The use of lentivirus-mediated gene delivery to investigate the role of the Brain specific transcription factor MYT1L In-vitro and In-vivo

Martinez Medina, Lourdes

Awarding institution:
King's College London

Title: The use of lentivirus-mediated gene delivery to investigate the role of the Brain specific transcription factor MYT1L In-vitro and In-vivo

Author: Lourdes Martinez Medina

THE USE OF LENTIVIRUS-MEDIATED GENE DELIVERY TO INVESTIGATE THE ROLE OF THE BRAIN SPECIFIC TRANSCRIPTION FACTOR *MYT1L* *IN-VITRO* AND *IN-VIVO*

Lourdes Martinez Medina

A thesis submitted to King's College London for the degree of Doctor of Philosophy in Social, Genetic and Development Psychiatry

2014

Be still,

Wild and young

And may your limits be unknown

And may your efforts be your own

If you ever feel you can't take it anymore

Brandon Flowers

This thesis is dedicated to my mother and grandparents

Abstract

The *Myt1l* gene, which encodes a neuron-specific transcription factor, is highly expressed in the developing brain, suggesting a crucial role in the processes of neurodevelopment. Although the expression of this gene decreases after birth, it continues to have a good level of expression throughout adulthood in localized areas. Nevertheless, the role of this gene in neural development and resultant behaviours has not been firmly established yet. In an effort to elucidate its function, lentiviral vectors containing synthetic microRNA-adapted short hairpin (shRNAmir) targeting *Myt1l* were produced to significantly decrease its expression. The knockdown efficiency of these vectors was corroborated *in-vitro* in the human neural stem cell line (SPC04) and the mouse cell line Neuro-2A. The effects of downregulating *MYT1L* at gene expression level during differentiation of SPC04 were assessed at two time points: pre-differentiation and day 7 differentiation. The results from this experiment identified five genes being co-expressed with *MYT1L* during stem cell differentiation: *BCL11B*, *MYT1*, *SYN1*, *SNAP25* and *JPH3*. Further *in-silico* analysis localized a MYT1L binding site in the promoter region of each one of those genes, suggesting that they might be direct targets of MYT1L. In order to expand our understanding of the possible behavioural effects of this gene, an *in-vivo* study was also performed in which adult mice received microinjections of lentiviruses expressing *Myt1l* shRNAmir in the dorsal hippocampus. These mice manifested a very subtle and transient increase in anxiety-like behaviour, which normalised with time. Even though the dorsal hippocampus has been only weakly linked to anxiety, our results seem to support this association when the expression of *Myt1l* is reduced. The findings of this thesis have laid the foundations of understanding the function of *MYT1L* pathway and the impact it has on behaviour.

Table of Contents

Table of Figures

Table of Tables

Acknowledgements

First of all, I'm deeply grateful to my supervisors Dr Sylvane Desrivières and Dr Christian Müller for giving the opportunity to study a PhD under their guidance. I would like to thank them both for their endless patience and invaluable support throughout these years. I would also like to thank Dr Cathy Fernandes for being like a third supervisor to me in the last part of my PhD and for her support and dedication towards my research project.

I'm deeply grateful to Dr Andrew Wong, Dr Graham Cooks, Dr Alanna Easton and Hannah Grayton for the kindness and patience they demonstrated while teaching me and sharing their knowledge with me.

I would like to extend my thanks to the Schumann past and present lab members for all their help and friendship, especially to Dr Barbara Ruggeri for her time and advice.

A special mention goes to Consejo Nacional de Ciencia y Tecnología (CONACyT) for believing in me and financially supporting me throughout my PhD.

I would like to thank my mum and grandparents for always believing in me, I could not have done it without them. Last but not least, I'm so grateful to all my

amazing friends and extended family, they might not know it, but each one of them help me achieving this dream.

Chapter 1 : General introduction

1.1 Introduction

Explaining the structure and function of the brain represents one of the greatest challenges to science; even more convoluted is determining the role that the genomic mechanisms behind this powerful organ play. The brain, considered one of the most complex systems in the body, is composed of 100 billion nerve cells that are precisely interconnected through trillions of synapses, giving rise to highly specialized structures which shape the characteristics of our species (Colón-Ramos and Shen 2008, Johnson, Kawasawa et al. 2009). The proper development of the mammalian brain is essential to creating a well-integrated and functional system capable of cognitive functions. Therefore, the programmes that regulate its development are extremely complex and must be tightly controlled to guarantee a functional outcome; these processes are largely driven by genetic factors (Stiles 2008). Failure to adequately execute these programmes can lead to a wide variety of phenotypes such as brain malformation, body growth deficiency and tumour susceptibility among others that can, in extreme cases, be fatal (Latchman 1996, Semenza 1998).

In recent years, scientific advances have enhanced our understanding of the mechanisms relating to brain development. Remarkable milestones have been the sequencing, in their totality, of the mouse and human genome in the early 2000s (Venter, Adams et al. 2001, Mouse-Genome-Sequencing-Consortium

2002). It was widely expected that knowing the full nucleotide sequence would help with the task of identifying the relationship between genes and environment, and the role these two play in disease (Venter, Adams et al. 2001); however, these goals are far from being completed but it is certain that knowledge in the field is building every day.

1.2 How the brain develops

1.2.1 Prenatal brain development

Neurons begin to differentiate and consequently form networks during the early stages of life in embryogenesis but the process will continue throughout the life of an individual. The differentiation of all the embryonic cells is conducted by a series of well-orchestrated signalling cascades (Stiles and Jernigan 2010). Specifically, the event that marks the emergence of the brain is the derivation of the ectoderm during gastrulation (Tam and Beddington 1987). During this period of development, the blastula reorganizes itself to form three layers: the endoderm, the mesoderm and the ectoderm (Lumsden and Chris 2003). Each one of these layers contains specific progenitor cells capable of producing the different structures of the embryo. For instance, the ectoderm will differentiate into different cell populations such as neural progenitor cells, progenitor cells for the neural crest, and the epidermal ectoderm (Tam and Beddington 1987).

A key aspect not only involved in deciding which cells will become part of the

future nervous system, but also important in defining the location of organs in the embryo is patterning. The establishment of the rostral-caudal axis through signalling molecules is a crucial step for this regional patterning (Yamaguchi 2001). In addition, further cues, varying in time and location, influence the release of signalling molecules to assist in delimitating this axis and guide cell differentiation (Stiles 2008). Special signalling tissues like the organizer node are also involved in patterning (Gritsman, Talbot et al. 2000, Mareschal, Johnson et al. 2007, Stiles and Jernigan 2010). In addition, the products of the genes expressed in this site help to establish the dorsal ventral axis (Anderson, Lawrence et al. 2002), as well as the asymmetry seen in the left and right axis. This third spatial patterning is important for organogenesis (Ohuchi, Kimura et al. 2000).

This process in which the foundations of the central nervous systems are properly established is called neurulation, which culminates in the formation of the neural tube. The development of the neural tube begins when a specialized dorsal region of the ectoderm enlarges and its edges are brought together to form the neural tube. It is largely dependent on the presence of morphogenes (Copp, Greene et al. 2003, Mareschal, Johnson et al. 2007, Brodal 2010), which code for diffusible proteins whose effects during development vary according to their concentration (Brodal 2010).

After its closure, the morphology of the neural tube evolves rapidly. The rostral part of the tube forms the primary vesicles which will generate the embryonic precursor of the forebrain (proencephalon), mid brain structures

(mesencephalon), and the hind brain (rhomboencephalon) and spinal cord (posterior neural tube) (Gilbert 2010). The proencephalon and the rhomboencephalon will further divide as shown in Figure 1.1.

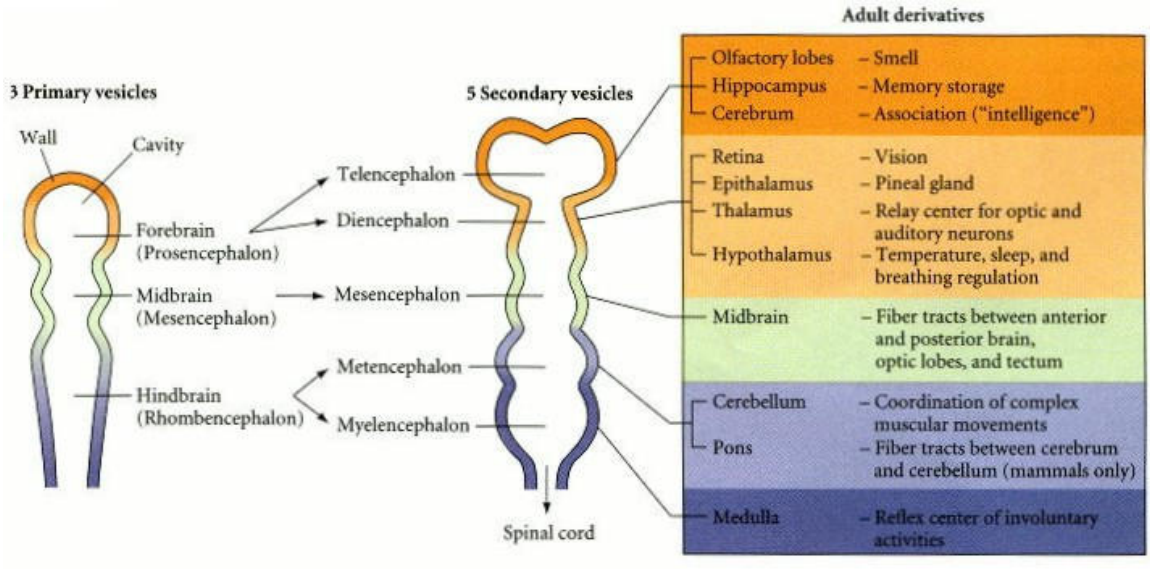

Figure 1.1 **This figure illustrates how the neural tube develops into different parts of the central nervous system.**

The rostral part of the neural tube forms 3 vesicles, which through development are subdivided into 5 secondary vesicles. On the right side of the figure, there is a list of the mature derivatives of those vesicles and their functions. The image was taken from Gilbert (Gilbert 2010).

All the pouches shown in Figure 1.1 are organized along the rostral-caudal axis of the embryo and will enlarge and bend to further accommodate the developing structures (Gilbert 2010). The cells that will develop into neural progenitor cells are not selected randomly, but rather by genetic signalling emanating from the organizer node. This node is responsible for guiding ectodermal cells into becoming neural progenitor cells (Stiles 2008). For example, one of the most important groups of genes involved in patterning and inducting neural phenotypes is composed of antagonists of bone morphogenic protein 4 (*BMP4*)

(Wilson, Lagna et al. 1997). Their importance was demonstrated when knockout mice lacking *noggin* and *chordin*, both *BMP4* antagonists, were seen to have a reduced neural plate. As a consequence, the brain was smaller and more importantly, the forebrain was absent (Anderson, Lawrence et al. 2002). Hence, the importance of establishing a dorso-ventral gradient of *BMP4* is necessary to aid the development of the brain and other organs (Lumsden and Chris 2003). Other morphogens like Wingless (*Wnt*), Sonic Hedgehog (*Shh*), epidermal growth factor (*EGF*), and fibroblast growth factor (*FGF*), which establish their effects in a concentration-dependent manner, are also required for brain patterning and help cells elicit their final lineage (Stiles 2011).

1.2.1.1 The creation of a circuit: neurogenesis and cell differentiation and synapse formation

When neurulation is complete, the gross morphology of the central nervous system has been established. As illustrated in Figure 1.2, further stages are dedicated to the proliferation, migration and differentiation of neurons, as well as axonal and dendritic outgrowth leading to synaptogenesis and the creation of neural networks and circuits (Paczkowski and Chun 2009). A neural network is simply defined as interconnected neurons that activate a linear pathway. In contrast, a circuit is a cluster of interconnected neurons that receives, modifies and transmits information through electrochemical signals to other circuits with the purpose of serving a particular function (Tau and Peterson 2009).

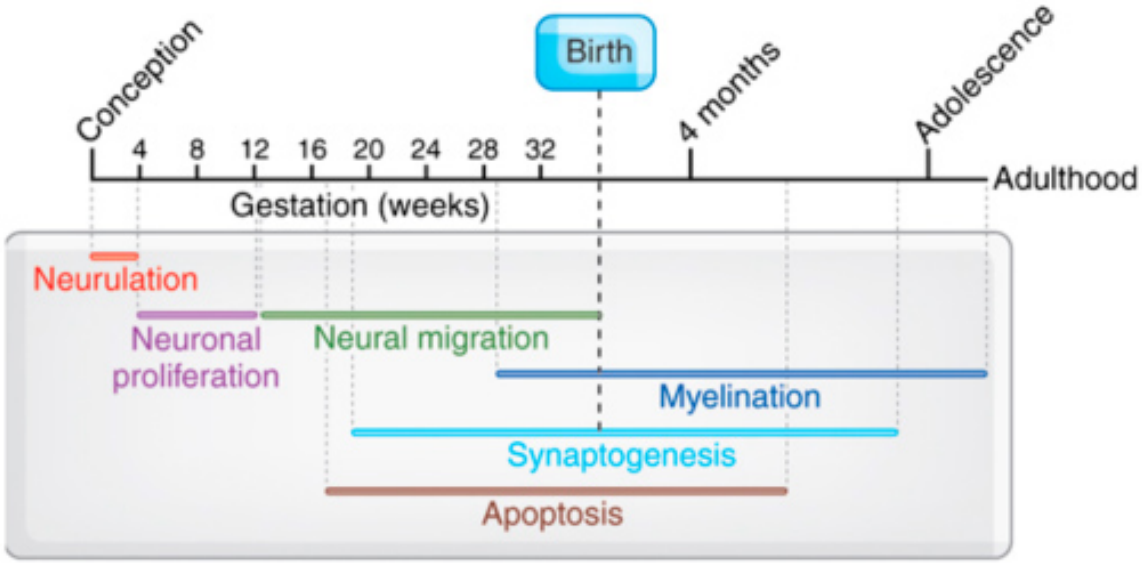

Figure 1.2 **Timeline of the major events occurring during brain development.**

This figure shows the major events involved in brain development across time. The image was taken from Tau et al. (Tau and Peterson 2009).

After the neural tube has formed, an increase in neurogenesis is observed (Figure 1.2). The lumen of the neural tube encloses an area of neural stem cells which expands in number before differentiating into neurons and glial cells that eventually migrate to other regions of the brain (Farkas and Huttner 2008). This process of expanding the neural stem cell pool follows both symmetrical and asymmetrical division: vertical cleavage of the neural stem cells increases division in a symmetrical manner, meaning daughter cells are the same as the parent cell; on the other hand, horizontal cleavage results in asymmetrical division, meaning each parent cell gives rise to one neural stem cell and one neural progenitor cell. These cells then differentiate into a neuron or a glial cell, with the former continuing to divide in the proliferative zone while the latter migrates into its final location. The proportion of cells undergoing symmetrical and asymmetrical division changes with time, increasing drastically when cortical neurogenesis begins (Chenn and McConnell 1995).

The cortex is formed from neurons generated in the ventricular zone (Meyer, Schaaps et al. 2000). These neurons require radial and tangential migration to reach their final location (Meyer, Schaaps et al. 2000). Cell migration in this case is performed in an “inside-out” fashion (from layer 6 to layer 1), meaning that the newly formed neurons populate the deeper layers of the cortex, while those formed just after migrate to the more external layers (Francis, Koulakoff et al. 1999). Disturbances in the genes required to regulate these complex processes of cell differentiation, neuron migration, and connectivity, can lead to cortical malformations resulting in disorders such as mental retardation and epilepsy (Francis, Koulakoff et al. 1999, Meyer, Schaaps et al. 2000).

Continuing with the development of the cortex, transplantation experiments have shown the importance of time-controlled expression of environmental cues when establishing the six morphological and functional distinctive layers of the cortex (Fukuchi-Shimogori and Grove 2001). For example, when cortex progenitor cells were transplanted from a younger donor, which were building cortex layer 4, into an older donor, whose progenitor cells were already building layers 2 and 3, the newly added cells followed the older cells’ differentiation and built the appropriate layers (layers 2 and 3). This demonstrated that cells in layer 4 are still multipotent. To the contrary, when progenitor cells belonging to an older donor (building layer 4) were transplanted into a much younger donor (layer 6), the cells were unable to acquire the characteristics of layer 6 and they migrated to layer 4. These results were interpreted as evidence that the environmental cues change along development and their presence is determinant of the progression towards an irreversible cell lineage (Desai and

McConnell 2000). However, recent studies have refuted the idea of permanent cell commitment after skin cells were able to be converted into functional neurons using transcription factors involved in brain development (Vierbuchen, Ostermeier et al. 2010).

Further research on the impact of migration and time-specific environmental cues have shown that once the cells have reached their final destination, cell to cell recognition and adhesive interactions among neurons, glia and the surrounding tissue possibly trigger additional signalling cues for neuron differentiation (Ghashghaei, Lai et al. 2007). This interaction of proximal neural cells is important for the establishment of neural networks and circuits (Dermietzel and Spray 1993). These circuits are seen as the primary mediators of the functional capacities of the brain (Tau and Peterson 2009).

The establishment of neural networks and circuits is tightly coupled to neuron differentiation and the development of special junctions called synapses (Li and Sheng 2003, Tau and Peterson 2009). Synapses between neurons occur through electrochemical signalling and their formation requires the neurites (axons and dendrites) of the neuron to elongate and come into proximity (Tau and Peterson 2009). For instance, the process of guiding axons towards their target dendrites depends on cell-related cues, chemical gradients and some extracellular signals (Palka, Whitlock et al. 1992). Axons travelling long distance depend on intermediate targets consisting of guidepost cells, which can be neurons, immature neurons (Sanes and Yamagata 1999) or glial cells (Pfrieger 2010). The chemical gradient provides additional guidance, just like in brain

patterning, by attracting or repelling the axon within a considerable distance (Chédotal and Richards 2010).

While a neuron can only have one axon, it can possess more than one dendrite. The dendrites emanate from the neuron and ramify in the proximity during development (Hof, Trapp et al. 2003). Since these ramifications vary in size and can define the properties of a neuron, the development of dendritic branching has to be well regulated at the molecular level and guided by intrinsic mechanisms (Perycz, Urbanska et al. 2011). It has been hypothesized that cytoskeleton dynamics and synthesis of proteins within the dendrites contribute to correct spine formation and neuronal connection (Crino, Khodakhah et al. 1998).

Shortly after the neuron has extended its neurites, genes coding for proteins involved in formation, accumulation and trafficking of synaptic vesicles begin to be expressed. These synaptic vesicles contain neurotransmitters that are cell-specific, determining the phenotype and function of a neuron. The specificity of neurotransmitters is largely regulated by transcription factors (Goridis and Brunet 1999). For example, transcription factors Forkhead box A1 (*FOXA1*) and A2 (*FOXA2*) were found to be necessary to regulate and maintain the phenotype of dopaminergic neurons (Stott, Metzakopian et al. 2013).

1.2.1.2 Morphological changes and cell pruning

After all the effort and resource spent on the generation of neurons and their synapses during the early prenatal stages, it is surprising that the latter stages of central nervous system development involve the death of at least half of the cells and connections created in the process (Mareschal, Johnson et al. 2007, Stiles, Reilly et al. 2012). This programmed cell death or apoptosis is not a fortuitous event, but a well-regulated process controlled by several intrinsic and extrinsic factors (Mareschal, Johnson et al. 2007). Even though the purpose of apoptosis during differentiation is not yet fully understood, there are some hypotheses as to why it may occur. After an extensive literature review, Oppenheim (Oppenheim 1991) suggested that different functions for apoptosis may depend on the embryonic stage in which they took place. In the early embryonic stages, it could be useful to eliminate defective cells. Later on, other cells that were created to perform a transient task may die after having fulfilled it, such as that of guiding axonal projections to their final destination. Right before birth, the massive pruning of cells might be the answer to adjusting the final number of neurons and synaptic connections.

1.2.2 Postnatal brain development

After birth, the brain does not develop in a continuous fashion, but it follows a non-linear pattern consisting of distinct age-dependant stages. These are roughly outlined below.

1.2.2.1 Infant brain development

Although a massive wave of apoptosis occurs before birth, the brain continues to grow in a linear and rapid manner right before the individual is born (Hüppi, Warfield et al. 1998). This linear growth of the brain continues throughout early childhood, reaching about 95% of its final size by age six (Dekaban and Sadowsky 1978, Lenroot and Giedd 2006). In order to assess the development of the brain, parameters such as intracranial space, cerebrospinal fluid, and grey and white matter volumes have been investigated through magnetic resonance imaging (MRI) (Courchesne, Chisum et al. 2000). For instance, white matter volume (myelinated axons and myelinating oligodendrocytes) normally follows a linear increase from birth to adolescence, when it reaches its peak (Giedd, Blumenthal et al. 1999, Matsuzawa, Matsui et al. 2001). The white matter volume augments due to differentiation and oligondedrocytes wrapping around the axons. These cells are in charge of enhancing connectivity by insulating the axons and upregulating the myelin protein (McTigue and Tripathi 2008).

By contrast, grey matter volume (neuronal cell bodies and glial cells) increases rapidly and continuously during foetal development, with it accounting for 50% of the total brain volume at the time of birth (Hüppi, Warfield et al. 1998, Lenroot and Giedd 2006). After birth, a non-continuous increase of grey matter volume is observed in a region-specific manner, peaking in late childhood and adolescence. For instance, the parietal lobe reaches its maximum volume by the age of 10, while the temporal lobe does not peak till around 16 years of age

(Courchesne, Chisum et al. 2000). The increase in grey matter volume is thought to be due to cell differentiation more than cell proliferation, as well as synaptogenesis. The functional implications of the augmentation of white and grey matter volume will be reviewed further below.

1.2.2.2 Brain development during adolescent and adulthood

Although adolescence is a period of development difficult to precisely define, it is usually described as the time between the start of sexual maturation to adulthood (Dahl 2004). It is characterized by an increase in gonadal steroid hormones (testosterone and estradiol), which are known to have an organizational effect on neural circuitry during foetal development and early childhood. Besides these effects in earlier development, these hormones induce sex-specific changes during adolescence, especially in brain areas that have gender dimorphisms like the amygdala and the hypothalamus (Jernigan, Baaré et al. 2011).

A neuronal event characteristic of adolescence involves a second wave of massive pruning, similar to the one observed before birth (Pfefferbaum A 1994, Andersen 2003, Crews, He et al. 2007). It is hypothesised that it shapes the brain and prepares its neural circuitry for mature adult behaviour (Crews, He et al. 2007) including cognitive traits such as abstract reasoning (Spear 2000).

MRI studies have quantified the effects pruning has on brain volume during adolescence. In regards to white matter volume, it does not seem to be affected, which is logical considering it increases linearly until it reaches a plateau around the age of 40 (Courchesne, Chisum et al. 2000). On the contrary, there is a volume reduction observed in grey matter that could be associated with synaptic and axonal pruning (Pfefferbaum A 1994). After the volume of grey matter in the different regions peaks in late childhood, it proceeds to decrease (Giedd, Blumenthal et al. 1999, Lenroot and Giedd 2006) at a rate of approximately 5% per decade (Courchesne, Chisum et al. 2000), with the exemption of the volume of the temporal lobe that peaks during adolescence (as noted above), which then also beings to decrease (Giedd, Blumenthal et al. 1999).

The variations in white and grey matter volume along development seem to be part of the ongoing maturation and remodelling of the brain. Abnormal changes could have consequences for the development of adult cognition. A study by Reiss (Reiss, Abrams et al. 1996) showed a positive correlation between intelligence, as measured by an intelligence quotient (IQ), and the total brain volume, particularly the grey matter volume in the prefrontal cortex. Other studies have supported this statement and have correlated IQ with the grey and white matter volumes of other specific brain regions in the different lobes (Haier, Jung et al. 2004). Social cognition, which represents the interplay between emotion-related processes and cognition, has also been correlated to changes in brain volume, especially white matter in the occipito-temporal lobe. The appropriate development of social cognition during adolescence is crucial in

interpreting verbal and non-verbal cues related to human interaction and communication (Paus 2005).

Brain function can be measured by using functional MRI (fMRI) to detect changes in blood flow and then associating these changes with neuronal activity in the grey matter when a particular task is being performed (Brown, Joanisse et al. 2013). Other imaging techniques such as diffusion tensor studies are capable of measuring the magnitude and direction of the water molecule diffusion inside the brain, allowing for measurements of the level of myelination and axon thickness (Gössl, Fahrmeir et al. 2002, Olesen, Nagy et al. 2003). When subjects are investigated using both techniques while performing a task, a correlation of the activation sites in each study can unravel the networks connecting grey and white matter (Werring, Clark et al. 1999, Olesen, Nagy et al. 2003). These techniques have been applied to children and adolescents in an effort to study neuropsychological traits such as working memory (Olesen, Nagy et al. 2003) and speech and motor functions (Paus, Zijdenbos et al. 1999).

Both MRI and functional MRI (fMRI) studies have, in combination with genetic studies, been used to determine the role genes play in structure and function of the brain (Bartley, Jones et al. 1997, Posthuma, De Geus et al. 2002, Toga and Thompson 2005), specifically in regards to the genetic influence on the frontal grey matter volume and its correlation to cognition (Thompson, Cannon et al. 2001, Posthuma, De Geus et al. 2002).

In addition to genetic factors, environmental factors could also impact on the size and function of the brain (Thompson, Cannon et al. 2001, Toga and Thompson 2005). Throughout the lifetime of an individual, the brain can respond to those factors by activating brain plasticity, which is characterized by changes in synapses and neural networks (Kolb, Gibb et al. 2003). One hypothesis about the purpose of plasticity is to adjust the neural networks according to the environment in which the organism lives (Bavelier, Levi et al. 2010). Brain plasticity cannot only be influenced by changes in the environment but also by factors like cognitive maturation (Lledo, Alonso et al. 2006), experience (Draganski, Gaser et al. 2004), learning (Poldrack 2000), memory (Bailey and Kandel 1993) and pathologies (Keyvani and Schallert 2002). For instance, one study observed that extensive navigational experience in taxi drivers was correlated with a larger grey matter density in the posterior hippocampus (the area of the brain is suggested to store spatial memory) in comparison to the general population (Maguire, Gadian et al. 2000).

More recently, neurogenesis in the adult brain has been proposed to contribute to brain plasticity. Although neurogenesis decreases markedly before birth, there are still two areas in the adult brain that serve as areas for the remaining neural stem cells. The neurons that differentiate from the subgranular layer in the dentate gyrus are thought to play a role hippocampal-related memory and learning, whilst the neurons generated in the subventricular zone are associated with olfaction (Lazarov, Mattson et al. 2010).

1.3 The importance of transcription factors

Changes in gene expression drive the structural alterations in the brain described in the previous chapter. Human post-mortem studies have suggested that these changes occur throughout the life of an individual in a spatio-temporal manner (Erraji-Benchekroun, Underwood et al. 2005). Transcription factors have a particular role in this gene expression because by binding to the promoters of their target gene and working closely with chromatin-remodelling factors, they regulate the transcription of the target genes (Maniatis, Goodbourn et al. 1987). In this manner, transcription factors create transcriptional networks that regulate brain patterning, cell proliferation, cell differentiation, cell migration, synaptogenesis and programmed cell death (Southall and Brand 2009, Studer 2011). Not surprisingly, neurons are one of the most transcriptionally active cells in the body, which enables them to obtain and maintain their phenotype throughout development (Nelson, Hempel et al. 2006).

Transcription factors are characterized by a DNA-binding domain that facilitates specific recognition of target genomic regions. It has been estimated that about 8% of the human genome (~2000-3000 genes) encode for putative transcription factors, as judged by the presence of a DNA-binding site in their amino acid sequence (Brivanlou and Darnell 2002, Babu, Luscombe et al. 2004). Out of those, zinc finger accounted for about 3% of the genome (Klug 2010). Similar results were obtained in mouse studies, which showed that over 7% of the genome, encode for putative transcriptions factors (~1445 genes). These results further concluded that more than 20% of those (~349 genes) were

restricted to the central nervous system and presented different patterns of expression during development. Moreover, the largest group of transcription factors were the zinc fingers (~678 genes). Around 10% of them were restricted to the central nervous system, highlighting the importance of zinc fingers in the brain (Gray, Fu et al. 2004).

It is thought that the zinc fingers are so widely used because the zinc ions offer structural stability to the folded domains that do not possess a stable hydrophobic core due to its length (Coleman 1992, Kim, Armstrong et al. 1997). The structure of zinc fingers normally comprises two small antiparallel beta-strands followed by an alpha helix [Figure 1.3(c)]. The DNA binding properties are created from the tertiary structure established between the tetrahedral complex (either four cysteines or two histidines and 2 cysteines) and a zinc ion (Pabo and Sauer 1992, Semenza 1998, Klug 2010). Further stabilization of the zinc fingers is given by the hydrophobic core, usually composed of three conserved amino acids: tyrosine, phenylalanine and leucine (Klug 2010).

In terms of their binding efficiency, the proteins require at least two zinc finger subunits to attach around the DNA (Coleman 1992). A classic proportion between a finger motif and DNA is one to one. This means that individual amino acids from the alpha helix typically recognize and interact with a specific adjacent three-base pairs site on the coding strand of the major groove of DNA. In addition, they have a fourth-amino acid docking a base overlapped with the previous finger; it is referred to as position ‘minus one’ and is situated before the alpha helix. One manner in which they are linked is a cross-strand interaction:

positions minus one, three and six are linked to the coding strand while position two binds to the non coding one [Figure 1.3(b)] (McBryant, Gedulin et al. 1996, Luscombe, Austin et al. 2000). Although this binding arrangement is common, some alterations in the way it is presented in the different families of zinc fingers have been noted (Klug 2005, Klug 2010).

In most cases, the specificity of the DNA binding protein increases with the number of finger units in it; this is because each finger functions as an individual unit recognizing a DNA base. Therefore, a protein with two fingers is less specific and can target more genes because it binds to fewer DNA bases, while one with six fingers can bind to a longer part of the coding strand, making it more selective (Luscombe, Austin et al. 2000, Klug 2010).

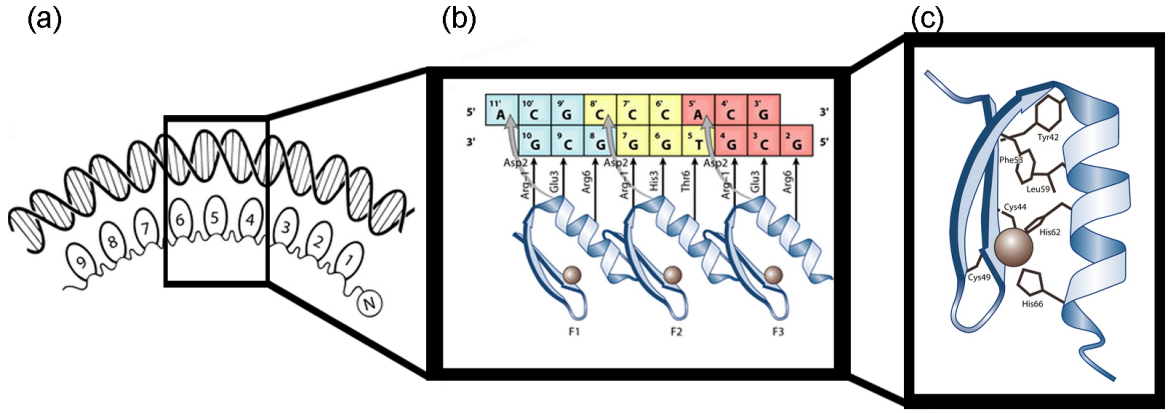

Figure 1.3 **Structure and binding sites of a zinc finger protein.**

(a) The protein structure of Transcription factor IIIA (TFIIIA). This transcription factor is composed of nine CCHH zinc fingers and was the first to be discovered. (b) Schematic diagram of the DNA recognition model by sequence specific amino acids in the alpha helix. This model particularly illustrates the case of three amino acids being cross-strand linked with three adjacent base pairs in the coding (positions -1, 3 and 6) and non-coding strand (position 2) of DNA. (c) Nuclear magnetic resonance of a two-finger protein study showed the structure of an individual finger CCHH motif. In this particular example, Tyr42, Phe53 and Leu59 compose the hydrophobic core. All images in this figure belong to Aaron Klug (Klug 2010).

1.3.1 Transcription factors and psychiatric diseases

The dysregulation and dysfunction of transcription factors is regarded as a cause of disease. More specifically, at least one third of disorders originating during development have been linked to their disruption (Vaquerizas, Kummerfeld et al. 2009). For instance, psychiatric disorders like autism, schizophrenia and mental retardation, among others, have linked their aetiology to disruptions in the sequence or the expression of transcriptions factors during brain development (Van Loo and Martens 2007). For example, in autism, genetic alterations of transcription factor Engrailed 2 (*EN2*) during cerebellar development were suggested to contribute to the observed pathology (Gharani, Benayed et al. 2004); in the case of schizophrenia, the expression of transcription factor SRY-related HMG-box 10 (*SOX10*), involved in developing and maturing glial cells like oligodendrocyte (Kuhlbrodt, Herbarth et al. 1998), was found to be decreased in a patient cohort (Tkachev, Mimmack et al. 2003); lastly, a candidate gene for X-linked mental retardation is Zinc finger protein 41 (*ZFP41*), which is suggested to be important for cognitive development (Shoichet, Hoffmann et al. 2003). These examples illustrate the importance of transcription factors. When disturbed, they can impact the correct development of the brain and ultimately affect the behavioural output (Vaquerizas, Kummerfeld et al. 2009).

1.3.2 Myelin transcription factor 1 like (*MYT1L*)

MYT1L, which is also called neural zinc finger 1, is a zinc finger transcription

factor that has been related to the operation and development of the brain (Kim, Armstrong et al. 1997). It was discovered while searching for proteins capable of binding beta-retinoic acid. In the mouse, they observed that *Myt1l* could not only recognize the promoter in the beta-retinoic acid receptor, but also the promoters of the other two POU Class 1 Homeobox 1 (*Pit-1*) genes (Jiang, Yu et al. 1996).

MYT1L belongs to the myelin transcription factor 1 family. This cluster of DNA-binding proteins, commonly referred as CCHHC domains, stands for its peculiar motif of five, instead of four, conserved residues arranged as follows: Cys-X_4-Cys-X_4-His-X_7-His-X_5-Cys (Jiang, Yu et al. 1996, Blasie and Berg 1999, Berkovits-Cymet, Amann et al. 2004). The involvement of the fifth metal ligand causes a spatial re-organization to the motif, which changes the potential binding of the zinc ion, modifying its folding domains and ultimately the structure. Specifically, MYT1L zinc finger is known to coordinate zinc in a tetrahedral manner by using one histidine and three cysteines (Berkovits-Cymet, Amann et al. 2004). The additional histidine residue is hypothesised to stabilize an internal loop by interacting with a tyrosine (Figure 1.4); however, this observation has not been duplicated yet (Besold, Lee et al. 2010).

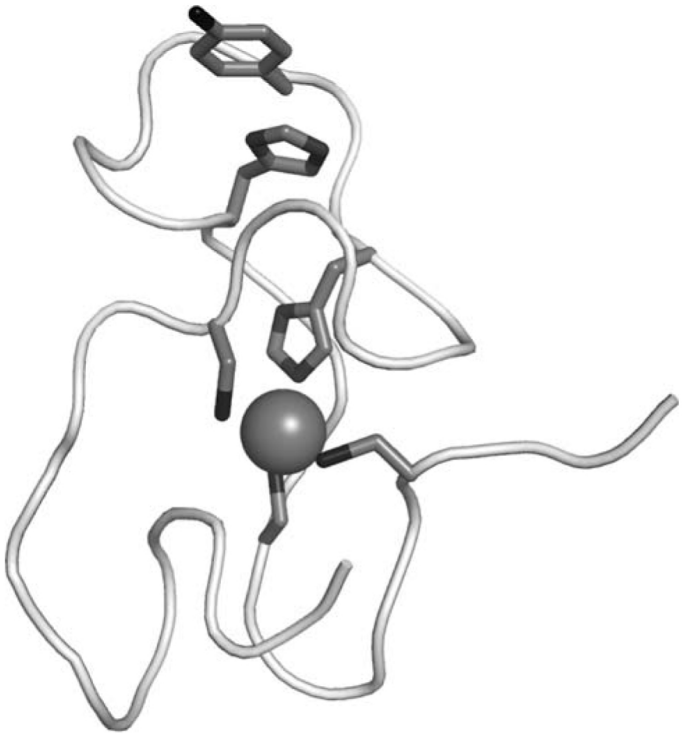

Figure 1.4 **Schematic structure of a single Myt1l zinc-binding domain.**

This figure represents the solution structure of a zinc finger. Three cysteine residues and a histidine are interacting with the zinc ion, along with the additional histidine and a semiconserved tyrosine. The image was taken from Besold et al. (Besold, Lee et al. 2010).

In the human genome, there are three members of this family: myelin transcription factor 1 (*MYT1*), myelin transcription factor 1 like (*MYT1L*) and suppression of tumorigenicity 18 (*ST18*) (Figue 1.5) (Wang, Zeng et al. 2010, Stevens, van Ravenswaaij-Arts et al. 2011). The *MYT1L* gene in humans is located in chromosome 2 (2p25.3) and is formed by 540,081 base pairs and 25 exons. From those, only exons 6 to 24 and the proximal part of exon 25 are coding regions (Wang, Zeng et al. 2010), resulting in a protein composed of 1186 amino acids (Meyer, Zweig et al. 2013). Interestingly, human MYT1L protein is similar to Myt1l rodent protein, being 95% equal to the mouse and 92% to the rat, showing its high conservation through evolution (Stevens, van Ravenswaaij-Arts et al. 2011). It is formed by six zinc finger domains internally

organized in groups of two and three, leaving the remaining finger in the N-terminus. An independent DNA binding domain is created by each one of the clustered zinc fingers. The cluster composed of three zinc fingers has a higher biding affinity (Jiang, Yu et al. 1996). Furthermore, a high degree of homology between the zinc fingers in *MYT1L* has been observed as both two and three-finger clusters can bind the same DNA sequence. Although this allows any of those domain clusters to activate the promoter, the ability to decide which set of fingers docks the target gene might be part of the mechanism regulating transcription (Besold, Lee et al. 2010).

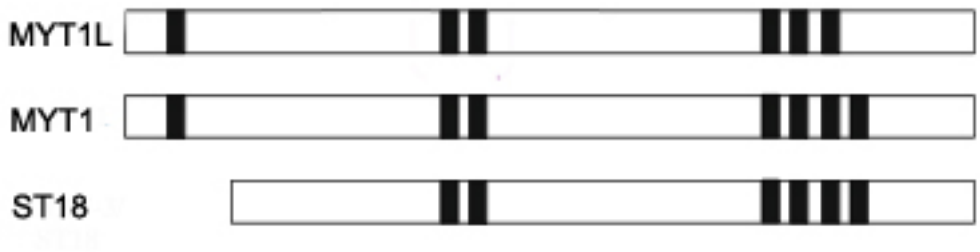

Figure 1.5 **Schematic representation of the clusters made by zinc finger in the MYT1 family.**

The black rectangles represent each one of the zinc fingers. The image was obtained from Besold et al. (Besold, Lee et al. 2010).

Normally, when the structure of a DNA-binding protein is known, inferences can be made about the docking to the target gene. However, this is not the case for *MYT1L*. It was demonstrated that the *MYT1L* zinc fingers lack alpha helix and beta sheets, the former structure being widely used by other zinc fingers to interact with the DNA (Berkovits-Cymet, Amann et al. 2004, Besold, Lee et al. 2010). Research performed on family member *MYT1* revealed no other clear contact areas and it was suggested that the whole *MYT1* zinc finger binds to the major groove of DNA, producing specific electrostatic and hydrophobic contacts

(Gamsjaeger, Swanton et al. 2008). This could also be the case for *MYT1L*.

As for its expression, this DNA-binding protein is brain specific, specifically restricted to neurons (Berkovits-Cymet, Amann et al. 2004). The microarray data obtained online from the quantitative atlas BioGPS (available at http://biogps.org/#goto=welcome) has helped to provide evidence of the restricted expression of *MYT1L* in human and mouse brain (Figure 1.6) (Wu, Orozco et al. 2009). In particular, this protein is predominantly expressed in the developing central nervous system (Kim, Armstrong et al. 1997). A second *in-silico* analysis using the Allen Developing Mouse Brain Atlas (available online at http://developingmouse.brain-map.org) has further corroborated this hypothesis by showing that the expression of *Myt1l* in the mouse appears to start around E13.5, reaching a peak around birth and lowering, but to still detectable levels, in adulthood (Figure 1.7). Previous *in-situ* hybridization experiments in rats found similar expression patterns, with *Myt1l* expression starting around days 13-15 and reaching its maximum expression right before birth (Kim, Armstrong et al. 1997).

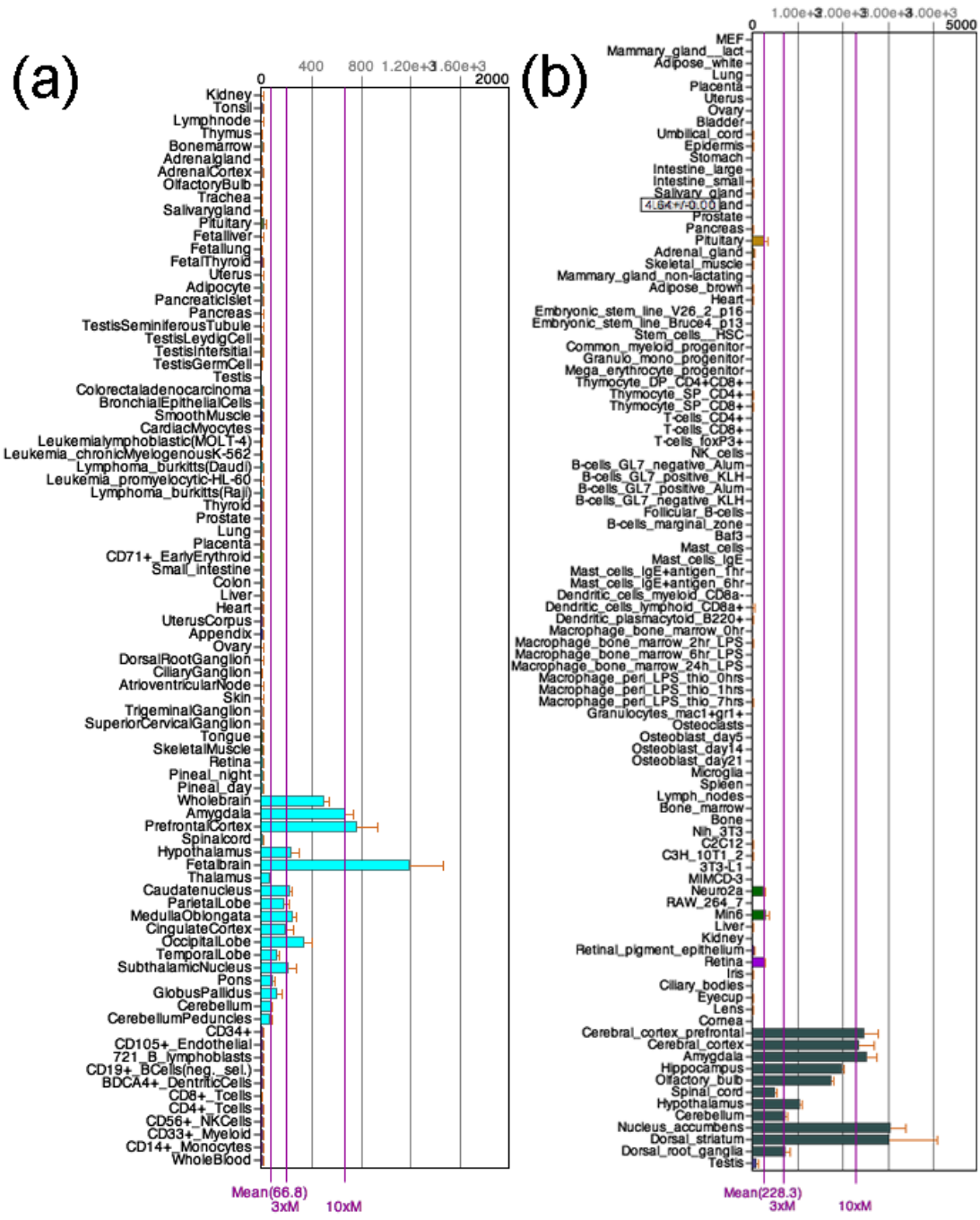

Figure 1.6 ***MYT1L*** **mRNA expression in different tissues in (a) human and (b) mouse.**

The tissue-specific patterns of mRNA levels in these graphs were obtained from BioGPS. The expression levels correspond to the results obtained in microarray experiments conducted with Affymetrix chips (Wu, Orozco et al. 2009). (a) For analysing human mRNA levels, the probe 210016_at on the Human Genome U133 array was used (Su, Wiltshire et al. 2004); while for the mouse, the probe 1421175_at on the mouse genome 430 array was used (Lattin, Schroder et al. 2008). All microarray data was normalized using Gene Chip Robust Multiarray Averaging (GC RMA).

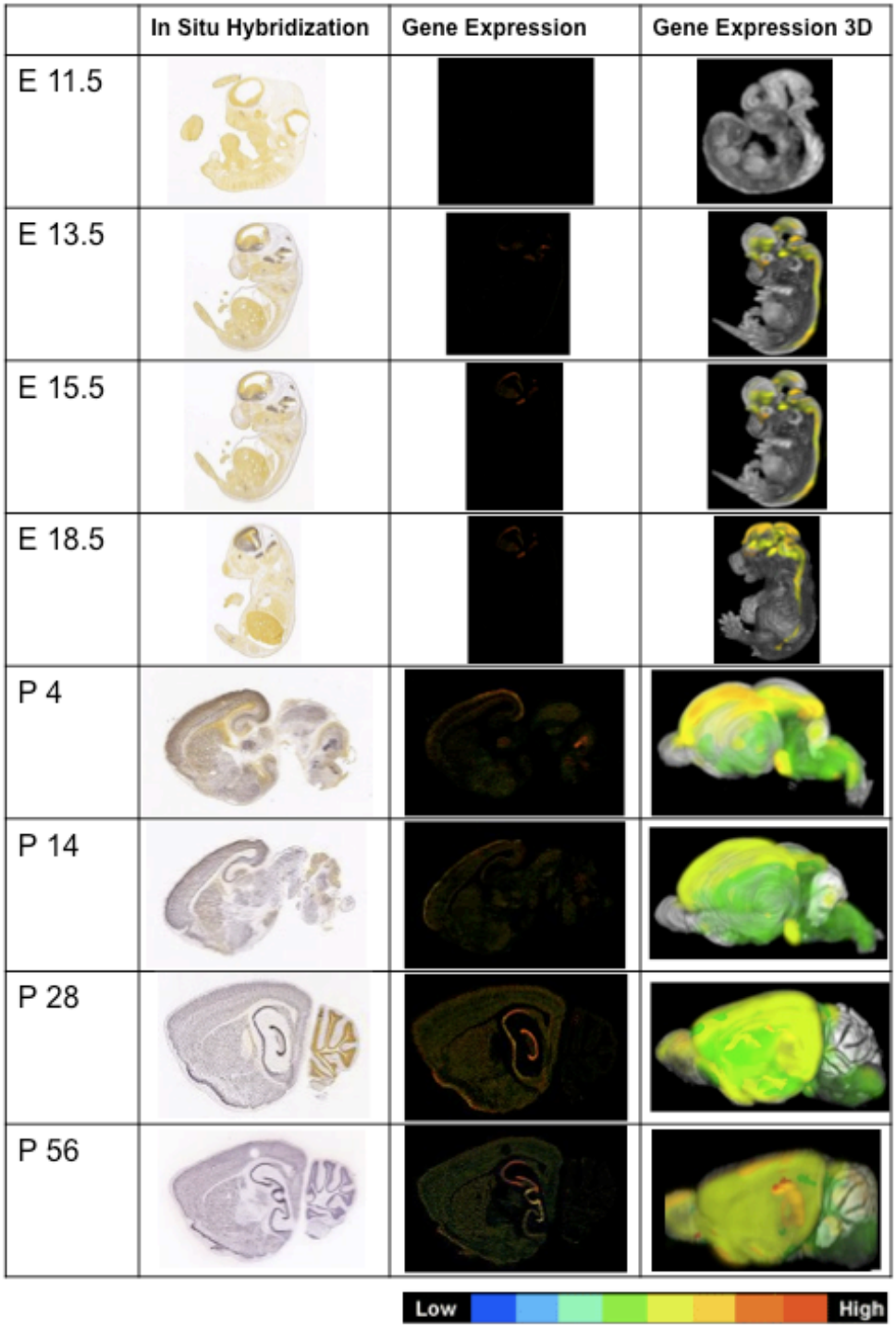

Figure 1.7 **Expression of *Myt1l* through different stages from embryonic (E) to postnatal (P) development in the mouse strain C57BL/6J.**

All images were obtained from the Allen Developing Mouse Brain Atlas. In the first column, *in-situ* hybridization (ISH) was used in sagittal brain sections to detect *Myt1l* mRNA. Images from the second column are another method of representing the gene expression obtained by ISH. Each ISH image undergoes a detection algorithm to create a high-resolution greyscale image to identify pixels that correspond to gene expression. The intensity of the signal is colour-coded, with blue representing the lowest gene expression and red the highest. Images in the third column are a 3D illustration of the gene expression (Lein, Hawrylycz et al. 2007).

1.3.2.1 The importance of *MYT1L* for neuronal induction *in-vitro*

The fact that *Myt1l* is expressed only in neurons and that its expression is higher before birth suggests its crucial role in neurodevelopment (Jiang, Yu et al. 1996, Kim, Armstrong et al. 1997). Moreover, its presence in later stages of life denotes its possible importance for brain function. The first evidence supporting these conjectures was reported by early findings that *Myt1l,* along with Achaete-scute homolog 1 (*Ascl1*) and POU class 3 homeobox 2 (*Brn2*), is capable of not only reversing cell lineage in mouse fibroblast but also reprogramming them as neurons. Although, fibroblasts acquire an immature neuronal phenotype when the expression of *Ascl1* is activated, the addition of *Myt1l* and *Brn2* is fundamental to obtaining a mature neuron capable of synapse connections and action potentials (Vierbuchen, Ostermeier et al. 2010). Characterization of the newly converted neurons indicate they are excitatory cells showing cortical neurons markers (Vierbuchen, Ostermeier et al. 2010), suggesting their involvement in cognitive functions (Stevens, van Ravenswaaij-Arts et al. 2011). When the other genes were tested individually, none of them were sufficient to induce neuronal cell fate (Vierbuchen, Ostermeier et al. 2010).

Similar to the previous experiment, a second study achieved the differentiation of human pluripotent stem cells into mature neurons through the addition of *ASCL1*, *BRN2* and *MYT1L*. By including Neuronal differentiation 1 (*NEUROD1*) in the previous pool of genes, the same outcome was yielded when converting human foetal and postnatal fibroblasts. *NEUROD1* aided these types of cells to

obtain the morphology and electrophysiological properties of a mature neuron. These studies were further corroborated when the newly transformed neurons were put in culture along with mouse cortical neurons to assess the integration into pre-existing neuronal networks. Further whole cell recording demonstrated the formation of neurotransmitter receptors and functional synapses. Moreover, the cell phenotype was maintained once these genes were no longer overexpressed (Pang, Yang et al. 2011).

An alternative set up used microRNA-124 (miR-124) instead of *ASCL1* plus *BRN2* and *MYT1L* to transform human postnatal and adult fibroblasts into functionally mature neurons. When either *BRN2* or *MYT1L* were tested separately in combination with mir-124, only *MYT1L* demonstrated the ability to promote a more elongated morphology. However, proper maturation and fully functional synapses still required all three factors (Ambasudhan, Talantova et al. 2011). Comparable results were obtained in an experiment using microRNA 9/9 (mir-9/9), mir-124, Neuronal differentiation 2 (*NEUROD2*), *ASCL1* and *MYT1L* (Yoo, Sun et al. 2011). Once again, *MYT1L* was necessary to enhance the level of maturation. These studies highlighted the possible role of microRNA in neurogenesis and phenotype determination (Ambasudhan, Talantova et al. 2011, Yoo, Sun et al. 2011).

In order to intentionally convert human embryonic fibroblasts and postnatal fibroblasts into functional dopamine neurons, the overexpression of *ASCL1*, *BRN2*, and *MYT1L*, supplemented by LIM homeobox transcription factor 1, alpha (*LMX1A*) and *FOXA2* (genes related to dopaminergic differentiation) was

necessary. Out of the resulting neurons, one out of ten exhibited morphological and electrophysiological characteristics of midbrain dopamine neurons (Pfisterer, Kirkeby et al. 2011). Son and colleagues (Son, Ichida et al. 2011) further corroborated the possibility of inducing different neuronal phenotypes by reverting mouse fibroblasts into motor neurons. This experiment required the addition of LIM Homeobox 3 (*Lhx3*), Motor neuron and pancreas homeobox 1 (*Hb9*), ISL LIM homeobox 1 (*Isl1*), and Neurogenin 2 (*Ngn2*) to the now well-known protocol (*Ascl1*, *Brn2* and *Myt1l*) to induce functional motor neurons. The addition of *NEUROD1* to the previous mix was enough to replicate the effect in human embryonic fibroblasts.

All of the experiments mentioned above relied on lentiviral vectors to increase expression of the genes in order to revert cell fate and obtain mature neurons. The use of this particular technique represents a challenge for further clinical application. A recent study in mouse embryonic fibroblasts proposed the use of plasmids *Ascl1*, *Brn2* and *Myt1l* to recreate the same effect observed with lentiviral vectors. Surprisingly, results showed high transfection efficiency and low toxicity in addition to providing comparable results to the lentiviral technique. These experiments not only provide insight into the putative importance of *MYT1L* for cell differentiation and cell identity, but could also play a valuable role in future neuron replacement therapy (Adler, Grigsby et al. 2012).

1.3.2.2 The association of *MYT1L* and disease

Considering the importance of *MYT1L* in neuronal development, it is logical that alteration in its sequence or expression could have an impact on psychiatric disorders. The development of new technologies like fluorescence *in-situ* hybridization and microarrays has helped the mapping of genomes of both the healthy and pathological populations (Rio, Royer et al. 2012). Both techniques have been able to extend the number of genes that can be analysed in a single experiment, providing a good approach to unravelling the genes that could be affected in a specific disease (Lee, Mattai et al. 2012).

Clinical studies, which rely on such techniques, have positioned *MYT1L* as a candidate gene for psychiatric disorders (Table 1.1). The first link was reported in a genomic study aiming to identify rare copy number variants (CNV) in schizophrenic patients. In two patients it was observed that the breakpoint of CNV duplication was located on the terminal part of *MYT1L*, which could impact on both the dosage variation and its expression (Vrijenhoek, Buizer-Voskamp et al. 2008). Additional evidence of CNV affecting *MYT1L* came from an analysis of childhood onset of Schizophrenia, in which two patients presented duplications which disrupted *MYT1L* (Addington and Rapoport 2009). Independently, these studies only displayed a trend of association between duplications in *MYT1L* and schizophrenia. However, the results of four published studies were combined together in a meta-analysis to provide stronger evidence of how variable size *MYT1L* duplications might be involved in this disease. The overall rate of disruption in *MYT1L* found in this study was

comparable to other CNVs that have been classified as high risk for schizophrenia (Lee, Mattai et al. 2012).

Table 1.1 **Mutations in *MYT1L* and their linkage to disease**

N/A: Not applicable; PANSS: Positive and Negative Syndrome Scale.

	Patient	Mutation	Diseases and other behavioural problems associated
Vrijenhoek (2008)	**P1**	Duplication of 1014 kb partially affecting *MYT1L*	Schizophrenia (Severe delusions/ hallucinations of sexual/aggressive content)
	P2	Duplication of 3134 kb afecting the whole *MYT1L*	Schizophrenia (Bizarre delusions/ hallucinations; aggressive behavior; anhedonia)
Addington (2009)	**P1**	Duplication of unknown size affecting *MYT1L*	Childhood onset of schizophrenia
	P2	Duplication of unknown size affecting *MYT1L*	Childhood onset of schizophrenia
Li (2012)	**N/A**	SNP mutation rs17039584 in *MYT1L* gene	Schizophrenia in the Han Chinese population (females associated with positive syndrome score on the PANSS)
	N/A	SNP mutation rs10190125 in MYT1L gene	Schizophrenia in the Han Chinese population (Associated with positive syndrome score on the PANSS)
Wang (2010)	**N/A**	SNP mutation rs3748989 in MYT1L gene	Major Depressive Disorder in the Chinese Han Population
Meyer (2012)	**P1**	Duplication of 281 kb partially affecting *MYT1L*	Non-verbal autistic patient
	P2	Duplication of 281 kb partially affecting *MYT1L*	Autistic patient with stereotypical autistic language
Rio (2012)	**P1**	Deletion that partially affects *MYT1L*	Developmental delay, absence of speech, overweight and hyperactivity
	P2	Somatic mosaicism with 3 cell population affecting *MYT1L:* 1/3 duplication, 1/3 deletion and 1/3 normal	Autism spectrum disorder without motor delay

Gruchy (2007)	**P1**	Inverted duplication of 28 Mb affecting *MYT1L*	Severe psychomotor and mental retardation
Bonaglia (2008)	**P1**	Inverted duplication of 10Mb affecting the whole *MYT1L*	Moderate mental retardation with motor and speech delay
	P2	Inverted duplication of 10Mb affecting the whole *MYT1L*	Severe mental retardation with motor delay, and severe speech delay
	P3	Inverted duplication of 10Mb affecting the whole *MYT1L*	Moderate mental retardation
Stevens (2011)	**P1**	Deletion of 2.77 Mb that affected *MYT1L*	Moderate mental retardation, hyperactivity, mood changes and obesity
	P2	Deletion of 2.77 Mb that affected *MYT1L*	Moderate mental retardation, hyperactivity, mood changes and obesity
	P3	Deletion of 2.77 Mb that affected *MYT1L*	Moderate mental retardation, hyperactivity, mood changes and obesity
	P4	Deletion of 3.13 Mb that affected *MYT1L*	Moderate mental retardation and obesity
	P5	Deletion of 1.33 Mb that affected *MYT1L*	Moderate mental retardation, psychomotor and speech delay, mild hypotonia, hyperlaxity and obesity
	P6	Deletion of 0.37 Mb that affected *MYT1L*	Moderate to severe mental retardation, autism and obesity

The association of a *MYT1L* polymorphism and schizophrenia was also explored in the Han Chinese population. In this study, six single-nucleotide polymorphisms (SNPs) were analyzed. The results showed that SNP rs17039584 and rs10190125 had a significant association with schizophrenic patients in comparison to the controls. The latter SNP was still significant after the participants were divided by gender (Li, Wang et al. 2012).

The first study to look for an association between *MYT1L* and major depressive disorder was also in the Han Chinese population. A set of eight SNPs was tested in a large population containing both affected and general population. It was found that SNP rs3748989 was significantly associated, indicating *MYT1L* might be a potential risk gene for major depressive disorder among the Han Chinese (Wang, Zeng et al. 2010).

Garbett and collaborators (Garbett, Ebert et al. 2008) first suggested an association between transcription factor *MYT1L* and autism after encountering a reduced expression of this gene in the temporal gyrus of autistic patients. A more recent clinical report, in which two male half-siblings were found to have de novo duplication in chromosome 2p25.3, further supported the role of *MYT1L* as a possible candidate gene for autism. The breakpoints included a full copy of peroxidasin homolog (Drosophila; *PXDN*) and seven exons of the terminal part of *MYT1L*. Their psychiatrically healthy mother was analysed and it was revealed that the transmission was due to germline mosaicism (Meyer, Axelsen et al. 2012).

In a case study of monozygotic twins, one twin was found to exhibit an autistic phenotype whilst her twin sister's phenotype included absence of speech, developmental retardation, hyperactivity and obesity. The former twin suffered from somatic mosaicism in which the chromosomal imbalance included deletion of 2p25.3 in one third of the cells; duplication in the same location in another third; and the remaining third was normal. The other sister presented only a deletion but in the same region. While the deletions and the duplication seen in

both twins were of different sizes, *MYT1L* and syntrophin gamma 2 (*SNTG2*) appeared to be affected in both cases (Rio, Royer et al. 2012). Considering the associations of this gene with neuronal maturation and synapse formation, it is not unexpected that *MYT1L* could contribute to the induction of this disorder,

Another psychiatric disease that has been linked to chromosome 2p25.3 is mental retardation. Inverted duplications with terminal deletions affecting this chromosomic region, hence *MYT1L*, were initially noted in a study involving four patients: two siblings (a boy and a girl), their father and a non-related girl. Although the deletions were different in size and specific location, the patients shared the following phenotypes: scoliosis, particular ear shape and mental retardation, the latter being more severe in the females (Gruchy, Jacquemont et al. 2007, Bonaglia, Giorda et al. 2008).

A more compelling study linking intellectual disability and *MYT1L* combined phenotypic and genotypic data from six patients, three siblings and three non-related. All patients shared moderate intellectual disability and were overweight. Five out of six had a square-shaped complexion and half of them suffered from hyperactivity. Microarray results identified a deletion in 2pq25.3 ranging from 0.37 to 3.13 Mb. The only gene which overlapped and which was disturbed in all cases was *MYT1L*. Along with *MYT1L*, the following genes were affected by the deletion in four of the patients (including all the siblings): Family with sequence similarity 110 member C (*FAM110C*), Family with sequence similarity 150 member B (*FAM150B*), Sh3 domain YSC-like 1 (*SH3YL1*), Acid phosphatase 1 (*ACP1*), *TMEM18*, Chromosome 2 open reading frame 90

(*C2ORF90*), Syntrophin, gamma 2 (*SNTG2*), Thyroid peroxidase (*TPO*) and *PXDN*. In contrast, one patient with a shorter deletion only had the following genes compromised: *MYT1L*, *SNTG2*, *TPO* and *PXDN*. For the remaining patient, only *MYT1L* and *PXDN* were disturbed in the deleted region. Taking these results into consideration, it was suggested that the cause of intellectual disability was due to *MYT1L* haploinsufficiency (Stevens, van Ravenswaaij-Arts et al. 2011).

In the light of the genome variations affecting the previously mentioned psychiatric disorders, it is not unexpected that *MYT1L* could play a role in causing them when disrupted (Wang, Zeng et al. 2010).

1.4 Underlying the function of genes

The large amount of genetic information generated by the distinctive types microarrays has increased the number of candidate genes for most psychiatric disorders (Thakker, Natt et al. 2004). Although these studies have been a remarkable achievement in delimitating the genes involved in a particular disease, further research is required to establish the contribution of each gene to the psychopathology. A logical method to establish the function of individual genes is by significantly increasing or reducing their expression and observing the changes produced in an organism (Vallier, Rugg-Gunn et al. 2004, Weber, Bartsch et al. 2008). Both *in-vitro* and *in-vivo* models have used this technique to screen for phenotypic and genotypic consequences of gene modification

(Paddison, Caudy et al. 2002). The phenotypic products resulting from the loss of gene expression represents one way to unravel how the gene works by identifying its pathways, biological function and connections (Silva, Li et al. 2005).

1.4.1 Gene Silencing

The knockout mouse model was one of the first approaches used to investigate gene function (Brunstein 2010). As 99% of genes between the mouse and the human are homologous, as revealed by the full sequencing of the mouse genome (Ahmad-Annuar, Tabrizi et al. 2003, Austin, Battey et al. 2004), this model provides an opportunity to study the possible consequences of blocking a particular gene from being expressed and observing the consequential effects on other genes, behaviour and physical characteristics. However, there are many disadvantages to this technique. First and foremost, it requires breeding mice injected with the modified sequence at least three times before a homozygous animal is obtained, making it time consuming and expensive (Rubinson, Dillon et al. 2003, Brunstein 2010). Furthermore, since the organism has to be genetically modified before birth, it is unsuitable for translation to human gene therapy (Rubinson, Dillon et al. 2003). It is inefficient at investigating the role of a gene in a very localized region, for example, a specific brain region (Hommel, Sears et al. 2003). In addition, because the gene modification starts early in development, there is a chance that some other genes will compensate for the deleted gene and the resulting animal will not be a clear representation of the gene deletion (Crawley 1999). Lastly, if the gene is

involved in vital functions or plays an essential part in development, it is highly possible that the knockout mouse will be incompatible with life (Blanchard, Iizuka et al. 1997, Sanford, Ormsby et al. 1997).

1.4.2 The RNA interference (RNAi) pathway and lentiviral mediated gene transfer

An alternative mechanism to silencing gene expression came after the discovery of the RNA interference (RNAi) pathway in 1998 (Tabara, Sarkissian et al. 1999, Hommel, Sears et al. 2003, Zamore and Haley 2005). This pathway occurs naturally in most eukaryotes and functions as surveillance machinery controlling gene expression in response to double-stranded RNA (dsRNA) (Tuschl, Zamore et al. 1999, Meister and Tuschl 2004, Thakker, Natt et al. 2004). Characterisation of the dsRNA has shown that it is formed by two strands of 21 to 23 nucleotides with symmetric overhangs of two or three nucleotides in the 3'. The size of dsRNA is restricted to 30 nucleotides; any sequences longer that that can provoke an adverse reaction leading to cell death (Thakker, Natt et al. 2004). Additional features of dsRNA include a phosphate group located at the beginning of 5' and a hydroxyl group at the start of 3' (Dykxhoorn, Novina et al. 2003).

Endogenously, the RNAi pathway is triggered either by precursory primary-microRNA (pri-microRNA) or a long dsRNA. The process is initiated with either RNase III enzymes Drosha and/or Dicer to further activate the RNA-induced

silencing complex (RISC) to accomplish gene silencing (Hammond 2005). Specifically referring to the pri-microRNAs, they are transcribed from the genome by RNA polymerase II (Figure 1.8). This sequence typically folds its 33 complementary nucleotides that end in a terminal loop (Carthew and Sontheimer 2009). Before leaving the nucleus, the pri-microRNAs encounter Drosha, presumably by recognizing the size of its loop (Hammond 2005). Subsequently, the RNase domains of Drosha form a pseudo-dimer that cleaves the pri-microRNA and produce a pre-microRNA (Hammond 2005, Carthew and Sontheimer 2009). After the cleaveage, the pre-microRNA is left with a PAZ domain consisting of 2-nucleotide overhanging in the 3' (required for Dicer recognition) and ready for Exportin-5 to transport it outside the nucleus for further processing. Once in the cytoplasm, pre-microRNA is ready to undergo additional modifications by Dicer (Hammond 2005).

In the case of the long dsRNAs, they are incorporated into the RNAi pathway as well as the pre-microRNAs when they are recognized and cleaved by Dicer (Paddison, Caudy et al. 2002, Caplen 2004, Hammond 2005, Carthew and Sontheimer 2009). Dicer, an RNase III enzyme, is characterised for having a dsRNA-binding domain (dsRBD), a PAZ domain and two tandem RNase III domains (Carthew and Sontheimer 2009). Structural, genetic and biochemical models agree that the way Dicer interacts with both premicro-RNA and dsRNA, is due to the overhang nucleotides in the 3'. These nucleotides bind to the PAZ domain, while the RNAase III domains engage in a pseudo-dimer, each domain hydrolysing one strand (Hammond 2005, Carthew and Sontheimer 2009). The resultant product has a new 2-nucleotide overhang on 3' and a monophosphate

group at 5', required for further silence processing (Carthew and Sontheimer 2009).

The small interfering RNAs (siRNAs) and the microRNA produced by the Dicer cleavage are integrated into a multi-component nuclease complex called RNA-induced silencing complex (RISC), which identifies the substrate mRNA for destruction (Paddison, Caudy et al. 2002, Tiscornia, Singer et al. 2003, Caplen 2004). It is important to note that when the double-stranded siRNA and microRNA enter RISC, the strands get separated and only one strand is required to guide the recognition of the mRNA (guide strand); the other strand gets dismissed (passenger strand) (Carthew and Sontheimer 2009).

Exogenously, this pathway can be modified by the introduction of synthetic silencing sequences (McIntyre and Fanning 2006). The study and consequently the understanding of the RNAi pathway brought the evolution of synthetic ways of silencing genes through it (Hannon and Rossi 2004). Scientists have been able to generate synthetic dsRNA such as siRNA, short hairpin RNA (shRNA) and microRNA-adapted short hairpin (shRNAmir) capable of being integrated into the RNAi pathway (Fewell and Schmitt 2006). The siRNA are small molecules consisting of 21 to 25 bp that are cleaved directly by Dicer enzymes. Their effect is dose-dependent and transient since they do not incorporate into the genome of the host cell (Rao, Vorhies et al. 2009). On the contrary, shRNA are encoded in a DNA plasmid that integrates into the genome of the cells and presumably is incorporated into the RNAi pathway as endogenous dsRNA (Wu, Wu et al. 2005, Rao, Vorhies et al. 2009). The sequence is modelled after a

premicroRNA (Figure 1.8) and is composed of around 70 nucleotides that form a sense, a loop and an antisense sequence (Paddison, Caudy et al. 2002, Fewell and Schmitt 2006). The shRNAmir, also known as second-generation shRNAs, includes the same structure as shRNA in addition to a microRNA-30 (miR30) sequence (Chang, Elledge et al. 2006). This extra sequence allows it to enter the pathway as a pri-microRNA, a precursor of premicroRNA (Figure 1.8) (Fewell and Schmitt 2006). This second generation of shRNA enters the pathway at an earlier stage, making it a more natural route capable of more effective silencing of the target gene (Chang, Elledge et al. 2006).

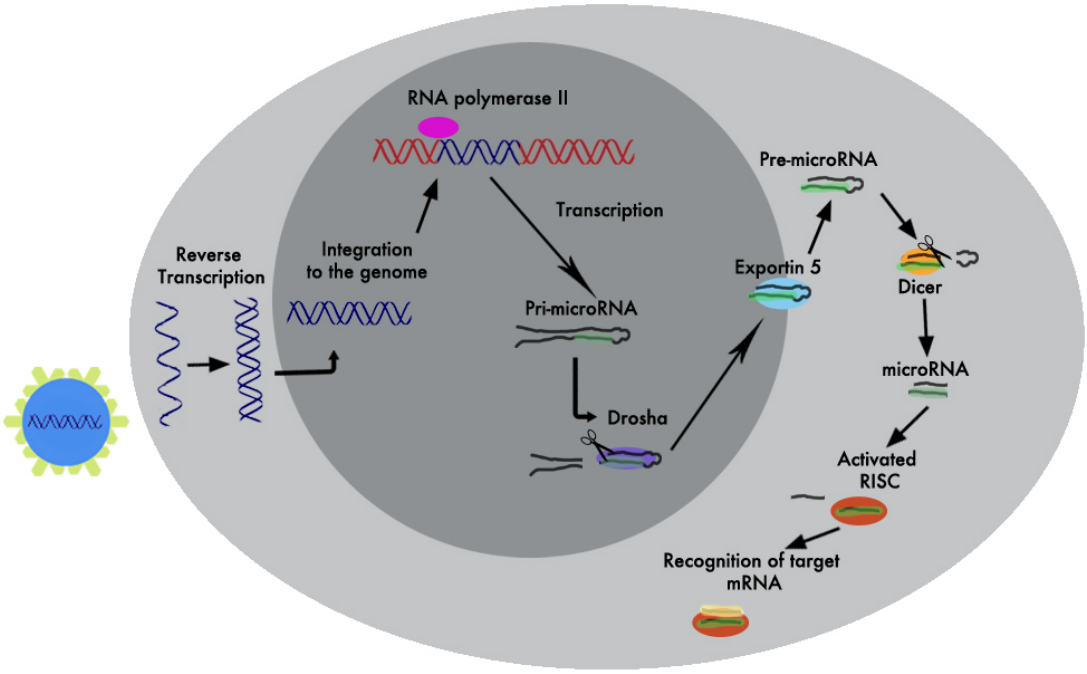

Figure 1.8 **The figure illustrates the RNAi pathway activated by lentiviral vectors containing shRNAmir to knockdown gene expression**.

The virus binds to the cell and delivers its engineered genome containing the shRNAmir specific to the target gene for knockdown. Once in the cytoplasm, it is reverse-transcribed and imported into the nucleus. Further integration into the cell genome takes place and pri-microRNAs are transcribed by the RNA polymerase II. Before leaving the nucleus, they are trimmed by Drosha complex to generate pre-microRNA. Pre-microRNA is then transported into the cytoplasm by exportin 5 proteins. The Dicer complex performs a second cutting, involving the removal of the loop and production of microRNA. The microRNA binds and activates RISC, which uses it as a guiding strand to identify target mRNAs. After recognition, the mRNAs are destroyed; hence their expression is reduced.

Previously, the synthetic sequences had been restricted to being delivered directly through microinjections into worms and flies, as these organisms possess an effective endogenous machinery capable of uptaking dsRNA (Fire, Xu et al. 1998, Misquitta and Paterson 1999, Tuschl, Zamore et al. 1999, Elbashir, Harborth et al. 2001). In the case of mammalian cell culture, their lack of this machinery requires a more sophisticated delivery method to effectively downregulate the target gene (Rozema and Lewis 2003). One such mechanism is the use of DNA vectors to deliver synthetic silencing sequences into the cells, with comes with the additional advantage of integration into the endogenous genome of the host cell (Shi 2003). This technique allows the transfected cell to synthesize siRNAs, shRNAs and shRNAmir in order to achieve a longer silencing effect (Brummelkamp, Bernards et al. 2002, Pebernard and Iggo 2004).

Even though the use of DNA vectors is useful to increase the gene knockdown effect, this is often insufficient, especially for *in-vivo* purposes (van den Haute, Eggermont et al. 2003). To circumvent this problem, the use of viral vectors such as lentiviruses (van den Haute, Eggermont et al. 2003, Weber, Bartsch et al. 2008), adenoviruses (Shen, Buck et al. 2003) and adeno-associated viruses (Tomar, Matta et al. 2003) came to be used and appear to be well suited to ensuring the stable long-term expression of the siRNA.

Although all of these viral vectors are capable of infecting dividing and non-dividing cells, there are certain characteristics, which made lentiviral vectors a better approach for this project. Firstly, although they reach their transgene

expression peak at around day 7, their effects can last for years, allowing for long-term experiments (Doherty, Schaack et al. 2011). Moreover, lentiviruses have a greater capacity to carry large fragments of foreign DNA such as transgenes (around 10 kb) in comparison to other viral vectors (Doherty, Schaack et al. 2011). Additionally, the integration of the transgene into the host genome allows for continuous expression: in case the transduced cell is still dividing, their progeny will carry on the transgene (Manjunath, Wu et al. 2009). Lastly, lentiviruses produce a minimal immune response from the cell after transduction (Howarth, Lee et al. 2010). All of these factors contribute to the extensive use of lentviruses to create research models *in-vitro* and *in-vivo*.

1.4.3 The peculiarities of pGPIZ vector

The *Myt1l* shRNAmir, which was cloned into a lentiviral vector in this project, belonged to the library developed by Dr Greg Hannon and Dr Steve Elledge (Thermo Scientific Open Biosystems pGIPZ shRNAmir). This gene silencing system distinguishes itself by its ability to highly activate the RNAi pathway with its unique short hairpin design. The silencing sequence is expressed as human microRNA-30 (miR30) primary transcripts. The full hairpin includes 22 nucleotides of dsRNA and the miR30 loop is composed of 19 nucleotides. The dsRNA sequence is made of two strands of 21 complementary nucleotides and one mismatch, located upstream towards the Drosha cut site. A Drosha processing site was added to the hairpin, which means greater numbers of pre-microRNA were released for further processing and increased efficiency for silencing genes (Figure 1.8). Also, the miR30 design enables the use of rule

based design such as destabilizing the 5' end of the antisense strand to incorporate strand specific microRNAs into the RISC machinery. All these peculiarities in the structure need to be maintained for proper incorporation into the RNAi pathway (Boudreau, Garwick-Coppens et al. 2011).

Furthermore, the success rate of the system also relies on the characteristics of the vector delivering the shRNAmir into the cell. pGIPZ lentiviral vector has proven to be a good candidate, as it is capable of infecting, with low toxicity rates, most types of cell, whether they are dividing or fully differentiated.

pGIPZ is a high copy plasmid composed of 11,774 base pairs containing different expression cassettes conferring its properties. For plasmid preparation, the pUC origin replication site in the plasmid allows high copy replication and maintenance when cloned in *Escherichia coli*. Additionally, the ampicillin-resistance element is useful for selecting only the bacteria that was transformed. The presence of the reverse response element allows the plasmid to be reverse transcribed inside the cytoplasm. Once it is integrated into the host genome, the RNA Polymerase II promoter CMV-EI (cytomegalovirus-immediate early promoter) is responsible for high transgene expression levels. The puromycin-resistance gene, encoded in the pGIPZ vector, permits further selection of infected cells. The visualization of transduced cells is granted by the expression of the turbo-Green Florescent Protein (GFP) site (Figure 1.9).

pGIPZ plasmid requires special packaging plasmids (pTLA1-Pak, pTALA1-Enz,

pTLA1-Rev and pTLA1-TOFF) coding for genes essential for lentivirus production. For safety reasons, these lentiviruses are composed of less than 30% of the human immunodeficiency virus type 1 (HIV-1) and they are replication-incompetent. This means that all the necessary genes and accessory genes necessary to produce viral progeny have been removed. However, all the cis-acting sequences essential for proper packaging, reverse transcription and integration are present but this lentivirus lacks HIV-1 pNL4-3 provirus (all information about pGIPZ was obtained from Thermo Scientific Open Biosystems).

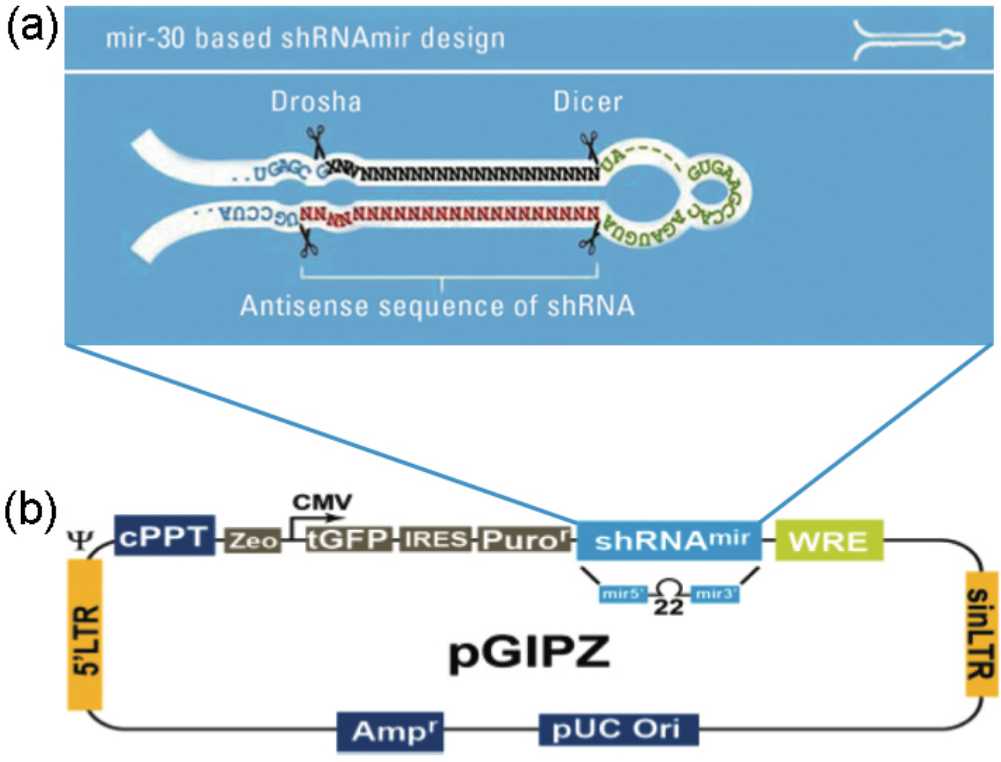

Figure 1.9 **The figure shows a graphical representation of pGIPZ vector (b) and an example of the shRNAmir cloned inside of it (a).**

The pGIPZ vector (b) is composed of a variety of cassette enclosing genes important for plasmid replication (pUC Ori); bacterial selection [ampicillin (Amp^r) and zeocin (Zeo) resistance]; transgene expression (CMV); visualization (tGFP) and selection of cell expressing shRNAmir ($IRES.Puro^r$); and the shRNAmir. The shRNAmir (a) is composed of 22 nucleotides (red) that have a complementary strand (black) forming a dsRNA and a miR30 loop (green). It was designed to have a Drosha and a Dice processing site to adequately integrate into the RNAi pathway. All images were obtained from the Thermo Scientific Open Biosystems protocol.

1.5 Aims of this project

As described above, early stages of neural development are characterized by neurogenesis, migration, differentiation of neurons into synaptically active phenotypes and pruning by programmed cell death (Andersen 2003, Toro and Deakin 2007). During adolescence, a new wave of neuronal rearrangement takes place, eliminating synapses and pruning more neurons (Andersen 2003). During adulthood, the brain can still modify its organization and function; this process is normally referred to as plasticity. These physical changes are normally associated with behavioural changes like learning, memory, maturation, recovery or addiction (Kolb, Gibb et al. 2003). In summary, brain development is a never-ending process and it is important to understand the role of genes throughout the different stages.

The candidate gene *MYT1L* has not been fully studied either in early or late development. The literature available strongly suggests a role in cell differentiation, maturation and possible synapse development. Given the tendency of *MYT1L* to influence neurons and its restricted expression in the brain, we hypothesise that disruption of this gene will have detrimental consequences on gene expression that ultimately will affect the behavioural outcome, in particular in relation to memory, learning and possibly anxiety. To address this hypothesis and further unravel the function of *MYT1L* in gene expression and behaviour, we decided to use shRNAmir to reduce its expression in a number of models. To delineate the scope of this project, we have subdivided the objectives as follows:

1. Chapter 2: *In-vitro* screening of possible candidate shRNAmir sequences designed to knockdown *Myt1l* in the rat, mouse and human.

2. Chapter 3: Infection of human neural stem cell line (SPC04) with *MYT1L* shRNAmir lentiviruses to identify possible downstream targets of *MYT1L* during cell differentiation.

3. Chapter 4: Microinjection of *Myt1l* shRNA lentiviruses into the dorsal hippocampus of the adult mouse brain to evaluate changes in behaviour such as anxiety, learning, memory and social interactions.

Chapter 2 : *In-vitro* screening of shRNA sequences targeting *Myt1l*

2.1 Introduction

As discussed in Chapter one, the increasing research on *Myt1l* has started to give a better perspective on the possible function of this gene. From the cellular point of view, it is known that this neuron-specific transcription factor is required along with *Ascl1*, *Brn2* and *NeuroD1* to reverse cell lineage and induce a functional neuronal phenotype (Vierbuchen, Ostermeier et al. 2010, Ambasudhan, Talantova et al. 2011, Pfisterer, Kirkeby et al. 2011, Yoo, Sun et al. 2011, Adler, Grigsby et al. 2012). Combining this finding with the observation that there is a high expression of *Myt1l* during development (Kim, Armstrong et al. 1997), it is possible to hypothesise that it has a role in cell differentiation during brain development. From the genetic perspective, the detection of variations in the genome sequence and the differences in gene expression of a large number of genes in a single experiment have helped scientists to infer candidate genes for most psychiatric disorders (Pongrac, Middleton et al. 2002, Stankiewicz and Lupski 2010). *MYT1L* is not an exception and in recent years it has been linked to disorders such as schizophrenia (Lodge and Grace 2007), mental retardation (Huttenlocher 1991), autism (Raymond, Bauman et al. 1995) and major depression disorder (Belmaker and Agam 2008). The specific role played by *MYT1L* in each one of those diseases is not clear yet. Currently there is no information regarding the phenotypic outcome of cells or organisms when only this gene is disrupted or its expression is compromised.

2.1.1 Gene silencing and validation in a cell model

One method used to investigate the effects of a gene in an organism is to either increase or decrease its expression (Vallier, Rugg-Gunn et al. 2004). The latter approach, where gene expression is inhibited, will be used in this model. This technique has proven to be especially effective since the discovery of the RNAi pathway as an endogenous silencing machinery in the *Caenorhabditis elegans* (Fire, Xu et al. 1998); it has revolutionized the development of techniques to investigate gene function (Hannon and Rossi 2004). This pathway allows the post-transcriptional downregulation of genes by recognizing dsRNA and using it as a template to identify mRNA of target genes in order to eliminate them; it essentially works as genetic surveillance machinery (Tabara, Sarkissian et al. 1999).

The biochemical understanding of this singular pathway helped to design siRNA to target specific sequences that could be incorporated into the RNAi pathway (Fewell and Schmitt 2006). Tuschl and his collaborators (Tuschl, Zamore et al. 1999) were able to transfect mammalian cells to further increase the scope of its applications; however, it was not until shRNAs could be cloned into vectors that mimicked the endogenous triggers of the RNAi pathway that this technique could be expanded to most kinds of cells and tissues present in an organism with more stable and longer expression (Hannon and Rossi 2004, Chang, Elledge et al. 2006). Following the evolution of such techniques, research groups such as the group lead by Hannon and Elledge (Paddison, Silva et al. 2004) were able to create large libraries of putative shRNAmir sequences which

target most genes in the human, mouse and rat genomes, and which are capable of obtaining a more robust reduction of gene expression (Chang, Elledge et al. 2006). This effort has helped researchers to better understand the role of genes.

It has been demonstrated that the knockdown efficiency of siRNA sequences *in-vitro* and *in-vivo* is highly dependent on their design, which is based on algorithms developed from empirical testing to predict efficient sequences (Reynolds, Leake et al. 2004, Pei and Tuschl 2006, de Fougerolles, Vornlocher et al. 2007). However, it is worth noting that even if there are sophisticated software programmes engineered to reduce the expression of the target gene available, they do not always succeed in providing sequences with good knockdown efficiency and thus it is important to test more than one sequence *in-vitro* (Rozema and Lewis 2003, Tiscornia, Singer et al. 2006). Even the commercially available shRNAmir libraries lack *in-vitro* validation for most of the clones since that is out of the scope of those companies (Chang, Elledge et al. 2006).

Moreover, not only is the type and design of the silencing sequence important in achieving high knockdown efficiency, but also the backbone vector used for their cloning. Lentiviral vectors have been shown to be a suitable choice because of their ability to infect non-dividing and fully differentiated cells, as well as dividing cells like stem cells (Rubinson, Dillon et al. 2003, Weber, Bartsch et al. 2008). In addition, it has been reported that the shRNA or transgene they encode is expressed for long periods of time, making it useful for long-term

experiments or clinical studies (Blomer, Naldini et al. 1997, Kafri, Blomer et al. 1997).

The required *in-vitro* validation for these sequences relies on suitable cell models to test their efficiency. When searching for one, the intrinsic characteristics of the target gene should be considered. In the case of *Myt1l*, since it is a neuron-specific transcription factor, it was appropriate to validate the knockdown effect of the sequences on neuron-related cells such as PC-12 and Neuro-2a (N2A), which have been widely used as neuronal models (Calderón, Bonnefont et al. 1999).

2.1.2 Aims

The development of this research project depended upon finding an oligonucleotide sequence whose expression resulted in efficient knockdown of *Myt1l*. This chapter had the purpose of testing the efficiency of three lentiviral vectors containing shRNAmir sequences designed to reduce the expression of human, rat and mouse *Myt1l in-vitro* and *in-vivo*.

2.2 Methods

2.2.1 Experimental setup

The *Myt1l* expression in the cell lines PC-12 and N2A was assessed in a single biological replication consisting of triplicates. Upon confirmation, PC-12 and Human Embryonic Kidney 293 T cells (HEK293T) were transduced in duplicates with each one of the lentiviral vectors containing one of the three shRNAmir sequences or a non-silencing shRNAmir for a control. HEK 293T cells do not express *Myt1l*, but they were used as a positive control for infection because they are easily transduced (Torres, García et al. 2011). This experiment consisted of three biological replications and the data were analysed together. The shRNAmir that caused the most significant decrease of *Myt1l* expression was used to transduce N2A cells. This experiment followed the same design as described for PC-12 (three biological replications consisting of two technical replications).

2.2.2 Mammalian cell culture

All cell lines were maintained at 37^{o} C in a humidified incubator at 5% CO_2. The media for all flasks and plates was changed to fresh complete media every second day, unless stated otherwise. The Fetal Bovine Serum (FBS) and horse serum were heat inactivated by incubation in a water bath at 56^{o} C for 30 minutes.

2.2.2.1 Culture N2A and HEK293T cells

N2A is a mouse cell line derived from neuroblastoma cells capable of

differentiating into neurons within days (Augusti-Tocco and Sato 1969, Tremblay, Sikorska et al. 2010). This cell line was bought from American Type Cell Collection (ATCC; USA).

HEK 293T cells, derived from human embryonic kidney cells, were modified to express the SV-40 large T antigen, which allows very high levels of plasmid replication (Wurm and Bernard 1999, Pham, Kamen et al. 2006). This cell line was purchased from ATCC (USA).

1) Cell media: The complete media was composed of high glucose (4500 mg/L) Dulbecco's Modified Eagle Medium (DMEM; Sigma, UK) supplemented with 10% inactivated FBS (Sigma, non-USA origin) and 1% penicillin/streptomycin (P/S; Sigma, UK).

2) Cell revival: The cells were revived from liquid nitrogen storage by immersing the cryogenic tube containing them in a water bath at 37^{o} C for 2 minutes. The cells were transferred into a tube containing 4 ml of complete media and centrifuged for 5 minutes at 1500 revolutions per minute (RMP). The supernatant was discarded and the cell pellets were resuspended in 10 ml of complete media before plating them all in a T75 flask.

3) Passaging: N2A and HEK 293T were expanded in Falcon T75 culture flasks and were passaged when they reached 80-90% confluency. For this, the

complete media was removed from the flask; the cells were washed using sterile Phosphate Buffered Saline (PBS) and then trypsinized using Trypsin-EDTA 0.05% solution (Gibco, UK) for 5 minutes at 37^{o} C. This last reaction was inactivated by the addition of complete media before the cells were collected and centrifuged for 5 minutes at 1500 rpm. The supernatant was carefully discarded, the cell pellets resuspended in fresh complete media and the cells plated into a T75 flask at a 1:3 ratio for further cell expansion. For RNA extraction, cells were seeded at a density of 1x10^{6} cells per well in 6-well plates and harvested two days later as detailed below (2.2.5).

4) Cell freezing: N2A and HEK 293T were frozen at a density of 3x10^{6} cells per vial in complete media supplemented with 10% Dimethyl Sulfoxide (DMSO; Sigma, UK). The vials were frozen at 1^{o}C per minute using a Mr Frosty freezing container (Nalgene®) for 24 hours at -80^{o}C and then transferred to liquid nitrogen storage.

2.2.2.2 Culture PC-12 cells:

PC-12 is a rat cell line derived from the rat adrenal phaeochromocytoma with the remarkable characteristic of responding to the nerve growth factors (NGF) and differentiating into neuron-like cells (Greene and Tischler 1976, Zhou, Xu et al. 2006). This cell line was bought from American Type Cell Collection (ATCC; USA).

1) Cell media: PC-12 cells were expanded in complete media composed of high glucose (4500mg/L) DMEM without pyruvate (Gibco, UK) supplemented with 10% inactivated horse serum (Gibco, UK), 5% inactivated FBS and 1% P/S.

2) Coating of flasks: T75 Falcon flasks were freshly coated with 2.5 ul/cm^2 rat-tail tendon collagen diluted in 0.2% acetic acid (2 mg/ml; Roche, USA) and left to air dry for two hours at room temperature before plating the cells.

3) Cell revival: The cells were revived as described for N2A and HEK293T cells (above).

4) Passaging and seeding: The cells were passaged when they reached 80-90% confluency. First, the cells were mechanically detached using a sterile cell scrapper and then the media-containing cells centrifuged for 5 minutes at 1500 RPM. The supernatant was discarded, the cells resuspended in complete media and plated at a 1:3 ratio into a T75 flask for further expansion. For RNA extraction, cells were seeded at a density of 1.5 x10^6 cells per well in 6-well plates and harvested two days later as detailed below (2.2.5).

5) Cell freezing: PC-12 were frozen at a density of 4x10^6 cells per vial in complete media supplemented with 10% Dimethyl Sulfoxide (DMSO; Sigma, UK). The vials were frozen as described for N2A and HEK293T cells (above).

2.2.2.3 Cell counting and seeding

Cells were counted and their viability was assessed before plating them for RNA extraction, transfection (non-viral introduction of nucleic acids into cells to produce virus) and transduction (viral introduction of nucleic acids into cells). Cell number and viability were analysed using NucleoCounter® NC-100 (Chemometec, Denmark). This device is an integrated fluorescence microscope capable of detecting signals from the fluorescent dye propidium iodine (PI). This dye is present in the interior of the NucleoCassette™ (Chemometec, Denmark) and binds to the DNA of the lysated cells.

For total cell number, a sample of at least 40 ul of resuspended cells was mixed with equal amounts of Reagent A (Chemometec, Denmark) and Reagent B (Chemometec, Denmark). The mixture was loaded into a NucleoCassette™ and placed into the NucleoCounter® to obtain the cell concentration. This value was multiplied by the dilution factor to obtain the total number of cells. The principle behind this device is that Reagent A disrupts the plasma membrane and Reagent B stabilizes the reaction. This allows the PI dye to interact with the DNA of all the cells.

For cell viability, at least 40 ul of the resuspended cells was mixed with equal amounts of PBS and Reagent B. The mixture was then loaded into a NucleoCassette™ (Chemometec, Denmark) and placed into the NucleoCounter® to obtain the cell concentration. This value was multiplied by

the dilution factor to obtain the total number of cells that were non-viable after resuspension. Since no Reagent A was added to the mixture, this reaction only quantified the cells that were already disrupted. Viability was calculated as follows:

$$V = \frac{C_t \times M_t - C_{nv} \times M_{nv}}{C_t \times M_t} \times 100$$

V : Viability
C : Cell concentration
M : Multiplication factor
t : Total cell count
nv : Non-viable cell count

2.2.3 Lentiviral vectors

Three different pGIPZ lentiviral vectors containing shRNAmir and which targeted *Myt1l* were selected and bought from the Open Biosystem shRNAmir library (Thermofisher Scientific Open Biosystems, UK). Additionally, a non-silencing shRNAmir was bought as a negative control. These sequences were developed in collaboration with Hannon and Elledge (Paddison, Silva et al. 2004) and cloned by them into a pGIPZ vector (a full description of the vector is provided in Chapter 1). The shRNAmir sequences were designed using a proprietary algorithm of Rosetta Inpharmatics (Chang, Elledge et al. 2006). The detailed sequences of each used for this chapter can be found in Table 2.1.

In-silico analysis blasting of all the sequences was performed to confirm their selectivity for *Myt1l* and the species affected. All blasts were done using the information provided on the National Centre for Biotechnology Information (NCBI) website (http://blast.ncbi.nlm.nih.gov/Blast.cgi).

Table 2.1 **shRNAmir sequences for the possible candidates to knockdown *Myt1l* and a non-silencing negative control**.

Oligo ID	Target	Homology Hs (Homo Sapiens) Mm (Mus musculus) Rn (Rattus norvegicus)	Sequence mir-30 context sense loop antisense
V2LMM_32678	*Myt1l*	Hs Mm Rn	TGCTGTTGACAGTGAGCG CCGTGACTACTTTGACGGAAAT TAGTGAAGCCACAGATGTA ATTTCCGTCAAAGTAGTCACGT TGCCTACTGCCTCGGA
V3LMM_428227	*Myt1l*	Mm Rn	TGCTGTTGACAGTGAGCG CCAAGGACATGGTGTTGTGCTA TAGTGAAGCCACAGATGTA TAGCACAACACCATGTCCTTGT TGCCTACTGCCTCGGA
V3LMM_90785	*Myt1l*	Hs Mm Rn	TGCTGTTGACAGTGAGCG CCCTCAGTATGGCTACAGAAAC TAGTGAAGCCACAGATGTA GTTTCTGTAGCCATACTGAGGA TGCCTACTGCCTCGGA
RHS4346	Non-silencing		TGCTGTTGACAGTGAGCG ATCTCGCTTGGGCGAGAGTAAG TAGTGAAGCCACAGATGTA CTTACTCTCGCCCAAGCGAGAG TGCCTACTGCCTCGGA

2.2.3.1 Generation of plasmid vectors

2.2.3.1.1 Transformation of bacteria

The manufacturer provided the pGIPZ lentiviral vectors as bacteria in glycerol stocks. After thawing and mixing by gentle pipetting, these stocks were used to transform *Escherichia coli* MAX efficiency Stbl2 competent cells (Invitrogen, UK) as follows: 50 ul of bacteria 50 ul was incubated with 5 ul of each construct for

30 minutes on ice, then heat-shocked for 25 seconds at 42^{o} C and incubated for an additional 2 minutes on ice. To maximize transformation efficiency, 0.9 ml of S.O.C. medium (Invitrogen, UK) was added to each transformation and the bacteria were incubated further at 30^{o} C (the ideal temperature to prevent DNA recombination) for 1.5 hours, while being shaken at 350 RPM. After incubation was complete, the transformed bacteria was gently mixed and evenly spread on Luria-Bertani (LB) broth (Lennox; Invitrogen, UK) agar plates containing 100 ug/ml Ampicillin (Sigma, UK). The plates were incubated overnight at 30^{o} C.

2.2.3.1.2 Preparation of DNA plasmids

Single bacteria colonies that grew on the plate were chosen and allowed to proliferate in a pre-culture of 5 ml of LB Broth media (Invitrogen, UK) containing 100 ug/ml Ampicillin at 30^{o} C overnight and used for small- or large-scale plasmid production as follows:

For small-scale plasmid production, the tubes containing the 5 ml of pre-culture bacteria were centrifuged at 1500 RPM for 5 minutes at room temperature. Only approximately 4 ml of the supernatant was carefully discarded, leaving 1 ml to resuspend the bacteria in before being transferred to a microcentrifuge tube for further centrifugation at 11,000 x g for 1 minute. The remaining supernatant was carefully removed and the bacterial pellet was used for DNA extraction using the NucleoSpin® Plasmid kit (Marcherey-Nagel, UK), as per the manufacturer's instructions. Briefly, the bacterial pellet was resuspended in 250 ul of RNase A-

containing buffer A1 (100 ug/ml). Following the addition of 250 ul of lysis buffer A2, the suspension was mixed by inversion (6 to 8 times), incubated at room temperature for 5 minutes and the lysis neutralized by the addition of 300 ul of buffer A3. Bacterial debris were pelleted by centrifugation at 11,000 x g for 5 minutes and the plasmid-containing supernatant was carefully removed and transferred into a NucleoSpin® Plasmid column. Column-bound plasmids were washed twice with 80% ethanol (in buffer A4) by centrifugation for 1 minute at 11,000 x g and plasmid DNAs eluted with 40 ul of buffer AE [5 mM TrisHCl (pH 8.5)].

For large-scale plasmid preparation, 1 ml of the pre-culture bacteria was added to 400 ml of LB Broth media (supplemented with 100 ug/ml Ampicillin) and incubated at 30^{o} C overnight. The bacteria were then collected by centrifugation at room temperature for 20 minutes at 1500 RPM. Supernatants were discarded and the bacterial pellets used for plasmid maxi-prep using the Qiagen Plasmid Maxi Kit (Qiagen, UK), as per the manufacturer's instructions. Briefly, bacteria were resuspended in 10 ml buffer P1 [50 mM TrisHCl (pH 8.0) and 10 mM EDTA] supplemented with RNase A (100 ug/ml) and lysed for 5 minutes at room-temperature by addition of 10 ml of buffer P2 (200 mM NaOH and 1% SDS). Lysates were neutralised by the addition of 5 ml of pre-chilled buffer P3 [3.0 M potassium acetate (pH 5.5)]; the neutralised lysates were cleared by filtration into a QIAfilter cartridge and further incubated on ice for 30 minutes in the presence of 2.5 ml of buffer ER. The filtered lysates were then applied into an equilibrated QIAGEN-tip 500 column and allowed to go through by gravity flow and washed twice with 30 ml of buffer QC [1 M NaCl, 50 mM MOPS (pH 7.0) and 15% isopropanol]. The plasmid DNAs were eluted in 15 ml of buffer

QN [1.6 M NaCl, 50 mM MOPS (pH 7.0) and 15% isopropanol], precipitated by the addition of 10.5 ml of isopropanol (Sigma, USA) followed by centrifugation at 30,000 x g for 30 minutes at 4^{o} C. After washing with 5 ml endotoxin-free 70% ethanol, the mixture underwent centrifugation for 10 minutes at 30,000 x g at 4^{o} C; the plasmid DNA pellets were then air-dried for 5 minutes and resuspended in 150 ul of TE buffer [10 mM Tris-HCl (pH 8.0) and 1 mM EDTA].

DNA plasmid concentration was measured by UV spectrophotometry using a nanospectrophotometer (NanoDrop 1000, Thermo Scientific) at a wavelength of 230 nm. By measuring the ratio of absorbance at 260nm and 280 nm (260/280), the purity of the plasmid was assessed. A ratio above 1.8 was accepted as “pure” for DNA. If the ratio was lower, it could indicate contamination of protein, phenol or other contaminant. The DNA plasmids were stored at -20^{o} C till required.

2.2.3.1.3 DNA restriction digestion

In order to verify the correct size of the vector, the plasmids were digested with EcoR1 (20,000 units/ml; New England Biolabs, UK). Each reaction included 1 ug of plasmid, 1 ul of 10 X NEBuffer EcoRI (New England Biolabs, UK), 10 units of EcoRI enzyme, and dH_2O up to a final volume of 10 ul. The reaction was incubated at 37^{o} C for 1 hour.

The DNA plasmid digestions were separated by electrophoresis on a 1.3%

agarose gel (Sigma, UK) made up with 1X TBE buffer (0.0089 M Tris, 0.089 M Borate, 0.002 M EDTA; Merck, Germany) and supplemented with 1% Ethidium Bromide (Electron, UK). The digestion samples were mixed with 2 ul of 6X gel-loading buffer (Thermo Scientific, UK) and loaded into the wells of the gel. Additionally, one well was used for loading the 1 kilobases DNA ladder (250-10,000 bp Sigma, UK). Electrophoresis was performed using 1X TBE buffer at 120 V for 1 hour. The DNA bands obtained in the gel were visualized using ultraviolet light.

In addition, the DNA plasmids were sent for DNA sequencing (Source Bioscience, UK) to check the correct shRNAmir sequence and verify no recombination of the sequence occurred while it was being amplified inside the bacteria.

2.2.3.1.4 Virus production

Replication incompetent lentiviruses containing *Myt1l* or non-silencing shRNAmir were created using the Trans-lentiviral GIPZ Packaging System (Thermofisher Scientific Open Biosystems, UK). To ensure high titre of lentiviruses, the HEK 293T cells were used for transfection till they reached a rapid replication state. This means that after the cells reached 70% confluency, they were passaged at a 1:2 ratio for at least two consecutive days, till the cells were able to reach 70% confluency the next day.

The day before transfection, HEK 293T cells were seeded at a density of 5.5 $x10^6$ into 10 cm dishes in 14 ml of regular media. The next day, the following mixture was prepared in a 15 ml-sterile tube for each plate: 42 ul lentiviral vector plasmid (containing either *Myt1l* or non-silencing shRNAmir), 30 ul of Trans-Lentiviral Packaging Mix (Thermofisher Scientific Open Biosystems, UK) and sterile dH_2O (Gibco, UK) up to a final volume of 945 ul. Then, 105 ul of calcium chloride (Thermofisher Scientific Open Biosystems, UK) was applied to each tube, followed by drop-wise addition of 1050 ul of 2X HBSS (Thermofisher Scientific Open Biosystems, UK) while the tube was being mixed by air bubbling using a serological pipette. The solution was left for incubation for 3 minutes at room temperature. The resulting 2.1 ml solution was then added drop-wise to each 10 cm plate and left in the incubator (37^o C and 5% CO_2) for the next 16 hours. The plates were microscopically examined for the presence of GFP (fluorescent reporter), an indicator of transfection efficiency. The media was changed to 14 ml of reduced serum media composed of high glucose DMEM, 5% inactivated FBS, 1% P/S and 2 mM L-glutamine (Sigma, UK). The plates were incubated for 48 hours (37^o C and 5% CO_2). Afterwards, the supernatant was collected and centrifuged at 1600 x g for 10 minutes at 4^o C to pellet the cell debris. The lentiviral supernatant was filtered before being aliquoted and stored at -80^o C till required.

2.2.4 Cell transduction

One day before transduction, 5 x 10^5 PC-12 cells were plated in each well of a 6-well plate and incubated overnight. The following day, the media was

removed and changed to 1 ml of serum free and antibiotic free high glucose DMEM media and 2 ml of lentiviral supernatant. Each received an additional 3 ul of 8 mg/ml polybrene (Sigma, USA) to increase transduction efficiency. The plates were centrifuged for 90 minutes at 2500 RPM and put at 37^{o} C in 5% CO_2 incubator for 2.5 hours. The media was then changed to 3 ml of complete media and incubation continued for a further 72 hours. After incubation, the media was removed and 3 ml of complete media supplemented with 5 ug/ml of puromycin (MP Biomedicals, France) was added to each well to selectively kill the non-transduced cells. After 48 hours, only transduced cells were observed and the media was changed to complete media. It has been reported that the peak in transgene expression for lentiviral vectors is around seven days (Doherty, Schaack et al. 2011), so the cells were left incubating for expansion for two more days.

HEK 293T cells and N2A cells followed the same transduction protocol. However, the puromycin concentration (5 ug/ml) was used only for cell selection of N2A as HEK293T cells were only required as a control for infection and for that reason not selected. In addition, the N2A cells required a further step after the 72-hour incubation following transduction owing to their high division rate. The cells therefore were trypsinized and plated into 10 cm dishes. The following day, the N2A cells underwent puromycin selection for two days and the cells were left for expansion for only one additional day. Images of both transduced cell lines were taken using Leica DMIL supplied by a Leica camera DFC420C (x10 objective).

2.2.5 RNA extraction

Before harvesting the cells for RNA extraction, all the equipment and surfaces were sprayed with RNAseZAP^{TM} (Sigma, UK) to eliminate RNAse and avoid RNA degradation. The media was removed from the wells or dishes and the cells were washed twice with sterile PBS. 350 ul of RLT buffer (QIAGEN, UK) supplemented with 1% β-mercaptoethanol (Sigma, UK) was added to each well or 600 ul to each dish. The cells were mechanically removed using a sterile cell scrapper. The lysate was placed in 2 ml collection tubes (QIAGEN, UK) and stored at -80^{o} C until RNA extraction took place.

The lysate was homogenized using a QIAshredder spin column (QIAGEN, UK) placed over a 2 ml collection tube and centrifuged at full-speed for 2 minutes. The RNA extraction was performed using the RNeasy® mini kit (QIAGEN, UK). One volume of 70% nuclease-free ethanol was added to each homogenized lysate and mixed well by pipetting. The mixture was then transferred into an RNeasy spin column over a 2 ml collection tube and centrifuged for 15 seconds at 21.1 x g. The flow was discarded and 350 ul of RW1 buffer was applied to each column before centrifuging it for 15 seconds at 21.1 x g. The flow was discarded and 80 ul at 1:8 ratio of DNase treatment mixed (DNase I and Buffer RDD; QIAGEN, UK) was applied to each column. The reaction was left to incubate for 15 minutes at room temperature before 350 ul of RW1 buffer was added. The columns were centrifuged again for 15 seconds at 21.1 x g. The flow was discarded and the column washed with 500 ul of RPE buffer followed by centrifugation for 15 seconds at 21.1 x g, discarding the flow at the end. A

second wash with 500 ul of the same buffer was applied and the column was centrifuged for 2 minutes at 21.1 x g. After the second wash, the column was centrifuged for an additional minute. The column was transferred into a clean RNase-free collection tube. RNA was eluted by adding 40 ul of RNase-free water directly to the membrane of the column and centrifuging it for 1 minute at 21.1 x g. RNA concentration was measured by UV spectrophotometry using a nanospectrophotometer (NanoDrop 1000; Thermo Scientific) at 230 nm wavelengths. By measuring the absorbance ratio (260/280) the purity of the plasmid was assessed. A ratio above 2 was accepted as “pure” for RNA. If the ratio was lower, it could indicate contamination of protein, phenol or other contaminant. The RNA was stored at -80^{o}C till required.

2.2.6 Reverse transcription

Reverse transcription was performed using the Superscript^{TM} III First-Strand Synthesis System for RT-PCR (Invitrogen, UK). Two micrograms of RNA were mixed with 1ul of 50 uM Oligo$(dT)_{20}$, 1 ul of 10 mM dNTP mix and RNAse-free water in a final volume of 10 ul and denatured by incubation at 65^{o} C for 5 minutes followed by incubation on ice for at least 1 minute. 10 microliters of cDNA synthesis mix composed of 2 ul of 10X RT buffer, 4 ul of 25 mM $MgCL_2$, 2 ul of 0.1 DTT, 1 ul of RNase OUT^{TM} (40 U/ul) and 1 ul of Superscript^{TM} III RT (200 U/ul) was added to the previous solution and the resulting 20-ul solution incubated at 50^{o} C for 50 minutes, followed by incubation at 85^{o} C for 5 minutes to deactivate the enzymes. 1 ul of RNase H (2 U/ul) was added and the solution was further incubated at 37^{o} C for 20 minutes to remove residual RNA. The

cDNA was then diluted with 179 ul of RNase free water to have an estimated final concentration of 10 ug/ul and stored at -20^{o} C till required.

2.2.7 Quantitative Polymerase Chain Reaction (qPCR)

qPCR amplification was performed in a 20 ul solution containing 4 ul of cDNA (10ug/ul), 10 ul of 2X *Power* SYBR® Green PCR master mix (Applied Biosystems, UK), 0.14 uM forward primer (Table 2.2), 0.14 uM reverse primer (Table 2.2) and 5.72 ul of RNase free water. All the amplifications were carried out in triplicate using a ABI Prism® 7900 HT Sequence detection system (Applied Biosystems) under the following thermal cycle: 95^{o} C for 15 minutes (initial denaturation); 40 cycles of 95^{o}C for 30 seconds and 60^{o}C for 30 seconds (amplification); finishing with 50^{o} C for 10 seconds and 95^{o} C for 10 seconds (dissociation stage). The ABI Prism® SDS 2.1 software (Applied Biosystems) was used to analyse the specificity and relative quantification of the amplicons. The dissociation curve generated by the software was used to determine the specificity of the PCR products. The relative quantification curve of the amplicon was calculated using the cycle threshold (Ct), which represents the number of cycles required by the sample to cross a fixed fluorescence threshold. The fewer cycles required to cross the threshold, the higher the expression of the gene in the sample. In the case of the first experiment quantifying the endogenous expression of *Myt1l*, this curve was used to assess the expression of this gene in both cell lines when compared to a positive control (housekeeping gene). An additional cell line was used as a negative control (cDNA from undifferentiated B35 cells, kindly provided by Dr Alinda Fernandes);

its amplification curve was also compared to the housekeeping gene.

For the experiments where cells were transduced with lentiviral vectors, the mean of the triplicate Ct values were normalized against the mean of the triplicates of the housekeeping gene, *β-Actin,* to produce ΔCT ($\Delta CT = Ct_{Myt1l} - Ct_{\beta\text{-}Actin}$). The difference in expression of *Myt1l* mRNA was compared in the two conditions--infected with non-silencing shRNAmir and infected with *Myt1l* shRNAmir--to calculate ΔΔCt ($\Delta\Delta Ct = \Delta Ct_{Myt1l\ shRNAmir} - \Delta Ct_{non\text{-}silencing\ shRNAmir}$).

Table 2.2 **Sequence of the qPCR primers for rodent *Myt1l* and β-Actin**

	Forward	**Reverse**
Rodent *Myt1l*	GAGCCAGTCCCTGATCCAC	CCGTCAAAGTAGTCACGTAAGC
β-Actin	GCTCGTCGTCGACAACGGCTC	CAAACATGATCTGGGTCATCTTCTC

2.2.8 Statistics

To assess the effect of the three different knockdown sequences in the expression of *Myt1l* in PC-12 cells, the ΔΔCt values were firstly tested for normality using the Shapiro-Wilk test. After corroborating that the data was normally distributed, the ΔΔCt values were analysed using one-way ANOVA with factor treatment followed by Turkey's LSD post-hoc. An independent sample t-test was carried out to compare the ΔΔCt values of *Myt1l* in N2A cells infected with *Myt1l* shRNAmir against non-silencing shRNAmir. All statistical analyses were done using IBM SPSS Statistics 20 (IBM Corp., USA). A p-value

<0.05 was considered statistically significant. The data was expressed as mean ± Standard Error of the Mean (S.E.M.). The graphs were presented as the relative change in expression. This was obtained by elevating 2 to the negative power of ΔΔCt (relative fold expression=$2^{-\Delta\Delta Ct}$) (Livak and Schmittgen 2001). The error bars were adjusted to reflect the logarithmic scale. They were calculated as follow, the upper and lower limits of the ΔΔCt (ΔΔCt minus or plus the standard error of Ct values) were converted to relative fold expression. Then, these limits were subtracted from the mean fold relative expression to get the size of the error bars.

2.3 Results

In order to accomplish this, two cell lines were tested to determine their endogenous expression of this gene. Once *Myt1l* expression was corroborated in those cell models, the silencing sequences were tested. The sequence with the highest efficacy as well as lowest toxicity would provide a useful tool to investigate the possible roles of *Myt1l*.

2.3.1 *In-silico* confirmation of selectivity of shRNAmir sequences for *Myt1l*

The shRNAmir sequences were blasted to confirm their specificity to recognize *Myt1l*. As expected, the sequences numbered 32678 [Figure 2.1 (a)] and 90785 [Figure 2.1 (b)] aligned 100% to the *Myt1l* mRNA sequence in the rat, mouse and human. On the other hand, the sequence numbered 428227 only had

perfect alignment with the rat and mouse *Myt1l* sequences. The alignment of this sequence with the human *MYT1L* sequence presented three mismatches: the first and last nucleotides and one in the middle of the sequence [Figure 2.1 (c)]. The correct design and specificity of the sequences are crucial to achieving gene silencing.

Additionally, the non-silencing shRNAmir structure, which consists just as *Myt1l* shRNAmir of a mir-30, sense, loop and antisense sequences, was inspected to verify its lack of specificity for any known gene sequence. The results demonstrated that neither the sense nor the antisense sequences targeted any known human, rat or mouse gene.

(a) Myt1l shRNAmir 32678

Rattus norvegicus myelin transcription factor 1-like (**Myt1l**), mRNA
Length: 4491 Number of Matches: 1 Identities: 22/22(100%)

```
Query  1     ATTTCCGTCAAAGTAGTCACGT  22
             ||||||||||||||||||||||
Sbjct  4259  ATTTCCGTCAAAGTAGTCACGT  4238
```

Mus musculus myelin transcription factor 1-like (**Myt1l**), mRNA
Length: 7198 Number of Matches: 1 Identities: 22/22(100%)

```
Query  1     ATTTCCGTCAAAGTAGTCACGT  22
             ||||||||||||||||||||||
Sbjct  4382  ATTTCCGTCAAAGTAGTCACGT  4361
```

Homo sapiens myelin transcription factor 1-like (**MYT1L**), mRNA
Length: 7152 Number of Matches: 1 Identities: 22/22(100%)

```
Query  1     ATTTCCGTCAAAGTAGTCACGT  22
             ||||||||||||||||||||||
Sbjct  4294  ATTTCCGTCAAAGTAGTCACGT  4273
```

(b) Myt1l shRNAmir 90785

Rattus norvegicus myelin transcription factor 1-like (**Myt1l**), mRNA
Length: 4491 **Number of Matches:** 1 **Identities: 22/22(100%)**

```
Query  1     GTTTCTGTAGCCATACTGAGGA  22
             ||||||||||||||||||||||
Sbjct  2649  GTTTCTGTAGCCATACTGAGGA  2628
```

Mus musculus myelin transcription factor 1-like (**Myt1l**), mRNA
Length: 7198 Number of Matches: 1 Identities: 22/22(100%)

```
Query  1     GTTTCTGTAGCCATACTGAGGA  22
             ||||||||||||||||||||||
Sbjct  2778  GTTTCTGTAGCCATACTGAGGA  2757
```

Homo sapiens myelin transcription factor 1-like (**MYT1L**), mRNA
Length: 7152 Number of Matches: 1 Identities 22/22(100%)

```
Query  1     GTTTCTGTAGCCATACTGAGGA  22
             ||||||||||||||||||||||
Sbjct  2690  GTTTCTGTAGCCATACTGAGGA  2669
```

(c) Myt1l shRNAmir 428227

Rattus norvegicus myelin transcription factor 1-like (**Myt1l**), mRNA
Length: 4491 Number of Matches: 1 Identities: 22/22(100%)

```
Query  1     TAGCACAACACCATGTCCTTGT  22
             ||||||||||||||||||||||
Sbjct  1614  TAGCACAACACCATGTCCTTGT  1593
```

Mus musculus myelin transcription factor 1-like (**Myt1l**), mRNA
Length: 7198 Number of Matches: 1 Identities: 22/22(100%)

```
Query  1     TAGCACAACACCATGTCCTTGT  22
             ||||||||||||||||||||||
Sbjct  1737  TAGCACAACACCATGTCCTTGT  1716
```

Homo sapiens myelin transcription factor 1-like (**MYT1L**), mRNA
Length: 7152 Number of Matches: 1 Identities: 19/20(95%)

```
Query  2     AGCACAACACCATGTCCTTG  21
             |||||||||| ||||||||
Sbjct  1654  AGCACAACACCGTGTCCTTG  1635
```

Figure 2.1 ***In-silico* analysis of the antisense strands of the shRNAmir numbered 32678 (a), 90785 (b) and 428227 (c).**

Each sequence was aligned to the *Myt1l* sequence belonging to the rat, mouse or human to confirm specificity.

2.3.2 Corroboration of *Myt1l* expression in two rodent cells lines

Using qPCR, the cDNAs were isolated from two neural rodent cell lines (PC-12 and N2A) and analysed in order to find whether they naturally expressed measurable quantities of *Myt1l*. Both PC-12 and N2A cells showed a good expression of *Myt1l* when their amplification curves (Figure 2.2) and Ct values (Table 2.3) were compared to that of *β-Actin* (positive control). *β-Actin* was selected as the housekeeping gene and positive control because of its good and invariant expression in the samples tested. High Ct values comparable to those observed for *β-Actin* indicated that the gene is well expressed in the cell line. The *Myt1l* amplification curve obtained from PC-12 and N2A was further compared to the curve obtain from undifferentiated B35 cells (negative control). The choice of this last cell line as a negative control was because of its undifferentiated state, hence its lack of *Myt1l* expression. The *Myt1l* amplification curve in PC-12 and N2A cells was closer to their housekeeping gene, indicating good expression [Figure 2.2 (a) and (b)]. As expected, the negative control had no *Myt1l* amplification curve [Figure 2.2 (c)].

By examining the dissociation curve, the specificity of the PCR products could be assessed. Figure 2.3 illustrates the changes in fluorescence which were observed as the temperature was increased. When the melting point was reached due to the dissociation of the double-stranded DNA, SYBR® was released and the fluorescence decreased. The melting point is different for every amplified product: it depends on several factors such as length, GC concentration and the presence of base mismatches. If a single peak is yielded

after amplification, as it is for *Myt1l* and *β-Actin* in N2A [Figure 2.3 (c) and (d)] and PC-12 [Figure 2.3 (a) and (b)] in this experiment, it indicates that the primers only amplified the region for which they were designed. These results together with the high Ct values observed for *Myt1l* in the N2A and PC-12 cell lines provided good evidence of their utility to assess the effects of *Myt1l* shRNAmirs.

Table 2.3 **Ct values obtained from analysing *Myt1l* expression in three cell lines: PC-12, N2A and B35.**

The data are expressed as mean ± S.E.M.

Cell Type	Ct *β-Actin*	Ct *Myt1l*
PC-12	20.75±0.36	24.01±0.41
N2A	19.42±0.39	23.39±0.28
B35	21.80±0.93	Undetermined

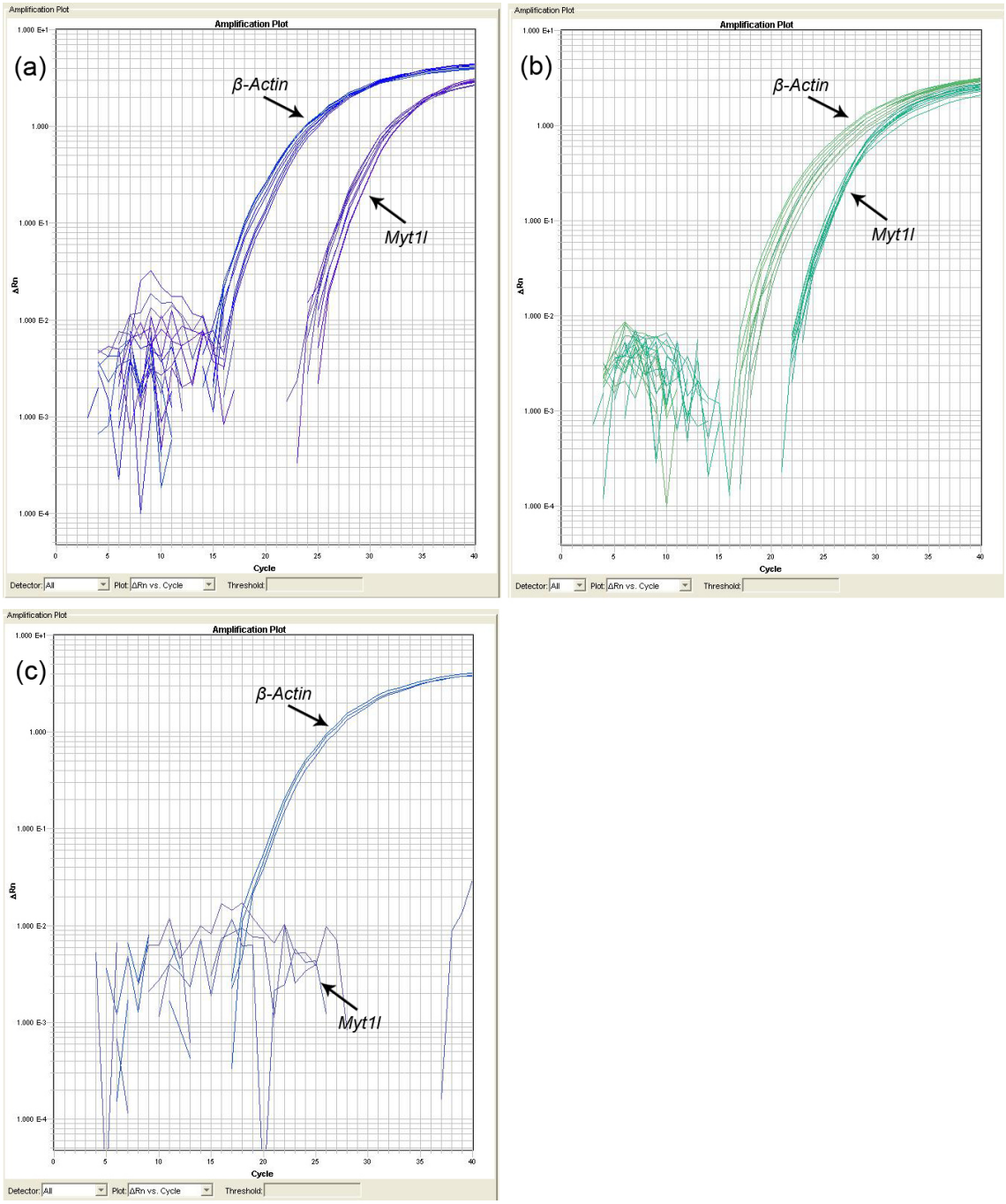

Figure 2.2 **The expression of *Myt1l* in four different cells lines:**

PC-12 cells (a), N2A (b) and undifferentiated B35 (c). This chart plots the changes in the magnitude of the signal generated by the amplicon across cycles. Each graph shows the amplification of *Myt1l* and the housekeeping gene used for normalization. PC-12 (a) and N2A (b) possess a good expression of *Myt1l* as the amplification curves are not far from the housekeeping gene curve. The last figure is an example of a cell line that does not express *Myt1l* (c).

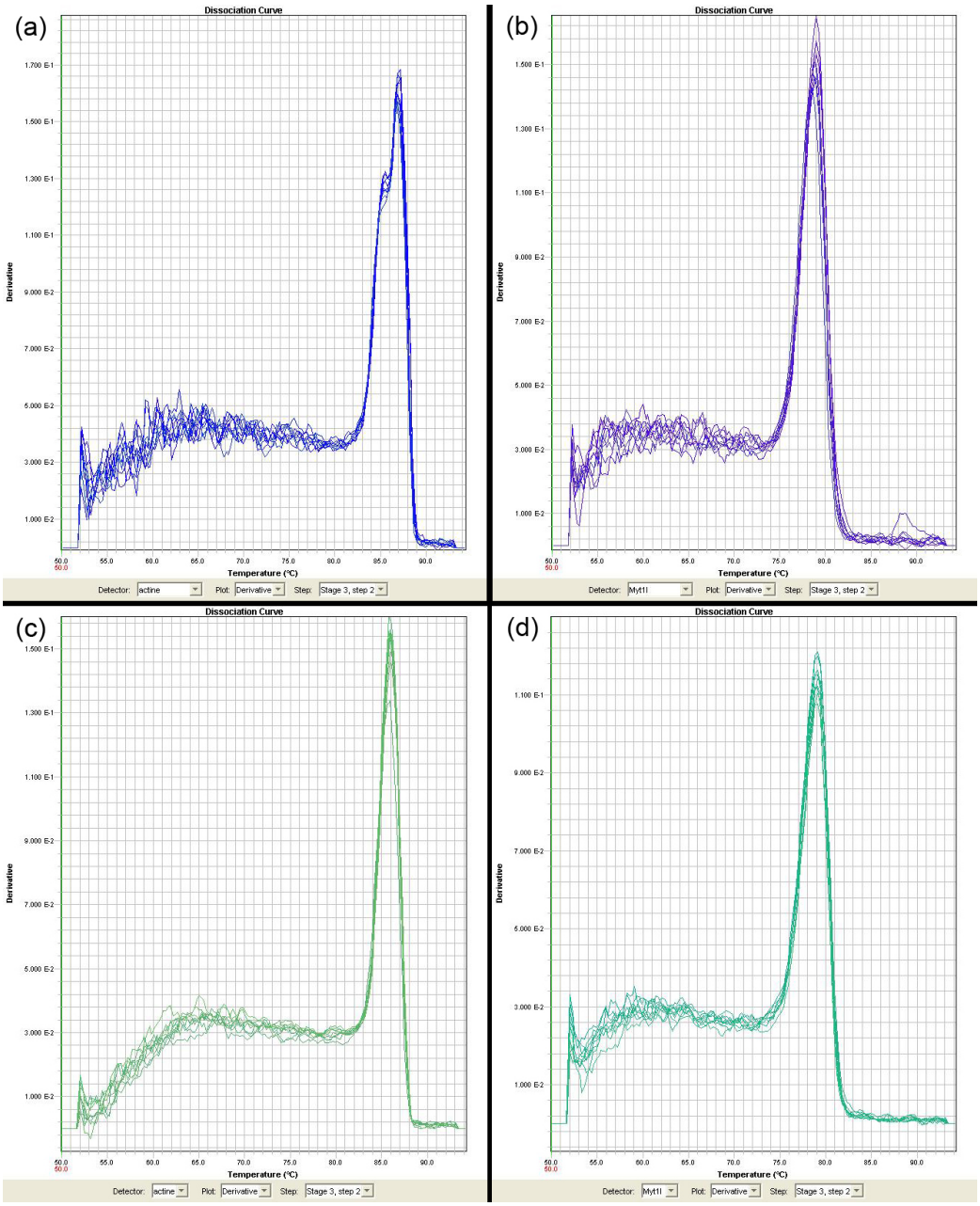

Figure 2.3 **Confirmation of *β-actin* (a and c) and *Myt1l* (b and d) qPCR primer specificity in the cell lines PC-12 (a and b) and N2A (c and d).**

The dissociation curves derived from the qPCR analysis of *Actin* and *Myt1l*, yielded only one peak (i.e., one PCR product) per primer pair in each cell line, indicating the specificity of these primers. The plot illustrates the derivative data (the rate of change in fluorescence as a function of temperature) versus the temperature interval at which fluorescence changes.

2.3.3 Screening for anti-*Myt1l* shRNAmir in rodent cells lines

Two cells lines commonly used as neuronal models were used to corroborate

the efficiency of *Myt1l* shRNAmir sequences: one derived from rat (PC-12) and the other one from mouse (N2A). For the first set of experiments, PC-12 cells were infected with each one of the three putative silencing sequences (*Myt1l* 32678, *Myt1l* 428227, or *Myt1l* 90785 shRNAmir) and one negative control (non-silencing shRNAmir). PC-12 was first investigated because its fluorescence is easier to detect under the fluorescent microscope in comparison to N2A. Following transduction, pictures were taken after the cells were selected using Puromycin in order to obtain only cells that were actively expressing the shRNAmir of interest as well as GFP (seen in Figure 2.4). This is because GFP is expressed from the same CMV-EI promoter that regulates the shRNAmir expression. Most cells are expressing green fluorescent, demonstrating that the cells were infected and were expressed either *Myt1l* or non-silencing shRNAmir.

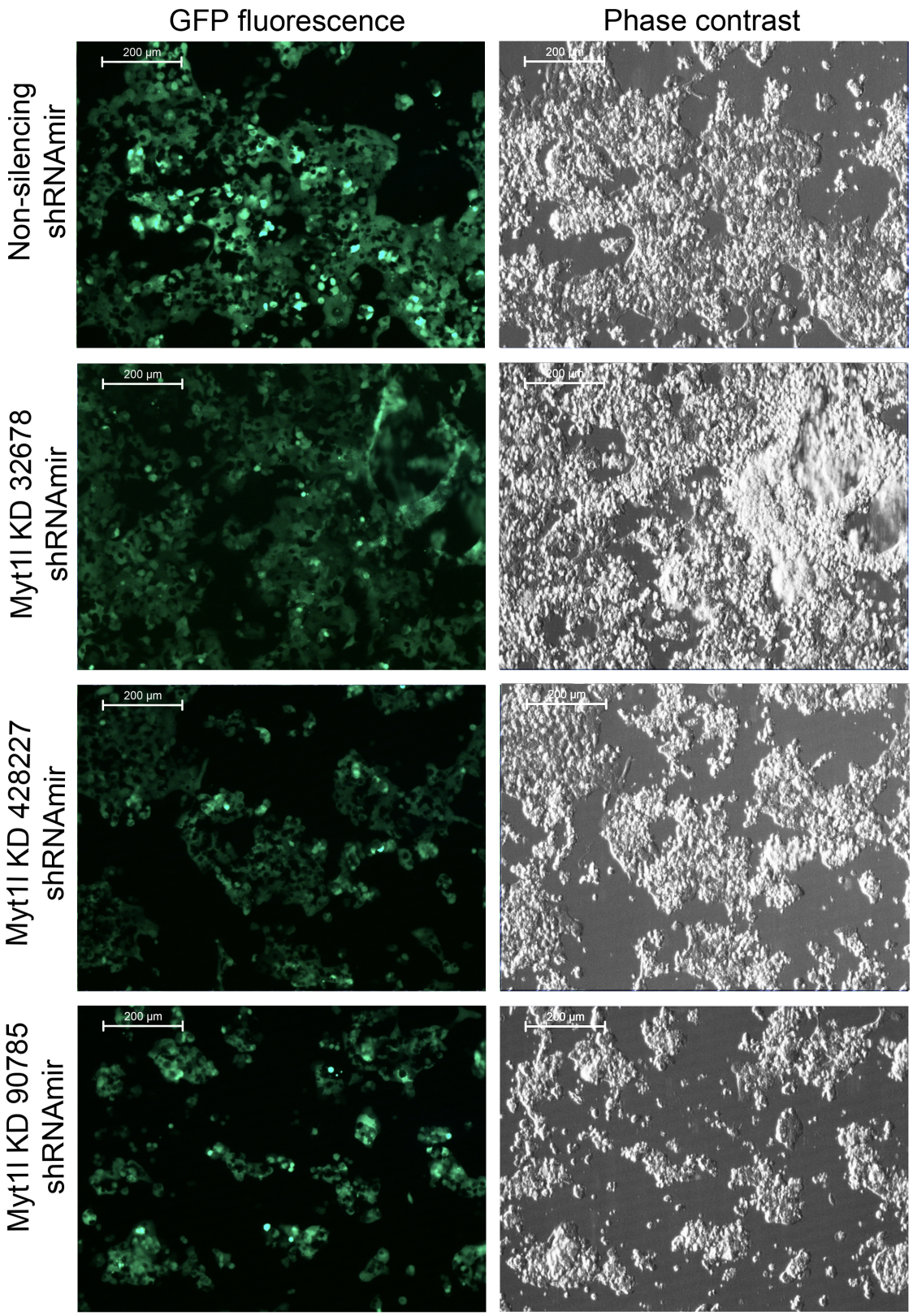

Figure 2.4 **The fluorescent microscope images on the right illustrate the GFP expression in PC-12 cells obtained with each of the three different *Myt1l* shRNAmirs and control 5 days after transduction.**

On the left, are the corresponding phase-contrast images. All photographs were taken using objective X10.

The RNA extracted from those transduced cells was used to perform a qPCR analysis to determine the effect of *Myt1l* shRNAmir *in-vitro*. The plots were obtained by calculating the relative fold expression of each *Myt1l* shRNAmir infection in comparison to non-silencing. As seen in Figure 2.5, the expression of *Myt1l* was found to be decreased by 55% in shRNAmirs 32678 (2.23-fold change), 26% in 428227 (1.35-fold change) and 31% 90785 (1.45-fold change) when compared to the control. A one-way ANOVA test analysing the $\Delta\Delta$Ct values indicated significant group differences when comparing *Myt1l* expression in the control and *Myt1l*-shRNAs infected samples ($F_{3,23}$=7.378, p=0.002). Post-hoc analyses using the Tukey LSD test found a significant reduction between the control and *Myt1l* shRNAmir 32678 (p=0.012), while the control versus either *Myt1l* shRNAmir 428227 (p=0.331) or *Myt1l* shRNAmir 90785 (p=0.127) was not significant.

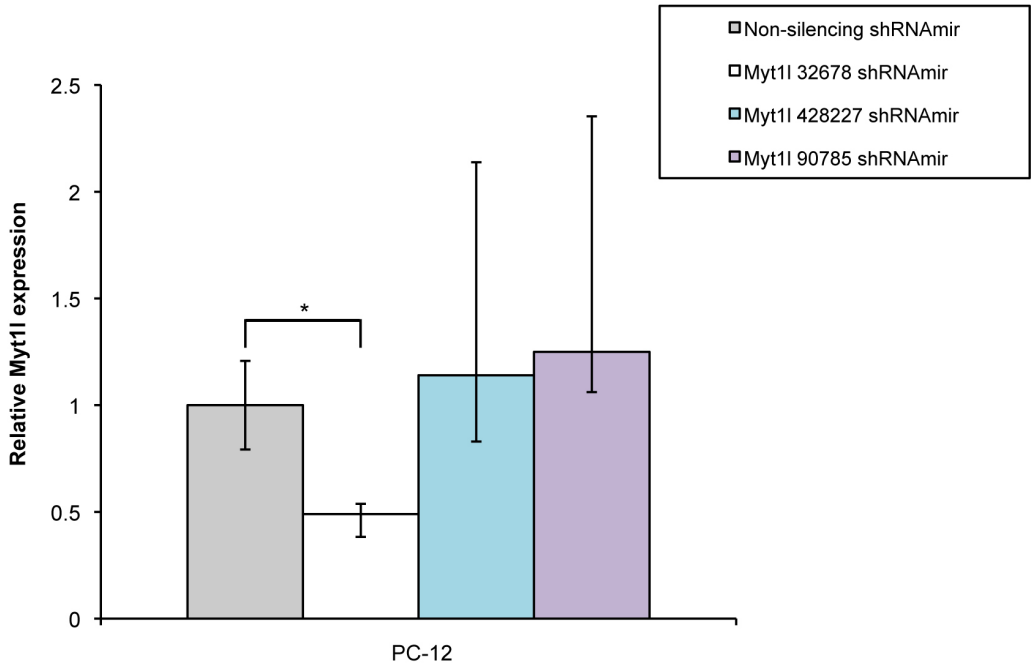

Figure 2.5 **This graph illustrates the relative fold expression of *Myt1l* in PC-12 cells after being transduced with either one of the three different *Myt1l* shRNAmirs or non-silencing shRNAmir.**

The data are expressed as mean ± S.E.M. *p<0.05 *Myt1l* knockdown versus control pre-planned pairwise comparison followed by Tukey LSD correction of ΔΔCt values (n=6 per group).

After analysing the results obtained from the experiments performed on PC-12 and corroborating the efficiency of at least one of the shRNAmir sequences, the transduction of the N2A cell was restricted to that shRNAmir construct. The reasons behind using N2A were to try to replicate the effect seen in PC-12 and to validate the shRNAmir construct in the mouse for the following *in-vivo* experiments.

Even though it was hard to capture the fluorescence of this cell line in pictures, the microscopy inspection of GFP expression in the cells indicated high transfection efficiency after Puromycin selection (Figure 2.6). This was further

corroborated when the RNA extracted from those cells was analysed. The relative expression of *Myt1l* in 32678 shRNAmir-transduced cells compared to control cells had a 2.64-fold reduction, which represented a reduction of 65% An independent t-test analysing the ΔΔCt values revealed a significant difference between the control and the treated cells [T(10)=-7.036; p=0.000036; Figure 2.7], indicating that the *Myt1l* shRNAmir sequence was capable of downregulating *Myt1l* in the mouse cell line too. The results of these experiments corroborated the efficiency of shRNAmir 32678 to significantly knockdown *Myt1l* in the rat and the mouse.

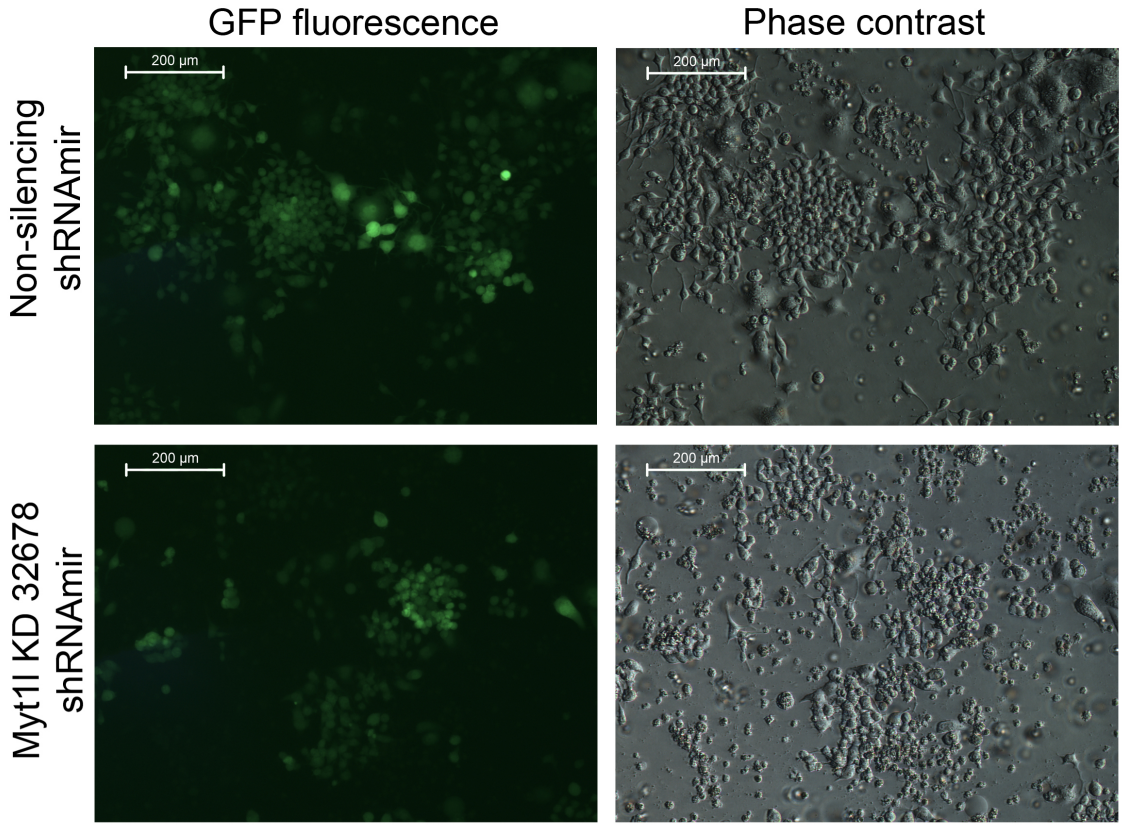

Figure 2.6 **The figures on the right illustrate the GFP expression in N2A cells of *Myt1l* shRNAmir and the control after 5 days of being transduced.**

On the left are the corresponding phase-contrast images. All photographs were taken using objective X10.

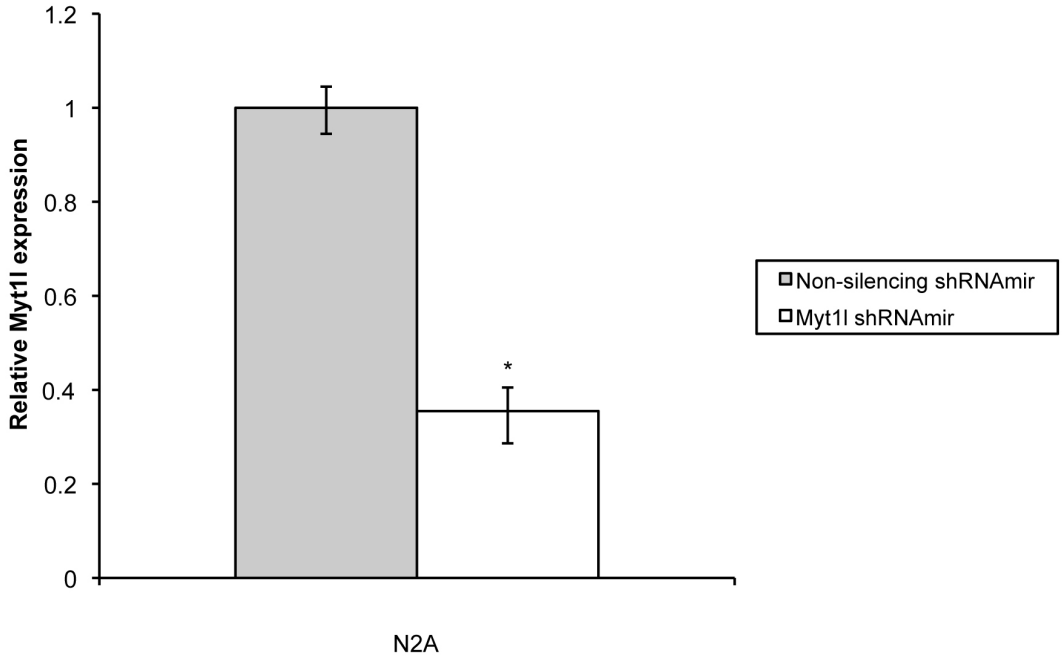

Figure 2.7 **This graph illustrates the relative fold expression of *Myt1l* in N2A cells after being transduced with either *Myt1l* 32678 shRNAmir or non-silencing shRNAmir.**

The data are expressed as mean ± 1 S.E.M. *p<0.0001 (n=6 per group).

2.4 Discussion

This initial experimental chapter focused on identifying a silencing sequence capable of downregulating the expression of *Myt1l*. To address this aim, three sequences designed for such a purpose were acquired from the shRNAmir library of Hannon and Elledge (Paddison, Silva et al. 2004) as well as a non-silencing shRNAmir as a negative control (Open Biosystems Thermo Scientific). The use of this last construct as a control was to make the experiment as similar as possible in terms of transgene incorporation into the host genome. The results yielded from this study have identified an shRNAmir sequence capable of significantly reducing the expression of *Myt1l in-vitro* in a rat and a

mouse cell line. This finding allowed us to address some of our current hypotheses about *Myt1l* involvement in cell development and the resultant adult mouse.

2.4.1 *Myt1l* knockdown

In order to validate their efficiency *in-vitro*, expression of *Myt1l* was assessed in two cell lines (one rat and one mouse) commonly used as neuronal models. Both of them showed a good expression of *Myt1l* when compared to the expression of a well-expressed gene. Following these results, the three *Myt1l* shRNAmirs were used to transduce the rat cell line PC-12 and *Myt1l* expression was compared between them and the control shRNAmir. Not surprisingly, only one of them (*Myt1l* 32678 shRNAmir) was capable of reducing the expression of *Myt1l* by 55.05 ± 9.13%. The other two failed to significantly decrease *Myt1l* expression when compared to the control. Although all the sequences were designed to decrease the expression of the gene of interest and their specificity was validated, it is common to find variability in the results when the sequences are tested *in-vitro*. One possible reason why the efficiency of shRNAs is variable could be due to the silencing sequence. It has been observed that the following factors are the most determinant on shRNA functionality: sequence specificity (Du, Thonberg et al. 2005); low guanine and cytosine content; internal stability of the 5' antisense; thermodynamic properties; and absence of internal repeats of the nucleotides (Reynolds, Leake et al. 2004). Most of the current software integrates these factors when designing shRNA sequences; but silencing is still not always achieved in its totality or a significant percentage.

Another possible explanation is because the secondary and tertiary structures of the targeted mRNA have an important impact on the activation of the RNA-induced silencing complex (RISC) (Brown, Chu et al. 2005, Overhoff, Alken et al. 2005). RNA is prone to forming this kind of structure and they can block the access to the target site sequence, which results in low cleavage of the endogenous mRNA (Brown, Chu et al. 2005).

Furthermore, the efficiency to downregulate *Myt1l* in a mouse cell line was replicated. In this case, validation *in-vitro* in a mouse cell line was necessary to further pursue the aims intended for Chapter 4. For this experiment, only the *Myt1l* shRNAmir vector that significantly reduced the gene expression in PC-12 cells was used to transduce N2A cells. The results further supported the finding in PC-12, that is, that the *Myt1l* shRNAmir was capable of reducing by 64.50±4.40% of the *Myt1l* mRNA in those cells in comparison to the non-silencing vector. Nevertheless, even though the expression of *Myt1l* recorded for *Myt1l*-shRNAmir infected PC-12 and N2A represented only a partial knockdown of the gene, this effect was not unforeseen as other studies have described similar knockdown effects (Moffat and Sabatini 2006, Singh, Spoelstra et al. 2008, Muruganandan, Dranse et al. 2013).

2.4.2 Conclusion and limitations

The results of these experiments were crucial to the future development of this project. A silencing sequence targeting *Myt1l* mRNA was necessary to address

the questions about the function of this gene in stem cell development and mouse behaviour. In the case of the animal model, the use of an shRNAmir cloned into a lentiviral vector was chosen over other techniques such as a conditional knockout the same construct can be used for *in-vitro* purposes as well (Davidson and Boudreau 2007). Moreover, the use of stereotaxic surgery and lentiviral vectors provided the opportunity to localize the manipulation of gene expression (Cetin, Komai et al. 2007). However, this could also be interpreted as a disadvantage depending on the size of the region where the gene would be downregulated. Another disadvantage of this approach is the subtle effects which may be created, possibly due to the decrease rather than elimination of the expression of the gene of interest (Gao and Zhang 2007). An additional shortcoming is the unknown temporal expression of the shRNAmir sequence, although this largely depends on the choice of vector, and lentiviral vectors are known to be expressed for long periods of time (Howarth, Lee et al. 2010); however, the exact time is unknown and it should be checked for every vector+shRNAmir construct. Lastly, an additional inconvenience of this approach is the possibility of causing off-target effects on other genes. Such effects are considerable due to the RISC machinery loading the passenger strand instead of the guiding strand and can be minimized by ensuring the precise Dicer cleavage of the guiding strand out the microRNA (Gu, Jin et al. 2012, Fellmann, Hoffmann et al. 2013). Although, the design of shRNAmirs used in this study tried to minimize such effects by mimicking the structure of the endogenous microRNAs, off-target effects cannot be dismissed. In the future, the results of these experiments could be replicated using an additional and capable shRNAmir sequence, in order to fully reject that the results obtained here were due to any off-target effect.

Chapter 3 : Effects of *MYT1L* knockdown on gene expression during differentiation of human neural stem/progenitor cells.

3.1 Introduction

A complex organ like the brain develops through multiple stages that rely on cellular processes such as neural stem cell proliferation, differentiation, migration and synaptogenesis, among others. The process of differentiation of neural stem cells is largely dependent on genes and their transcriptional products, which ultimately determine the end fate of these stem cells (Paczkowski and Chun 2009). In light of technological advances devoted to measuring the expression of large quantities of genes in a single experiment, new genes are being associated to neuronal cell differentiation (Wen, Gu et al. 2002). Among these, a wide repertoire of the genes coding for transcription factors seem to have an important input into deciding the cell-type specification (Bang and Goulding 1996). In the quest to investigate the impact of transcription factors such as *MYT1L* on the transcription of other genes, the use of stem cells as an *in-vitro* model of neuronal differentiation in parallel with gene knockdown appeared to be a suitable model. In this way, we sought out to unravel the importance of *MYT1L* in the genetic pathway of cell differentiation.

3.1.1 Stem cells as an *in-vitro* model of neurodevelopment

Tissue culture of neural stem cells is among the procedures commonly used to

understand the cellular processes taking place during the development of the central nervous system, in particular as a model of cell proliferation and differentiation (McKay 1997). The term ‘neural stem cells’ or ‘neural progenitors’, refers to cells that are able to differentiate into neural cells (neurons and glial cells) and which are capable of self-renewing as well as undergoing asymmetric cell division (Figure 3.1) (Gage 2000). The isolation and culture of neural stem cells is possible due to the protocols developed by Evans, Kaufman (Evans and Kaufman 1981) and Martin (Martin 1981) to obtain embryonic stem cells directly from a mouse embryo (Figure 3.1). The availability of these types of cell lines and their capacity to differentiate brought a new *in-vitro* approach to studying mammalian development and it represented a watershed in the field of developmental biology (Keller 1995).

New protocols have been developed to improve techniques to isolate stem cells from different regions of the brain at different stages of life (embryonic, foetal, adult) (Pollock, Stroemer et al. 2006). These cell lines can be expanded by the addition of growth factors such as fibroblast growth factor–2 (FGF-2) and epidermal growth factor (EGF). The removal of those factors consequently leads to the induction of differentiation (Reynolds and Weiss 1992, Rietze and Reynolds 2006). Moreover, depending on the cell line and the neuronal phenotypes pursued, other factors might be required for differentiation (Gage 2000). Although these protocols have produced good neurodevelopmental *in-vitro* models, these cells are prone to genetic instability as well as a tendency to create tumours. A protocol overcoming those difficulties was developed by Pollock and collaborators (Pollock, Stroemer et al. 2006) and it incorporated c-

mycER^{TAM} technology, which comprises a growth promoting gene (c-myc) and a hormone receptor that is activated by 4-hydroxy-tamoxifen (4-OHT). This selective growth regulator provides protection against uncontrolled division and tumour formation, in addition to the generation of genetically stable cell lines.

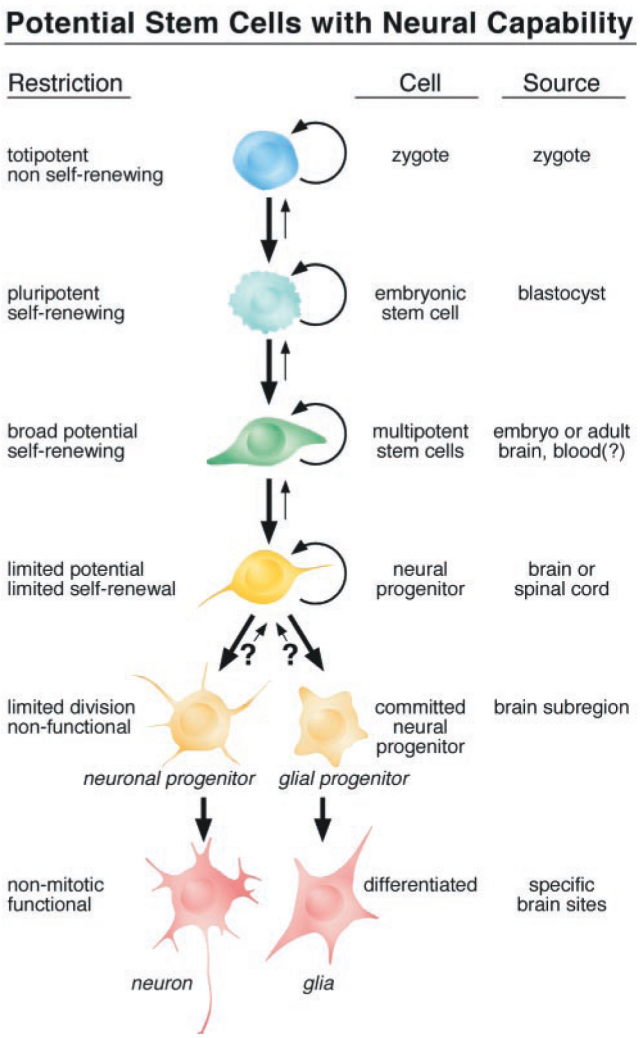

Figure 3.1 **This figure illustrates the different types of stem cells and their differentiation potential.** This figure was taken from Gage (Gage 2000).]

3.1.2 The use of microarrays to identify the genes involved in proliferation and differentiation

Even though the use of stem cells has facilitated the study of development, studying the genetic pathways that control it remains a long and extensive task. One manner of possibly solving this is by correlating the protein or mRNA expression patterns from the cell or tissue with the degree of development at which the sample was taken and comparing it to other earlier or later stage of development (Lillien 1998). Applying the same principles in a more ambitious approach, the use of large-scale gene profiling techniques such as microarrays has helped identify the genetic pathways leading to proliferation and differentiation of neural cells (Aiba, Sharov et al. 2006). This technology has evolved from the early work performed by Schena and collaborators (Schena, Shalon et al. 1995) and it has benefited from the advancements of technology such as an increase in the specificity and number of probes analysed per experiment (Peeters and Spek 2005).

Relying on the information provided by microarray analysis, an initial pool of the putative genes involved during proliferation was established for neural stem cells (Ramalho-Santos, Yoon et al. 2002, D'Amour and Gage 2003) and embryonic stem cells (Ramalho-Santos, Yoon et al. 2002, Tanaka, Kunath et al. 2002, D'Amour and Gage 2003). It was not surprising that both types of stem cells shared the expression of some common genes given the fact that embryonic stem cells and neural stem cells are still differentiating, although the latter had a more restricted phenotypic output in comparison to the former

(Figure 3.1). Among those genes, most of them belonged to transcription regulation, signalling and cell cycle regulation (Ramalho-Santos, Yoon et al. 2002, D'Amour and Gage 2003).

Further experiments using the same stem cell line tried to identify the genes whose expression differed significantly during differentiation in comparison to proliferation. It was found that a large number of genes coding for transcription factors and cell signalling were upregulated during differentiation (Karsten, Kudo et al. 2003, Ahn, Lee et al. 2004, Gurok, Steinhoff et al. 2004). Particularly, it was observed that the expression of transcription factors in a temporospatial manner had an important input into deciding the fate of progenitor cells (Levine and Davidson 2005). This is to regulate the expression of a large number of genes required to be expressed in order to switch the cell from an undifferentiated progenitor type to a highly specialized neural cell (Gurok, Steinhoff et al. 2004).

3.1.3 Neural stem cells and gene knockdown

The aforementioned studies have provided global gene expression profiles, which have laid down the roots for the discovery of the putative genes involved in cell proliferation and differentiation of stem cells. One way of investigating the role of those genes individually is by increasing or reducing their expression *in-vitro* and *in-vivo* and observing the changes at both phenotype and genotype level. The use of lentiviruses has demonstrated that foreign genes can be

efficiently introduced into the genome of stem cells, and therefore lentiviruses are a valuable tool to analyse gene function during developmental processes (Zaehres, Lensch et al. 2005, Wang, Oron et al. 2012). In addition, this particular type of vectors also offers the advantage of infecting dividing and non-dividing cells (Naldini, Blomer et al. 1996, Dissen, McBride et al. 2012). Moreover, transduction of embryonic stem cells has shown stable transgene expression, a long-lasting effect that continued throughout differentiation (Pfeifer, Ikawa et al. 2002). Furthermore, specifically referring to gene silencing, the use of lentiviral vectors containing shRNA sequences in these kinds of cells showed a stable expression of siRNAs capable of reducing gene expression (Rubinson, Dillon et al. 2003, Zaehres, Lensch et al. 2005, Wang, Oron et al. 2012).

One example of the use of lentiviral vectors to transduce human dividing cells was performed by Zaehres and collaborators (Zaehres, Lensch et al. 2005). They used lentiviral vectors to silence the expression of two transcription factors: octamer-binding transcription factor 4 (*OCT-4*) and Nanog homeobox (*NANOG*) in human embryonic stem cells. The phenotypic changes indicated that the cells were leaving the proliferation stage and were beginning cell differentiation. In terms of gene expression, they found that the expression of *OCT-4* had an impact on the expression of *NANOG* and vice versa when tested separately. In addition, the expression of markers associated with the undifferentiated stage indicated that these transcription factors might be involved in maintaining the pluripotency of these cells. These results were further confirmed by Wang and colleagues (Wang, Oron et al. 2012), who used

microarrays and siRNAs to demonstrate the coregulation of *OCT-4* and *NANOG* in cell self-renewal mechanisms. Moreover, the same study showed that over 100 genes expressed during human embryonic stem cell development required *OCT-4*, *NANOG* and SRY (sex determining region Y)-box 2 (*SOX2*) to maintain proper expression.

In a similar type of experiment which used non-dividing cells, Lin and collaborators (Lin, Bloodgood et al. 2008) tested the impact of removing transcription factor Neuronal PAS Domain Protein 4 (*Npas4*) through the use of lentiviral vectors in mouse neuronal cultures. The results indicated that the expression of this gene was involved in the development of inhibitory synapses and its absence disturbed the naturally occurring homeostatic balance between excitatory and inhibitory synapses. One of the putative downstream targets that stood out in this experiment was brain-derived neuro-trophic factor (*BDNF*), which is known to associate to inhibitory synapse maturation and function.

3.1.4 *MYT1L* and neuron development

The previous studies exemplified how the use of lentiviral vectors incorporating siRNA and shRNAs has been useful in understanding the pathways lead by transcription factors. Applying such technologies to other transcription factors such as *MYT1L*, whose downstream targets have not yet been discovered, could be helpful in better understanding the transcriptional pathway initiated by this gene. So far, it is known that this transcription factor is actively expressed in

the central nervous system, in particular in the neurons (Berkovits-Cymet, Amann et al. 2004). More precisely, its expression begins around embryonic day 13 in the rat and peaks right before birth, but continues to have a detectable expression during adulthood (Chapter 1, Figure 1.7) (Kim, Armstrong et al. 1997).

In-vitro studies have provided further evidence of the importance of *MYT1L* in neuron development. Since Vierbuchen and collaborators (Vierbuchen, Ostermeier et al. 2010) demonstrated that *Myt1l* in combination with transcription factors *Ascl1* and *Brn2* was sufficient to revert mouse fibroblast into functional neurons, other protocols with similar purposes have been developed. In addition to mouse fibroblasts, these new protocols adjusted the genes required to convert human pluripotent stem cells (Pang, Yang et al. 2011) and human fibroblasts (Ambasudhan, Talantova et al. 2011, Pfisterer, Kirkeby et al. 2011, Son, Ichida et al. 2011, Yoo, Sun et al. 2011) into functional neurons. All of the aforementioned protocols require the expression of *MYT1L* in order to obtain mature neurons capable of action potentials and synapse formation.

Additional information about the role of *MYT1L* has been provided by clinical studies. These studies which use genome maps or expression profiles of patients have found a disruption in *MYT1L* in major depression disorder (Wang, Zeng et al. 2010), schizophrenia (Vrijenhoek, Buizer-Voskamp et al. 2008, Addington and Rapoport 2009, Lee, Mattai et al. 2012), autism (Meyer, Axelsen et al. 2012, Rio, Royer et al. 2012) and mental retardation (Gruchy, Jacquemont

et al. 2007, Zou, Van Dyke et al. 2007, Bonaglia, Giorda et al. 2008, Stevens, van Ravenswaaij-Arts et al. 2011). These four complex disorders have been thought to be, to some extent, the result of disrupted genes and environmental factors during neurodevelopment (Van Loo and Martens 2007).

3.1.5 Aims

The role that *MYT1L* plays in the transcription of other genes during development has not yet been fully understood. The fact that it is highly expressed during development and that it is necessary to convert other cellular types into functional neurons provides evidence of its importance for neuronal development. Further support of this comes from associations some studies have made between *MYT1L* and psychiatric diseases developed during neurodevelopment. Taking into account all the information available about this gene, it is not surprising that its reduced expression during differentiation would have an impact on the expression of other genes and ultimately on the proper differentiation of the brain. The aims of this chapter are to examine the role of *MYT1L* in the differentiation of human neural stem/progenitor cell line SPC04 by selectively knocking it down using a lentiviral shRNAmir vector and analysing the consequences on gene expression profile through qPCR and microarray at two different time points: pre-differentiation and day 7 of differentiation. Due to limitations in the quantity of RNA, only the expression of nine genes was assessed. Those genes were chosen on the basis of being highly co-expressed with *MYT1L* in a previous experiment attempting to investigate the expression profile of SPC04 cells during differentiation (data not shown). The differences

found in gene expression due to *MYT1L* knockdown could help determine the genes that might require this transcription factor to initiate transcription. The results of this study would help unravel the putative downstream targets of *MYT1L* during differentiation.

3.2 Materials and Methods

3.2.1 Experimental setup

The human neural stem/progenitor cell line SPC04 cells were seeded into 6-well plates. The wells were infected with lentiviral vectors containing either *MYT1L* shRNAmir or non-silencing shRNAmir. RNA was extracted from those cells at two time points: pre-differentiation and day 7 of differentiation. The choice of those time points was decided after analysing data of a pilot study demonstrating a knockdown effect of *MYT1L* after 7 days of differentiation. The experiment consisted of 2 biological replications with 3 technical replications for each condition and time point.

The RNA was used to analyse gene expression through microarray analysis. Further validation was performed by qPCR but only on a handful of genes due to the limitation in the quantity of RNA. Unfortunately the results of the microarray were inconclusive and therefore this chapter is only based on the findings of the qPCR analyses. The genes that had a significant reduction in expression when treated with *MYT1L* knockdown in comparison to the control

underwent *in-silico* analysis of the transcription binding sites present in their promoter region. This last step was important in assessing the possibility of them being direct downstream targets.

3.2.2 Concentrated lentiviral production

The lentiviral supernatant containing shRNAmirs against *MYT1L* and the control was produced exactly as described in Chapter 2 (2.2.3). After the supernatant was filtered, it was loaded into ultracentrifugation tubes (Beckman Coulter) and spun down at 25,000 revolutions per minute (RPM) for 1.5 hours at 4^{o} C. The supernatant was carefully removed from the tubes without disturbing the lentiviral pellet. 30 ul of PBS was added to each tube and left overnight at 4^{o} C. The next day, the pellet was resuspended, aliquoted and stored at -80^{o} C.

3.2.3 Lentiviral titration

In order to determine the viral titre, $1x10^{5}$ HEK293T cells were seeded into each well in a 24-well plate using complete media (details about cell culture are found in 2.2.2). The next day, HEK293 cells were transduced with serial dilutions of the concentrated virus. The concentrated virus was diluted as follows: 10^{-2}, 10^{-3}, 10^{-4}, 10^{-5}, 10^{-6}, 10^{-7} and 10^{-8} in serum and antibiotic free high glucose DMEM media supplemented with polybrene (8 ug/ml). The plates were centrifuged at 2500 RMP for 1.5 hours, followed by 2.5 hours in the incubator (37^{o} C and 5% CO_2). The media was replaced with 1 ml of complete media and the cells were

incubated for 72 hours without disruption. Following this step, the cells were carefully washed twice with sterile PBS and trypsinised using Trypsin-EDTA 0.05% solution for 5 minutes at 37^{o} C. Once the cells were detached, 500 ml of sterile PBS was added to each well and centrifuged for 5 minutes at 1000 RPM. The supernatant was carefully discarded and each sample was resuspended in 500 ul of 4% paraformaldehyde (PFA). The samples were analysed by flow cytometry using a fluorescence-activated cell sorting (FACS) analysis to count the transduced cells, which were recognized by their GFP expression (fluorescent reporter). Only dilutions resulting in about 10 to 15% GFP positive cells were used for titre calculation. This percentage represents a single viral integration per cell.

The viral titre was calculated using the following formula:

Transducing units (TU/ml)= (%GFP positive cells/100%) x nb x dilution factor

nb= number of cells plated x 2 $^{\text{number of days after plating}}$

3.2.4 Human neural stem/progenitor cell line SPC04

The human neural stem/progenitor cell line, SPC04, used for this study is a conditionally immortalized cmyc-ER^{TAM} human spinal cord cell line (kindly provided by the Jack Price Lab), which was generated from 10-week old foetal cervical spinal cord tissue (Kubinová, Horák et al. 2010, Jeffries, Perfect et al. 2012, Růžička, Nataliya Romanyuk et al. 2013). In brief, the foetal cervical region of the spinal cord was finely cut into pieces to generate primary cells.

Those cells were gently dissociated using 0.25% trypsin in Dulbecco's modified Eagle's medium/Ham's F12 (DMEM:F12) at 37^{o} C. The reaction was inactivated using 0.25 mg/ml of soybean trypsin inhibitor (Cocks, Romanyuk et al. 2013). The cells were conditionally immortalized following the protocol described by Pollock et al. (Pollock, Stroemer et al. 2006). The cells were plated into laminin-coated plates. When 60% confluency was reached, they were transduced with the retroviral vector pLMCX-2 encoding the transgene cmyc-ER^{TAM} for 12 hours. This gene combines the cmyc transcription factor with a mutant of oestrogen receptor regulated by 4-OHT. The transfected cell colonies were selected using neomycin before being expanded as a clonal cell line. In the presence of 4-OHT, the conditional cell line continues to proliferate remaining phenotypically and karyotypically stable.

3.2.4.1 Cell growth

1) Cell media: Reduced modified media plus (RMM+) was composed of DMEM:F12 (Gibco, UK) supplemented with 4-OHT (100nM; Sigma, UK) and all the components written in Table 3.1 (preparation of stock solution is described in Table 3.2). The media was filtered through a 0.2 uM Stericup filter (Millipore, UK) and stored at 4^{o} C for a maximum of 4 weeks. Differentiation media RMM- was prepared in the same manner but this media was depleted from the growth factors and 4-OHT.

Table 3.1 **RMM composition**

Components	Concentration	Company
Human Albumin Solution	0.03%	Baxter
Human Transferrin	100 μg/ml	Sigma-Aldrich
Putrescine DiHCL	16.2 μg/ml	Sigma-Aldrich
Human recombinant Insulin	5 μg/ml	Sigma-Aldrich
Progesterone	60 ng/ml	Sigma-Aldrich
L-glutamine	2 mM	Sigma-Aldrich
Sodium Selenite	40 ng/ml	Sigma-Aldrich
bFGF (basic Fibroblast Growth Factor)	10 ng/ml	PeproTEc
EGF (Epidermal Growth Factor)	20 ng/ml	PeproTEc

Table 3.2 **Preparation of stock solutions for RMM and differentiation factors**

Component	Stock	Preparation	Storage
Human albumin solution	20%	No preparation was required	4° C
Human Transferrin	50mg/ml	Dissolved in DMEM:F12 containing 1mM of HEPES (pH 7.4; Sigma, UK)	-20° C
Putrescine DiHCL	8.1mg/ml	Dissolved in tissue culture grade water (Gibco, UK)	-20° C
Human recombinant Insulin	10 mg/ml	No preparation was required	4° C
Progesterone	20 ul/ml	Dissolved in molecular biology grade ethanol (Sigma, UK)	-20° C
L-glutamine	200mM	No preparation was required	-20° C
Sodium Selenite	20 ug/ml	Dissolved in DMEM:F12	-20° C
bFGF	10 ug/ml	Dissolved in DMEM:F12 containing 1mM HEPES and 0.03% human albumin solution	-20° C
EGF	10 ug/ml	Dissolved in DMEM:F12 containing 1mM HEPES and 0.03% human albumin solution	-20° C
4-OHT	1mM	Dissolved in molecular biology grade ethanol	-20° C
ATRA	10mM	Dissolved in DMSO (Sigma, UK)	-20° C
DAPT	10mM	Dissolved in DMSO	-20° C

2) Coating of flasks: cell expansion was carried out in Nunc Delta surface treated (Thermo Scientific, UK) T75 and T175 culture flasks freshly coated with mouse laminin and DMEM:F12 at a ratio of 1:50 (20ug/ml; Sigma, UK) for at least three hours at 37° C in a humidified incubator at 5% CO_2. Prior to cell seeding, the excess laminin was aspirated and the flask was washed with

DMEM:F12 to remove any extra laminin present in the flask. This media was aspirated and replaced by RMM+ before returning it to the incubator.

3) Cell revival: In order to revive the cells from liquid nitrogen storage, they were thawed and centrifuged with RMM+ at 900 revolutions per minute (RPM) for 5 minutes. The supernatant was carefully removed and the cell pellet was resuspended in RMM+. Before plating, the cells were counted and their viability was analysed using NucleoCassettes™ and the NucleoCounter® (Chemometec, Denmark) as indicated in Chapter 2. The SPC04 cells were seeded at a density of 20,000 per cm^2 in freshly coated flasks and they were proliferated in RMM+. The media was changed for fresh RMM+ every two days.

4) Cell passaging: The cells were passaged when they reached 80% confluency. For passaging, the flask was washed with Hank's Balanced Salt Solution (HBSS) without calcium and magnesium (Gibco, UK) before trypsinising using TrypZean EDTA (Lonza, UK) for 3 to 5 minutes at 37^o C. Deattachment of the cells was verified using an inverted microscope. This was followed by the addition of trypsin inhibitor solution [DMEM:F12, 0.023 U/ml of Benzonase (Merck, UK), 0.5 mg/ml of Trypsin inhibitor (Sigma, UK) and 0.91% human albumin (Baxter, UK)] and centrifuged for 5 minutes at 900 RPM. The cell pellet was resuspended and they were either seeded in a freshly coated flask (20,000 per cm^2) or frozen.

5) Cell freezing: The SPC04 cells were frozen at a density of $2x10^6$ cells per

vial in RMM+ supplemented with 10% DMSO. The vials were frozen at 1^{o}C per minute using a Mr Frosty freezing container (Nalgene®) for 24 hours at -80^{o}C and then transferred to liquid nitrogen storage. The isopropanol in the Mr Frosty container was changed after 4 freezes.

3.2.4.2 Cell differentiation

For differentiation and transduction, the cells were plated at a rate of 15,000 per cm^2 in freshly laminin-coated 6-well plates (Nunc Delta surface treated; Thermo Scientific, UK). After the cells reached around 80% confluency, the cells were washed twice with RMM- to remove any traces of growth factors. Subsequently, differentiation was triggered by the addition of RMM- supplemented with 10 uM of the γ-secretase inhibitor DAPT (Sigma, UK) and 100 nM all-trans-retinoic acid (ATRA; Sigma, UK). Additionally, for transduction, a 3.50x10^5 TU/ml concentrated stock of lentiviruses containing *MYT1L* or non-silencing shRNAmir was added to the media. Cells were transduced at this stage because preliminary observations showed that there was a higher cell survival rate in comparison to infection during undifferentiation. The SPC04 cells were incubated in this media for 48 hours prior to replacing it with RMM-. The stage at the end of the 48-hour incubation was known as “pre-differentiation”. Differentiation day 1 was counted as the day after pre-differentiation had finished. The plates were microscopically examined for phenotypic differences and the presence of GFP, an indicator of transfection efficiency. The media was changed every 2 days till the end of the experiment. Images of transduced cells

were taken using Leica DMIL supplied with a Leica camera DFC420C (x10 objective).

3.2.5 Cell harvesting and RNA extraction

Before harvesting the cells, all the equipment and surfaces were sprayed with RNAseZAP^{TM} (Sigma, UK) to eliminate RNAse and avoid RNA degradation. The media was carefully removed from the wells and 350 ul of RLT buffer (Qiagen, UK) supplemented with 1% β-mercaptoethanol was added to each one (Sigma, UK). The cells were mechanically disturbed using a sterile cell scraper. The lysate was placed in 2 ml collection tubes (Qiagen, UK) and stored at -80^{o} C until RNA extraction took place.

The lysate was homogenized using a QIAshredder spin column (Qiagen, UK) placed over a 2 ml collection tube and centrifuged at full-speed for 2 minutes. The RNA extraction was performed using the RNeasy® mini kit (Qiagen, UK) and followed the same protocol as in Chapter two (2.2.5), including the optional on-column DNAse digestion using the RNase-Free DNase Set (Qiagen, UK). RNA was eluted in 30 ul of RNase-free water added directly to the membrane of the column and centrifuged for 1 minute at 21.1 x g. RNA concentration was measured using UV spectrophotometry using the nanospectrophotometer NanoDrop 1000 (Thermo Scientific) at 230 nm wavelength. Measuring the ratio sample absorbance at 260 nm and 280 nm (260/280) assessed plasmid purity. A ratio above 2 was accepted as “pure” for RNA. If the ratio was lower, it could

indicate contamination of protein, phenol or other contaminant. The RNA was stored at -80^{o}C till required.

3.2.6 Reverse transcription

Reverse transcription was performed in 1 ug of RNA using Superscript^{TM} III First-Strand Synthesis System for RT-PCR (Invitrogen, UK). The same protocol described in Chapter 2 was followed here (2.2.6). The cDNA was then diluted in 79 ul of RNase free water to have a final concentration of 10 ug/ul. The cDNA was stored at -20^{o} C till required.

3.2.7 Quantitative Polymerase Chain Reaction (qPCR)

qPCR was used to validate the microarray data. Unfortunately due to limitations in the quantity of RNA, only the expression of nine genes was assessed. These analysed genes were selected because of their co-expressed with *MYT1L* in a previous experiment performed by Dr Desrivières (data not shown) that intended to show the gene expression profile of SPC04 during differentiation [B-cell lymphoma/leukemia 11B (*BCL11B*), Cyclin-dependent kinase 5 activator 1 (*CDK5R1*), Junctophilin 3 (*JPH3*), Myelin transcription factor 1 (*MYT1*), Neural cell adhesion molecule 2 (*NCAM2*), seizure related 6 homolog (mouse)-like 2 (*SEZ6L2*), Synaptosomal-associated protein 25kDa (*SNAP25*), Synaptosomal-associated protein 91kDa (*SNAP91*) and Synapsin 1 (*SYN1*)]. qPCR amplification was performed in a 20 ul volume containing 4 ul of cDNA

(10ug/ul), 10 ul of 2X *Power* SYBR® Green PCR master mix (Applied Biosystems, UK), 0.14 uM forward primer (Table 3.3), 0.14 uM primer reverse (Table 3.3) and 5.72 ul of RNase free water. All the amplifications were carried out in triplicate using the ABI Prism® 7900 HT Sequence detection system (Applied Biosystems) under the following thermal cycle: 95^{o}C for 15 minutes (initial denaturation); 40 cycles of 95^{o}C for 30 seconds and 59^{o}C for 30 seconds (amplification); finishing with 50^{o}C for 10 seconds and 95^{o}C for 15 seconds (dissociation stage). The ABI Prism® SDS 2.1 software (Applied Biosystems) was used to analyse the specificity and relative quantification of the amplicons. The dissociation curve generated by the software was used to determine the specificity of the PCR products. The relative quantification curve of the amplicon was calculated using the cycle threshold (Ct). The mean Ct values of the triplicates were normalized against the mean of the triplicates of the housekeeping gene Ribosomal Protein L18 (*RLP18*) to produce ΔCT ($\Delta CT=Ct_{Gene}-Ct_{\text{-RPL18}}$). To calculate ΔΔCt, the difference in expression of each gene mRNA was compared against undifferentiated and non-infected SPC04 cells ($\Delta\Delta Ct=\Delta Ct_{Gene}-\Delta Ct_{undifferentiated}$).

Table 3.3 **qPCR primers**

Gene	Forward	Reverse
Human *RPL18*	GAGAGGTGTACCGGCATTTC	CTCTGGCACGCTCGAACT
Human *MYT1L*	TGGAGAGCAACCTGAAGACC	ATTCCTCTCACAGCCTGCTT
Human *BCL11B*	CGAAGATGACCACCTGCTCT	GCAAATGTAGCTGGAAGGCT
Human *CDK5R1*	CAGTGTGAAGCCTGTCGTGT	CTTCATAGCAGCATGGCAAA
Human *JPH3*	AATCCTTGCCTGTCGCTCTA	GAGCAAGATCACCATGACCA
Human *MYT1*	TTCATGATTGCTTTCCGTGA	CCGTGTGTCCACCTCTGATT
Human *NCAM2*	CAAGACTGACTGGCACCAAC	CATACACATGCAGGGCCTTC
Human *SEZ6L2*	CACTCCTACAGCCCCATCAC	GTCTTGGGGTTCAGATGGAA
Human *SNAP25*	CTGTCTTTCCTTCCCTCCCT	AGTGACGGGTTTGGCTCTG
Human *SNAP91*	AGCGTTACAGGCTCTGCTGT	CATTGGTCTCGTTGGTAGCC
Human *SYN1*	TCAGACCTTCTACCCCAATCA	GTCCTGGAAGTCATGCTGGT

3.2.7.1 *In-vitro* validation of *MYT1L* primer specificity

The approximately 20ul of MYT1L products obtained after qPCR amplification were separated by electrophoresis on a 1.2% agarose gel made up with 1X TBE buffer and supplemented with 1% Ethidium Bromide. The samples were mixed with 4 ul of 6X gel loading buffer (Thermo Scientific, UK) and loaded into the wells of the gel. Additionally, two wells were used for loading the 1 kilobase DNA ladder (250-10,000 bp Sigma, UK). Electrophoresis was performed using 1X TBE buffer at 120 V for 1.5 hours. The DNA bands obtained in the gel were visualized using ultraviolet light.

3.2.8 Bioinformatic analysis of the putative downstream targets of *MYT1L*

Additional *in-silico* analyses were performed on the genes investigated in this chapter through qPCR assays. Special attention was given to the genes that appeared to be affected when *MYT1L* was knocked down. This additional investigation had the purpose of identifying whether the genes could be direct or indirect downstream targets of MYT1L. Firstly, the MYT1L binding site was obtained from Matrix Library 9.0 (www.genomatix.de). This sophisticated software creates nucleotides or position weight matrices, which are selective descriptions of DNA patterns. They are based on nucleotide distributions detected after aligning DNA sites where a particular transcription factor is known to have a binding site. Then, the programme records each one of the nucleotides and their position to determine their frequency there. In this way, the binding site for that transcription factor is obtained (Stormo 2000).

In order to determine whether the putative genes analysed by qPCR had a MYT1L binding site, ElDorado software in conjunction with MatInspector V 8.06 software (www.genomatix.de) were used. ElDorado extracted the proximal promoter regions following the patterns established by the "Genomatix optimized length". This region was normally defined as 500 bp upstream of the first transcription start site (TSS) and 100 bp downstream of the last TSS. In case no MYT1L binding sites were found in that region, the parameters were increased to cover up to 3000 bp upstream and 300 bp downstream. This modification caused an increase in the length of the DNA sequence inspected for transcription factor binding sites. ElDorado automatically provided the TSS

to all possible transcripts of each gene on the basis of the 5' cap site. Then, MatInspector used the large library of transcription factor binding sites obtained through weight matrices to locate which ones could be a match for the DNA sequence of the gene of interest (Cartharius, Frech et al. 2005).

3.2.9 RNA labelling and microarray analysis

All the necessary processing of RNA samples for microarray analysis was performed by Eric Nasser at the NIHR comprehensive BRC, King's College London. A representative number of samples were re-quantified using Qubit® RNA assay kit (Life Technologies, UK) on a Qubit® 2.0 fluorometer following the manufacturer's protocol. Since the sample concentrations matched the ones obtained with the nanospectrophotometer, the concentrations obtained with the nanospectrophotometer were used for the following step. Additionally, the RNA integrity was analysed using Agilent RNA 6000 Nano Kit© (Agilent Technologies, Inc; Germany) on an Agilent 2100 Bioanalyzer© (Agilent Technologies, Inc).

500 ng of mRNA taken from each of the samples were labelled (biotinylation) using TargetAmp™ Nano Labeling Kit (Cambio Ltd.) and the procedure was followed according to the manufacturer's instructions. The biotinylated samples were then hybridised into Illumina HumanHT-12 v4 Expression BeadChips (Illumina Inc., USA) following the recommendation of the manufacture. The BeadChips were scanned using an Illumina Bead array confocal scanner

(Illumina Inc.). All samples were done in triplicate using a loading pattern determined by the BRC team.

3.2.10 Statistical analysis

3.2.10.1 qPCR quantification

To assess the effect of the *MYT1L* shRNAmir on the expression of the selected genes in the SPC04 cell line, the ΔΔCt values obtained for each gene were analysed using a 2-way ANOVA with the factors 'differentiation stage' and 'treatment'; additionally 'biological replication' was used as a covariance. Unfortunately, one of the biological replications was composed of only two technical replications due to a small quantity of RNA in the third replication (n=5 samples per treatment and differentiation stage). All results were presented as mean± standard error of the mean (S.E.M.). The graphs plotted the relative change in expression. This was obtained by elevating 2 to the negative power of ΔΔCt (relative fold expression=$2^{-\Delta\Delta Ct}$) (Livak and Schmittgen 2001). Additionally, the error bars of the graphs were adjusted to reflect the logarithmic scale as described in Chapter 2 (2.2.8). Also, the variance due to the biological replication was removed. A p-value <0.05 was considered statistically significant.

3.2.10.2 Microarray quantification

The data were analysed by Dr Venu Pullabhatla (NIHR comprehensive BRC, King's College London) using GenomeStudio Data Analysis Software (Illumina). The data were processed as follows:

1) Background subtraction

2) Quantile normalisation

3) Within a group independent t-test model for identifying differentially expressed probes and genes between pre-differentiation and day 7 of differentiation. The reference group here was pre-differentiation.

4) Within treatment independent t-test model for identifying differentially expressed probes and genes between treatments on day 7 of differentiation. The reference group was non-silencing shRNAmir samples.

5) Benjamini and Hochberg error correction for multiple testing (FDR).

The differences in gene expression were assessed using the Differential Score, which is a transformation of the p-value that provides the directionality (i.e. upregulated or downregulated) of the difference between the average signal in the tested group in comparison to the reference group. A Differential Score of ± 13 was considered significant and equivalent to a p-value of 0.05, while a Differential Score of ± 22 was comparable to a p-value of 0.01.

3.3 Results

3.3.1 SPC04 viral infection and differentiation

The human neural stem/progenitor cell line SPC04 was used as neural development model *in-vitro*. The cells were transduced with either *MYT1L* or non-silencing shRNAmir at the same time as differentiation was being induced. This model brought the possibility to test the effects of *MYT1L* knockdown in the transcription of other genes throughout differentiation. The pictures in Figure 3.2 showed SPC04 cells without infection (a and d) or after infection with either non-silencing shRNAmir (b, and e) or *MYT1L* shRNAmir (c, and f) at two different time points of differentiation. The morphology of the cells in all conditions changed noticeably within differentiation, specifically in regards to neurite elongation. No apparent differences were found between cells treated with *MYT1L* knockdown, control or uninfected cells at any time point of differentiation.

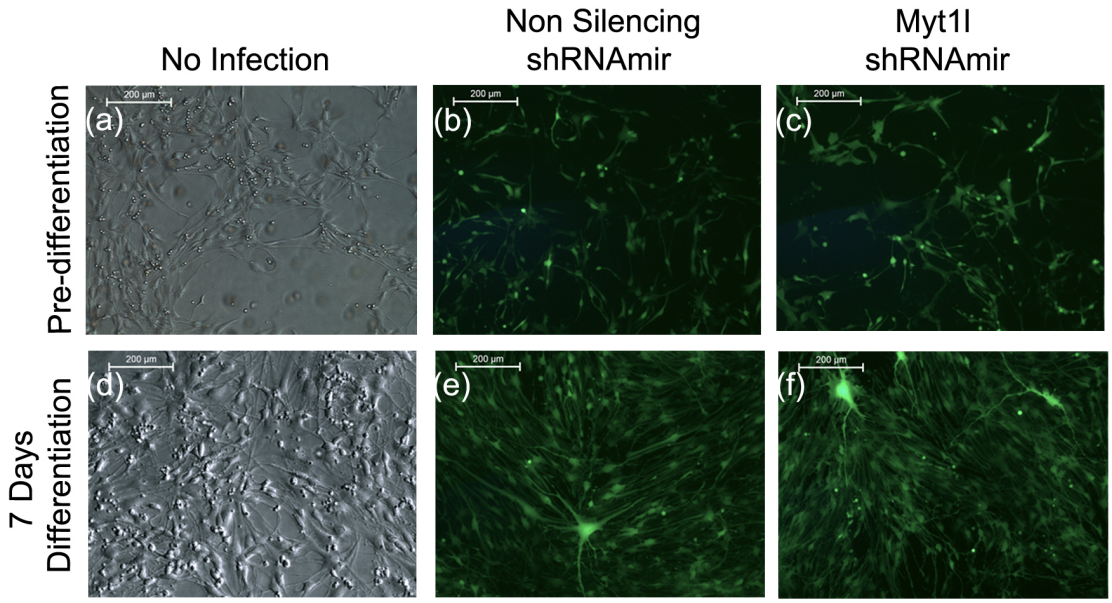

Figure 3.2 **This figure illustrates the human neural stem/progenitor cell line SPC04 differentiation and transduction with *MYT1L* shRNA and non-silencing shRNA.**

Each row shows a differentiation stage and each column represents one condition obtained for this experiment. The first column contains phase-contrast pictures of normal differentiation occurring without transduction. The second and third rows have fluorescent microscope images indicating the GFP expression of transduced cells. All photographs were taken using objective x10.

3.3.2 qPCR analysis

The RNA harvested from the transduced SPC04 cells (n=5 per treatment and differentiation stage) was firstly used to test the knockdown efficiency of *MYT1L* shRNAmir, which was about a 59% reduction [Figure 3.5 (a)]. Secondly, it was used to analyse the differences in the expression of a handful of genes that could be possible downstream targets of *MYT1L*: *BCL11B*, *CDK5R1*, *JPH3*, *MYT1*, *NCAM2*, *SEZ6L2*, *SNAP25*, *SNAP91* and *SYN*. These genes were chosen because they were co-expressed with *MYT1L* when SPC04 cells were differentiating in a previous experiment performed by our group (data not shown). Figure 3.3 illustrates the dissociation curves of the PCR products obtained for abovementioned genes. The single peak yielded during

amplification ensured that the PCR product was specific for each gene. Further corroboration of the specificity of *MYT1L* required the amplified PCR product to be separated by electrophoresis. The single band observed in this test agreed with the size determined by the primer design (Figure 3.4). In addition, the samples corresponding to *MYT1L* knockdown during day 7 of differentiation were fainter in comparison to the control, indicating the lower expression of *MYT1L* and thus downregulation of this gene in these samples.

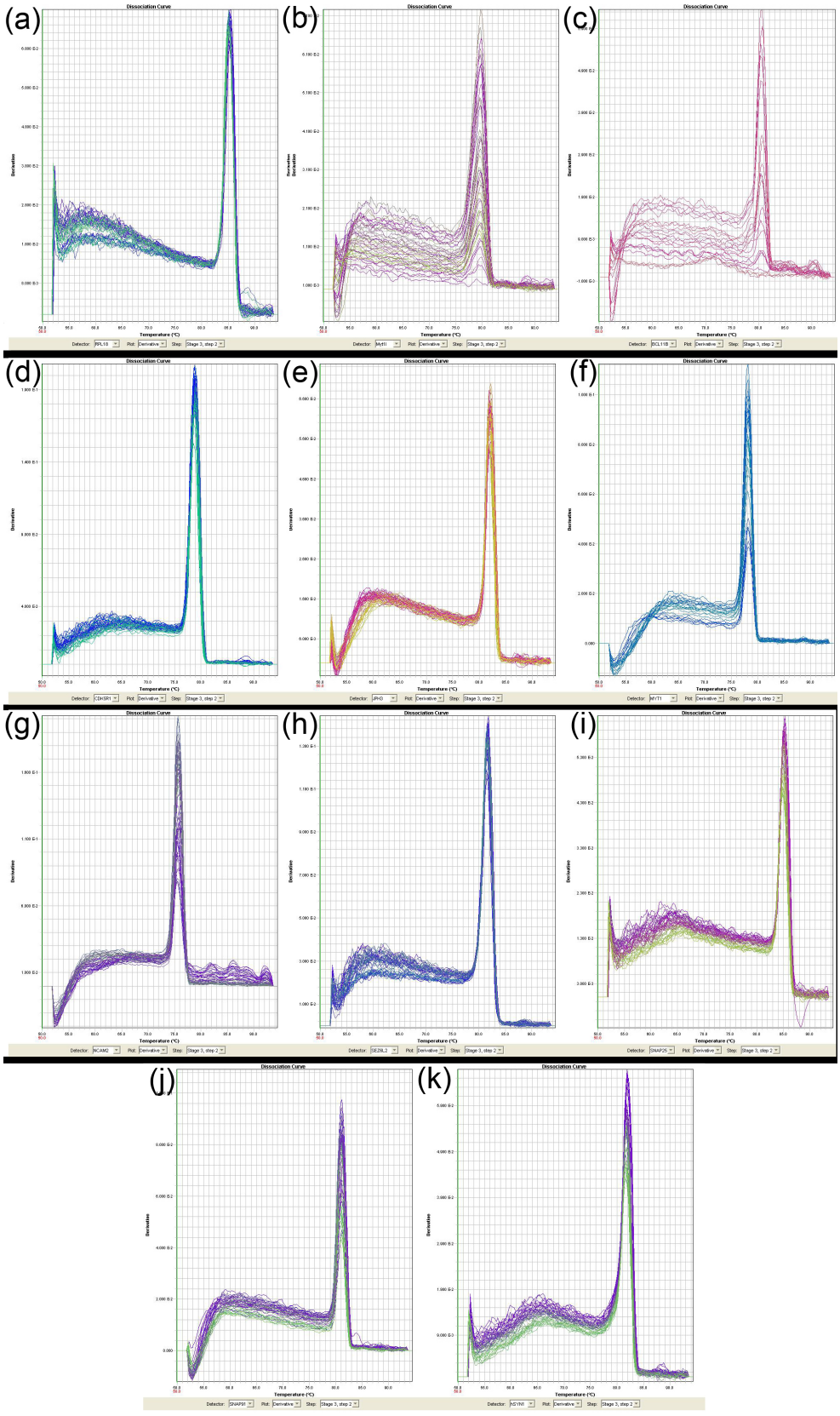

Figure 3.3 **Confirmation of *RLP18* (a), *MYT1L* (b), *BCL11B* (c), *CDK5R1* (d), *JPH3* (e), *MYT1* (f), *NCAM2* (g), *SEZ6L2* (h), *SNAP25* (i), *SNAP91* (j), *SYN* (k) qPCR primer specificity.**

The dissociation curves derived from the qPCR analysis yielded only one peak (i.e., one PCR product) per primer pair in each cell line, indicating the specificity of these primers. The plot illustrates the derivative data (the rate of change in fluorescence as a function of temperature) versus the temperature interval at which fluorescence changes.

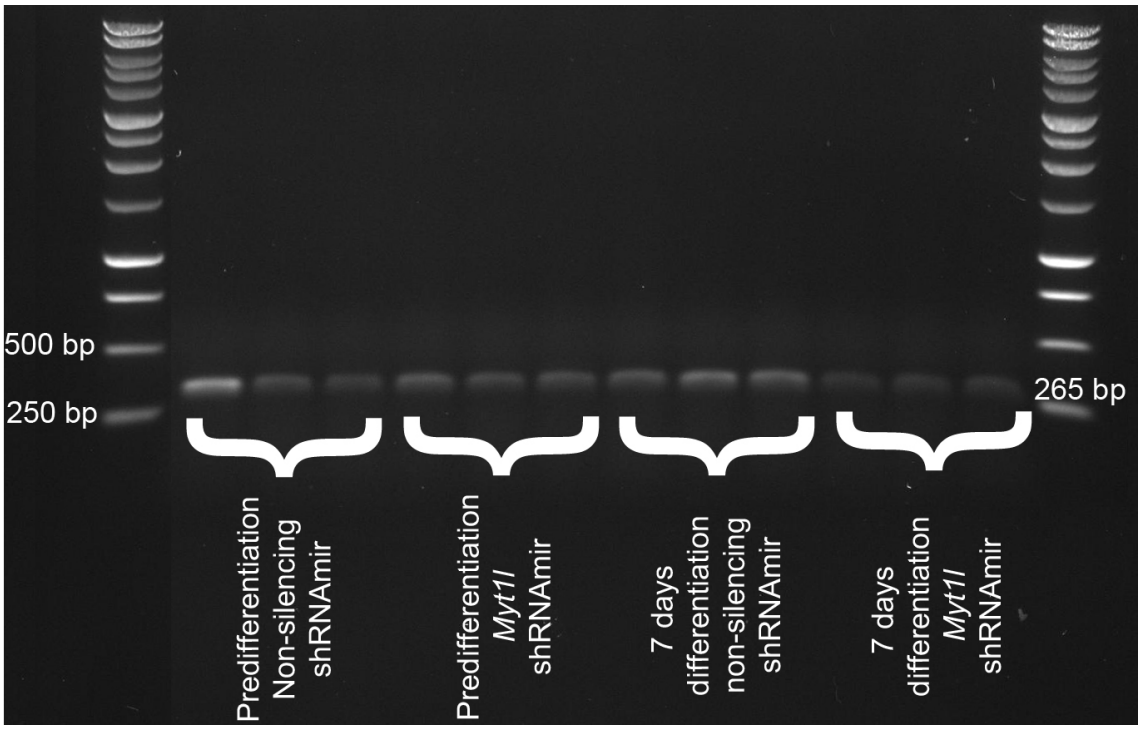

Figure 3.4 **Agarose electrophoresis patterns of qPCR *MYT1L* amplification product.**

The pre-differentiation and 7 day differentiation samples for *MYT1L* knockdown (n=3) and control (n=3) were used for electrophoresis. They corresponded to the second technical replication. The last and first columns belong to the 1kb DNA ladder used as a marker (1.2% agarose in 1xTE buffer, 120 V for 1.5 h).

3.3.3 Validation of *MYT1L* knockdown in SPC04 cells

The efficiency of *MYT1L* knockdown in differentiating SPC04 cells was assessed through a two-way ANOVA. Although there were no significant differences due *MYT1L* shRNAmir alone ($F_{1,15}$=0.486, p=0.496), the results found a significant interaction between the treatment and differentiation day ($F_{1,15}$=11.322, p=0.004). Specifically, pre-planned pairwise comparisons followed by Bonferroni correction demonstrated a significant reduction in the expression of *MYT1L* when the cells were treated with *MYT1L* shRNAmir (p=0.012) in comparison to the cells treated with the control vector at differentiation day 7. In terms of relative fold expression, this reduction of expression was about 2.42-fold and represented 59% less *MYT1L* mRNA

[Figure 3.5 (a)]. The results also indicated that the expression of *MYT1L* increased as differentiation progressed to day 7 ($F_{1,15}$=12.209, p=0.003). Particularly, control cells had a 3.99-fold increase in *MYT1L* expression at day 7 of differentiation in comparison to the pre-differentiation stage, while *MYT1L* mRNA levels remained unchanged during this period in *MYT1L* shRNAmir-containing cells [Figure 3.5 (a)].

3.3.4 Possible downstream targets of *MYT1L*

In brief, after verifying the efficiency of *MYT1L* shRNAmir to decrease *MYT1L* expression in SPC04 cells after 7 days of differentiation, the expression of a small number of genes was assessed to determine whether they were affected by this downregulation. Statistical analysis of the data produced through qPCR assays showed that the expression of all tested genes (*MYT1L*, *BCL11B*, *CDK5R1*, *JPH3*, *MYT1*, *NCAM2*, *SEZ6L2*, *SNAP25*, *SNAP91* and *SYN*) increased, as expected, throughout differentiation. After 7 days of differentiation, the expression of *BCL11B*, *MYT1*, *JPH3*, *SYN1* and *SNAP25* was significantly decreased due to the knockdown effect of *MYT1L* shRNAmir in comparison to the control. The remaining tested genes (*SNAP91*, *CDK5R1*, *NCAM2* AND *SEZ6L2*) were unaffected by the aforementioned construct.

Analysing genes individually, a 2-way ANOVA found a significant effect of treatment ($F_{1,14}$= 14.565, p= 0.002) on the expression of *BCL11B*. Pairwise comparison with Bonferroni correction showed a significant effect of *MYT1L*

shRNAmir in comparison to the control at day 7 of differentiation (p=0.004). In terms of relative fold expression, a 3.35-fold decrease was observed during this differentiation stage [Figure 3.5 (b)]. No interaction between treatment and differentiation was observed ($F_{1,14}$= 0.922, p= 0.353). Moreover, the results demonstrated that the expression of this gene was significantly induced during differentiation ($F_{1,14}$= 52.547, p= 0.000004). Comparisons within groups showed that non-silencing treated cells had a 7.72-fold increase, while cells treated with *MYT1L* knockdown only had a 4.17-fold change [Figure 3.5 (b)].

The decreased expression of *MYT1L* seemed to also have an effect on the expression of *JPH3*. A 2-way ANOVA revealed that there was an interaction between treatment and differentiation ($F_{1,15}$= 5.157, p=0.038). This test was followed by pairwise comparison with Bonferroni correction that showed a significant decrease in the expression of *JPH3* when cells were transduced with *MYT1L* shRNAmir in comparison to the control (p=0.006). Figure 3.5 (c) illustrates this decrease, which was about 1.85-fold. The test also revealed a significant treatment effect ($F_{1,15}$= 5.119, p=0.039). Moreover, the expression of this gene had a statistically significant increase due to differentiation ($F_{1,15}$= 194.006, p=5.50x10^{-10}). When comparing pre-differentiation to 7 days differentiation, the cells infected with non-silencing shRNAmir had a 6.81-fold increase. On the other hand, cells transduced with *MYT1L* shRNAmir augmented only 3.39 times [Figure 3.5(c)].

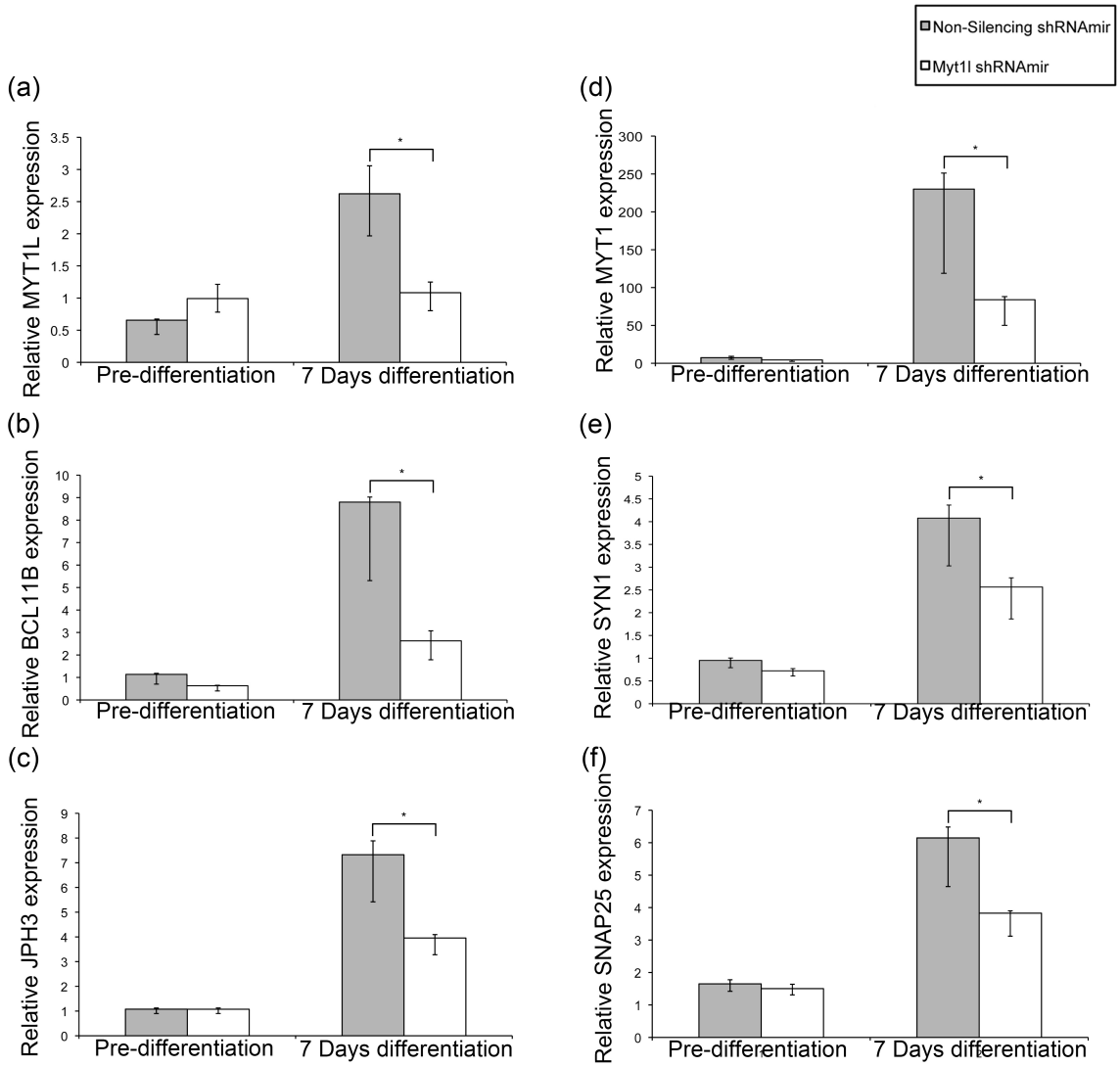

Figure 3.5 **This graph illustrates the relative fold expression of *MYT1L* (a), *BCL11B* (b), *MYT1* (c), *JPH3* (d), *SYN1* (e) and *SNAP25* (f) in SPC04 cells transduced with *MYT1L* and non-silencing shRNAmir at two different points of differentiation.**

The relative expression was obtained by elevating 2 to the negative power of ΔΔCt. The data are expressed as mean±adjusted S.E.M. (n=5 per group). *p<0.05 *MYT1L* knockdown versus control pre-planned pairwise comparison followed by Bonferroni correction of ΔΔCt values.

Another gene that was disrupted when *MYT1L* was knocked down is a family member of *MTY1L* called *MYT1*. The expression of this gene due to treatment showed to be statistically different when analysed using a 2-way ANOVA ($F_{1,15}$= 8.187, p= 0.012). During day 7 of differentiation, pre-planned pairwise comparison followed by Bonferroni correction showed a significant reduction in

the expression of *MYT1* in cells transduced with *MYT1L* shRNAmir when compared to the control (p=0.047). This was a 2.74-fold reduction in *MYT1L* shRNAmir treated cells in comparison to the non-silencing construct [Figure 3.5 (d)]. The test also indicated no interaction between factors ($F_{1,15}$= 0.041, p=0.842). However, similar to the other genes, the expression of *MYT1* changed significantly from pre-differentiation to 7 days differentiation ($F_{1,15}$= 118.619, p=1.607x10^{-8}). In terms of relative fold expression, the control cells underwent an increase of 31.05 times, while cells with reduced *MYT1L* expression had a 19.30 fold change [Figure 3.5 (d)].

The expression of *SYN1* was also compromised when *MYT1L* was knocked down, as indicated by a 2-way ANOVA ($F_{1,15}$= 8.112, p=0.012). A significant decrease in *SYN1* expression was observed during day 7 of differentiation in comparison to non-silencing construct when pre-planned pairwise comparison with Bonferroni correction was employed (p=0.026). The difference was a 1.60-fold reduction in SPC04 treated with *MYT1L* shRNAmir in comparison to the control [Figure 3.5 (e)]. Although there was no significant interaction between treatment and differentiation ($F_{1,15}$= 0.426, p=0.524), a significant change in expression was observed along differentiation ($F_{1,15}$= 100.130, p=4.954x10^{-8}). Figure 3.5 (e) illustrates this change, which accounted for a 4.29-fold increase in cells infected with the non-silencing vector and a 3.55-fold increase for cells infected with *MYT1L* shRNAmir.

In case of the expression of *SNAP25,* a 2-way ANOVA showed that the *MYT1L* shRNAmir had a knockdown effect on the expression of this gene ($F_{1,15}$= 4.668,

p=0.047). A pairwise comparison followed by Bonferroni correction demonstrated a significant decrease of *SNAP25* mRNA when *MYT1L* was decreased (p=0.03). This reduction was equivalent to a 1.61-fold change, as seen in Figure 3.5 (f). No interaction between factors was found ($F_{1,15}$= 2.028, p=0.175). However, similar to the expression of the aforementioned genes, the expression of *SNAP25* did significantly increase during differentiation ($F_{1,15}$= 85.006, p=1.439x10^{-7}). This change within treatment was about 3.73-fold in control cells and 2.55-fold in cells with reduced *MYT1L* expression [Figure 3.5 (f)].

Analysing the expression of *SNAP91* with a 2-way ANOVA also indicated it had been affected during differentiation ($F_{1,15}$= 9.785, p=0.007). A 5.92-fold increase was observed when SPC04 cells were treated with non-silencing shRNAmir, while a more modest 1.80-fold change was seen when they were treated with *MYT1L* shRNAmir. Although a decrease of 2.85 fold in SNAP91 expression between treatments was observed on day 7 of differentiation [Figure 3.6 (a)], the result failed to be significant due to treatment ($F_{1,15}$= 1.649, p=0.219) or interaction ($F_{1,15}$= 3.656, p=0.075).

Similar results were seen when the expression of *CDK5R1* was analysed with a 2-way ANOVA. Both treatments increased the expression of this gene during differentiation ($F_{1,15}$= 23.479, p=0.0002) without a significant effect of treatment ($F_{1,15}$= 0.202, p=0.659) or an interaction between factors ($F_{1,15}$= 0.003, p=0.960). In terms of fold expression, there was a 1.44-fold change for cells

treated with the control vector and a 1.40-fold change for cells that underwent *MYT1L* knockdown [Figure 3.6 (b)].

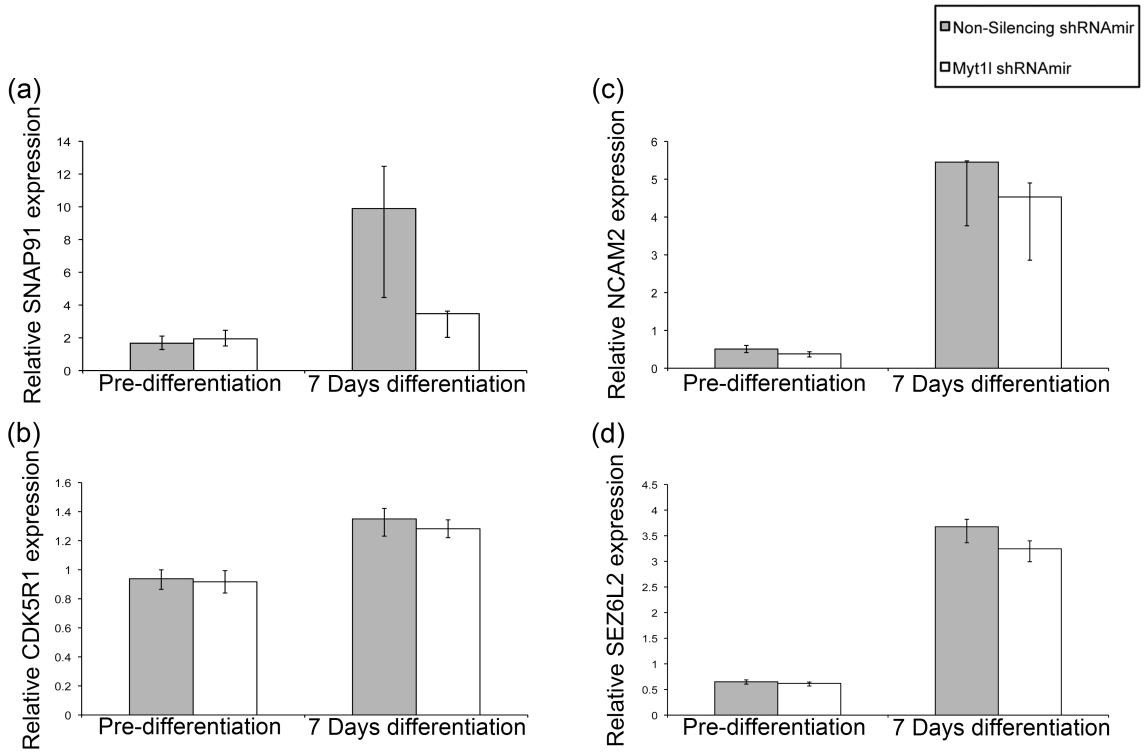

Figure 3.6 **This graph illustrates the relative fold expression of *SNAP91* (a) and *CDK5R1* (b) in SPC04 cells transduced with *MYT1L* and non-silencing shRNAmir at two different points of differentiation.**

The relative expression was obtained by elevating 2 to the negative power of ΔΔCt. The data are expressed as mean±S.E.M. (n=5 per group).

NCAM2 expression also had a significant increase during differentiation, as reported by a 2-way ANOVA ($F_{1,15}$= 141.400, p=4.890x10^{-9}). This increase due to treatment was not significant ($F_{1,15}$= 2.552, p=0.131) nor was the interaction between this and differentiation ($F_{1,15}$= 0.16, p=0.906). Both groups had a similar within-group increase in fold expression when comparing pre-differentiation to 7 days differentiation [Figure 3.6 (c)]. The expression of *NCAM2* increased 10.72 times in cells transduced with non-silencing shRNAmir and an 11.90-fold change for cells which were infected with *MYT1L* shRNAmir.

When analysing the expression of *SEZ6L2,* a significant effect attributed to differentiation was observed in a 2-way ANOVA ($F_{1,15}$= 194.006, p=4.837x10^{-14}), both without a treatment effect ($F_{1,15}$= 2.038, p=0.174) and interaction between factors ($F_{1,15}$= 0.171, p=0.685). The *SEZ6L2* expression in both, the control and the *MYT1L* knockdown samples, had an increase in fold expression of 5.65 and 5.23 respectively [Figure 3.6 (d)].

3.3.5 Bioinformatic analysis of putative MYT1L target genes

3.3.5.1 Identification of MYT1L binding site

In order to determine whether the genes that were affected by the *MYT1L* shRNAmir could be direct targets of this transcription factor, *in-silico* analyses were performed. The first one, Matrix Library 9.0, was used to determine the binding site for MYT1L. Figure 3.7 shows the graphical representations of the results obtained from aligning the MYT1L binding site weight matrices. Figure 3.7 (a) shows the degree of conservation of the nucleotides at each position through varying stack height. The red letters indicate that those nucleotides were highly conserved at each position across the matrices; the capital red letters denote the core sequence of the binding site and were used by MatInspector to predict binding sites. Figure 3.7 (b) provided a more precise description of the frequency of the nucleotides yielded by the matrix alignment with the height of the nucleotide letter corresponding to their frequency in that position.

Additional information provided by the *MYT1L* weight matrices indicated that it matched approximately 36.7% of the promoters present in vertebrates (human, rat and mouse). It has 0.82 random matches for every 1000 bp in the human genome and only 0.66 for every 1000 bp in the promoter sequences.

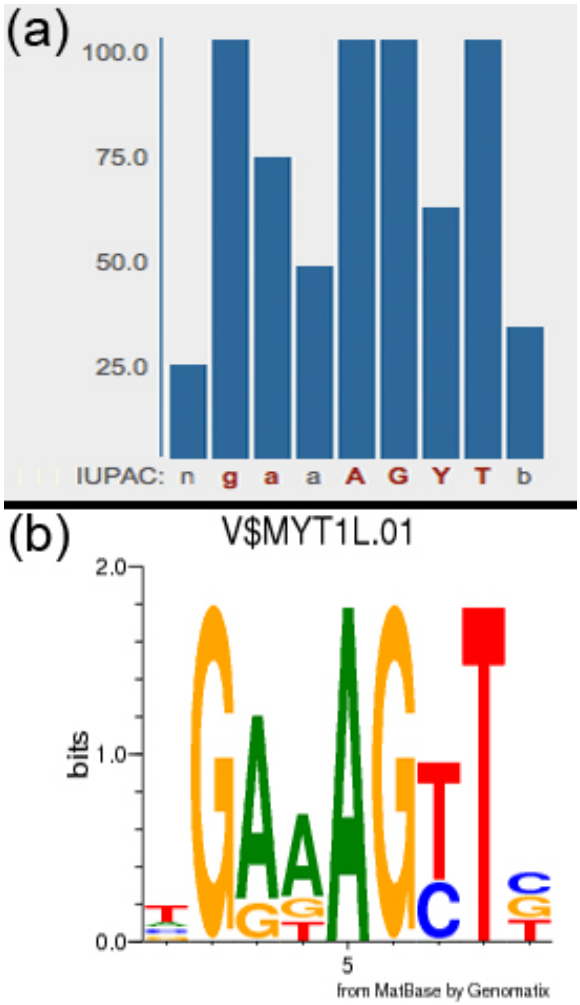

Figure 3.7 **Graphical representation of MYT1L binding site.**

Figure (a) illustrates the results of the MYT1L binding site weight matrix. The single nucleotides (A, C, G, T) are written when its frequency is above 50% and at least twice as high as the second most frequent nucleotide. Letter "Y" represents when 2 nucleotides occur in more than 75% of the underlying sequences but none of them is present in less than 50%. The letter "n" represents all other distributions. Figure (b) is a graphical illustration of the weight matrix, illustrating the nucleotides observed at each position. The height of each stack of nucleotides represents its conservation at that position. The height of the letter is a reflection of its frequency in the position. The images were created using Genomatix software (www.genomatix.de).

3.3.5.2 Identification of *MYT1L* putative downstream targets

Having found a *MYT1L*-specific binding matrix in the Matrix Library 9.0, we matched it against the promoter regions of the genes tested using qPCR, giving special attention to the genes selected above whose expression depended on *MYT1L*. The results yielded by the MatInspector software indicated putative MYT1L binding sites in *BCL11B*, *CDK5R1*, *JPH3, MYT1*, *NCAM2, SEZ6L2 SNAP25, SNAP91* and *SYN1* (Figure 3.8) within 3000 bp upstream and 1000 bp downstream of the first TSS. The indicated core similarity is based on how similar the core sequence of the transcription factor binding site and its potential binding site located in the promoter region of the analysed gene are; however, the matrix similarity is more important since it takes into account all the bases over the whole matrix length. A perfect match for any of the previous similarity scores is 1. The core and matrix similarity values for each one of the potential MYT1L binding sites in the analysed genes was higher than 0.8, indicating a good match with the MYT1L binding site.

Table 3.4 **Location of MYT1L binding sites within the promoter region of putative target genes using MatInspector.**

Accession no. indicates the particular transcript where a binding site was found. The start and end positions are relative to upstream and downstream nucleotides from the TSS used to localize MYT1L binding sites. The capital letters in red represent the core sequence.

Gene Symbol	Accession no.	Start position	End position	Core similarity	Matrix similarity	Sequence
BCL11B	GXP_121128	340	352	0.818	0.927	tgaaAGATcaact
CDK5R1	GXP_122933	54	66	0.909	0.95	ggaaAGCTgtccc
JPH3	GXP_107484	418	430	1	0.986	ggaaAGTTgcctg
MYT1	GXP_3671835	456	468	0.909	0.95	ggaaAGCTtggtg
MYT1	GXP_3671836	1419	1431	0.818	0.927	tgaaAGATcacat
NCAM2	GXP_196197	717	729	1	0.931	ggacAGTTtcaaa
NCAM2	GXP_1819684	6	18	1	0.967	agaaAGTTaagtg
NCAM2	GXP_1819684	393	405	1	1	tgaaAGTTttgta
NCAM2	GXP_2055710	191	203	1	0.958	tgatAGTTcatgt
NCAM2	GXP_3185310	291	303	0.909	0.964	tgaaAGCTggcca
SEZ6L2	GXP_91352	328	340	1	0.945	agagAGTTtcctt
SEZ6L2	GXP_3662955	334	346	1	0.945	ggagAGTTgtcgc
SNAP25	GXP_153694	217	229	1	0.945	ggatAGTTtaaac
SNAP25	GXP_153695	1019	1031	1	0.945	ggatAGTTtaaac
SNAP25	GXP_3183905	466	478	0.909	0.922	tgagAGCTtatat
SNAP91	GXP_1502044	416	428	1	0.925	agagAGTTaaaaa
SNAP91	GXP_1826254	50	62	0.818	0.927	tgaaAGGTgctag
SNAP91	GXP_3206048	97	109	1	0.967	agaaAGTTactct
SNAP91	GXP_3206048	332	344	1	0.945	agagAGTTttact
SNAP91	GXP_3206050	1	13	0.818	0.927	tgaaAGGTttact
SNAP91	GXP_3206050	183	195	1	1	tgaaAGTTtaatg
SNAP91	GXP_3206051	401	413	1	0.931	ggacAGTTgttac
SNAP91	GXP_3678501	121	133	0.909	0.95	ggaaAGCTcacaa
SYN1	GXP_261907	440	452	1	0.931	agacAGTTtgggg
SYN1	GXP_261907	1860	1872	1	0.986	ggaaAGTTcttgg

The parameters to locate a MYT1L binding site in *BCL11B* and *SYN1* were adjusted since they were outside the “Genomatix optimized length”. Both genes had only one possible promoter region. While the gene *BCL11B* had only one MYT1L binding site [antisense strand over 2500 bp upstream from the TSS; Figure 3.8 (a) and Table 3.4]; *SYN1* had two [both on the sense strand, one within 1200 bp and the other one less than 2500 bp upstream from the TSS; Figure 3.8 (d) and Table 3.4]. As for *MYT1*, there was a MYT1L binding site present in two out of the five possible promoter regions for this gene. The first one was located less than 50 bp upstream on the antisense strand, while the second was over 800 bp downstream from the TSS [Figure 3.8 (b) and Table 3.4]. In the case of *JPH3*, it had a MYT1L binding site in only one of the five possible promoter regions identified for this gene [less than 100 bp upstream of the TSS; Figure 3.8 (c) and Table 3.4]. Lastly, there were seven possible promoter sites for *SNAP25* and there was a MYT1L binding site in three of them. For two of them, the binding sites were in the upstream region, one on the sense strand (within 300 bp from the TSS) and one on the antisense strand (less than 150 bp from the TSS). The third one was around 1550 bp downstream of the TSS on the sense strand [Figure 3.8 (e) and Table 3.4].

The results for the remaining genes (*CDK5R1*, *NCAM2, SEZ6L2* and *SNAP91*), which were not affected by fluctuations in *MYT1L* expression, were not reported in detail, but the main features of their MYT1L binding sites were written in Table 3.4.

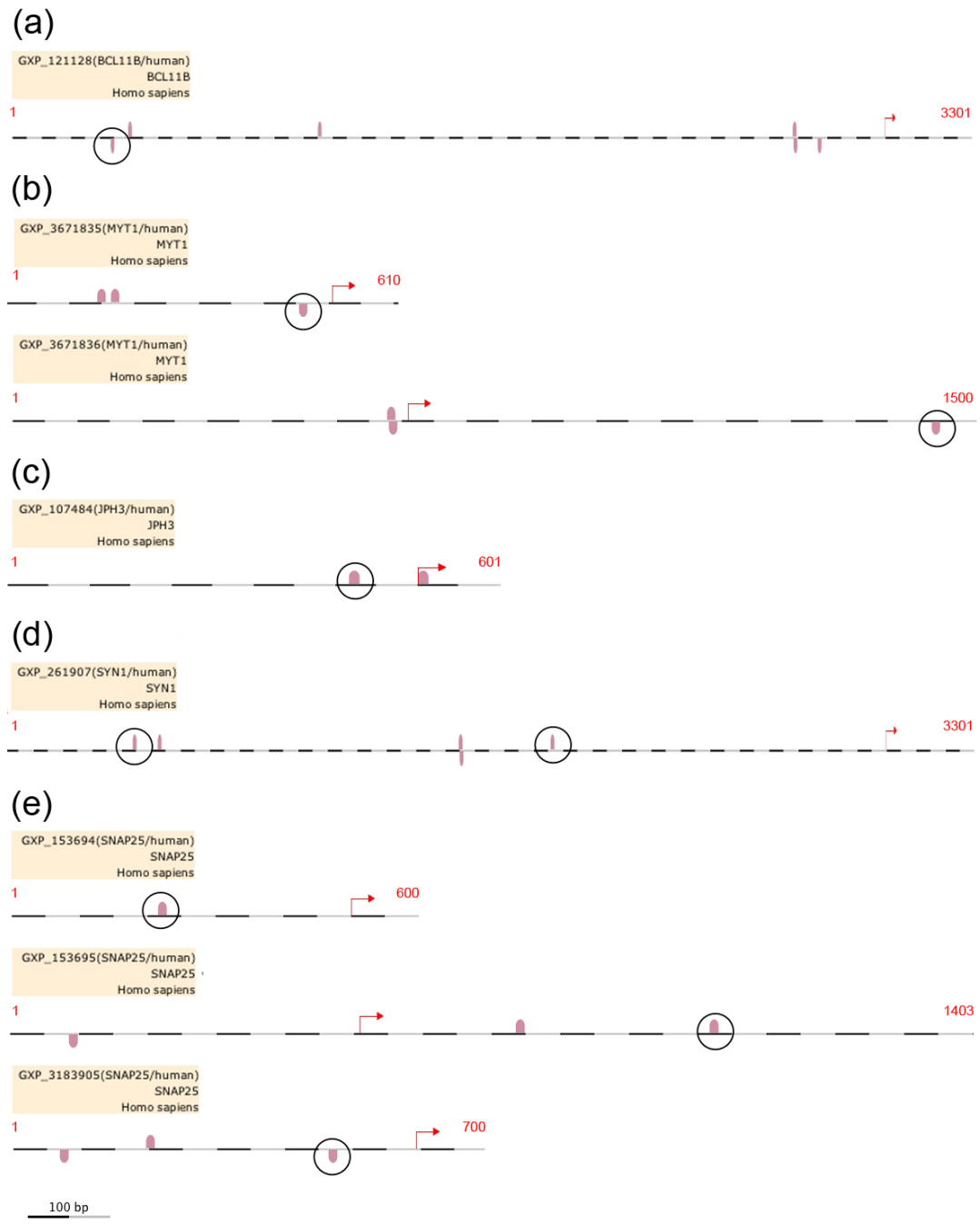

Figure 3.8 **Graphical representation of the location of MYT1L binding site in *BCL11B* (a), *MYT1* (b), *JPH3*·(c), *SYN1* (d) and *SNAP25* (e).**

The pink semi-ovals represent the binding sites for the *MYT1* family; the *MYT1L* binding sites are circled. The red arrows represent the location of the TSS in each transcript.

3.3.6 Microarray

In the quest to expand the analyses described above and identify a more

comprehensive list of possible downstream targets of *MYT1L*, microarray analyses were performed to compare the gene expression profiles of SPC04 cells infected with *MYT1L* or non-silencing shRNAmir harvested at the pre-differentiation (n=3 per treatment) and day 7 differentiation (n=3 per treatment) stages. Unfortunately, when the expression was compared within groups between pre-differentiation and 7 days differentiation, no statistically significant differences were found (data not shown). Moreover, the statistical analysis of the microarray data did not show any differences when comparing the gene profile expression of SPC04 infected with either *MYT1L* or non-silencing shRNAmir during day 7 of differentiation. The expression of any of the genes in the aforementioned comparisons led to a Differential Score ≥ 13. The entire dataset is not shown in this thesis, only the results obtained when comparing gene expression of the neurodevelopmental genes previously tested with qPCR at day 7 of differentiation (non-silencing versus *MYT1l* shRNAmir) (Table 3.5). It is worth mentioning that the directionality of the effect seen across technical replicates (n=3 for each condition and time point) is inconsistent, which is reflected in the large standard deviations calculated for the expression of each gene. This could be a reason for the lack of significant differences in gene expression observed in this experiment.

Table 3.5 **Differences in gene expression between SPC04 cells treated with non-silencing shRNAmir and *MYT1L* shRNAmir harvested at day 7 of differentiation (n=3 per treatment).**

The Differential Score is a transformation of the p-value providing the directionality of the p-value. It is based on the difference between the average signal of *MYT1L* shRNAmir versus non-silencing shRNAmir. A value of ± 13 (equivalent to p-value 0.05)

	Non Silencing shRNAmir		***MYT1L* shRNAmir**		
Symbol	**Average Signal**	**Array Standard Deviation**	**Average Signal**	**Array Standard Deviation**	**Differential Score**
MYT1L	8.3	12.912	5.1	17.437	0
BCL11B	-1.2	6.551	-2.4	5.987	0
CDK5R1	1164.2	381.941	958.2	64.412	-0.001
JPH3	0.7	3.365	-17	4.296	-0.001
MYT1	199.8	327.315	42.7	28.328	-0.001
NCAM2	-2.2	10.264	-0.7	7.445	0.001
SEZ6L2	44.5	42.884	31.7	18.181	0
SNAP25	775.8	637.544	409.4	159.661	-0.001
SNAP91	39	26.075	5.7	4.055	-0.001
SYN1	58.8	49.832	27.7	13.297	-0.001

3.4 Discussion

The information acquired in this chapter by knocking down *MYT1L* in the stem cell line SPC04 and the bioinformatic data retrieved from MatInspetor (Genomatix) have provided valuable evidence about the downstream targets of this transcription factor. Even though the analysis of the microarrays was inconclusive, the qPCR assays found that *BCL11B*, *JPH3*, *MYT1*, *SNAP25* and *SYN1* had decreased expression due to *MYT1L* shRNAmir after 7 days of differentiation. Further *in-silico* analyses of the promoter regions of these genes

revealed they all have a binding site for MYT1L, suggesting that they could all be direct targets of this transcription factor.

3.4.1 Possible *MYT1L* downstream targets according to qPCR

Due to the unfortunate results obtained through microarrays, this chapter had to rely only on the results obtained by qPCR. Firstly, these results validated the knockdown efficiency of the *MYT1L* shRNAmir in the human neural stem/progenitor cell line SPC04 at day 7 of differentiation. *MYT1L* expression observed in these experiments was very low during the undifferentiated and pre-differentiated stages, gradually increasing as differentiation progressed. At day 7 of differentiation, there was around 59% less *MYT1L* mRNA present in the SPC04 cells transduced with *MYT1L* shRNAmir in comparison to cells infected with the control vector. As a consequence, this reduction in *MYT1L* expression was significantly associated with decreased expression of five out of the nine genes tested in this experiment during day 7 of differentiation: *BCL11B*, *MYT1*, *JPH3*, *SYN1* and *SNAP25*. The nine genes had been selected on the basis of being co-expressed along with *MYT1L* during the differentiation of the SPC04 cell line in a previous experiment (data not shown).

In order to determine whether these genes could be directly affected by the expression of *MYT1L*, their promoter regions were matched against the MYT1L binding site. Interestingly, seven of them (*CDK5R1, JPH3, MYT1, NCAM2*, SEZ6L2, *SNAP25* and *SNAP91*) had a MYT1L binding site within 1000 bp

upstream of a TSS, while *BCL11B* and *SYN1* that had one within 2500 bp upstream. Still, it has been reported that both distal and proximal transcription factor-binding sites can promote transcription (Koudritsky and Domany 2008).

It is worth mentioning that the MatInspector software, which provided the previous *in-silico* results, has been optimized to reduce the number of false positives. Additionally, the MYT1L binding site obtained by the programme was quite specific. Randomly, it only matched 0.66 for every 1000 bp of the promoter region. Nevertheless, this software only infers the binding potential of a transcription factor, but not the functionality of such site. The functionality can only be assessed through an *in-vitro* experiment (Cartharius, Frech et al. 2005). The results yielded by the qPCR assay performed in this chapter only supported a co-expression between *MYT1L* and *BCL11B*, *MYT1*, *JPH3*, *SYN1* and *SNAP25*. This outcome possibly suggests that the *MYT1L* binding site located on the aforementioned genes is functional, making those genes downstream targets of *MYT1L*.

Among the genes disrupted by *MYT1L* expression, *MYT1* and *BCL11B* are also transcription factors. The former belongs to the same CCHHC zinc finger family as *MYT1L* (Jiang, Yu et al. 1996, Kim, Armstrong et al. 1997). It is highly expressed during brain development in neural progenitor cells (Kim, Armstrong et al. 1997). It has potentially been involved in oligodendrocytes differentiation by regulating the expression of myelin specific genes (Nielsen, Berndt et al. 2004). Similarly, *BCL11B* is increasingly expressed in the brain during development (Leid, Ishmael et al. 2004). It has been linked to the Brain-derived

neurotrophic factor (*BDNF*) signalling pathway (Tang, Di Lena et al. 2011), critical for neuronal differentiation and survival (Bekinschtein, Cammarota et al. 2008). Specifically, Arlotta and collaborators (Arlotta, Molyneaux et al. 2008) confirmed that *BCL11B* is an important factor in the differentiation of striatal medium spiny neurons and the development of axonal projections of the corticospinal motor neurons.

The expression of *MYT1L* seemed to have an effect on two genes related to synaptic vesicles and the release of neurotransmitters: *SNAP25* and *SYN1*. The former codes for presynaptic plasma membrane protein which regulates vesicle trafficking (Bark, Hahn et al. 1995); at synaptic level, SNAP25 is important for neurotransmitter release evoked by action potentials (Washbourne, Thompson et al. 2002) and during development, it helps the growth cone to extend by modulating vesicle fusion, which promotes axonal growth (Osen-Sand, Staple et al. 1996). On the other hand, *SYN1* codes for a neuron-specific phosphoprotein present at nerve terminals (De Camilli, Harris et al. 1983, Huttner, Schiebler et al. 1983), which also regulates neurotransmitter release by controlling the anchoring of synaptic vesicles to the cytoskeleton (Moretto, de Mattos-Dutra et al. 1999) and clustering them in a pool near the synaptic terminal (Greengard, Valtorta et al. 1993). One study showed that during neuron development in a *Syn1* knockout mouse, the formation of synapses occurred at a slower rate and the neuron elongation was shorter and less branched (Ferreira, Chin et al. 1998).

Lastly, *MYT1L* expression also modified *JPH3* expression. This gene belongs to

a family of junctional membrane complexes between the plasma membrane and the endoplasmic reticulum. This family is present in excitable cells and is believed to participate in the foundation of crosstalk between ion channels in order to regulate calcium influx (Nishi, Mizushima et al. 2000, Takeshima, Komazaki et al. 2000), a process which is important for synaptic plasticity in the neurons (Bardo, Cavazzini et al. 2006, Garbino, van Oort et al. 2009).

3.4.2 Microarray results

Microarrays represent a good approaches to acquiring gene expression profiles (Hoheisel 2006). Unfortunately, in this study there were discrepancies in the results obtained through the microarray and qPCR analyses. According to the microarray data, there were no significant differences between the genes expressed by SCP04 cells transduced with non-silencing or *MYT1L* shRNAmirs on either pre-differentiation or 7 days differentiation. Additionally, no differences were found within group when the expression was compared between the two time points of differentiation. The lack of differences between the genes expressed during pre-differentiation and 7 days differentiation is incongruent with the phenotypic changes observed during differentiation (Gurok, Steinhoff et al. 2004).

The results obtained through qPCR assay and the incongruence observed in directionality among technical replications during the analysis of microarray data suggested possible technical problems (e.g. with the processing of the RNAs for

the hybridisations, the chip itself or its loading). Irizarry and collaborators (Irizarry, Warren et al. 2005) noted in a multiple laboratory comparison of microarray platforms that the variability observed between microarray results among different laboratories was likely due to the laboratory techniques. RNA samples require the synthesis of double stranded cDNA and biotin labelling before being hybridized into the microarray chips. This process can be a tedious and time-consuming protocol making it prone to human error. Any error in the protocol or mislabelling can lead to inconclusive results (Knight 2001). Since this part of the experiment was not directly performed in our laboratory, it is only possible to speculate on this being the possible cause for the failure of the experiment.

Another possible reason why the microarray analysis did not perform as excepted is the RNA quality. Although RNA was carefully extracted, underwent quality control and all possible measures were taken to avoid its degradation throughout the process performed by us, it is known to be less stable than DNA (Kim, Zakharkin et al. 2010). One of the problems encountered when dealing with low quality RNA is the degree of degradation of the samples between different time points, which could lead to differences in expression (Gingrich, Rubio et al. 2006). In this experiment, all samples were always kept in optimal storage condition and samples belonging to each time point were extracted and stored simultaneously. If degradation occurred within storage, then the variance should be similar between all the samples belonging to a specific time point of differentiation. Gingrich and collaborators (Gingrich, Rubio et al. 2006) have noted that using degraded RNA in microarrays can compromise the detection of

genes, especially those whose expression is low. By contrast, qPCR has been reported of being capable of amplifying degraded RNA such as the RNA coming from formalin fixed and paraffin-embedded tissue (Specht, Richter et al. 2001).

Even though microarray technology has matured in the past decades and standardized protocols have been implemented, it still has its limitations. Among these limitations is its lack of consistency in data extracted from different platforms or different laboratories, especially with low expressed genes, as confirmed by qPCR validation (Irizarry, Warren et al. 2005, Liu, Kuo et al. 2012). Moreover, the data acquired through microarrays are still subject to qPCR validation (Larkin, Frank et al. 2005). Whilst qPCR has shown to produce more reliable, powerful and replicable data (Bustin and Nolan 2004, Bahat, Kedmi et al. 2013), there is still variability which could cause issues and it has been determined that it largely depends on technical replications (Taylor, Wakem et al. 2010). Optimizing the reaction has been useful in homogenising the results and reducing variability. The two most important measures which should be taken are avoiding the amplification of genomic DNA by removing it when RNA is extracted and using optimal primer design (Sinicropi, Cronin et al. 2007). In this study, both were followed. One extra step was undetaken while extracting the RNA to remove genomic DNA. In addition, the optimal primer design was corroborated by the analysis of the dissociation curves, which provided evidence of the specificity of the primers to detect the correct gene.

3.4.3 Conclusions and limitations of this study

Dysregulations in the sequence and expression of *MYT1L* have been linked to some neurodevelopmental disorders such as major depression disorder (Wang, Zeng et al. 2010), schizophrenia (Vrijenhoek, Buizer-Voskamp et al. 2008, Addington and Rapoport 2009, Lee, Mattai et al. 2012), autism (Meyer, Axelsen et al. 2012, Rio, Royer et al. 2012) and mental retardation (Gruchy, Jacquemont et al. 2007, Zou, Van Dyke et al. 2007, Bonaglia, Giorda et al. 2008, Stevens, van Ravenswaaij-Arts et al. 2011). The pathology of these disorders appears to be caused by impairments, which arise during the course of brain development (Van Loo and Martens 2007). Additionally, information obtained from *in-vitro* trials has demonstrated the importance of *MYT1L* expression for the development of functional neurons. Although, it can be inferred that the appropriate expression of *MYT1L* is important for neurogenesis, the precise genetic pathway in which this transcription factor is active during brain development remains largely unknown. The use of human/progenitor stem cells to model neural differentiation along with gene silencing techniques has brought about the possibility of studying at least one important part of development: cell differentiation. The results from this study have enriched the knowledge of the possible downstream targets of *MYT1L* during brain development. According to the results of Kim and collaborators (Kim, Armstrong et al. 1997), the expression of *Myt1l* in the rat started around embryonic day 13-15. Coincidentally in the rat, neurogenesis in some brain structures such as the cranial sensory and vestibular nuclei begin around the same day and there is no record of neurogenesis starting earlier than embryonic day 12 (Finlay and Darlington 1995, Workman, Charvet et al. 2013). The fact that it continues to

express and reaches its maximum expression right before birth coincides with the formation of synaptic connections and the peak in neurogenesis for most areas of brain (Workman, Charvet et al. 2013). This overlap, coupled with evidence indicating the importance of *Myt1l* for neuronal maturation, could possibly indicate that this transcription factor is responsible, to some degree, for the induction of neurogenesis and synaptogenesis in the rat and possibly in the human. The fact that all the genes that appeared to be targets of *MYT1L* in this study, apart from *JPH3*, are known to be involved in brain development further supports this hypothesis. In the particular case of *JPH3*, it might not be involved directly in the development of the neuron but, it is believed to play a role in the formation of the junctional membrane complex (Holmes, O'Hearn et al. 2001). This complex is thought to anchor the plasma membrane and the endoplasmic reticulum to connect intracellular and extracellular channels to allow the release of intracellular calcium required for cell signalling (Nishi, Sakagami et al. 2003, Garbino, van Oort et al. 2009). This mechanism is likely to be present in some forms of synaptic plasticity (Rose and Konnerth 2001, Kakizawa, Kishimoto et al. 2007), which may contribute to the reorganization of neuronal networks (Johnston 2009).

The results obtained in this chapter should be taken with caution. First, SPC04 is an immortalized cell line derived from week 12 of foetal development and it is possible that the genes expressed by this line differ from the mature *in-vivo* spinal cord cells. Another important limitation was the sample size. Taylor and collaborators (Taylor, Wakem et al. 2010) have suggested that having three biological replications consisting of two technical reapplications each is enough

to mitigate the variability. In order for this study to fulfil these criteria, an additional biological replication would be required to decrease the variance and possibly increase the significance of the results.

A further limitation of this study was the lack of results obtained through microarray. The genes that were analysed through qPCR were very limited and a global expression profile could have broadened the MYT1L downstream targets. The study of MYT1L downstream targets could be further expanded and enriched by repeating the microarray experiment and the production of a MYT1L antibody. The former could provide evidence of other possible MYT1L downstream targets, while the latter would allow for additional tests such as chromatin immunoprecipitation and DNA sequencing (ChIP-sequencing). ChIP-sequencing has the goal of identifying functional elements in the DNA such as transcription factors (Yip, Cheng et al. 2012). In this type of experiment, the proteins that bind the DNA are cross-linked to their binding site and an antibody against the protein of interest recognizes the site of interaction. This site is isolated by immunoprecipitation and a readout of the binding site can be produced to identify the gene it belonged to (Valouev, Johnson et al. 2008). Finally, the study also has limitations due to the specificity of the antibody and might have been unable to detect transient binding of transcription factors (Tang, Di Lena et al. 2011). If the study presented in this chapter could be complemented with consistent data from microarray experiments and ChIP-sequencing, more robust results could be achieved to unravel the transcriptional pathway in which MYT1L participates.

Chapter 4 : Behavioural characterization of *Myt1l* knockdown in the dorsal hippocampus of adult mice

4.1 Introduction

As previously mentioned in Chapter 1, the discovery of the endogenous RNAi pathway was followed by the development of new experimental techniques to modulate the activity of a gene (Hommel, Sears et al. 2003, Zamore and Haley 2005). This alteration of gene expression has opened new possibilities not only for the study of gene function but also for the therapeutic applications it offers (Blomer, Naldini et al. 1997). An indispensable element to modify genetic material in-vitro and in-vivo is a reliable vector capable of efficiently integrating into the genome of the host cell (Amado and Chen 1999). Lentiviral vectors have been proven to achieve this task in cell culture, as shown in Chapter 2 and 3, but they also may be used for in-vivo experiments (Baekelandt, Claeys et al. 2002). Neuroscience research has benefited from these approaches to widen our understanding of the role of genes in neurobiological processes (Genc, Koroglu et al. 2004).

4.1.1 Lentivirus mediated gene delivery in the mouse brain by stereotactic surgery

Producing animal models is essential to studying the function of a gene. These models provide an insight into the physical and behavioural consequences of

modifying gene expression (Heldt and Ressler 2009). The production of transgenic animals using conventional approaches such as gene knockout remains expensive and time consuming (Jaenisch 1988). In the particular case of reducing the expression of a gene, an alternative method uses viral vectors containing small interfering RNAs capable of integrating into the RNAi pathway of the host cells as described in Chapter 1 (Hommel, Sears et al. 2003). One type of vector commonly employed in animal work because of their long-term gene expression is the lentiviral vector (Baekelandt, Claeys et al. 2002). These vectors offer great advantages over other types of vectors due to their ability to infect proliferating and non-proliferating cells; they are replication defective to avoid spread of infection, do not trigger a humoral response from the host animal (Naldini, Blömer et al. 1996); and they integrate complex expression cassettes like the shRNA into the host genome (Jakobsson and Lundberg 2006). The delivery of these vectors into the brain is through stereotactic surgery. In the past, this technique has been a valuable tool to create lesions to mimic diseases, insert probes for microdialysis or implant electrodes to stimulate or record brain activity (Messier, Émond et al. 1999). In recent years, this surgery has been helpful for virus mediated gene delivery, allowing the manipulation of gene expression within a particular region of the brain (Cetin, Komai et al. 2007). Additionally, the surgery can be performed at any stage of the life of an organism, giving the opportunity to study the impact of gene expression at particular time points (Kuroda, Kutner et al. 2008).

Rodents have been extensively used as models for gene modification because of the number of pure genetic lines commercially available (Messier, Émond et

al. 1999). In particularly the mouse has been employed because 99% of the human genes have a mouse homolog gene (Ahmad-Annuar, Tabrizi et al. 2003, Austin, Battey et al. 2004). Furthermore, when the gene expression of the brain was compared between those two species, it was found that there is a high correlation between gene expression profiles in human and mouse (Strand, Aragaki et al. 2007). Moreover, humans and mouse have similar physiology and mice are prone to some of the human pathologies (Rosenthal and Brown 2007). Although these are good arguments in favour of the mouse as a model, it is important to consider that the complexity and size of the brain in humans and mice is quite different and mice do not have the same higher cerebral functions as humans (Seong, Seasholtz et al. 2002).

4.1.2 Using a mouse model to study *Myt1l* function

Taking advantage of the techniques described above, it is possible to investigate the function of *Myt1l* in the mouse brain. As previously mentioned in Chapter 1, the expression of *Myt1l* remains at detectable levels in the adult brain of both human and mouse. Interestingly, as observed in Figure 4.1, there is an increased expression of *Myt1l* in the dorsal hippocampus in comparison to other regions, especially in the pyramidal and oriens cell layers of the dorsal hippocampus. It is well-known that the hippocampus plays a crucial role in memory and learning (Gilbert and Kesner 2003), in particular the dorsal hippocampus is involved in spatial learning (Moser, Moser et al. 1993). However, the hippocampus also has been associated with emotional behaviours like anxiety (Gray and McNaughton 2000, Rezayat, Roohbakhsh et

al. 2005). The observation of increased *Myt1l* expression in the dorsal hippocampus during adulthood might indicate that this gene is required in this area for learning and memory, and emotional behaviour. Additionally, genome studies have associated the following mental disorders with *Myt1l*: schizophrenia (Vrijenhoek, Buizer-Voskamp et al. 2008, Addington and Rapoport 2009, Lee, Mattai et al. 2012, Li, Wang et al. 2012), major depression disorder (Wang, Zeng et al. 2010), autism (Garbett, Ebert et al. 2008, Meyer, Axelsen et al. 2012) and mental retardation (Gruchy, Jacquemont et al. 2007, Bonaglia, Giorda et al. 2008, Stevens, van Ravenswaaij-Arts et al. 2011); and these disorders all have been related, at least in part, to neuropathological changes in the hippocampus (Huttenlocher 1991, Raymond, Bauman et al. 1995, Lodge and Grace 2007, Belmaker and Agam 2008). Owing to these reasons, it is reasonable to assess the behavioural outputs resulting from decreasing *Myt1l* expression in this region.

The aforementioned diseases are very different from one another and they are thought to be caused by a diverse set of genes (Chelly, Khelfaoui et al. 2006, van Os, Rutten et al. 2008, Wall, Esteban et al. 2009, Bosker, Hartman et al. 2011). Since the function of *Myt1l* in the adult brain remains largely unknown, this chapter focused on the effects *Myt1l* has on certain behavioural patterns instead of trying to model the psychiatric disorders linked to *Myt1l*. The behaviours of interest for this chapter were learning and memory, anxiety, and social interaction. These behaviours were selected based on a careful review of the literature on *Myt1l*.

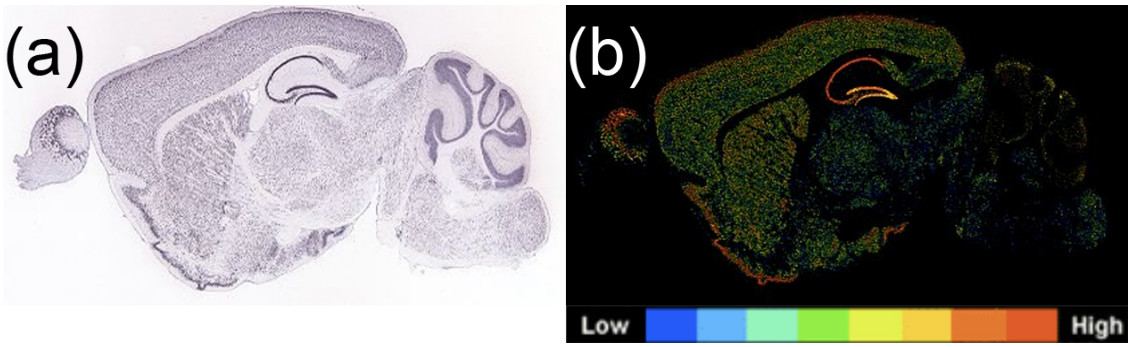

Figure 4.1 **Expression of *Myt1l* in the mouse inbred strain C57BL/6J (Postnatal day 56).**

All images were obtained from the Allen Mouse Brain Atlas. (a) In situ hybridization (ISH) for *Myt1l* mRNA in a sagittal brain section. (b) This image is another form of representing the gene expression obtained by ISH. Each ISH image undergoes a detection algorithm to create a high-resolution greyscale image to identify pixels that correspond to gene expression. The intensity of the signal is colour-coded, with blue representing the lowest gene expression and red the highest (Lein, Hawrylycz et al. 2007).

4.1.3 Aims of the study

Recent evidence has named *Myt1l* as a putative candidate gene for a wide range of psychiatric disorders (schizophrenia, autism, major depressive disorder and mental retardation) that might suggest its importance during adulthood. The aim of this chapter was to investigate the role *Myt1l* plays in the dorsal hippocampus of the adult mouse by selectively knocking it down using shRNAmir lentiviral vectors. The dorsal hippocampus was selected because of its high *Myt1l* expression, possibly suggesting a role of this gene in memory and learning, or emotional behaviours that have been associated with this brain region. Moreover, it was observed that the psychiatric diseases linked to *MYT1L* presented some neuropathological changes in the hippocampus, probably indicating the relevance of this structure to each one of those pathologies. Although, those diseases appeared to be neurodevelopmental, it is unclear whether the reduced expression of *MYT1L* in the adult could induce some of the symptoms presented in the disorders. Therefore, it was decided to use adult

mice in this project, since creating an adult model represented a more cost-efficient approach. After surgery and in order to elucidate the possible effect of knocking down this gene on behaviour, the animals underwent a battery of tests that included locomotor activity, anxiety, memory and learning, and social interactions. These tests were selected based on some of the dorsal hippocampus-associated behaviours and symptoms shown by the patients affected with mutations in *MYT1L*. It is hoped the results of this study will give insight into the impact of *Myt1l* expression in the dorsal hippocampus.

4.2 Methods

4.2.1 Lentiviral vectors

pGIPZ lentiviral vectors containing shRNAmir targeting *Myt1l* and non-silencing shRNAmir (negative control) were produced as described in Chapter 2. The viral particles were further concentrated and the titre was measured as described in Chapter 3. The lentiviral stock titre used for subsequent behavioural studies was adjusted with sterile PBS to 3 x 10^{-9} TU/ml for both constructs.

4.2.2 Animals

Upon arrival, male C57BL/6J mice (7 to 8 weeks old; Charles River Ltd., UK) were housed in Tecniplast cages (32cm x 16 cm x 14 cm) containing sawdust

(Litaspen premium), a cardboard house and bedding material (Sizzlenest, Datasand Ltd., UK) in groups of 4 or 5 mice per cage. After surgery, animals were single housed and allowed to recover for 4 weeks and then remained singly housed for the duration of the behavioural test battery. The mice were housed in a room of their own in order to minimize any behavioural disruption caused by other mice or people. The sawdust and bedding material were changed every two weeks and cages were changed once a month, on days when the mice were not being tested or after the daily experiment was over to minimize disruption to the mice.

The conditions of the housing room were kept constant with a temperature of 21^{o} C, humidity of 45% and under a 12-hour light/dark cycle, lights were on at 8:00 am (270 lux). They had *ad libitum* access to food (Rat and Mouse No.3 Diet, Special Diet Services, UK) and water. The weight of the mouse was recorded before surgery, one week after surgery, two months after surgery and on the day of perfusion.

Mice were left for 2 to 3 weeks to adapt before surgery. All procedures and tests were scheduled at least 1 hour after the lights were on and ended 1 hour before the lights went off. All housing and experimental procedures were performed according to the Animals (Scientific Procedures) Act 1986 and they were carried out at the Biological Services Unit located in the Institute of Psychiatry, King's College London. All efforts were made to reduce animal suffering.

4.2.3 Experimental setup

Mice were divided into two experimental groups (n=19/group). One group received lentiviral vectors containing non-silencing shRNAmir and the other group received *Myt1l* shRNAmir. Three mice in each group were used for validation of the *in-vivo* knockdown effect and did not undergo behavioural testing. The remaining 16 mice in each group were separated into two batches for testing: testing of batch 1 and 2 was separated by 7 days. Each animal received two viral vector injections, one in each hemisphere targeting the dorsal hippocampus. Before the start of behavioural tests, the identity of each mouse was blinded by a separate experimenter. The initial test battery included: open field, novel object recognition and Morris water maze. Based on preliminary findings, the mice then were tested on the elevated plus maze, light/dark box, three-chamber social approach, food burying task and social investigation (Figure 4.2). The last three tasks were performed on a smaller cohort of animals (shRNAmir non-silencing n=11 and shRNAmir *Myt1l* n=11) because eight mice were required for immunohistochemical verification of the injection site. Reducing the number of animals was taken into account when designing the experiment.

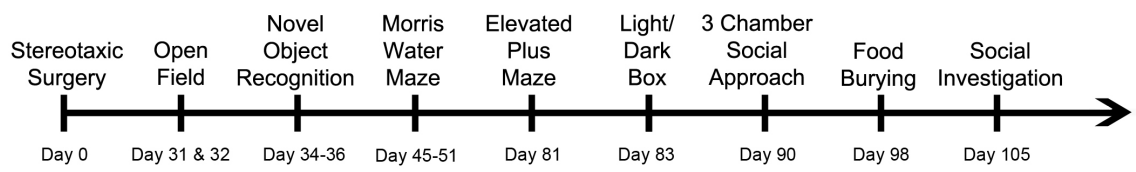

Figure 4.2 **Flow diagram of the experimental design.**

4.2.4 Stereotaxic surgery and validation of site of injection

The mouse was deeply anaesthetised by an intraperitoneal injection (IP) of 0.2 ml per 100 g of a mixture composed by Ketamine (37.5 mg/ml; Pfizer, UK), Medetomidine (0.38 mg/ml; Janssen, Finland) and sterile water (Hameln, UK). To deepen analgesia, the mouse received a subcutaneous (SC) injection of Rimadyl (5 mg/Kg; Pfizer, UK) immediately before surgery. The animal was then mounted onto a Kopf stereotactic frame, followed by a midline incision in the skull and skin retraction to localize Bregma. Coordinates were adjusted to this anatomical point to bilaterally drill burr holes above the dorsal hippocampus (AP -2 mm, ML ± 1.5 mm) (Paxinos and Franklin 2003). A cannula, connected through polyethylene tubing to a 10ul-Hamilton syringe mounted into syringe pump (CMA 400) was lowered (DV -1.8 mm from the top of the brain) to inject 1 ul of lentiviral viral stock of pGIPZ shRNAmir non-silencing (n=19) or pGIPZ shRNAmir *Myt1l* (n=19). The delivery rate of the virus was 0.1 ul per minute. Following injection, the cannula was left for 2 minutes to allow diffusion of the virus and then removed in steps of 0.5 mm every 2 minutes till the cannula was out of the brain. The holes in the skull were covered with dental cement and the incision was sutured using silk braided non-absorbable suture (Ethicon, UK). After surgery, the mouse received a SC injection of 0.1 ml/100 g Antisedan (1mg/ml; Janssen, Finland) to revert the sedative effect; and was put in heated cage until it awakened. Mice were checked daily and allowed to recover for four weeks before starting behavioural testing.

After behavioural testing was completed, the tested mice (n=16 mice each

group) received a lethal dose of the anaesthetic pentobarbital sodium (200 mg/ml IP; Merial, UK) before being transcardially perfused. Once the animal was fully anaesthetized, an incision below the rib cage and another one along the diaphragm helped to expose the heart. A single injection of 0.1 ml of heparin (5000 U/ml; Leo, UK) was administered into the bottom of the left ventricle to prevent clotting and allow better flushing of the blood. Subsequently, a cannula connected through polyethylene tubing to a pump (Watson-Marlow, UK) was inserted into the location of the injection. The pump was adjusted to deliver 40 to 50 ml of 0.1 M filtered PBS (pH adjusted to 7.4) at a rate of 3 ml per minutes. The right atrium was cut to allow the incoming flow of blood and PBS out of the system. After the volume of PBS had been exhausted and the emerging fluid from the atrium was clear, the pump was switched to administer 40 to 50 ml of 4% of filtered PFA (pH adjusted to 7.4). Early signs of perfusion such as body tremors were observed. Once the tissue fixative had finished passing through the mouse, it was decapitated and the extracted brain was postfixed in 4% PFA for 24 hours at 4^{o} C. The brains were washed with 0.1M PBS and transferred into a cryoprotective solution composed of 30% sucrose, 0.5 M Tris-buffered saline (TBS, pH 7.6) and 0.05% sodium azide (NaN_3; Sigma, UK) and left at 4^{o} C until the brains sunk before proceeding to sectioning.

Brain sectioning was performed in order to corroborate the site of injection. The brain was removed from the solution and placed over embedding matrix (Thermofisher scientific, UK) on the already frozen specimen clamp of the sliding microtome (Microm). Additional embedding matrix was applied over the brain before freezing it with crushed dry ice. Once the brain was fully frozen, 50

um-coronal sections were cut and stored in anti-freezing cryoprotective solution [30% ethylene glycol (Sigma, UK), 15% sucrose (Sigma, UK) and 0.05% NaN_3 in 0.5 M TBS] at -20^{o} C. Unfortunately, one mouse was found dead (cause unknown) and its brain could not be collected.

4.2.5 *In-vivo* Myt1l knockdown validation

4.2.5.1 RNA extraction

Mice designated for RNA extraction to validate the *in-vivo* knockdown of *Myt1l* were killed by cervical dislocation. The brains were quickly extracted and frozen on crushed dry ice. Brains were kept at -80^{0} C until dissection. Before starting the RNA extraction, all the equipment and surfaces were sprayed with RNAseZAP^{TM} (Sigma, UK) to eliminate RNAse and minimise RNA degradation. The frozen brain was placed in a brain matrix (Stoelting, USA) and the area targeted by the central injection was cut using a razor blade (Stoelting, USA). The resulting 1 mm-coronal slice was dissected using a scalpel to isolate the dorsal hippocampus of both sides. The tissue was put in microcentrifuge tubes containing 600 ul of RLT buffer (Qiagen, UK) supplemented with 1% β-mercaptoethanol (Sigma, UK). The brain tissue was first disrupted using a plastic pestle. Then, the tissue lysate was homogenized by passing it through a 20-gauge needle eight times using an RNAse-free syringe. Additional homogenization was carried out using the QIAshredder kit (Qiagen, UK). The lysate was transferred into a spin column placed in a 2 ml collection tube and centrifuged at full-speed for two minutes. Once finished, the spin column was

removed and the collection tube was capped for an additional three minutes of centrifugation at full-speed. The supernatant was carefully transferred to a new microcentrifugation tube for further processing using RNeasy® mini kit (Qiagen, UK). The following steps for RNA extraction were performed as described in Chapter 2 (2.2.5), including the optional on-column DNAse digestion (Qiagen, UK). The resulting RNA was eluted in 30 ul of RNAse-free water (Qiagen, UK) and the RNA concentration was quantified by UV spectrophotometry using a nanospectrophotometer (NanoDrop 1000; Thermo) at 230 nm wavelengths. A absorbance ratio (260/280) above 2 was accepted as "pure" for RNA. If the ratio was lower, it could indicate contamination of protein, phenol or other contaminant. The RNA was stored at -80^{o} C till required for reverse transcription. The correct placement of the viral injection was confirmed by visual inspection using the Paxinos and Franklin brain atlas (Paxinos and Franklin 2003).

4.2.5.2 Reverse transcription

Reverse transcription was performed in 1 ug of RNA using Superscript^{TM} III First-Strand Synthesis System for RT-PCR (Invitrogen, UK). The same protocol described in Chapter 2 was followed here (2.2.6). The cDNA was then diluted in 79 ul of RNase free water to have a final concentration of 10 ug/ul. cDNA was stored at -20^{o} C till required.

4.2.5.3 Quantitative Polymerase Chain Reaction (qPCR)

qPCR amplification was performed in a 20 ul volume containing 4 ul of cDNA (10ug/ul), 10 ul of 2X *Power* SYBR® Green PCR master mix (Applied Biosystems, UK), 0.14 uM forward primer (Table 4.1), 0.14 uM primer reverse (Table 4.1) and 5.72 ul of RNase free water. All the amplifications were carried out in triplicate using the ABI Prism® 7900 HT Sequence detection system (Applied Biosystems) under the following thermal cycle: 95^{o} C for 15 minutes (initial denaturation); 40 cycles of 95^{o}C for 30seconds and 59^{o}C for 30 seconds (amplification); finishing with 50^{o} C for 10 seconds and 95^{o} C for 15 seconds (dissociation stage). The ABI Prism® SDS 2.1 software (Applied Biosystems) was used to analyse the specificity and relative quantification of the amplicons. The dissociation curve generated by the software was used to determine the specificity of the PCR products. The relative quantification of the amplicon was calculated using the cycle threshold (Ct), which represents the number of cycles required by the sample to cross a fixed threshold. The mean Ct values of the triplicates were normalized against the mean triplicates of the housekeeping gene *β-Actin* to produce ΔCT ($\Delta CT = Ct_{Myt1l} - Ct_{\beta\text{-}Actin}$). The difference in expression of *Myt1l* mRNA was compared in two conditions: infected with non-silencing shRNAmir and infected with *Myt1l* shRNAmir, to calculate ΔΔCt ($\Delta\Delta Ct = \Delta Ct_{Myt1l\ shRNAmir} - \Delta Ct_{non\text{-}silencing\ shRNAmir}$).

Table 4.1 **Sequence of the qPCR primers for rodent *Myt1l* and *β-Actin***

	Forward	**Reverse**
Rodent *Myt1l*	GAGCCAGTCCCTGATCCAC	CCGTCAAAGTAGTCACGTAAGC
β-Actin	GCTCGTCGTCGACAACGGCTC	CAAACATGATCTGGGTCATCTTCTC

4.2.6 Behavioural testing

4.2.6.1 Open Field

The open field is a widely used test to measure locomotor activity as well as a validated test for anxiety-like behaviours (Prut and Belzung 2003, Crawley 2007). When mice are exposed to the open field arena, they will explore it in order to collect information about the environment. Following repeated exposure to the open field, their behaviour will change and this process is normally referred to as habituation (Crusio and Schwegler 1987, Thiel, Müller et al. 1999). Mice placed in a new environment will tend to explore the periphery of the arena and avoid the inner area, which is seen as a threatening and potentially dangerous zone. The time spent in, and latency to enter, the inner zone are indicators of reduced anxiety (Prut and Belzung 2003).

The open field arena used in this experiment was a TruScan arena (26 cm wide x 26 cm long x 38.5 cm height; Coulbourn Instruments, USA) placed in a sound-isolated room evenly lit (20 lux) by a white light lamp on the floor below the arena. Before and in-between trials, the apparatus was wiped clean with a 1%

Trigene® solution to avoid build-up of olfactory cues that could affect behaviour. At the start of each trial, a mouse was taken out of its home cage and placed in the peripheral zone of the arena facing an outer wall. The trial was recorded using an overhead camera for 20 minutes. At the end of the experiment, the mouse was returned to its home cage. Each animal was tested the next day following the same protocol. The recordings were analysed using the automated tracking EthoVision software (Noldus, Spink et al. 2001, Spink, Tegelenbosch et al. 2001). A squared area (13 cm x 13 cm) equidistant from the periphery was defined as the inner zone. The locomotor activity, in both the outer and the inner zone of the arena (distance moved and velocity), time spent in each zone and the number of entries to the inner zone were measured. Two types of habituation were calculated: the first was within the same trial by comparing the performance of the animal across four 5 minute time bins; the second was calculated by comparing the activity observed on day one with day two. The locomotion in the outer arena was used to calculate habituation instead of the total arena since these measurements are confounded by anxiety as it included the activity in the inner zone (anxiogenic).

4.2.6.2 Novel Object discrimination (NOD)

The NOD task relies on the natural tendency of mice and rats to be attracted to novel objects. It has been shown that after a single explorative session with an object, the rodents can differentiate between a familiar object and a novel one (Dere, Huston et al. 2007, Antunes and Biala 2012). The amount of time that the mouse spends interacting with the new object indicates the capacity of the

animal to discriminate between the familiar and novel (Bevins and Besheer 2006). Depending on the delay between the first contact with the objects and the presentation of the new one, both short-term memory (after one hour) and long-term memory (after 24 hours) could be assessed (Stefanko, Barrett et al. 2009).

An empty home cage (i.e. without sawdust and bedding material) was used as the arena for the NOD task along with 4 different objects (white cubes, black cubes, white pyramids, black pyramids). Preliminary observations using these objects suggested the preference of the mouse for a specific type. In order to avoid this preference, only cubes were used for short-term memory and only pyramids for long-term memory (Figure 4.3). Before and in-between trials, the test cage and the objects were washed with commercially available washing up liquid (Fairy Original, UK) and wiped with 1% Trigene® solution to avoid any olfactory cues that could lead to a side preference. The cages were placed in a sound-isolated room and a lamp located on and facing the floor provided low white light (20 lux) to the test room. For trial one, either two white or black cubes were attached to the cage through hook-and-loop fasteners to prevent the objects from being displaced by the mouse. The mouse was removed from its home cage and placed in the centre of test cage facing an outer wall. The trial lasted for 10 minutes and was recorded with an overhead camera. At the end of each trial, the mouse was returned to its home cage. One hour later, the same mouse was tested again following the same protocol, but this time one of the cubes had a different colour from the one seen before. Long-term memory was assessed using the same procedure except white or black pyramids were used

and the inter-trial interval was 24 hours (Figure 4.3). The order and location of the new cube/pyramid (i.e. top or bottom) was counterbalanced within groups to avoid laterality bias. The exploration of the objects was hand coded using EthoVision software to calculate frequency and duration for each object. Exploration was defined as: a) direct look at the object (within 1 cm), b) direct sniff of the object, c) direct contact of the nose with the object. Discrimination ratios were calculated to establish whether or not the mouse was exploring the objects above the 0.5 chance ratio, which indicated a preference for that object (Bevins and Besheer 2006), where the preference for the novel object was calculated as follows: time spent exploring the novel object divided by the total exploration time (time spent exploring the familiar object + time spent exploring the novel object). A discrimination ratio assuming no preference for the novel object was calculated by dividing the time spent exploring the familiar object between the total exploration time.

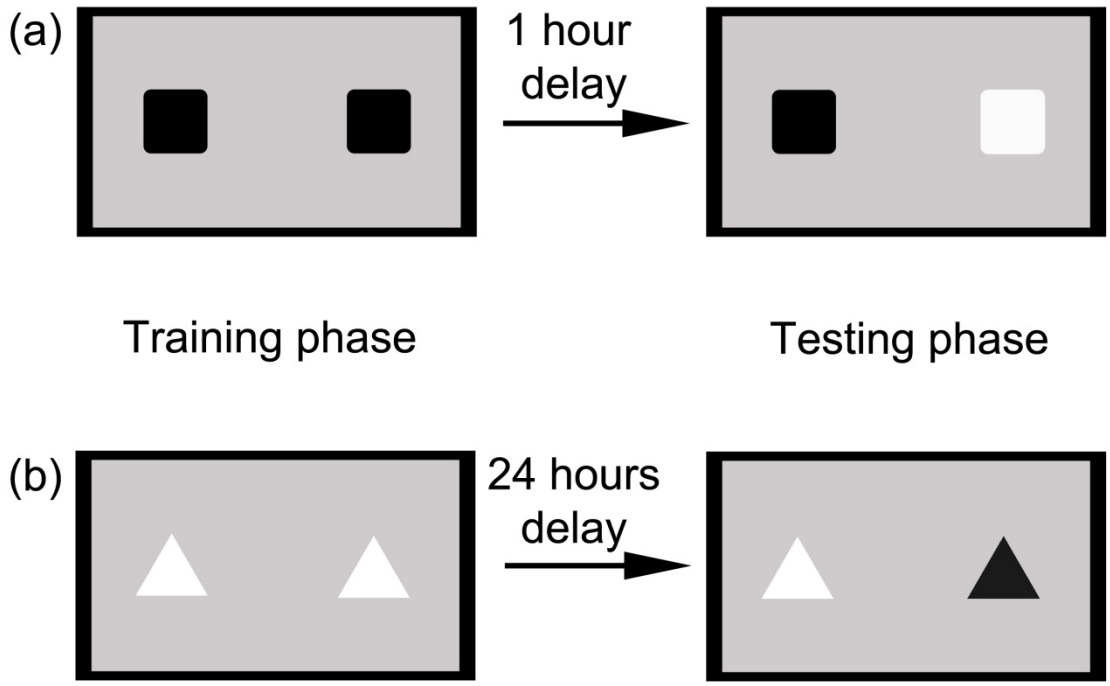

Figure 4.3 **Graphical representation of the object presented during the NOD task**.

Figure (a) shows the setup used to assess short-term memory. Cubes could be either all black or all white for the first contact test, counterbalanced across groups. Figure (b) presents a similar setup, using white or black pyramids (counterbalanced across group) and a 24-hour delay between trials.

4.2.6.3 Morris Water Maze (MWM)

The water maze developed by Morris is a validated test to examine spatial learning in rodents (Morris 1984). The spatial learning ability is tested through the acquisition phase consisting of repetitive trials in which a mouse is forced to swim and locate a submerged platform inside a circular pool by relying on distal cues (D'Hooge and De Deyn 2001, Vorhees and Williams 2006). Additionally, retention of spatial memory is assessed when the platform is removed and the time spent swimming where the platform was located is measured (Rodgers and Johnson 1995, Fernandes, Liu et al. 2004).

For this experiment, a large pool, 1.3 m in diameter and 60 cm of height was used. Even though there is no standard size of pool, previous experiments have shown that 1.3 m in diameter is sufficient to have reliable estimates of learning without being overly stressful to the mouse (van der Staay 2000). The pool was filled with tap water (room temperature around 21^{o} C) up to 30 cm of depth. To prevent the mouse from seeing the platform and to enhance video tracking using EthoVision software, 2 cups of white non-toxic aqueous emulsion (Acusol OP301 Opacifier, Tohm & Haas, Sweeden) were added to the water. Faecal boli were removed from the pool between trials and the water was changed weekly. The pool was lit from below using 4 lamps of white light (100 lux). To isolate the pool and prevent extra cues from affecting the behaviour, the periphery of the pool was delimitated using cream-coloured curtains. Big and bright extra-maze visual cues were hanging from this curtain to help navigation. The pool was virtually divided into 4 equally–sized quadrants in the EthoVision software: target (platform location; T), opposite to target (O), right of the target (R) and left of the target (L) (Figure 4.4). These quadrants were pseudorandomly assigned as the different starting points for the mouse in the successive daily trials and they were alternated between the testing days. The platform had a circular shape (10 cm in diameter) and was always positioned in the target quadrant.

Each experimental batch was run in squads of 5 and 6 mice and each mouse underwent 4 trials (starting from either T, O, R and L) per day for 7 days. The starting points were alternated between daily trails. For each session, the mice were taken into the testing room in squads and left there till all of them

completed their trials. Afterwards, they were taken back to the housing room and the next squad would come into the testing room. Batch 2 was tested after Batch 1 had completed all 7 days of testing.

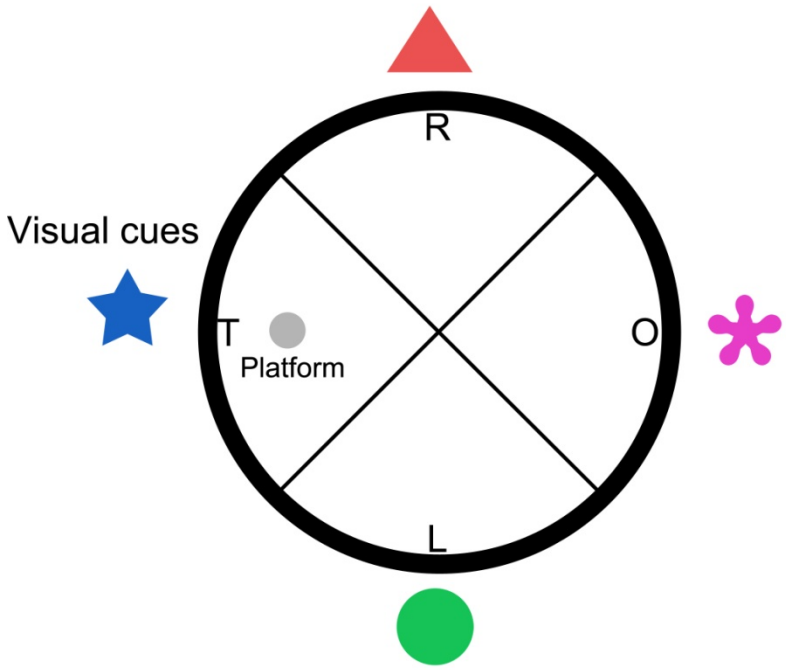

Figure 4.4 **Graphical representation of the Morris Water Maze pool division by quadrants**: **target (T), right (R), opposite (O) and left (L).**

The four figures drawn outside the pool represents the different cues attached to the curtain surrounding the pool.

On day one (visible trial), the platform was positioned about 1 cm above the water level and the mouse was trained to identify and locate the platform. The trial started when the mouse was placed by the tail inside the pool close to and facing the wall in one of the four starting points. The mouse was allowed to swim and find the platform for 60 seconds. Finding the platform was defined as having the four paws on the platform. If the mouse could not locate it in the established time, it was guided towards it. Once on the platform, the mouse was permitted to remain there for 15 seconds before removing it. The mouse was

returned to its home cage and the rest of the squad tested before starting the 2nd trial for each mouse, with an inter-trial interval of approximately 10 min. The mice groomed themselves dry in between trials. The subsequent three trials started in a different quadrant and the order was pseudorandomly assigned. From day two to day seven (hidden trial 1 to hidden trial 6), the same protocol was applied except that the pool was filled with more water to hide the platform 1 cm below the water level. The latency was measured with a stopwatch from the moment the mouse was left inside the pool till it found the platform. On day seven, after completing the four trials, a fifth trial was added to the test (probe trial). In the probe trial, the platform was removed from the pool and the mouse was allowed to swim for 60 seconds. Retention was measured in this trial by comparing the time spent in the target quadrant to the time spent in the other quadrants. Times significantly above 25 seconds chance level were taken as an indication of retained memory of the platform location.

The trials were recorded using an overhead camera for tracking locomotor activity (distance swum and swim speed) analysis using the EthoVision software. For the probe trial, the swimming activity was nested according to the quadrant location.

4.2.6.4 Elevated plus maze (EPM)

The elevated plus maze (EPM) has been described as a reliable model to measure anxiety-like behaviours in the mouse (Lister 1987). It relies on the

conflict between exploring a new environment and avoiding the aversive features of openness and height (Treit, Menard et al. 1993, Fernandes and File 1996, File, Lippa et al. 2001). Hence, the avoidance of the open arms is measured as indicative of an anxiety response (Rodgers and Johnson 1995, Fernandes and File 1996). The floor of the EMP runway was 0.5 cm thick black Perspex and it consisted of four arms measuring 30 cm x 5 cm, having a centre in between them of 5 cm x 5 cm. Two arms opposite to each other were enclosed using two 15 cm high grey Perspex walls on each side and one at the end. The other 2 arms were open. It was supported in the centre by a Perspex stand that positioned the apparatus 40 cm over the floor. The apparatus was placed in a sound-isolated room and a lamp of white light facing the floor was used to light the testing room. The light intensity in the closed arms was (10 lux) and in the open arms (30 lux). Before testing and in between trials, the apparatus was wiped clean~~ed~~ using 1% Trigene® solution to minimise olfactory cues that might interfere with behaviour. The trial started when the mouse was taken out of its home cage by the tail and placed in the centre of the EPM facing a closed arm. Each trial lasted for five minutes and then the mouse was returned to its home cage. An overhead camera recorded the session for further hand scoring using the EthoVision software. The exact number of entries and time spent in each arm were hand scored as well as the latency to enter into an open arm. An arm entry was considered only when the four paws were inside, while an exit was counted when at least two paws were out, in which case, the mouse was located in the central square. The additional behaviours scored were head-dipping (when the mouse lowered its head over the sides of an open arm while being located in the open arms or central square, (Rodgers and Johnson 1995) and scanning of the environment (when the mouse was on an

open arm and its head was moving from one side to the other, (Silva and Brandão 2000). The EthoVision software was used to track the distance moved and velocity in each arm and the central square. Unfortunately, due to a defective batch of recordable DVDs only 16 out 32 trials were available for hand scoring (n=7 from the shRNAmir group and n=9 from the shRNAmir Myt1l group).

4.2.6.5 Light/Dark Box

The light/dark test takes advantage of the innate conflict of mice to explore new environments and avoid open, brightly-lit areas (Crawley and Goodwin 1980). The apparatus consists of a larger, brightly-lit compartment and a smaller, dark compartment. Mice tend to stay in the dark compartment and increased time spent in the brightly-lit compartment is taken as a measure of anxiety (Crawley and Goodwin 1980, File, Lippa et al. 2001, Bourin and Hascoët 2003). The apparatus used for this experiment was a white acrylic box measuring 44 cm x 21 cm x 21 cm divided by a tall, white acrylic separator into two chambers. It was located in a sound-isolated testing room and a white light lamp behind the separator faced only the larger chamber to provide bright illumination. This setup consisted of a larger compartment (two thirds of the box) which was brightly lighted (120 lux) and a small chamber with low lighting (<20 lux). Free transition of the mouse from one chamber to the other was possible through a small opening (5 cm x 7 cm) in the separator. Before testing and between trials, the box and the separator were wiped clean using 1% Trigene® solution to minimise olfactory cues. The mouse was removed from its home cage and

transferred into the dark compartment of the box facing the wall. The trial lasted for five minutes and it was recorded using an overhead camera. Once finished, the mouse was returned to its home cage. The recordings were later hand scored using a manual behaviour module in the EthoVision system. The behavioural patterns measured were the number of entries and time spent in the light compartment, as well as the number of rearings against the wall. Entry to either the light or dark compartment was counted only when all four paws were inside. Rearing against the wall was defined as a mouse standing upright on its hind legs with the two front paws on the wall. In addition, locomotor activity was automatically tracked by the EthoVision software and the data nested according to the two different compartments.

4.2.6.6 Three-chamber social approach task

Based on the natural tendency of a mouse to approach and investigate unknown conspecifics, the three-chamber social task was developed by Crawley and co-workers (Nadler, Moy et al. 2004). The mouse is known to be a social species and a low social approach could be analogous to the social deficit observed in patients suffering from autism. This behavioural test provides a relatively quick screen for impairments in sociability in mouse models of autism. It monitors social approach behaviours by letting the subject mouse choose between spending time with another mouse or a novel object. Sociability is defined in terms of the time spent in the chamber containing the mouse instead of the object. A subsequent test can be performed to investigate social novelty; it is important to note that this is not as relevant to autism-like

symptoms of sociability. In this case, the subject mouse is presented with the choice to interact with either the familiar mouse (presented in the previous trial) or a novel one. The experiment was performed as described by Yang et al., differing only by the fact that the conspecific mice were habituated in wire cups for 15 minutes before undergoing a trial (Yang, Silverman et al. 2001). The three-chambered social test apparatus was a rectangular acrylic box consisting of three equally sized chambers (20 cm x 40.5 cm x 22 cm). The dividing walls were made of clear Plexiglas with openings (10 cm x 5 cm) to allow the mouse access to the chambers (Figure 4.5). The apparatus was placed in a sound-isolated room with a lamp placed and facing the floor to provide dim white light to the testing room (10 lux). All three compartments were filled with equally distributed clean sawdust and the sawdust was changed every time a new subject mouse was tested. Before testing and between subject mice, the box, the wire cups and the glass cups used to weigh down the wire cups were cleaned using 1% Trigene® solution to avoid olfactory cues which might interfere with behaviour. Additionally, between subject mice, both the wire and glass cups were washed using commercially available washing up liquid (Fairy Original, UK). The box was only washed with washing up liquid between test batches. The experiment was composed of three 10-minute trials. Trial one was used for habituation to the apparatus and it did not contain any objects. The trial started when the subject mouse was removed from its home cage and put into the central chamber facing the wall opposite to the experimenter. In trial two, an empty wire cup was placed upside down on either side of the chamber (novel object stimulus) and a novel juvenile same-sex conspecific mouse (novel mouse stimulus) was placed on another upside down wire cup on the other side chamber, leaving the central chamber empty. For trial three, a novel juvenile

same-sex conspecific mouse was placed inside the empty wire cup and the now familiar conspecific remained in the other wire cup. All trials were recorded using an overhead camera and were tracked using EthoVision. The location of the novel mouse across trials was counterbalanced within each group to avoid any bias related to a chamber preference. The tracked data obtained from EthoVision included the number of entries, time spent in, and latency to enter, each chamber, as well as locomotor activity (distance moved and velocity) nested by chamber. The data obtained from trial two (novel object vs. novel mouse) and three (familiar mouse vs. new mouse) were used to assess social approach and social novelty, respectively.

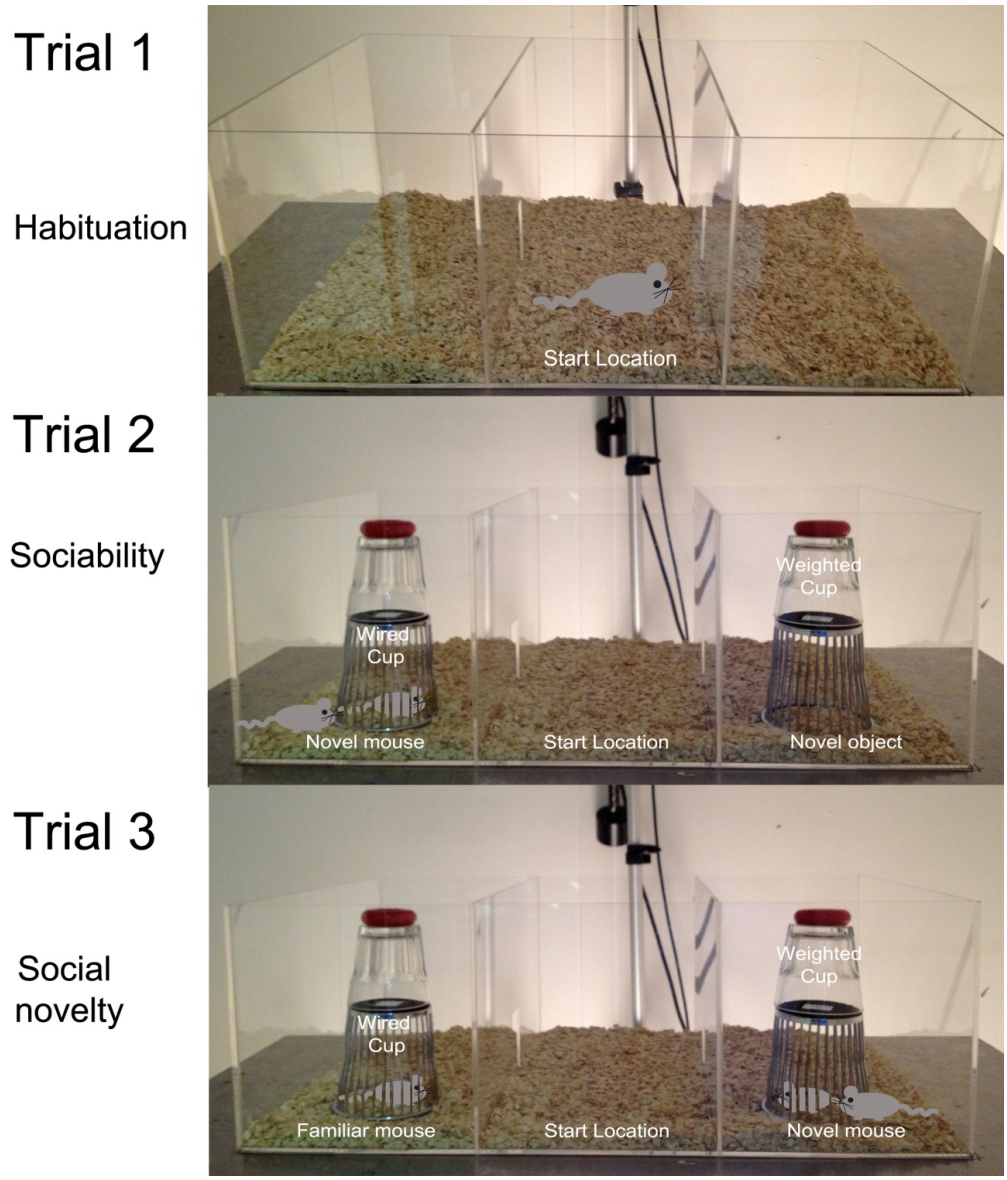

Figure 4.5 **This image illustrates the three-chamber social approach task.**

The image also represents the content of each chamber depending on the trial. During habituation (trial 1), the subject mouse is alone. To test sociability (trial 2), one chamber contains a novel mouse inside a wire glass and the other chamber just contained the wire cup. For the third trial (social novelty), a new mouse was place in the empty wire glass. A glass cup and a lead weight were placed above the wire glass to avoid the mouse from moving or climbing on top of the wire cups.

4.2.6.7 Social investigation task

The social investigation task provides a general assessment of the capacity of a mouse to respond to other conspecifics. Considering that the mouse possesses

a repertoire of well-characterized behavioural patterns, establishing an inventory (sometimes referred as an ethogram) of its behaviour while encountering a new mouse is relatively easy (Winslow 2001). In this experiment, clean home cages with only sawdust were used for the test arena. The cages were located in a sound-isolated room. A white light lamp located and facing the floor provided the lighting for the test room (10 lux). One hour before the experiment, the subject mouse was transferred from its home cage to the clean, test cage and it was left in the housing room. The trial began when the mouse in its test cage was transferred to the testing room and one juvenile same-sex conspecific was put inside the subject's test cage. They were allowed to interact for five minutes after which the subject mouse was returned to its home cage. The trial was recorded using an overhead camera for further analysis using the EthoVision software. Social behaviours initiated by the subject mouse included anogenital sniffing, social sniffing (any sniffing from the trunk upwards), aggression and allogrooming (defined as the grooming performed by the test mouse on the conspecific mouse) were hand scored.

4.2.6.8 Buried food task

Odours provide critical information to mice that can influence behaviours such as navigation, foraging, mouse recognition, bond formation, mate selection, sexual behaviour, and parental behaviour (Keverne and Brennan 1996, Brennan and Keverne 2004, Restrepo, Arellano et al. 2004). A wide range of behavioural tests measuring social abilities and certain cognitive tasks rely on olfactory cues and therefore deficits in olfaction can confound the results from

these tests. The buried food task is a simple way to assess olfaction in mouse. This test was essentially performed using a well-established protocol by Yang and Crawley (Yang and Crawley 2001). Cleaned home cages evenly filled with 5 cm of sawdust were used as test cages. The test room was sound-isolated and it was lit using a white light lamp placed on and facing the floor (lux 10). A small chocolate cookie (Nestle Cookie Crisp®, UK) was given to the mice in their home cages for three consecutive days. Every morning, the experimenter searched the home cage to check whether the cookie had been eaten. The mice then were food deprived for 24 hours before testing. On the day of the test, the mouse was transferred from its home cage to the test cage and was left to habituate for five minutes. Then, it was removed from the test cage and a cookie was hidden in the bottom of the test cage (right, left, centre). The location of the cookie was counterbalanced within groups across the trials. The mouse was returned to the test cage and allowed 60 seconds to find the cookie. The latency of the mouse to find the cookie was recorded using a stopwatch.

4.2.7 Immunohistochemistry

50 um-coronal brain sections were washed three times in 0.1 M PBS (pH 7.4) for 10 minutes to remove the cryoprotective solution in which they had been immersed, followed by one hour incubation at room temperature in blocking solution [0.2 M PBS containing 1% bovine serum albumina fraction V (Roche; USA), 0.3% Triton X-100 (Sigma, UK) and 1% of normal goad serum (Invitrogen, USA); pH adjusted to 7.4]. The slices were further washed as described before and incubated overnight at 4^{o} C in blocking buffer containing

rabbit polyclonal anti-GFP (1:1000; Abcam, UK). The next day, the brain slices were again washed in the same manner and incubated for one hour at room temperature in blocking buffer with fluorescently conjugated secondary antibody Alexa Fluor 488 antirabbit (1:1000; Invitrogen, UK). The slices were washed one last time before being mounted on microscopes slices using Vecta Mount™ (Vector, USA) under a cover slip. Images were taken using Leica DMIL supplied with a Leica camera DFC420C (x10 objective).

4.2.8 Statistics

All statistical analyses were done using IBM SPSS Statistics 20 (IBM Corp., USA). A p-value <0.05 was considered statistically significant.

4.2.8.1 *In-vivo* validation

In order to validate the efficiency of shRNAmir targeting *Myt1l* mRNA *in-vivo*, an independent sample t-test was carried out comparing the $\Delta\Delta$Ct obtained from brains infected with shRNAmir *Myt1l* against non-silencing shRNAmir. The graph plotted the relative fold expression, which was obtained by elevating 2 to the negative power of $\Delta\Delta$Ct (relative fold expression=$2^{-\Delta\Delta Ct}$) (Livak and Schmittgen 2001). The error bars were adjusted to reflect the logarithmic scale as described in Chapter 2 (2.2.8).

4.2.8.2 Behavioural testing

The sites of injection for all mice that underwent behavioural testing were confirmed using immunohistochemistry. The animals that had misplacement of the injection were not included in the statistical analysis. In addition, the brain from the mouse found dead was too degraded to corroborate injection site, hence it also was excluded from the analysis. The data for all behavioural tests were expressed as mean± standard error of the mean (S.E.M.). Before analysing the data, the differences between batches were analysed and since there were no significant differences between them, batch effect was not used as a cofactor for statistical analysis. Different analyses were performed according to the behaviour studied in order to assess the differences in behaviour between the mice having Myt1l knocked down in the dorsal hippocampus in comparison to the control mice. For open field, a two-way ANOVA with the factors ‘treatment’ and ‘time interval’ was performed to assess within trial habituation. Between days habituation employed a two-way repeated measure ANOVA to compare day one against day two. Mauchly's sphericity test was used to validate the results of the two-way repeated measure ANOVA. If this test was significant, a Greenhouse-Geisser correction was applied to adjust the value of F and the degrees of freedom. To test for specific group differences within a test day, a paired t-test was used. A two-way ANOVA with the factors ‘treatment’ and ‘time interval’ was employed to analyse the anxiety-like behaviours in the open field. In the particular case of NOD, a paired t-test was used to compare the time spent exploring the novel object in comparison to the familiar one. Additionally, one sample t-test was employed to compare the discrimination ratios against 50% chance ratio. An independent sample t-test

was used to analyse the differences between Myt1l knockdown mice and the control in the EPM, light/dark box, social investigation task and buried food task. For MWM and the three-chamber social approach task, a two-way repeated measures ANOVA was used with between-factor of Mtyl1 treatment and within-factor of chamber (three-chamber social approach task) or session (Morris water maze). The results from the ANOVA were adjusted with a Greenhouse-Geisser correction if the Mauchly's sphericity test was significant.

4.3 Results

4.3.1 *Myt1l* knockdown in the dorsal hippocampus using pGIPZ lentiviral vector microinjection

pGIPZ lentiviral vector containing *Myt1l* shRNAmir (n=3) and non-silencing shRNAmir (n=3) were bilaterally injected in the dorsal hippocampus of the mouse to verify the knockdown efficiency of this construct. A 1-mm coronal brain slice for each mouse was obtained by isolating the injection site and extracting the dorsal hippocampus from both hemispheres. The RNA obtained from this tissue was used to carry out a qPCR analysis to determine the effect of *Myt1l* shRNAmir *in-vivo*. The specificity of the PCR products was assessed by examining the dissociation curve; in both cases, only one peak was observed after amplification (Figure 4.6).

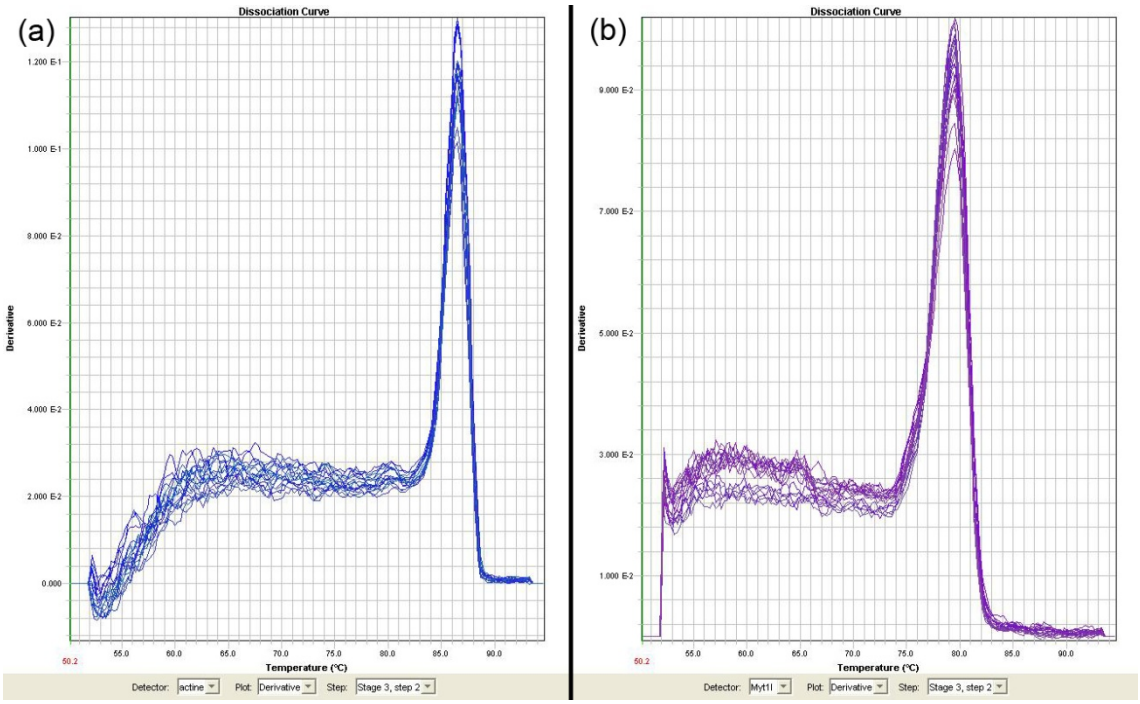

Figure 4.6 **Confirmation of *β-actin* (a) and *Myt1l* (b) qPCR primer specificity.**

The dissociation curves obtained from the qPCT analysis of *β-actin* and *Myt1l* indicate its specificity by yielding only one peak per gene.

The ΔΔCt values of mice infected in the dorsal hippocampus with *Myt1l* shRNAmir and non-silencing shRNAmir were analysed using independent samples t-test. The results (Figure 4.7) confirmed a significant decrease of about 49% in the expression of *Myt1l* compared to the non-silencing control [T(4)=-3.207; p=0.033)]. This result proves the efficiency of *Myt1l* shRNAmir in the mouse brain.

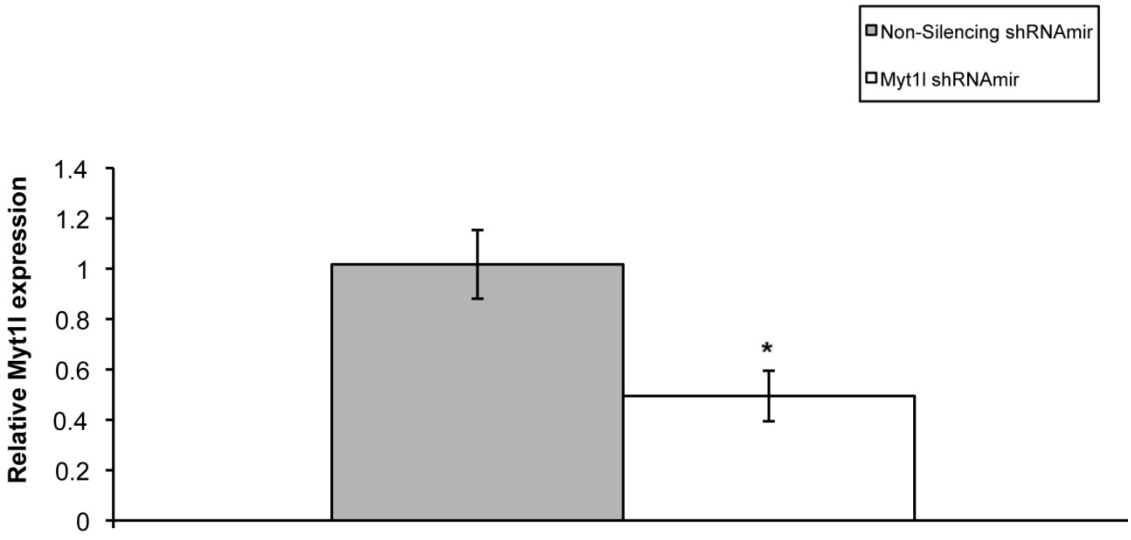

Figure 4.7 **This graph illustrates the relative fold expression of *Myt1l* in mice microinjected with *Myt1l* shRNAmir and non-silencing shRNAmir.**

The data are expressed as mean ± 1 S.E.M. (n=3 per group). * p<0.01

4.3.2 Stereotactic lentiviriral injections and immunohistochemical analysis

In order to investigate the effects of knocking down *Myt1l in-vivo*, lentiviruses containing *Myt1l* and non-silencing shRNAmir (n=16/group) were bilaterally injected in the dorsal hippocampus of the mouse. Given the presence of the marker GFP in the lentiviral vector, the infected cells could be tracked and the injection site detected. The sites of injection in the 31 mice (one mouse died during behavioural testing) that underwent behavioural testing were located by immunohistochemical analysis (Figure 4.8). Only three animals had misplacement of the injection. The viral spreading observed was very limited, around 300 um. This was likely due to the size of the lentiviral vectors (over 100 nm) in comparison to the extracellular space width (40-60 nm) (Cetin, Komai et al. 2007).

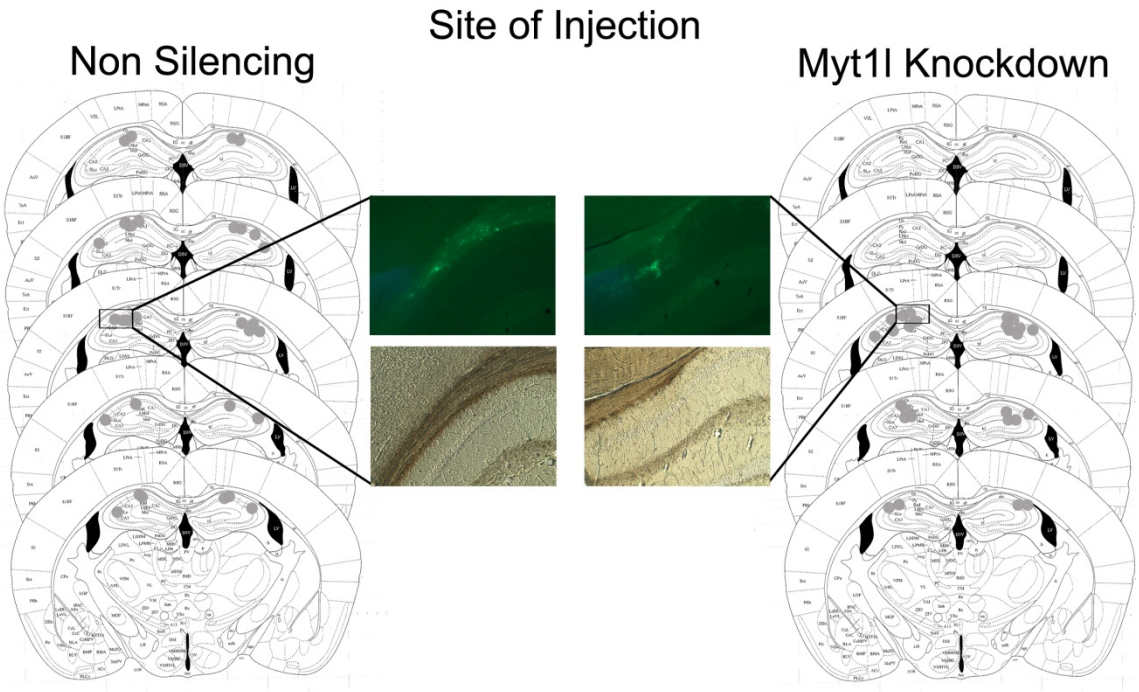

Figure 4.8 **These figures show a graphical representation of the injection site for mice injected with *Myt1l* and non-silencing shRNAmir.**

The grey dots represent each injection site in the mouse (n=14 per group). The pictures in the upper centre were taken after anti-GFP staining and the fluorescence indicates where the lentiviruses were expressed for both control and *Myt1l*; while the lower centre pictures are the corresponding phase-contrast images.

An additional variable that was measured across the study was body weight. It was recorded at four time points (before surgery, one week after surgery, two months after surgery and at cull). Repeated measures ANOVA with Greenhouse-Geisser correction demonstrated a significant time effect ($F_{1.674, 53.571}$=75.127, p=4.82x10^{-15}; Figure 4.9) but no treatment effect ($F_{1.686, 53.571}$=0.436, p=0.614).

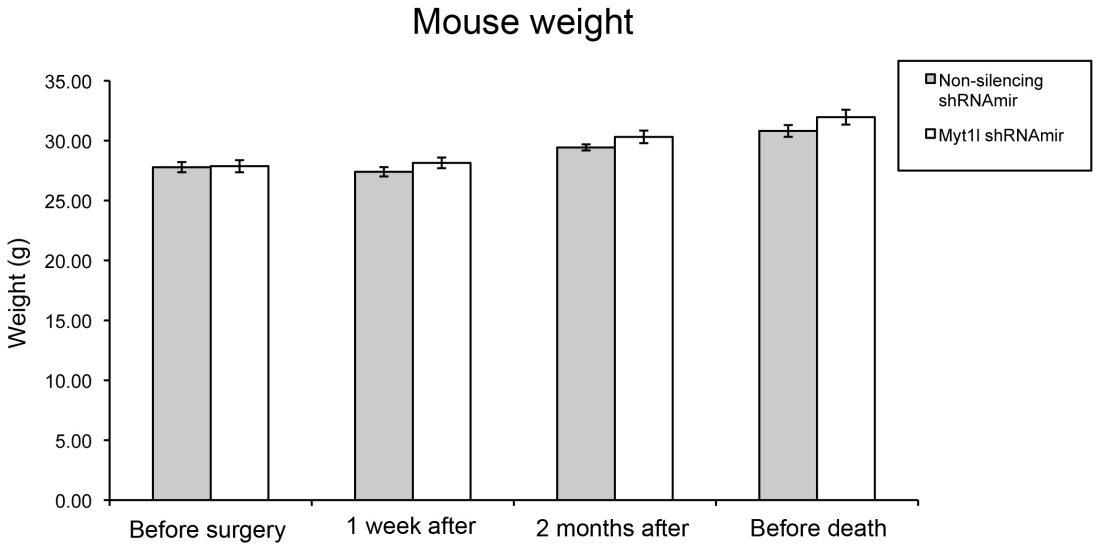

Figure 4.9 **This graph illustrates the differences found in body weight at 4 different time points.**

The weight of both *Myt1l* knockdown and control mice increased significantly 2 months after surgery and at cull. There were no differences according to the treatment. The data are expressed as mean ± 1 S.E.M. (n = 17 per group).

4.3.3 Open field

The open field test was used to measure both the locomotor activity and anxiety-like behaviours of the modified mice. In order to analyse the within-trial habituation, the distance moved across the outer arena was divided in time intervals of four x 5 minutes. During day one, the two-way repeated ANOVA results indicated that *Myt1l* knockdown mice overall moved a significantly greater distance in trial one in comparison to the control ($F_{1,\ 103}$= 4.542, p=0.035). However, there was no significant effect of treatment at any of the specific time bins. The same analysis applied to the data obtained on day two did not find any significant differences between treatment ($F_{1,\ 100}$= 0.307, p=0.581) or time intervals ($F_{3,\ 100}$= 2.137, p=0.100), indicating no within-trial habituation in either day [Figure 4.10 (a)]. Habituation between trials was

analyzed by an repeated measures ANOVA between trials and followed by Greenhouse-Geisser correction. The test showed no significant changes in the distance moved on day one in comparison to day two due to treatment ($F_{1, 99}$=1.202; p=0.276) or time point ($F_{3, 99}$=1.013; p=0.391), possibly indicating no habituation between days [Figure 4.10 (a)].

The velocity at which mice moved around the outer zone in the overall 20-minute trial was also measured. An independent t-test indicated no significant differences between the *Myt1l* knockdown and control on day one [T(25)=-0.761, p=0.454] or day two [T(25)=1.280, p=0.212; Figure 4.10 (b)]. A repeated measures ANOVA with a Greenhouse-Geisser correction revealed a significant decrease in velocity on day two in comparison to day one due to treatment [$F_{1, 24}$=3.552; p=0.072; Figure 4.10 (b)].

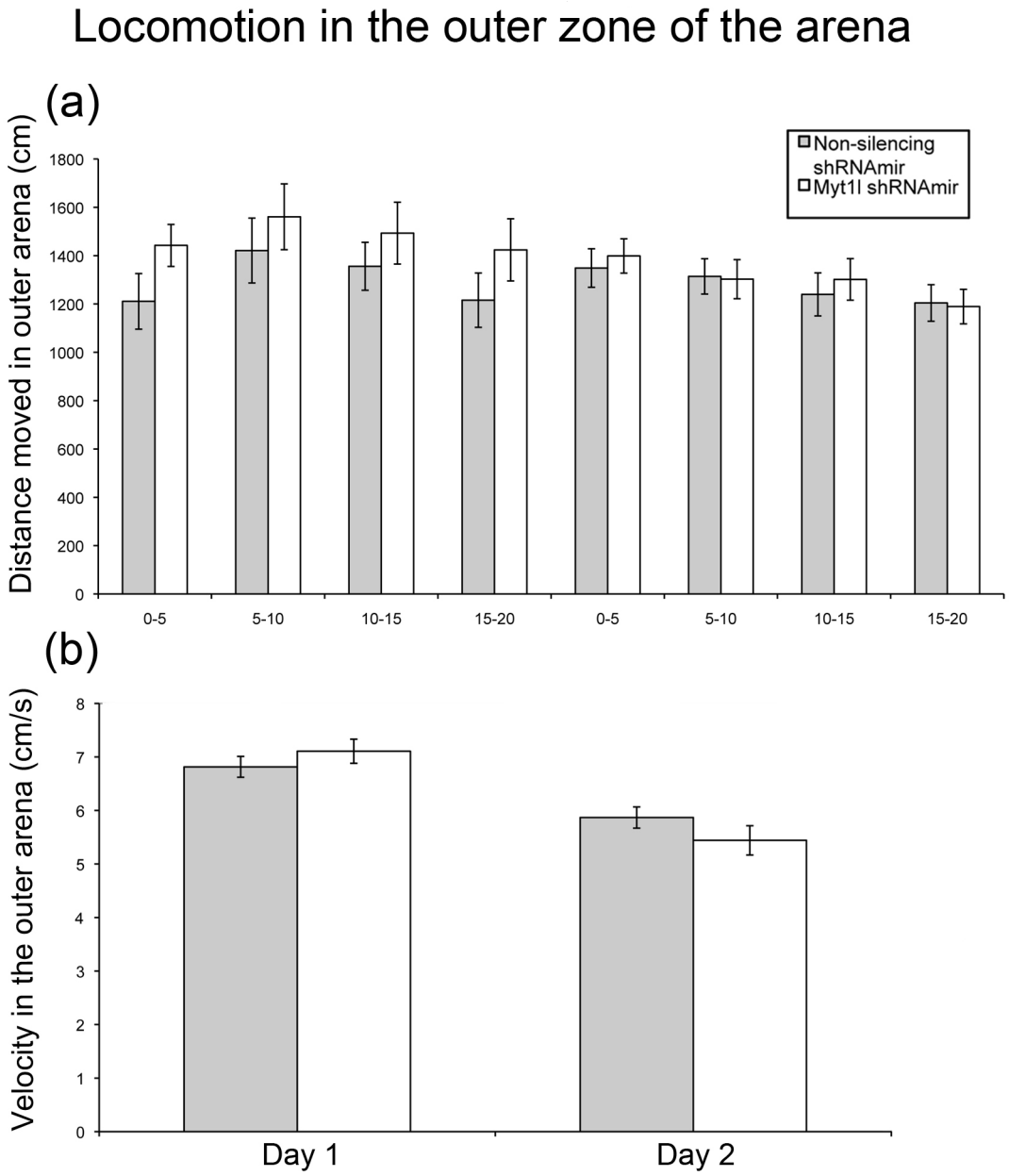

Figure 4.10 **These graphs illustrate the distance moved (a) and velocity (b) recorded in the outer zone of the open field over the 20-minute trial on day 1 and day 2**.

The data are expressed as mean ± 1 S.E.M. (n = 14 per group).

As mentioned previously, the open field can be used to study anxiety-like behaviours by measuring certain behavioural patterns. The first of those is the latency to enter the inner zone of the arena. An independent t-test indicated no differences in this latency between *Myt1l* knockdown and control mice either on

day one [T(26)=0.144; p=0.886] or day two [T(25)=0.324; p=0.749; Figure 4.11 (a)]. However, a repeated measures ANOVA with a Greenhouse-Geisser correction showed significant differences between the trial performed on day one and two ($F_{1, 25}$ =27.068; p=0.000022), without interacting with treatment ($F_{1, 25}$ =0.121; p=0.731). A paired t-test applied to both the *Myt1l* knockdown (p=0.002) and the control (p=0.008) found a significant increase in the latency to enter the inner zone of the arena.

A second possible indicator of anxiety-like behaviours is the number of entries to the inner zone [Figure 4.11 (b)]. In this experiment, a two-way ANOVA did not show any significant differences between groups ($F_{1, 103}$=0.967; p=0.328) or time intervals on day one ($F_{3, 103}$=0.721; p=0.542). During day two, both groups showed a significant increase in the number of entries into the inner zone across the time intervals ($F_{3, 100}$=15.288; p=2.9x10^{-8}) without any treatment effect ($F_{1, 100}$=2.307; p=0.459). A repeated measures ANOVA with a Greenhouse-Geisser correction demonstrated a significant decrease in the number of entries to the inner zone along the time intervals when comparing day one versus day two ($F_{3, 99}$=39.021, p=1.1x10^{-8}), without a significant treatment effect ($F_{1, 100}$=2.307; p=0.459). A further paired t-test comparing time bins from day 1 against day 2 found a significant decrease for *Myt1l* knockdown mice in the number of entries over the first three time intervals of open field testing (p=0.002; p=0.007; p=0.001). Similarly, control mice had a significant decrease in the frequency to enter the inner zone but only for the first and third 5-minute intervals (p=0.001; p= 0.023).

Another measure of anxiety is the time spent in the inner arena. The results showed that there was a significant difference in treatment [$F_{1,103}$=6.212, p=0.014; Figure 4.11 (c)]. Specifically, a pairwise comparison followed by Bonferroni correction indicated that *Myt1l* knockdown mice spent less time in the inner zone in the first five minutes in comparison to the control (p=0.009). The data recorded during day two indicated an overall treatment effect without interaction across time ($F_{1,100}$=5.397; p=0.022). Moreover, changes between time intervals were also statistically significant ($F_{3,\ 100}$=17.506; p=3.27x10^{-9}), probably indicating within-trial habituation. Between day differences were calculated using repeated measures ANOVA with a Greenhouse-Geisser correction; this test demonstrated an interaction between treatment, time interval and trial day ($F_{3,99}$=2.776, p=0.045). Paired t-tests showed that *Myt1l* knockdown mice spent less time in the inner zone on day two across the first and second time intervals when comparing it to day one (p=0.001; p=0.005); while during interval four, knockdown mice spent more time in the inner area in comparison to day one (p=0.037). On the contrary, control mice only spent significantly less time on the first time interval when comparing between day trials (p=0.004). It is important to mention that the baseline for the time spent in this area was less than 20% of the duration in either the first five minutes or the 20-minutes trial and it rarely went over into any other time bin (Table 4.2).

Table 4.2 **Summary of the percentage of the total time spent in the inner zone for both *Myt1l* shRNAmir and non-silencing shRNAmir recorded in the open field during the first five minutes and the 20-minute trial**.

The data are expressed as the mean ± S.E.M. (n = 14 per group). The percent duration for time intervals was calculated as follows: time spent in time interval/300, multiplied by 100. The percent duration for the total time spent was calculated as follows: total time spent inner zone/1200, multiplied by 100. * $p<0.05$ two-way ANOVA *Myt1l* knockdown versus control pre-planned pairwise comparison followed by Bonferroni correction

	% Total time spent inner zone 0-5 min	**% Total time spent inner zone 5-10 min**	**% Total time spent inner zone 10-15 min**	**% Total time spent inner zone 15-20 min**	**% Total time spent inner zone (20 minutes)**
Day 1					
Myt1l shRNAmir	11.78±2.18 *	15.29±2.03	14.72±1.35	14.23±1.42	14.04±1.22
Non-silencing shRNAmir	21.12±4.31	15.31±2.17	16.08±1.70	20.27±3.22	18.22±1.99
Day 2					
Myt1l shRNAmir	3.36±0.85	11.64±1.49	14.34±1.79*	20.47±2.05	12.49±1.09
Non-silencing shRNAmir	7.52±2.34	16.14±2.03	20.27±3.30	20.16±2.37	16.07±1.86

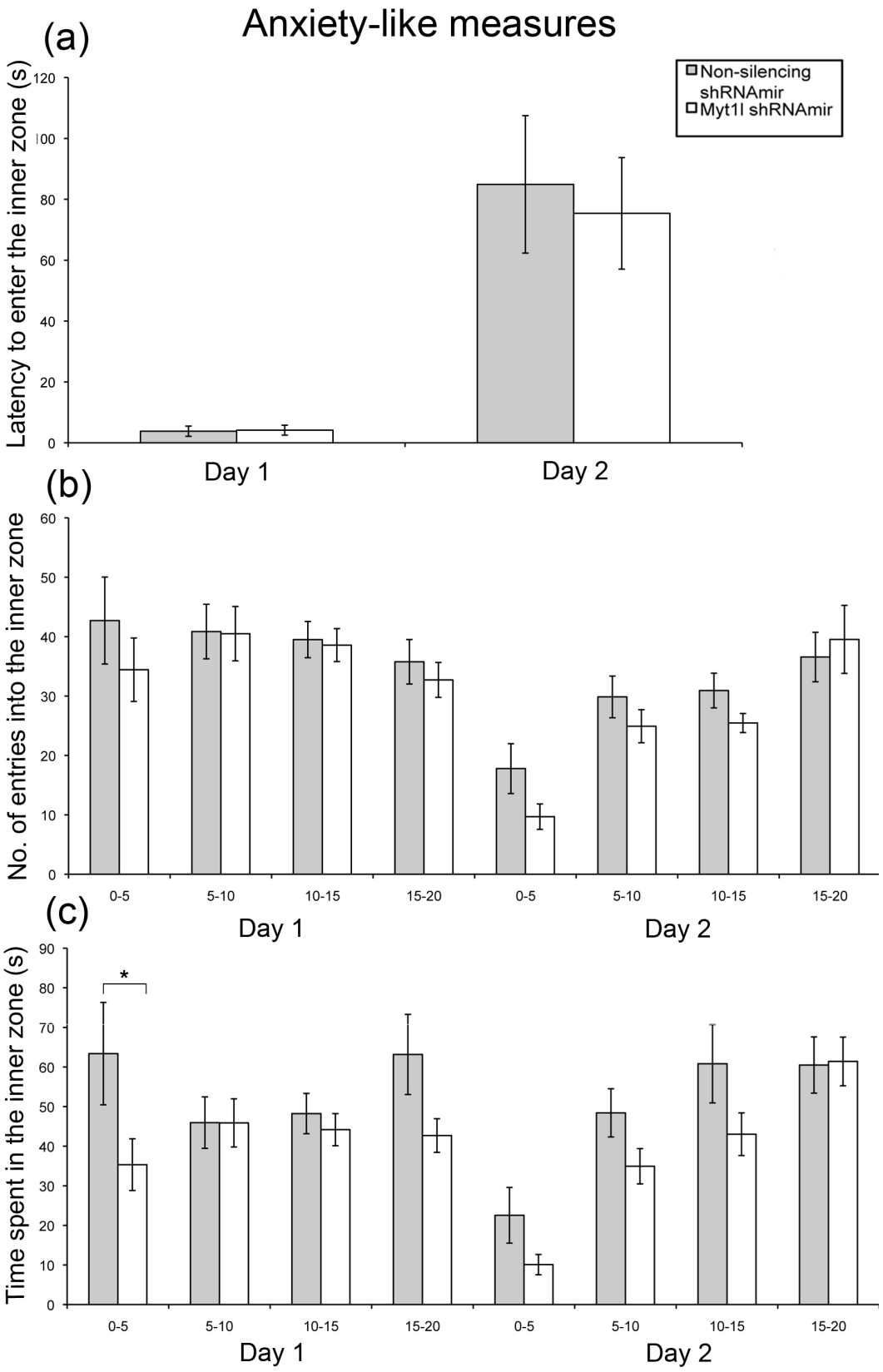

Figure 4.11 **These graphs illustrate the latency to enter (a), the number of entries into (b) and time spent in (c) the inner zone of the open field arena over the 20-minute trial on day 1 and day 2**.

The data are expressed as mean ± 1 S.E.M. (n = 14 per group). * p <0.05 *Myt1l* knockdown versus control pre-planned pairwise comparison followed by Bonferroni correction.

The overall 20-minute locomotion recorded in the inner zone was analysed using an independent t-test. The results showed that the distance moved by *Myt1l* knockdown mice was not significantly different from the control on day one [T(25)=1.337, p=0.193; Figure 4.12 (a)]. However, during day two, there was a statistically significant difference between these groups [T(25)=2.613, p=0.015; Figure 4.12 (a)]. Habituation was analyzed by a repeated measures ANOVA between trials followed by a Greenhouse-Geisser correction. The test showed a statistically significant difference between the distance moved in the inner zone between trials ($F_{1,24}$=25.752, p=3.45x10^{-5}), without a treatment effect ($F_{1,24}$=0.013, p=0.910).

The overall velocity at which mice moved around the inner zone was also measured. The results of an independent t-test did not show any significant differences regarding the velocity either on day one [T(25)=-1.202, p=0.241] or day two [T(25)=0.389, p=0.700). The velocity was compared between day one and day two using repeated measures ANOVA with a Greenhouse-Geisser correction. The test indicated a significant decrease in the velocity on day two in comparison to day one ($F_{1,24}$=67.283; p= 2.02x10^{-8}) without an effect of treatment [$F_{1,24}$=3.926; p=0.059; Figure 4.12 (b)].

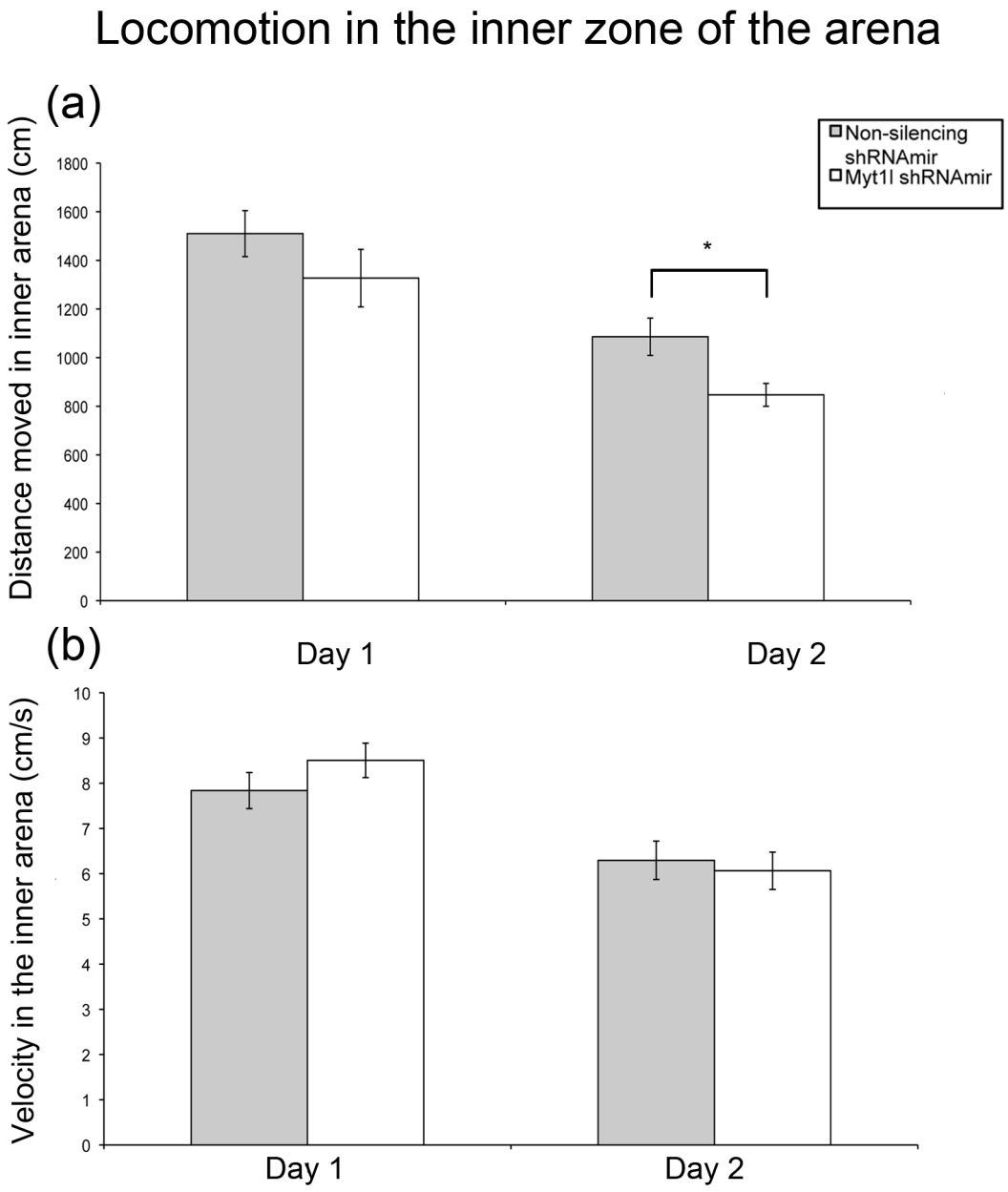

Figure 4.12 **These graphs illustrate the locomotion (a) and velocity (b) recorded in the inner zone of the open field arena over the 20-minute trial on day 1 and day 2**.

The data are expressed as mean ± S.E.M. (n = 14 per group). * $p<0.05$

4.3.4 Novel object recognition

During the training phase of the NOD test for short-term memory, mice were presented with two identical objects to explore for 10 minutes. Both groups

spent similar amounts of time exploring each object. Neither the mice with reduced expression of *Myt1l* [T(13)=0.166; p=0.870] nor the control mice [T(13)=1.386; p=0.189] showed any significant difference in time spent exploring the novel object [Figure 4.13 (a)]. The discrimination ratio was not significantly above 0.5 for the Myt1l knockdown [T(13)= ±0.239; p=0.815] or control [T(13)= ±1.228; p=0.241] suggesting this task was not sensitive enough to detect NOD above chance level in any of the groups [Figure 4.14 (a)]. There was not an effect of treatment on the overall exploration time [T(26)=0.553; p=0.585; Table 4.3].

Table 4.3 **Summary of the mean exploration time during training and testing phase for both a 1 hr delay and 24 hr delay.**

The exploration is presented as total exploration time and then divided into exploration of novel or familiar objects. Novel and familiar measures do not apply to the training test since identical objects were presented for the first time during training. The data are expressed as mean ± S.E.M. (n = 14 per group). The percent duration was calculated as follows: total time spent exploring/300, multiplied by 100.

		Mean exploration time (s) ± S.E.M.			
Training	**Treatment**	**%Total time spent exploring**	**Total**	**Novel**	**Familiar**
Training	*Myt1l* shRNAmir	12.61±1.27	75.66±7.60	40.29±4.35	35.37±3.83
	Non-silencing shRNAmir	14.77±1.42	88.64±8.53	46.31±6.55	42.33±3.46
1 hour delay	*Myt1l* shRNAmir	14.56±1.22	87.37±7.31	44.27±5.06	43.11±5.05
	Non-silencing shRNAmir	15.54±1.29	93.25±7.72	50.93±5.73	42.32±4.03
Training	*Myt1l* shRNAmir	18.09±1.35	108.52±8.12	49.18±4.31	59.34±4.90
	Non-silencing shRNAmir	16.95±1.29	101.70±7.71	51.06±4.51	50.64±4.83
24 hour delay	*Myt1l* shRNAmir	17.76±1.04	106.55±6.26	56.22±4.87	50.33±4.21
	Non-silencing shRNAmir	16.24±1.13	97.47±6.81	52.37±4.54	45.10±5.12

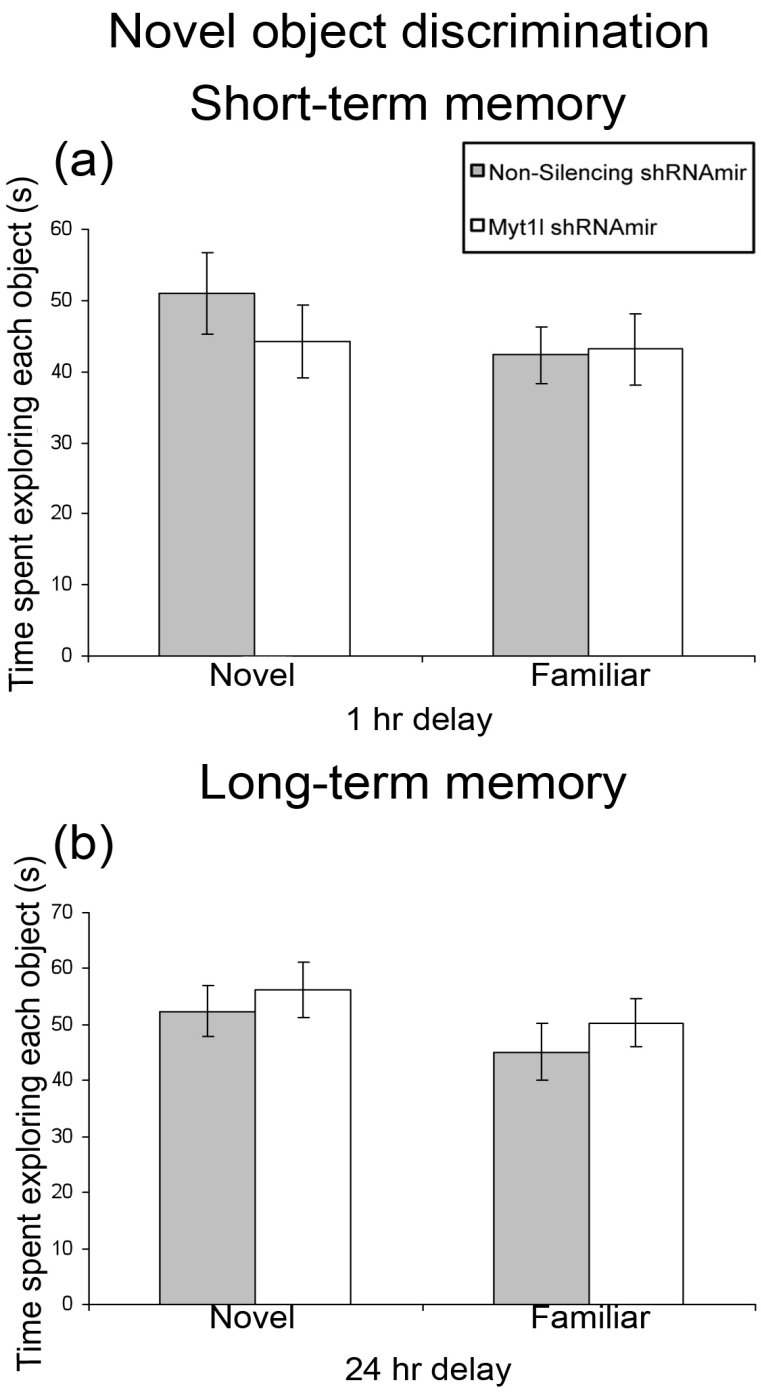

Figure 4.13 **These graphs illustrate the time spent exploring the novel object while testing for short-term (a) and long-term memory (b).**

Data are expresses as the mean ± S.E.M. (n=14 per group).

When testing long-term memory, both groups of mice spent equal amounts of time exploring the objects in the training phase. After the 24-hour delay, the *Myt1l* knockdown [T(13)=0.890, p=0.389] and the control [T(13)=1.056,

p=0.310] spent similar time exploring the novel and familiar object [Figure 4.13 (b)]. Moreover, neither *Myt1l* knockdown [T(13)= ±0.770; p=0.455] nor non-silencing [T(13)= ±1.350; p=0.200] mice showed a significant NOD above chance level [Figure 4.14 (b)]. There was no effect of treatment on the total exploration time [T(26)=-0.982; p=0.335; Table 4.5].

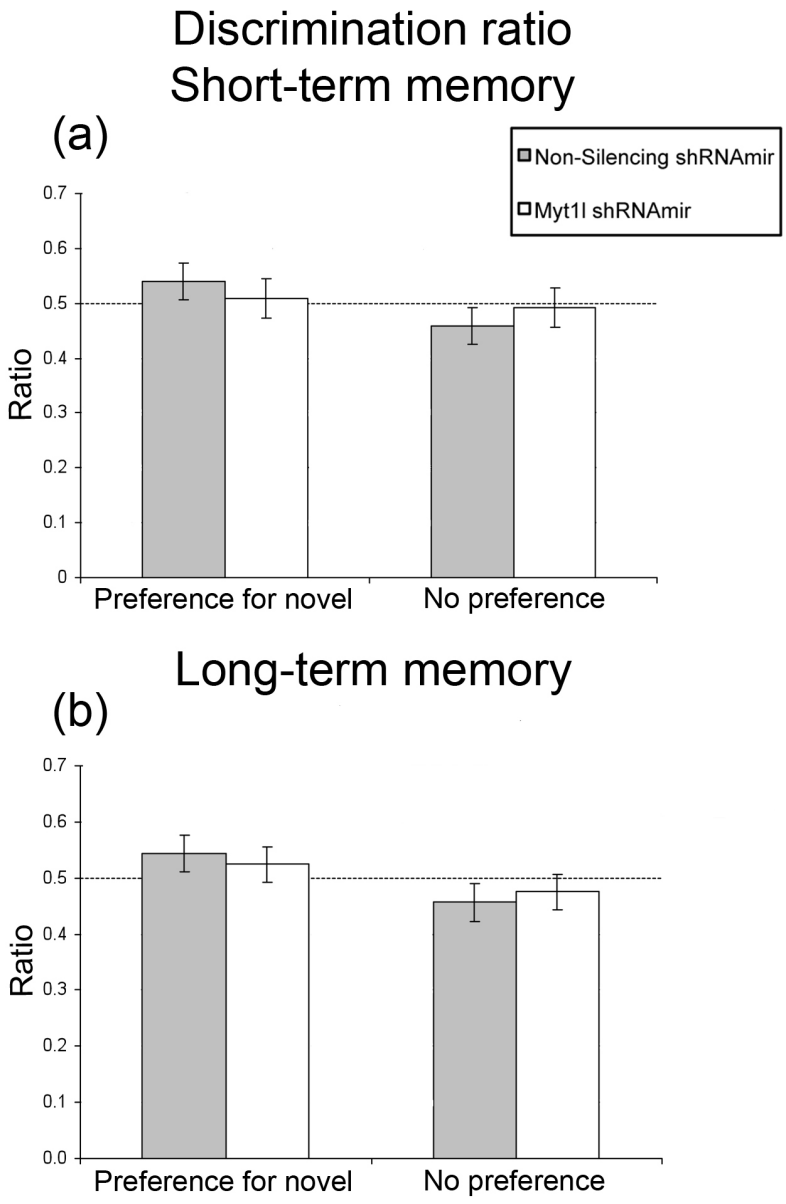

Figure 4.14 **These figures illustrate the discrimination ratio calculated for short-term and long-term memory.**

Data are expressed as the mean ± S.E.M. (n=14 per group). The exploration time was used to calculate the discrimination ratio for assumed preference for novel (novel object exploration time/total exploration time) and assumed no preference (familiar exploration time/total exploration time). The dashed line represents the 50% chance.

4.3.5 Morris water maze

Mice microinjected with *Myt1l* shRNAmir and the control non-silencing shRNAmir exhibited similar performance in the visible session of the Morris water maze (MWM). There was no significant change in MWM performance across the hidden sessions and therefore, no treatment effects could be assessed as this task did not work in either the control or *Myt1l* treated mice [$F_{5,130}$=1.309;p=0.268; Figure 4.15 (a)]. There was no effect of treatment on the distance [$F_{5,130}$=1.245; p=0.294; Figure 4.15 (b) or swim speed across the hidden sessions [$F_{5,130}$=0.324;p=0.857; and Figure 4.15 (c)].

During the probe trial, repeated measure ANOVA with a Greenhouse-Geisser correction indicated a significant difference in the distance moved across the quadrants of the pool [Figure 4.16 (a); $F_{2.322,60.370}$=10.278, p=6.6x10^{-5}] and the time spent in each quadrant [Figure 4.16 (b); $F_{2.440,63.443}$=10.135, p=5.3x10^{-5}]. However, the difference was not significant between *Myt1l* knockdown mice and control mice. Bonferroni post hoc tests revealed a preference for both groups to swim longer and further in the target quadrant in comparison to the left (distance moved p<0.0003; time spent p<0.0004) and opposite to target (distance moved p<0.004; time p<0.002) quadrants [Table 4.4; Figure 4.16 (a) and (b)]. There was no statistically significant difference in the distance moved or time spent between the right and target quadrants. It is important to mention that all mice started the probe trial from the right quadrant and this could have led the mice to swim more than a 25% chance rate in this quadrant. However, given the lack of significant learning in the previous hidden sessions, it is more

likely that the mice had not fully learned the target location in the MWM.

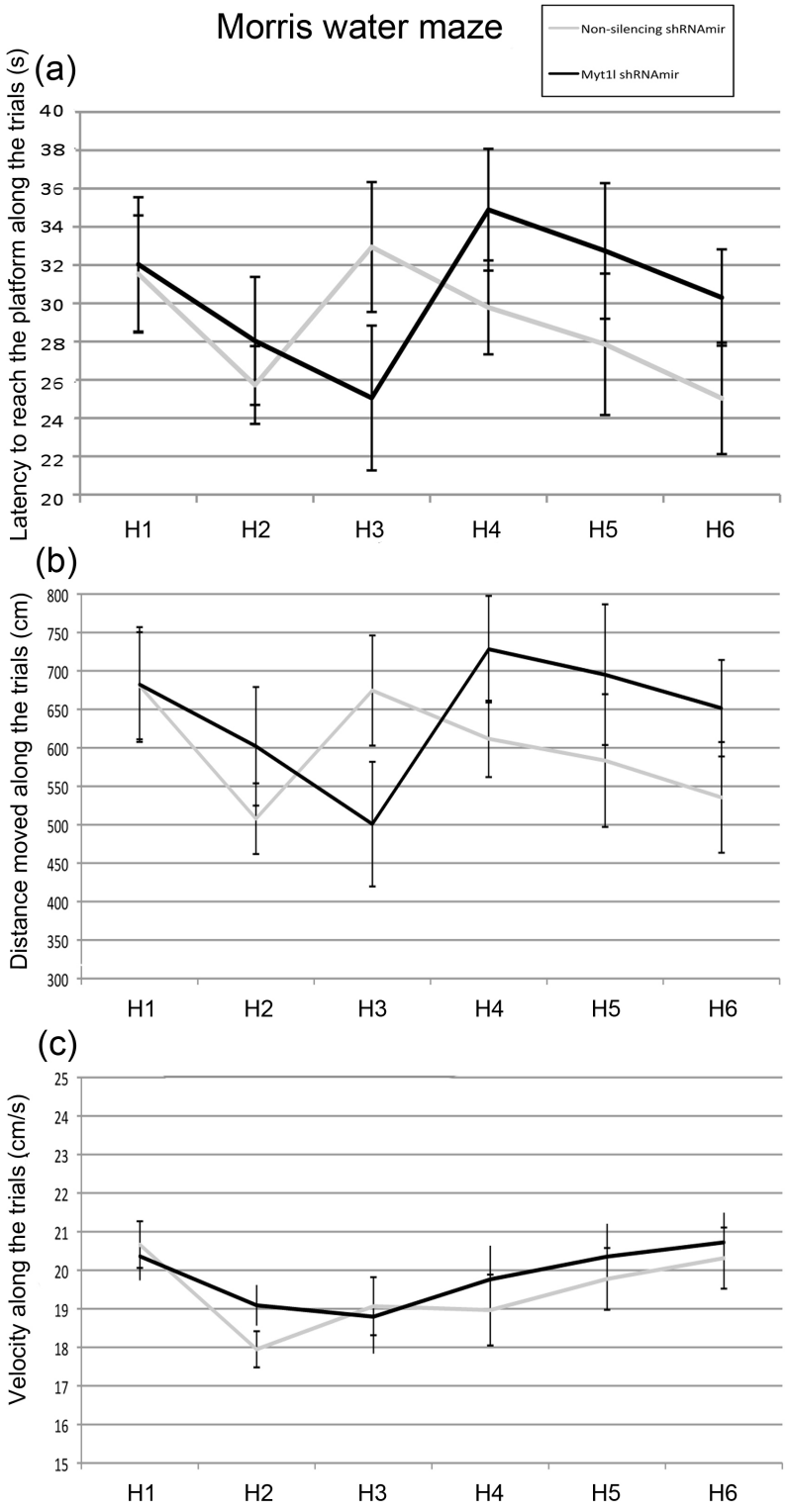

Figure 4.15 **These graphs illustrate the latency to locate the platform (a), distance swum to the platform (b) and swim speed (c) of mice in the Morris water maze during the visible and hidden trials.**

Data are expressed as the mean ± S.E.M. (n = 14 per group).

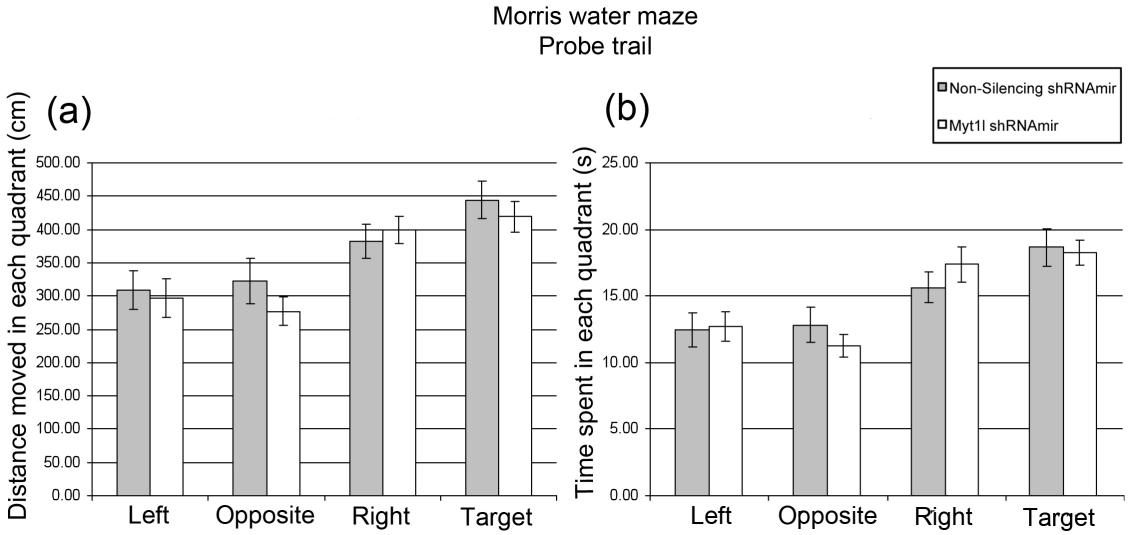

Figure 4.16 **These graphs illustrate the distance swum (a) and time spent (b) in each of the quadrants during the probe trial.**

Both the *Myt1l* shRNAmir and non-silencing shRNAmir mice, swam longer distances and spent more time in the right and target quadrant. Data are expressed as the mean ± S.E.M. (n = 14 per group).

Table 4.4 **Summary of the percentages of time spent in each quadrant during the probe trial.**

The data are expressed as mean ± S.E.M. (n = 14 per group). The percent duration was calculated as follows: time spent in quadrant/300, multiplied by 100.

	Quadrant			
	Left	**Opposite**	**Right**	**Target**
Myt1l shRNAmir	21.17±1.83	18.77±1.48	28.95±2.21	30.43±1.60
Non-silencing shRNAmir	20.75±2.09	21.36±2.18	26.07±1.91	31.08±2.41

4.3.6 Elevated plus maze

The results obtained from the EPM did not show any differences in the number of entries into [open arm T(14)=0.517, p=0.613; closed arm T(14)=0.725, p=0.480], or time spent in [open arm T(14)=0.561, p=0.584; closed arm T(14)=-0.667, p=0.516], each arm between treatment groups (Figure 4.17). Similarly, there was no significant difference in the latency to enter an open arm [T(14)=-

0.623, p=0.543; Figure 4.17 (a)]. Both groups of mice preferred to enter the closed arm [Figure 4.17 (b)] and spent most of the trial time in the closed arms [Figure 4.17 (c)]. Regarding the ethological measures, neither the frequency nor duration of head dipping [T(14)=0.454, p=0.657; T(14)=0.327, p=0.748; Figure 4.17 (d) and (e)] or scanning showed a significant difference between groups [T(14)=0.888, p=0.390, T(14)=0.708, p=491; Figure 4.17 (f) and (g)]. The analysis of the distance moved and velocity further corroborated no locomotion impairment between groups.

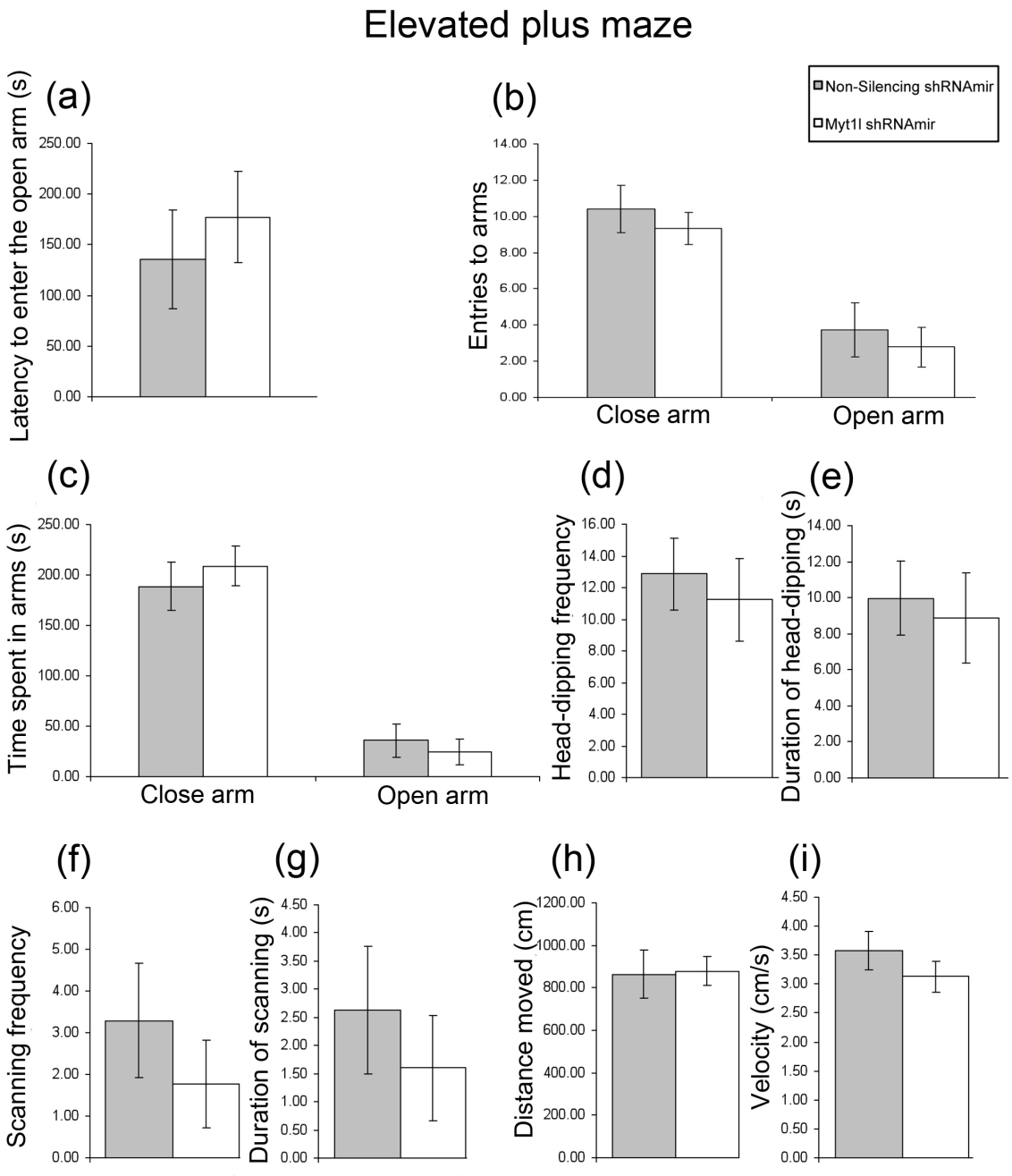

Figure 4.17 **These graphs illustrate the main findings of the EPM test.**

Data are expressed as the mean ± S.E.M. (*Myt1l* shRNAmir n = 9 per group and non-silencing shRNAmir n=7).

4.3.7 Light/dark box

As can be inferred by observing the graphs from Figure 4.18, the light/dark box test results did not show a significant difference in the latency to enter the light

compartment [(a); T(26)=-0.845, p=0.406], the number of entries to each compartment [(b); light T(26)=0.390, p=0.699; dark T(26)=0.272, p=0.787] or the time spent in each compartment [(c); light T(26)=1,219, p=0.234; dark T(26)=-1,219, p=0.234] between the mice injected with *Myt1l* or non-silencing shRNAmir. Both groups of animals made a similar number of entries to, and spent a similar time in, the light compartment. Additionally, no locomotion differences were observed in the velocity [Figure 4.18 (d); light T(26)=0.711, p=0.483; dark T(26)=0.344, p=0.733] or distance travelled [Figure 4.18 (e); light T(26)=-0.895, p=0.379; dark T(26)=0.908, p=0.372] between groups.

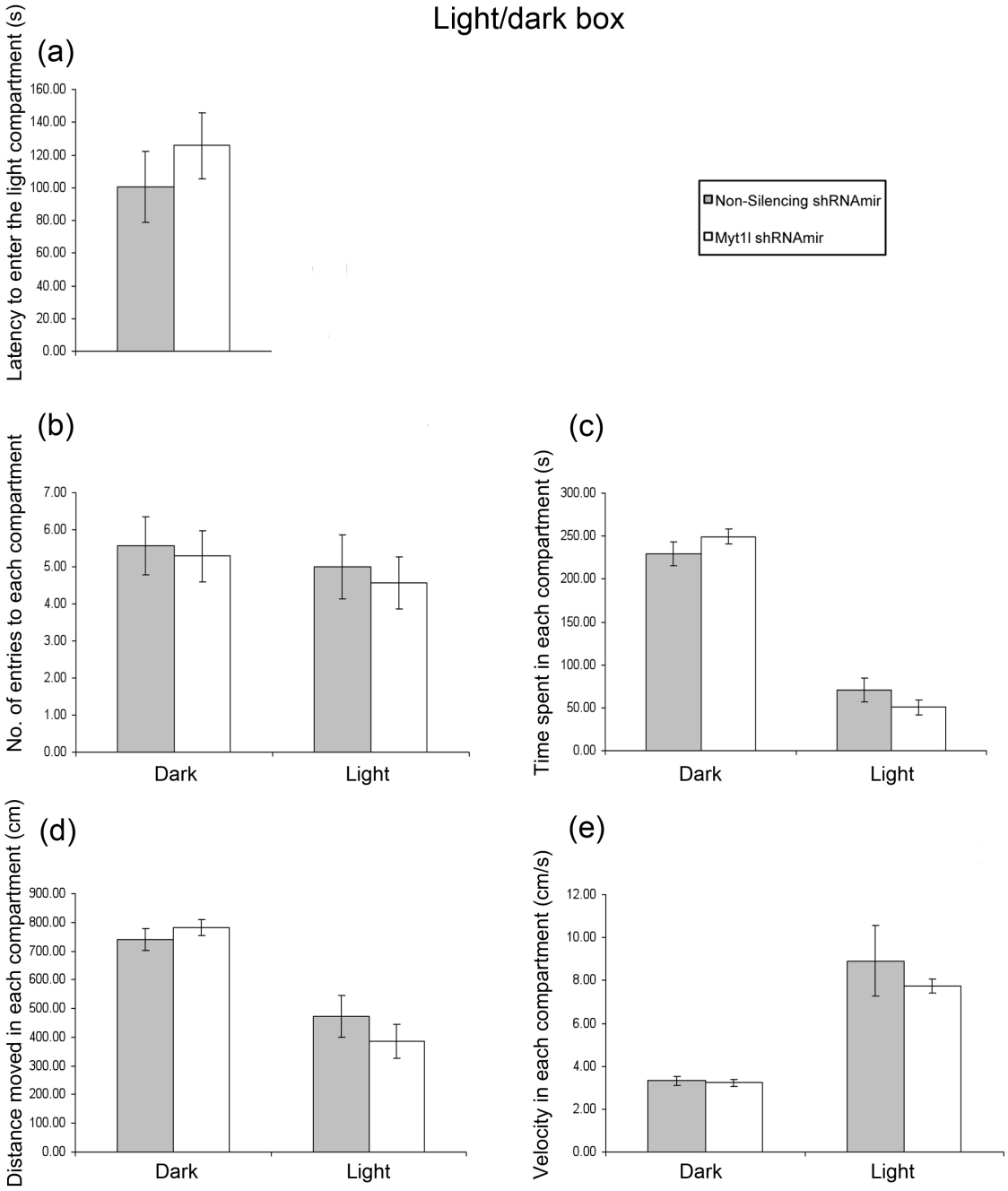

Figure 4.18 **These graphs illustrate the main findings regarding the light/dark box.** Data are expressed as the mean ± S.E.M. (n = 14 per group).

4.3.8 Three-chamber social approach task

During the habituation phase, mice that underwent *Myt1l* knockdown in the dorsal hippocampus and the control mice explored the three chambers of the

apparatus in a similar manner. There was no effect of treatment on the number of entries into ($F_{1,20}$=2.899, p=0.104), or time spent in ($F_{1,20}$=0.973, p=0.336), either the left or right chamber [Figure 4.19 (a) & (b)], showing no preference for either side in the habituation test (Trial 1). The analyses of the locomotor activity data showed no difference between groups in the velocity ($F_{1,20}$=0.051, p=0.823) or distance travelled ($F_{1,20}$=0.823, p=0.375) by the mice (Table 4.5).

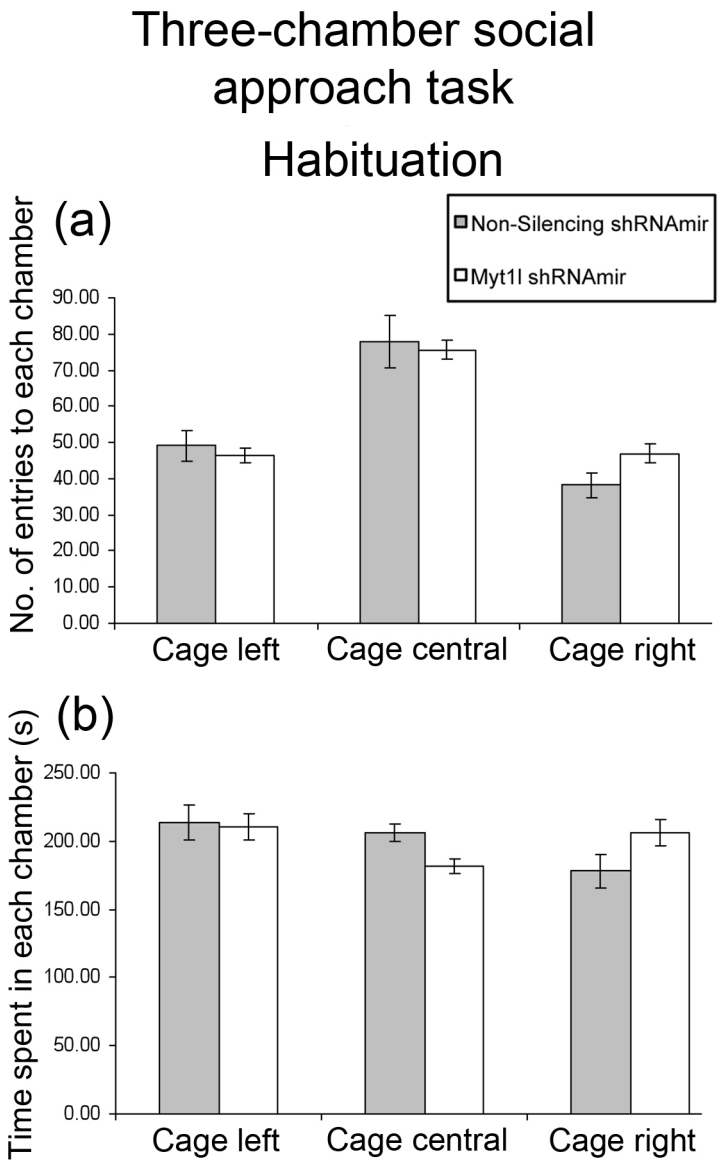

Figure 4.19 **These graphs illustrate the results obtained in the habituation phase of the three-chamber social approach task.**

Data are expressed as the mean ± S.E.M. (n = 11 per group).

During the sociability test (Trial 2), both groups made a significantly greater number of entries into the chamber containing the mouse [$F_{1,20}$=5.932, p=0.024; Figure 4.20 (a)] compared to the chamber with the novel object; but there was no significant difference between *Myt1l* knockdown and control groups ($F_{1,20}$=0.274, p=0.606). The same effect was seen in the time spent in each chamber, with an overall increase in the time spent in the chamber with the novel mouse [$F_{1,20}$=34.750, p=9.0x10^{-6}; Figure 4.20 (b)], but there was no effect of treatment ($F_{1,20}$=0.027, p=0.872). There were no differences in the velocity ($F_{1,20}$=4.597, p=0.055) or the distance ($F_{1,20}$=0.645, p=0.431) moved by the mice due to treatment (Table 4.5).

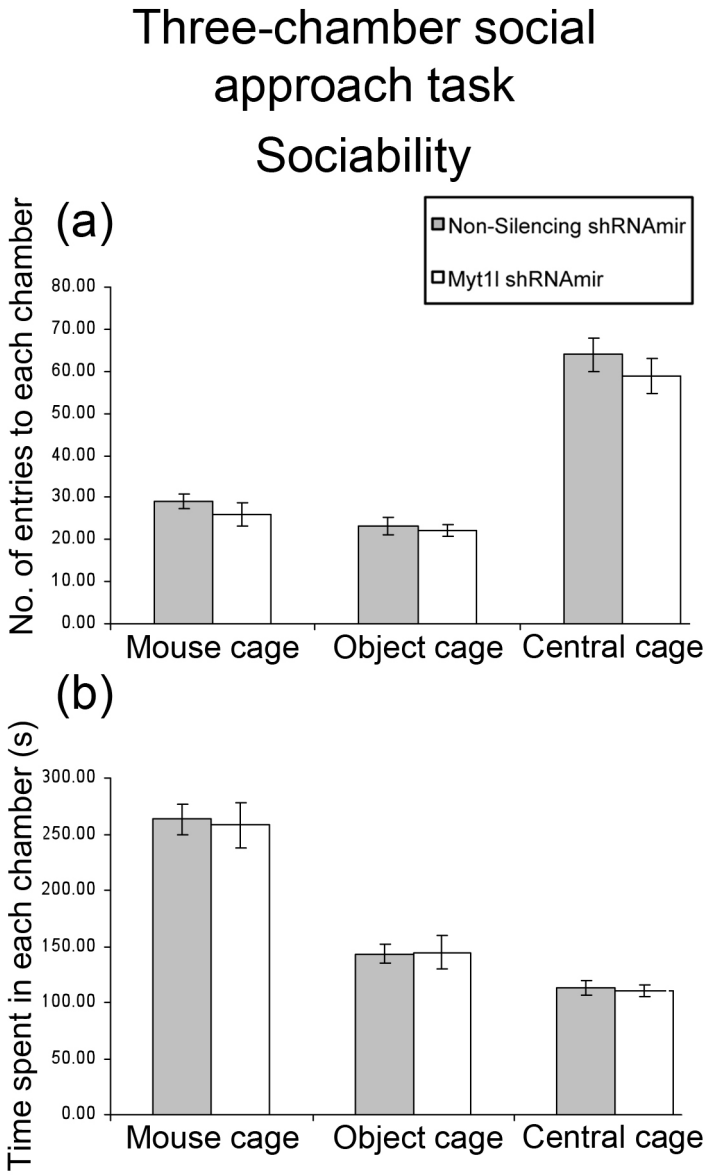

Figure 4.20 **These graphs illustrate the results obtained during the sociability phase of the three-chamber social approach task.**

Data are expressed as the mean ± S.E.M. (n = 11 per group).

During the last trial, preference for social novelty was assessed but neither group showed a significant difference in the number of entries to the chambers containing the new mouse compared to the chamber containing the previously explored mouse [$F_{1,20}$=1.525, p=0.231; Figure 4.21 (a)]. However, both groups spent more time in the cage containing the new mouse [$F_{1,20}$=5.277, p=0.033; Figure 4.21 (b)]. There was no effect of treatment on the preference for social

novelty ($F_{1,20}$=0.035, p=0.854). The analyses of the locomotor activity data showed no difference between groups in the velocity ($F_{1,20}$=0.116, p=0.737) or distance travelled ($F_{1,20}$=0.002, p=0.964) by the mice in any of the three trials (Table 4.5).

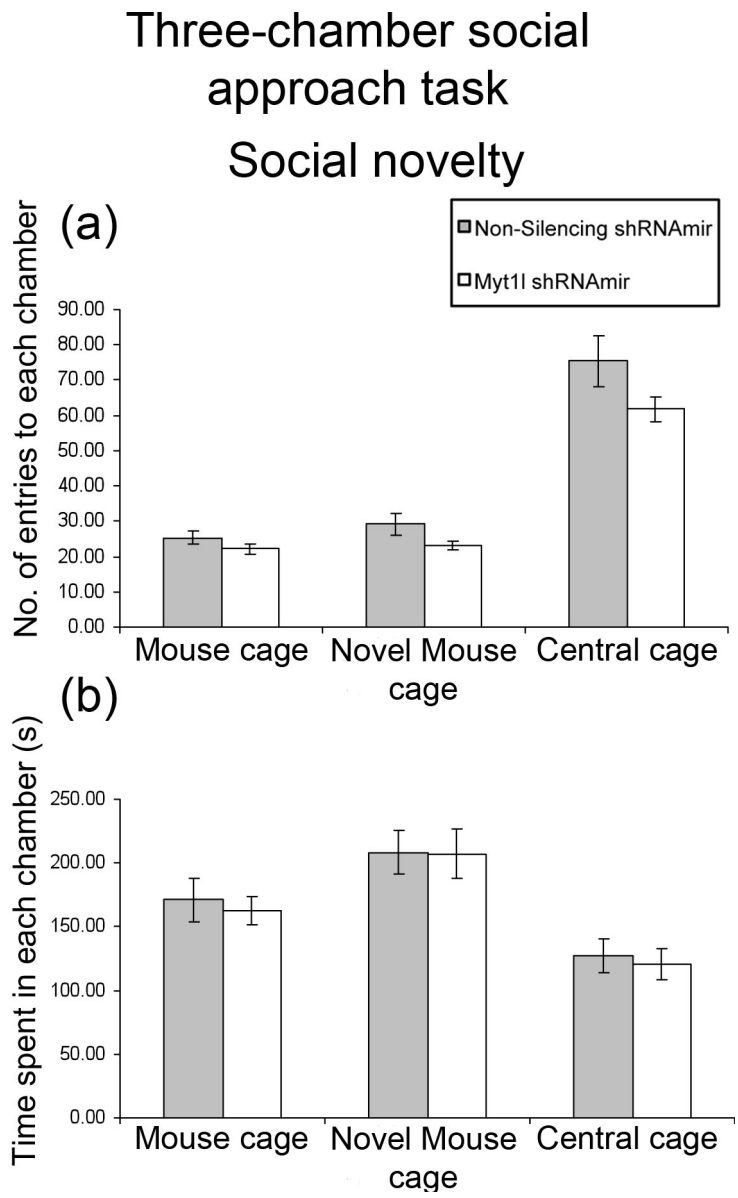

Figure 4.21 **These graphs illustrate the results obtained in the social novelty phase of the three-chamber social approach task.**

Data are expressed as the mean ± S.E.M. (n = 11 per group).

Table 4.5 **Summary of the distance travelled and the velocity for *Myt1l* knockdown and non-silencing groups of mice.**

The data are presented as mean ± S.E.M.

	***Myt1l* shRNAmir**		**Non-silencing shRNAmir**	
	Distance	**Velocity**	**Distance**	**Velocity**
Habituation				
Left	1669.11±99.92	8.63±0.27	1620.73±11.04	8.54±0.45
Right	1504.59±79.95	8.00±0.33	1292.19±100.54	8.00±0.33
Central	1791.79±69.39	9.13±0.47	1844.26±74.61	9.13±0.47
Sociability				
Novel mouse	1994.88±278.41	8.26±0.54	1757.52±110.75	7.64±0.35
Novel object	1028.73±96.93	8.51±0.49	1096.34±96.93	8.87±0.41
Central	1205.69±67.27	11.19±0.40	1298.17±96.72	12.14±0.63
Social novelty				
Mouse	1154.41±128.08	7.82±0.58	1286.52±134.98	8.80±0.44
Novel mouse	1521.78±235.74	7.84±0.44	1638.28±198.82	8.67±0.47
Central	1225.50±72.79	10.94±0.57	1507.97±140.64	12.49±0.83

4.3.9 Social investigation task

The results of the behavioural patterns observed during the social investigation task are shown in Figure 4.22. There was no significant effect of treatment on any of the measures taken in the social interaction task [social sniffing $T(20)=0.506$, $p=0.618$; anogenital sniffing $T(20)=-0.203$, $p=0.841$; following $T(20)=1.701$, $p=0.112$].

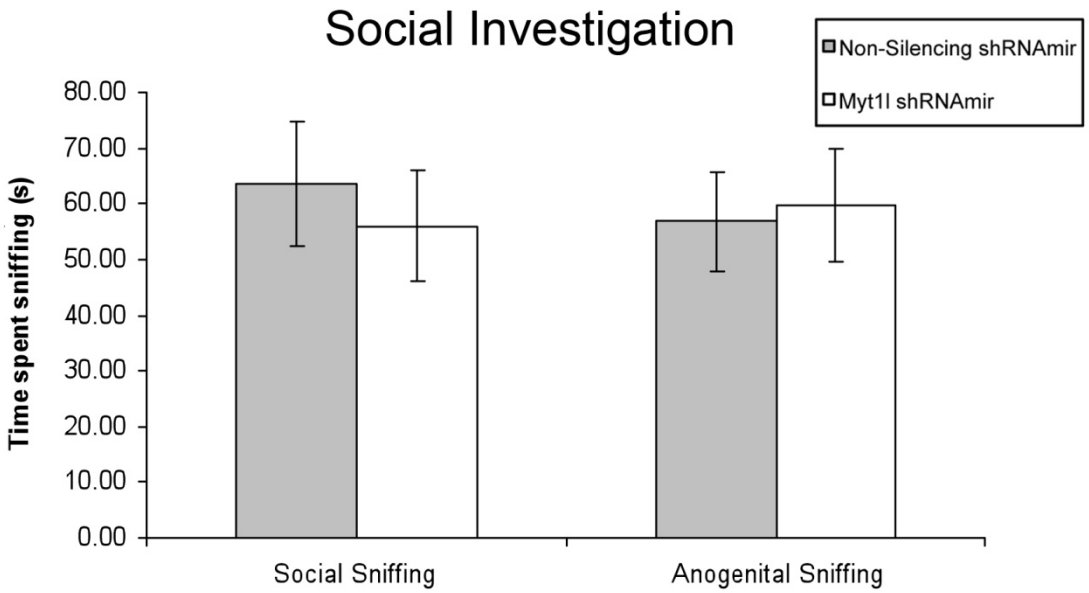

Figure 4.22 **This graph illustrates the results for the social investigation task**.

The data are expressed as the mean ± S.E.M. (n = 11 per group).

Both *Myt1l* knockdown and control mice displayed minimal aggressive behaviours towards the conspecific and the duration of this aggression did not differ between groups according to independent-samples Mann-Whitney U test ($U(20)=70.0$, $p=0.562$; Table 4.6). This test was performed on these data because it was not normally distributed. Allogrooming was rarely observed and it was not analysed.

Table 4.6 **Summary of the aggression observed during the social investigation task.**

	Aggression	
	Mean± S.E.M.	Median
Myt1l shRNAmir	5.94±3.03	0.00
Non-silencing shRNAmir	8.16±2.01	5.16

4.3.10 Food burying task

Olfaction appeared to be normal for both groups as all mice found the cookie within the allotted time and there were no significant differences between groups [T(20)=-0.772, p=0.449; Figure 4.23).

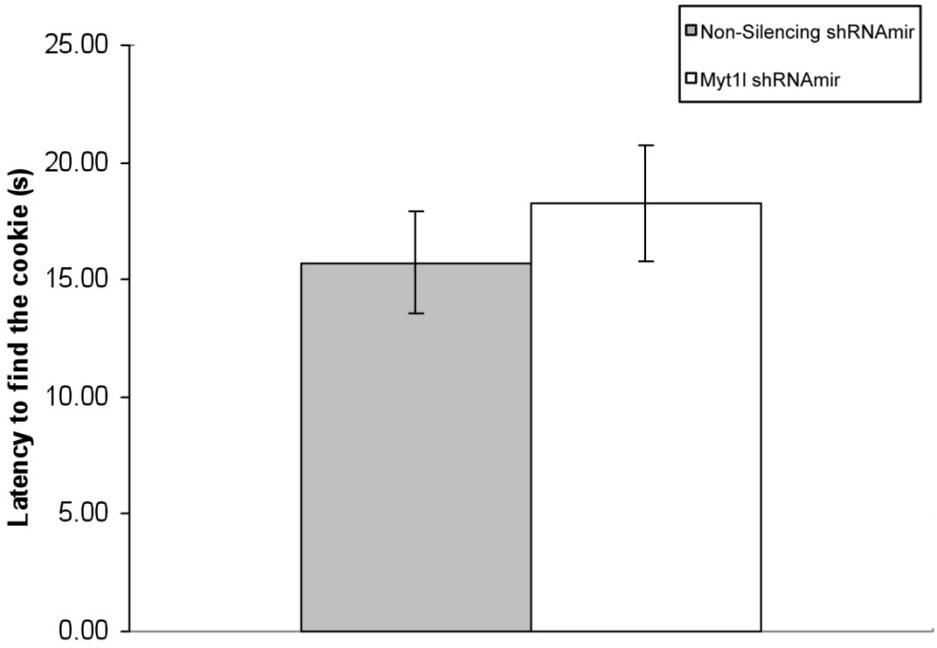

Figure 4.23 **This graph illustrates the latency (s) of the mice to find the hidden cookie in the home cage.**

Data are expressed as the mean ± S.E.M. (n = 11 per group).

4.4 Discussion

Although *Myt1l* has been recently linked to psychiatric disorders along with other genes, the precise function of this individual gene remains unknown. The application of the methodological manipulation of gene expression discussed

here has made it possible to widen our understanding of gene function *in-vivo* (Blomer, Naldini et al. 1997). Combining it with stereotactic surgery brings the opportunity to modify the function in particular brain regions and at specific time points in the life of the organism. Mouse models produced in this manner have given a powerful insight into the impact of genes on the complex biological processes like development and behaviour (Gossen and Bujard 2002). In this chapter, the function of *Myt1l* in the dorsal hippocampus was investigated using lentiviral vectors containing *Myt1l* shRNAmir and non-silencing shRNAmir (control) microinjected in this area of the brain. The behavioural results suggested that a decrease in *Myt1l* expression in the dorsal hippocampus of the brain resulted in a very subtle, transient increase in anxiety-like behaviour, in the open field only, that normalized within time. This inference was reached after assessing *Myt1l* knockdown animals in the open field. Unfortunately, these results were not replicated in the EPM or the light/dark box tests. No other effects were seen across the other tasks aiming to determine the impact of this gene on memory and learning and social approaches in comparison to control mice.

4.4.1 Anxiety-like behaviours

The mice were first tested in the open field arena for two reasons: to analyze anxiety-like behaviours and to verify any locomotion effects due to the injection that could contribute to the changes observed in behaviour. This test relies on the conflict between the desire to explore the novel arena and to avoid the openness of the arena. A measure of anxiety is provided by the time the mice

spent in the inner area of the apparatus (Prut and Belzung 2003). According to the data obtained for this particular test, a subtle anxiogenic effect was observed on the *Myt1l* knockdown mice. This modified group of mice started the test on day one with differences in the time spent in the centre of the arena, without showing any within-trial habituation. This lack of habituation was also observed in the control mice and given the low baseline of time spent in the inner zone, it could be hypothesised that both groups of mice found the test too anxiogenic. The baseline exploration of this zone in the first five minutes of the first trial was around 12% for the knockdown and 21% for control, showing not only a clear difference but it was barely above one fifth of the test. During day two, initially both groups of mice showed longer latencies to enter the inner zone and spent significantly less time in this zone during the first five minutes of the task in comparison to the day before, giving further evidence for an effect of treatment on anxiety. As for the rest of the trial, *Myt1l* knockdown had an overall significant decrease in the time spent, and distance moved, in the centre in comparison to control, but by the end of the 20-minute trial they normalized and they reached the same level as the control. This indicates that the anxiogenic effect of treatment is not permanent in these mice but requires time to be overcome. Within-trial habituation was observed on day two for both groups, which could be an additional indicator of how anxiogenic this test was for these modified mice, considering that habituation to anxiety in this strain had not occurred on the first day (Bolivar, Caldarone et al. 2000). Also, it can be hypothesised from this within-trial habituation that the hippocampus was not fully disturbed as a consequence of the microtrauma caused by the injection, given that mice with considerable hippocampal damage do not habituate (Crusio and Schwegler 1987). Contradictory evidence to the previous

hypothesis was found in the distance travelled in the outer arena by these mice, as neither the *Myt1l* knockdown or control showed any differences in their locomotor activity within-trial or between-trials, with the exception of velocity, which did show habituation by exhibiting a decrease on day two. A possible explanation could be that behavioural habituation is dependent on cognitive and emotional components (Cerbone and Sadile 1994). The injection might have caused damage to the dorsal hippocampus that prevented the mice from creating a cognitive map of the arena. O'Keefe and Nadel (O'Keefe and Nadel 1978) have suggested that this map is built within time and trials and that the mouse tends to reduce its exploration in the process. In this particular case, it could be possible that neither the knockdown mice nor control were able to fully create this map explaining why the overall arena exploration was not reduced. But the emotional component, that is the anxiety, might have encouraged these mice to explore the inner zone more and increase their cognitive map of the arena during trial two after realising no real danger occurred during trial one, hence the habituation observed for the anxiety measure.

This anxiogenic effect of *Myt1l* in the dorsal hippocampus could not be replicated in the EPM or the light/dark box tasks. It is important to note that both of these tests were performed after the open field, NOD and MWM. Therefore, the mice were used to being handled on a daily basis. It is possible that the subtle anxiety effect found for *Myt1l* knockdown could have been overcome by handling habituation. Supporting information of this statement comes from some studies that have found handling rodents before EPM testing can significantly decrease the anxiety shown in these test (Andrews and File 1993, Lapin 1995,

Hogg 1996, Schmitt and Hiemke 1998). In the particular case of the light/dark box, it is also possible that the size of the arena could have been less threatening for the mice than the open field, failing to uncover the weak anxiety phenotype shown by the knockdown mice. Moreover, this test has shown high variability of results within and between the different laboratories, making it difficult to estimate the real value of this test for anxiety (Bourin and Hascoët 2003).

4.4.2 Memory and learning tasks

In order to assess the cognitive effect of *Myt1l* knockdown in the dorsal hippocampus, NOD was used. This test relies on the tendency of mice to explore new objects over familiar ones (Dere, Huston et al. 2007). Both short (one hour later) and long memory (24 hours later) were measured dependent on the delay between presenting the first set of identical objects and the new one (Stefanko, Barrett et al. 2009). The results obtained in this experiment indicated that the mice failed to differentiate the new object from the old one after either a one or 24 hr-delay. Neither groups had a statistically significant discrimination ratio above chance (50%), suggesting that this test did not work in either group of mice. It is not possible to determine whether this result is related to the potential microlesion caused to the hippocampus by the lentiviral vector injection (Hammond, Tull et al. 2004, de Lima, Luft et al. 2006, Antunes and Biala 2012) or of it was an indicator of the failure of the NOD test for some other reason. One hypothesis which would explain these results would be that the familiar and the novel object were not different enough for the mouse to

discriminate between them, given the objects only differed in colour (Ennaceur 2010). Moreover, the percentage of exploration was below 20% in all trials, which might be an indicator that the objects were not interesting enough to catch the mouse's attention. Furthermore, the literature has provided evidence suggesting the susceptibility of mice to handling and the stress and anxiety caused by handling can have detrimental effects on the mouse's performance during NOD (Dere, Huston et al. 2005). This test has the limitation of lacking a non-surgical group of animals and/or the handling of a naive group; without it, it is not possible to determine the reason for this outcome in NOD.

Spatial learning and memory were analyzed using the MWM test. However, no significant learning was observed in either group of mice. Data from the probe trial were indicative of the presence of some memory for the platform location; the mice swam above the chance level in the target quadrant (around 30% for *Myt1l* knockdown and control) and the right quadrant where they started the test (below 30% for both groups) in comparison to the others. The lack of a non-surgical group was a limitation to this study. Without this group it is not possible to determine whether the task did not work in these mice or, similar to the results obtained from the NOD test, whether the low learning ability shown in this test was due to a lesion affecting their learning (Moser, Moser et al. 1993, Logue, Paylor et al. 1997).

4.4.3 Social approaches

The three chamber social approach task is a well-validated test which assesses differences in mouse sociability and preference for social novelty (Yang, Silverman et al. 2001). In this case, it was used to investigate whether *Myt1l* had a role in these behaviours. During the first trial of this test where the mice had the option of interacting with a novel object or a novel mouse, both the *Myt1l* knockdown and control preferred the novel mouse, showing a significant preference for social cues. The following trial gave the test mice the choice of spending time with the previously presented mouse or a novel mouse. Similarly, both groups spent a longer time with the novel mouse, indicating a social approach, a social memory, and a preference for social novelty. There were no significant differences in either trial between the mouse treatments suggesting no effect of *Myt1l* on these behaviours.

Following this test, the mice were put through an additional test to measure some social behavioural patterns displayed by the mouse when encountering a conspecific mouse (Winslow 2001). The results from this test replicated the findings from the previous test, showing that the mouse exhibited social behaviours and little aggression. Moreover, there were no differences in social behaviours that could be attributed to *Myt1l* knockdown. An additional test was performed at the end of the experiment to assess the olfactory ability of the mice. This test demonstrated no significant differences between treatments.

4.4.4 Conclusion and limitations of this study

In conclusion, the behavioural outcome caused by knocking down *Myt1l* in the dorsal hippocampus in this study was a subtle anxiety-like effect that normalized over time. However, not only was this effect only seen in the open field arena, in addition it appeared to only be caused by very stressful test conditions without prior excessive handling. Further data corroborated that the effect could not be attributed to differences in locomotory activity or animal weight since there was an effect of treatment on these measures. In addition, *in-vivo* validation of the lentiviral vector in the overall dorsal hippocampus confirmed the efficiency of the shRNAmir to reduce the expression of *Myt1l* mRNA by approximately 50%. Therefore, any behavioural effects potentially could be attributed to this knockdown. It is important to highlight that the injection targeted a small portion of the dorsal hippocampus and therefore a subtle effect was not unexpected (Cetin, Komai et al. 2007).

Although the hippocampus has been linked to mainly cognitive processes, there are some authors that have found a connection between this brain region and emotional behaviours. The hippocampus was first described by Papez (Papez 1937) as an important participant in the “emotion circuit”. Further support came when MacLean’s theory included the hippocampus as part of the emotional brain (MacLean 1949). It was not till Gray (Gray and McNaughton 2000) in the first edition of his book “The Neuropsychology of Anxiety” in 1982 that the concept of a “behavioural inhibition system” was proposed, which is activated by anxiogenic situations and responds by increasing attention and awareness

towards the environment. Interestingly, one of the main components of this system is a connection between the septum and the hippocampus. Data from additional studies supported this hypothesis, including studies looking at the effect of damage to extensive areas of the hippocampus. These studies indicated that the rodents suffering from this damage exhibit less anxiety-like behaviours in comparison to control, further supporting the role of hippocampus in anxiety (Deacon, Bannerman et al. 2002).

Although a putative role of the hippocampus in some emotional processes is accepted now, the link between this region and anxiety remains poorly understood. Some studies have divided the hippocampus into the ventral and dorsal regions and investigated it separately. The vast majority of results suggest that the dorsal hippocampus is more related to cognitive functions, while the ventral hippocampus is more involved in anxiety-related behaviours (Kjelstrup, Tuvnes et al. 2002, Bannerman, Rawlins et al. 2004, Engin and Treit 2007, McHugh, Fillenz et al. 2011). Nonetheless, there are some studies that have found that lesions to the dorsal hippocampus can produce a decrease in anxiety-like behaviours, suggesting a weak connection between anxiogenic-like behaviours and this brain region (Degroot and Treit 2004, Bertoglio, Joca et al. 2006). Moreover, it has been demonstrated that low expression of fibroblast growth factor 2 (*FGF2*) in the dorsal hippocampus results in an anxiogenic phenotype in rats. This study not only associated *FGF2* with anxiety, but also demonstrated the importance of the dorsal hippocampus in this behaviour (Perez, Clinton et al. 2009, Eren-Koçak, Turner et al. 2011).

A second hypothesis which would explain the relationship between the hippocampus and anxiety infers that memory and anxiety are both part of the hippocampal function, but their regulation is mediated by different neurotransmitter systems or/and receptors (Engin and Treit 2007). Evidence supporting this theory along with the aforementioned theory came when a laboratory discovered that infusing substance P (known to be involved in behaviours like learning, memory, anxiety, fear and stress) into the dorsal, but not the ventral, hippocampus induced an anxiogenic-like reaction in rats. Specifically, after microdialysis, this study found that the substance P receptors were responsible for the effect (Carvalho, Masson et al. 2008).

One of the most important limitations of this study is the site and size of the infection. Lentiviral vector microinjections induced a very localized gene modification (Cetin, Komai et al. 2007) unable to reach the whole of the dorsal hippocampus. Moreover, *in-vivo* validation demonstrated that there was only a 50% decrease in *Myt1l* expression in the overall dorsal hippocampus. Perhaps this was not sufficient to alter behaviours in these mice. In case of the anxiety-like behavioural pattern, it would be necessary to replicate these studies by tasking mice first with the anxiety tests and then with the other tests and also to include a non-surgical group. This would allow mice to be tested in the EPM and light/dark box without prior, potentially excessive, handling and test experience. As for the memory and learning tests, replication would require also an additional non-surgical group to compare and determine whether the effect observed was caused by a microlesion. The non-surgical group would be required only to determine whether the test setup worked itself with the chosen

mouse strain, but not as a control for *Myt1l* modified animals. Moreover, the lack of effect of this particular knockdown of *Myt1l* in the dorsal hippocampus does not necessarily mean that this gene is not involved in memory and learning and social approaches. It would be interesting to study the effect of *Myt1l* knockdown in a wider area of the dorsal hippocampus in addition to other parts of the brain related to memory, learning, anxiety and social approaches.

Chapter 5 : Discussion

The overall aim of this thesis was to investigate the functional role of the transcription factor *MYT1L.* This gene is highly expressed in the developing brain, indicating a possible role in neurodevelopment. Although the expression of *MYT1L* decreases after birth, it continues to have good expression throughout adulthood. In addition, clinical studies have associated impairments in *MYT1L* expression with psychiatric disorders, which would imply that *MYT1L* also has a function during adult life. Despite this information, the specific role played by this gene has not been fully elucidated. To further expand our understanding of this gene, the expression of *MYT1L* was reduced *in-vitro* during cell differentiation and *in-vivo* in the adult mouse *s*o that the underlying changes in gene expression and behaviour could be assessed, respectively.

5.1 *Myt1l* shRNA remarks

In order to undertake these experiments, we first had to find a silencing sequence that uniquely and significantly downregulated the expression of *Myt1l* in rat, mouse and human (see Chapter 2). For this purpose, the use of shRNAmirs over other types of silencing sequences such as siRNAs and shRNAs is preferred because they can produce a more efficient silencing effect since they can mimic the endogenous triggers of the RNAi machinery – microRNA (Silva, Li et al. 2005, Chang, Elledge et al. 2006, Fewell and Schmitt 2006). Lentiviral vectors were the method of delivery for the shRNAmirs both *in-vitro* and *in-vivo*. This was to ensure the long-term expression of the silencing

sequence, whether the cells are dividing or terminally differentiated, with minimal immune response from the host cell (Weber, Bartsch et al. 2008, Doherty, Schaack et al. 2011).

In the search for a suitable *Myt1l* shRNAmir, the efficiency of three commercially available shRNAmirs designed to downregulate *Myt1l* in the rat, mouse and human were cloned into a lenvitviral vector. The *in-vitro* assessment was done in a neuron-related cell line derived from rat. Out of the three sequences, only one shRNAmir provided a significant 55% reduction of *Myt1l* expression. In order to achieve the *Myt1l* knockdown mouse model planned for Chapter 4, this sequence required further validation in a neuron-related mouse cell line, where it was shown to decrease *Myt1l* mRNA expression by a significant 65%. The findings obtained in this first experimental chapter produced the necessary tools to further investigate, *in-vitro* and *in-vivo,* the role of *Myt1l* during both neurodevelopment and adulthood.

5.2 Possible downstream targets of MYT1L

Rodent studies have shown that during neurodevelopment, *Myt1l* is highly expressed in the brain, implying its possible importance during this stage (Kim, Armstrong et al. 1997). This conjecture was supported by a study which showed that *Myt1l* was one of the three necessary transcription factors, along with *Ascl1* and *Brn2*, required to revert the phenotype of a mouse fibroblast and convert it into a functional neuron (Vierbuchen, Ostermeier et al. 2010); however, this was

not unexpected considering that transcription factors are involved in cell-type specification (Bang and Goulding 1996). At the moment, none of the current literature has tried to investigate the importance, at gene expression level, of *MYT1L* during the differentiation of stem cells. It was hoped that the use of stem cells in parallel with gene knockdown would allow the possible downstream targets of individual transcription factors to be determined. In doing so, the research could help unravel the transcriptional pathway of *MYT1L*.

Thus, Chapter 3 was dedicated to testing the effects of the *MYT1L* shRNAmir construct in the differentiation of the human neural stem/progenitor cell line SPC04. Cells were transduced with *MYT1L* shRNA as differentiation was induced. In order to assess the differences in gene expression along differentiation, cells were harvested at two time points: two days after induction (pre-differentiation) and 7 days differentiation. Upon validation of a 59% reduction of *MYT1L* mRNA in SPC04 cells transduced with *MYT1L* shRNAmir at day 7 of differentiation, the gene expression of possible downstream targets was analyzed. Given the limitations in the quantity of RNA, the expression of only nine genes was assessed through qPCR assay. These genes were selected on the basis of being co-expressed with *MYT1L* when SPC04 cells progressed from proliferation to pre-differentiation and differentiation (3 days and 7 days), which our group had determined in a previous experiment (data unpublished). The qPCR results confirmed that *BCL11B*, *MYT1*, *JPH3*, *SYN1* and *SNAP25* were co-expressed along with *MYT1L*. Furthermore, the decrease of *MYT1L* expression due to the shRNAmir resulted in the decrease of the expression of those five genes. Therefore, a further *in-silico* analysis was

performed which found a MYT1L binding site located in the promoter region of each one of the co-expressed genes used in this study, suggesting they could possibly be direct downstream targets of *MYT1L*.

At the moment there is no link between neurodevelopment, MYT1L and the putative direct targets identified by our co-expression study. Nevertheless, it is important to emphasise that these genes belong to various categories related, to some degree, to brain development: neural cell differentiation (*BCL11B* and *MYT1*), neurotransmission -synaptic vesicles and neurotransmitters release- (*SYN1* and *SNAP25*) and synaptic plasticity -through functional crosstalk between intracellular and extracellular channels to release calcium- (*JPH3*). When comparing the start of *Myt1l* expression in the developing rat at the beginning of neurogenesis, in most areas of the rat brain, both processes overlap. Furthermore, the peak in *Myt1l* expression is directly prior to birth, coinciding with the peak of synapse formation and cortex neurogenesis (Workman, Charvet et al. 2013). These facts combined with the information recorded about the importance of *MYT1L* for neuronal maturation (Vierbuchen, Ostermeier et al. 2010) could suggest that *MYT1L* is involved in neurogenesis and synaptogenesis in the rat and possibly in the human.

5.3 *Myt1l* shRNAmir mouse model

Further support for the importance of *MYT1L* comes from clinical studies. The incoming evidence acquired through genome mapping and gene expression

profiles of patients suffering from psychiatric diseases such as mental retardation (Gruchy, Jacquemont et al. 2007, Bonaglia, Giorda et al. 2008, Stevens, van Ravenswaaij-Arts et al. 2011), schizophrenia (Vrijenhoek, Buizer-Voskamp et al. 2008, Addington and Rapoport 2009, Lee, Mattai et al. 2012, Li, Wang et al. 2012), autism (Garbett, Ebert et al. 2008, Meyer, Axelsen et al. 2012) and major depression disorder (Wang, Zeng et al. 2010) has linked their aetiology with impairments in the sequence and expression of *MYT1L*.

Even though all of the aforementioned diseases are the result of a complex combination of genes and environmental factors during early neurodevelopment (Van Loo and Martens 2007), it is important to remember that brain development continues throughout the lifespan of an organism. During adulthood, the brain remains plastic and can still modify its organization (Kolb, Gibb et al. 2003). Plasticity occurs through changes in synapses and networks in response to behavioural changes like memory and learning (Milner, Squire et al. 1998, Kandel and Pittenger 1999, Kandel 2001, Spedding, Jay et al. 2005).

In order to explore the role played by *Myt1l* during adulthood, the behavioural consequences of downregulating this gene in the dorsal hippocampus of the adult mouse brain were investigated by bilaterally injecting the *Myt1l* shRNA into the dorsal hippocampus of mouse. This area of the brain was chosen because of its high expression of *Myt1l* in the adult mouse in comparison to other areas. Moreover, the previously mentioned psychiatric disorders have different aetiologies, but they are all related, at least in part, to neuropathological changes in the hippocampus (Huttenlocher 1990, Raymond,

Bauman et al. 1995, Lodge and Grace 2007, Belmaker and Agam 2008). In addition, the dorsal hippocampus has been linked to cognitive processes, which rely heavily on plasticity (Spedding, Jay et al. 2005). It is therefore reasonable that disruptions in *Myt1l* expression in this area of the adult brain could contribute to modifications in behaviour.

Interestingly, this experiment produced a mouse with a very subtle and transient increase in anxiety-like behaviour that normalized within time. This effect was seen in terms of the time spent in the inner zone of the open field arena, where the *Myt1l* knockdown mouse spent significantly less time in the inner zone during the first five minutes in comparison to the control. Despite this, by the end of the 20-minute trial, both groups of mice were spending similar amounts of time in the inner arena. In this experiment, both *Myt1l* knockdown and control mice had a low baseline of exploration of the inner area and a lack of within-trial habituation, possibly indicating that both groups of mice found this test very anxiogenic. Unfortunately, no anxiety-like behaviour was triggered during EPM or light/dark box tests (performed approximately 7 weeks after the open field test). This led to the inference that the *Myt1l* shRNAmir mouse model elicited an increase in anxiety-like behaviour only in very stressful tests, without prior excessive handling. In terms of locomotion, no differences were found between the treated and control mice.

Validation of the correct place of injection, as well as the spread of the virus was performed through immunohistochemical staining of the brain slices. The quantification of the knockdown efficiency *in-vivo* through qPCR showed a 49%

reduction in *Myt1l* expression. It is therefore likely that the effects seen in the *Myt1l* knockdown mouse model are related to the decrease in *Myt1l* expression in the dorsal hippocampus.

Although the dorsal hippocampus has been mainly linked to cognitive processes, it was not completely unexpected to find an association between this brain region and anxiety. Early work from Gray and McNaughton (Gray and McNaughton 2000) proposed a link between anxiogenic situations and a system between the hippocampus and the septum. A further association between anxiety and the dorsal hippocampus was found in rodents with lesions in that area, which were found to exhibit a reduction in anxiety-like behaviours (Deacon, Bannerman et al. 2002, Degroot and Treit 2004, Bertoglio, Joca et al. 2006). Another study showed that low expression of *FGF2* in the dorsal hippocampus of the rat produced an anxiogenic phenotype (Perez, Clinton et al. 2009, Eren-Koçak, Turner et al. 2011). Although the link between the dorsal hippocampus and anxiety is still poorly understood, the results obtained in this last experimental chapter would seem to support it.

5.4 Study limitations

In this thesis only one common limitation was found and it will be discussed. The individual limitations observed in each experimental chapter have been previously discussed and will not be repeated here.

It is important to first note that although the *Myt1l* shRNA used for this thesis resulted in only a partial knockdown, the size of the reduction observed *in-vitro* (rat, mouse and human) and *in-vivo* (mouse) was comparable to other published studies (Thibault, Calvino et al. 2012, Li, Xiong et al. 2013, Shi, Chang et al. 2013, Zeng, Zhang et al. 2013). This limited reduction of gene expression can act as both an advantage and a limitation. One advantage of using an incomplete ablation of *MYT1L* instead of a complete deletion is that it is still unknown if the *MYT1L* knockout is incompatible with cell survival. Although it would be interesting to analyse the consequences of complete deletion of *MYT1L* in a stem cell model, it was safer in this case to only downregulate the gene in order to find the downstream targets of *MYT1L,* which was the aim of Chapter 3.

However, in the case of Chapter 4, it was more a limitation than an advantage since the incomplete ablation of *Myt1l* expression resulted in subtle behavioural effects. Nonetheless, this was anticipated considering only a fraction of the dorsal hippocampus was infected and only about half of *Myt1l* mRNA was reduced in the region. To overcome this limitation, future experiments should aim for a greater reduction to verify the results obtained here.

5.5 Future directions

Due to unfortunate circumstances (possibly technical difficulties) the microarray global expression profile intended for the study described in Chapter 3 failed. I

strongly recommend repeating this experiment to broaden the investigation of the number of genes co-expressed alongside *MYT1L* and to possibly identify more downstream targets of this transcription factor. In addition, the creation of MYT1L antibody could provide the necessary tool to perform ChIP-sequencing and further validate the previous results.

Additionally, it would be interesting to use immunocytochemistry to characterise the SPC04 cells transduced with *MYT1L* shRNAmir. This would show the differentiation potential of this cell line when *MYT1L* is downregulated. For this, cells would need to undergo staining of different markers along differentiation. The time frame would also need to go beyond the time point used for this study (7 days), until mature neurons are observed. Possible markers to use would be Nestin (stem cells), Glial fibrillary acidic protein (GFAP; astrocytes), Adenomatous polyposis coli (APC; oligodendrocytes), Neuronal Nuclei (NeuN; neurons) and Tau (mature neurons). Estimating and comparing the number of mature neurons found in SPC04 transduced with *MYT1L* shRNAmir and the control could further validate the *in-vitro* studies and give an idea of the importance of *MYT1L* for neuron maturation (Vierbuchen, Ostermeier et al. 2010, Pang, Yang et al. 2011). These results would help further expand our knowledge of *MYT1L* during differentiation.

Regarding the experiments described in Chapter 4, it would be advisable to repeat them, adding a non-surgical group of animals. This would be particularly important for the memory and learning paradigms to determine whether the lack of significant results was due to failure of the test or due to the micro-lesions in

the brain caused by the stereotactic surgery. In addition, all the anxiety-like related tests should be prioritized when retesting the knockdown mice. By starting with these tests, the anxiety-like behaviours might be easier to assess and the possible variance due to habituation to handling might be reduced. An alternative solution could be the use of a different mice batch for each paradigm; in this way it is possible to overcome the handing and testing sequence effects.

Another possible improvement might be to increase the number of injections to two per hemisphere to augment the infecting area of the dorsal hippocampus since the knockdown efficiency was only about 49%. Although most experiments injecting viral vectors or plasmids into the mouse brain are restricted to only two injections per brain (Mao, Ge et al. 2009, van Hooijdonk, Ichwan et al. 2009), there are studies that have reported satisfactory results when increasing the volume and injections per mouse brain (Rodriguez-Lebron, Denovan-Wright et al. 2005). Nevertheless, this would not be without its hazards since more intrusion into the brain can lead to additional microlesions affecting the animal phenotype.

An additional mouse model can be engineered through the conditional knockout approach, which has the advantage of selectively silencing gene expression in a spatio-temporal manner. In brief, this type of knockout mouse uses binary transcription transactivation systems that are dependent on doxycycline, offering the versatility to decide when the transgene would be expressed (Lewandoski 2001, Skarnes, Rosen et al. 2011). However, this technique had

carried with it the disadvantage of being time-consuming and expensive (Tong, Huang et al. 2011). Fortunately, the European Conditional Mouse Mutagenesis Program (EUCOMM) has been working on generating about 12,000 conditional mutations across the mouse genome and inserting them into mouse embryonic stem cells. This last procedure allows the generation of conditional knockout mouse models (The-International-Mouse-Knockout-Consortium 2007). At the moment, EUCOMM was able to generate both, embryonic stem cells and a mouse model containing a confirmed conditional knockout for *Myt1l*. However, only the embryonic stem cells are currently available for purchase, while the mouse remains under development (https://www.mousephenotype.org/data/genes/MGI:1100511). It is hoped that the future use of this model will help understand the cellular and behavioural consequences of eliminating *Myt1l* expression at different time points of the life of the mouse.

Even though the study presented in this thesis failed to find an association between the downregulation of *Myt1l* in the dorsal hippocampus and cognitive afflictions (rather than anxiety producing ones), the decreased expression of this gene in other areas of the brain could have repercussions on cognition. It has been hypothesised that *Myt1l* may be involved in cognitive processes given the resemblance to cortical neurons produced by this transcription factor in *in-vitro* experiments transforming fibroblasts (Vierbuchen, Ostermeier et al. 2010, Ambasudhan, Talantova et al. 2011, Pang, Yang et al. 2011). It would be advisable to apply either the EUCOMM *Myt1l* conditional knockout mouse or *Myt1l* shRNAmir model to brain regions involved in cognition, like the cortex,

and analyze the behavioural outcome. For instance, a reduced expression of *MYT1L* was noted in the temporal cortex of patients suffering from autism, which could possibly be the cause of defects in neuronal maturations and synapses in this area (Garbett, Ebert et al. 2008).

Lastly, previous studies have suggested that *MYT1L* plays a role in synaptogenesis. I suggest that both the *in-vitro* and *in-vivo* approaches mentioned above would be greatly benefited by further staining of the cells or tissue for two purposes. Firstly, the samples could be immunostained with synaptic markers for excitatory synapse such as: bassoon, anti-glutamate receptor 2/3 (GluR2/3), Postsynaptic density protein 95 (PSD-95) and Anti-Glutamate Receptor NMDAR1 (NR1), among others (Woolfrey, Srivastava et al. 2009). The choice of analysing the excitatory synapses comes from the study showing that the majority of neurons, which matured through the addition of *Myt1l*, were excitatory and glutamatergic neurons (Vierbuchen, Ostermeier et al. 2010). Secondly, the cells or tissue infected with the *MYT1L* shRNAmir could undergo GFP immunostaining to analyse the dendritic spines (Srivastava, Woolfrey et al. 2011). Notably, it has been observed that changes in the size, shape or number of the spines were associated to psychiatric disorders like schizophrenia (Glantz and Lewis 2000), major depressive disorder (Kang, Voleti et al. 2012), autism (Hutsler and Zhang 2010) and mental retardation (Kaufmann and Moser 2000), among others. This is relevant to our study, since the diseases mentioned before have been all linked to mutation in the *MYT1L* gene. The findings from any of the suggested studies would further increase our knowledge of the role of *MYT1L* at the genetic, cellular and functional levels.

5.6 Conclusions

Carefully dissecting and assessing the role of individual genes in the molecular process could help us to ultimately understand the underlying basis of behavioural patterns. The validation of the *MYT1L* shRNAmir sequence presented in this thesis provided a valuable tool by which to study the function of *MYT1L*. This method of using the shRNAmir sequence in conjunction with lentiviral vectors to specifically knockdown *MYT1L* proved useful in both cell (*in-vitro)* and mouse (*in-vivo)* models. The *MYT1L* shRNAmir cell model provided valuable information about the putative *MYT1L* downstream targets. As a result, this study has laid the foundations for determining the *MYT1L* pathway during neurogenesis. Furthermore, the animal model offered insight on a possible association between subtle anxiety-like behaviour and downregulation of *Myt1l* in the dorsal hippocampus. The results presented throughout this thesis represent the beginning of solving the puzzle of the *MYT1L* pathway and its role in behaviour.

References

Addington, A. and J. Rapoport (2009). "The genetics of childhood-onset schizophrenia: When madness strikes the prepubescent." Current Psychiatry Reports **11**(2): 156-161.

Adler, A. F., C. L. Grigsby, K. Kulangara, H. Wang, R. Yasuda and K. W. Leong (2012). "Nonviral Direct Conversion of Primary Mouse Embryonic Fibroblasts to Neuronal Cells." Molecular Therapy — Nucleic Acids **1**: e32.

Ahmad-Annuar, A., S. J. Tabrizi and E. M. C. Fisher (2003). "Mouse models as a tool for understanding neurodegenerative diseases." Current Opinion in Neurology **16**(4): 451-458.

Ahn, J.-I., K.-H. Lee, D.-M. Shin, J.-W. Shim, J.-S. Lee, S. Y. Chang, Y.-S. Lee, M. J. Brownstein, S.-H. Lee and Y.-S. Lee (2004). "Comprehensive transcriptome analysis of differentiation of embryonic stem cells into midbrain and hindbrain neurons." Developmental Biology **265**(2): 491-501.

Aiba, K., A. A. Sharov, M. G. Carter, C. Foroni, A. L. Vescovi and M. S. H. Ko (2006). "Defining a developmental path to neural fate by global expression profiling of mouse embryonic stem cells and adult neural stem/progenitor cells." Stem Cells **24**(4): 889-895.

Amado, R. G. and I. S. Y. Chen (1999). "Lentiviral Vectors--the Promise of Gene Therapy Within Reach?" Science **285**(5428): 674-676.

Ambasudhan, R., M. Talantova, R. Coleman, X. Yuan, S. Zhu, Stuart A. Lipton and S. Ding (2011). "Direct reprogramming of adult human fibroblasts to functional neurons under defined conditions." Cell Stem Cell **9**(2): 113-118.

Andersen, S. L. (2003). "Trajectories of brain development: point of vulnerability or window of opportunity?" Neuroscience & Biobehavioral Reviews **27**(1-2): 3-18.

Anderson, R. M., A. R. Lawrence, R. W. Stottmann, D. Bachiller and J. Klingensmith (2002). "Chordin and noggin promote organizing centers of forebrain development in the mouse." Development **129**(21): 4975-4987.

Andrews, N. and S. E. File (1993). "Handling history of rats modifies behavioural effects of drugs in the elevated plus-maze test of anxiety." European Journal of Pharmacology **235**(1): 109-112.

Antunes, M. and G. Biala (2012). "The novel object recognition memory: neurobiology, test procedure, and its modifications." Cognitive processing **13**(2): 93-110.

Arlotta, P., B. J. Molyneaux, D. Jabaudon, Y. Yoshida and J. D. Macklis (2008). "Ctip2 Controls the Differentiation of Medium Spiny Neurons and the Establishment of the Cellular Architecture of the Striatum." The Journal of Neuroscience **28**(3): 622-632.

Augusti-Tocco, G. and G. Sato (1969). "Establishment of functional clonal lines of neurons from mouse neuroblastoma." Proceedings of the National Academy of Sciences of the United States of America **64**(1): 311-315.

Austin, C. P., J. F. Battey, A. Bradley, M. Bucan, M. Capecchi, F. S. Collins, W. F. Dove, G. Duyk, S. Dymecki, J. T. Eppig, F. B. Grieder, N. Heintz, G. Hicks, T. R. Insel, A. Joyner, B. H. Koller, K. C. K. Lloyd, T. Magnuson, M. W. Moore, A. Nagy, J. D. Pollock, A. D. Roses, A. T. Sands, B. Seed, W. C. Skarnes, J. Snoddy, P. Soriano, D. J. Stewart, F. Stewart, B. Stillman, H. Varmus, L. Varticovski, I. M. Verma, T. F. Vogt, H. von Melchner, J. Witkowski, R. P. Woychik, W. Wurst, G. D. Yancopoulos, S. G. Young and B. Zambrowicz (2004). "The knockout mouse project." Nature Genetics **36**: 921-924.

Babu, M. M., N. M. Luscombe, L. Aravind, M. Gerstein and S. A. Teichmann (2004). "Structure and evolution of transcriptional regulatory networks." Current Opinion in Structural Biology **14**(3): 283-291.

Baekelandt, V., A. Claeys, K. Eggermont, E. Lauwers, B. De Strooper, B. Nuttin and Z. Debyser (2002). "Characterization of lentiviral vector-mediated gene transfer in adult mouse brain." Human Gene Therapy **13**(7): 841-853.

Bahat, A., R. Kedmi, K. Gazit, I. Richardo-Lax, E. Ainbinder and R. Dikstein (2013). "TAF4b and TAF4 differentially regulate mouse embryonic stem cells maintenance and proliferation." Genes to Cells **18**(3): 225-237.

Bailey, C. H. and E. R. Kandel (1993). "Structural changes accompanying memory storage." Annual Review of Physiology **55**(1): 397-426.

Bang, A. G. and M. D. Goulding (1996). "Regulation of vertebrate neural cell fate by transcription factors." Current Opinion in Neurobiology **6**(1): 25-32.

Bannerman, D. M., J. N. P. Rawlins, S. B. McHugh, R. M. J. Deacon, B. K. Yee, T. Bast, W. N. Zhang, H. H. J. Pothuizen and J. Feldon (2004). "Regional dissociations within the hippocampus—memory and anxiety." Neuroscience & Biobehavioral Reviews **28**(3): 273-283.

Bardo, S., M. G. Cavazzini and N. Emptage (2006). "The role of the endoplasmic reticulum Ca2+ store in the plasticity of central neurons." Trends in Pharmacological Sciences **27**(2): 78-84.

Bark, I. C., K. M. Hahn, A. E. Ryabinin and M. C. Wilson (1995). "Differential expression of SNAP-25 protein isoforms during divergent vesicle fusion events of neural development." Proceedings of the National Academy of Sciences of the United States of America **92**(5): 1510-1514.

Bartley, A. J., D. W. Jones and D. R. Weinberger (1997). "Genetic variability of human brain size and cortical gyral patterns." Brain **120**(2): 257-269.

Bavelier, D., D. M. Levi, R. W. Li, Y. Dan and T. K. Hensch (2010). "Removing brakes on adult brain plasticity: from molecular to behavioral interventions." The Journal of Neuroscience **30**(45): 14964-14971.

Bekinschtein, P., M. Cammarota, I. Izquierdo and J. H. Medina (2008). "Reviews: BDNF and memory formation and storage." The Neuroscientist **14**(2): 147-156.

Belmaker, R. H. and G. Agam (2008). "Major depressive disorder." New England Journal of Medicine **358**(1): 55-68.

Berkovits-Cymet, H. J., B. T. Amann and J. M. Berg (2004). "Solution structure of a CCHHC domain of neural zinc finger factor-1 and its implications for DNA binding." Biochemistry **43**(4): 898-903.

Bertoglio, L. J., S. R. L. Joca and F. S. Guimarães (2006). "Further evidence that anxiety and memory are regionally dissociated within the hippocampus." Behavioural Brain Research **175**(1): 183-188.

Besold, A., S. Lee, S. J. Michel, N. Lue Sue and H. Cymet (2010). "Functional characterization of iron-substituted neural zinc finger factor 1: metal and DNA binding." Journal of Biological Inorganic Chemistry **15**(4): 583-590.

Bevins, R. A. and J. Besheer (2006). "Object recognition in rats and mice: a one-trial non-matching-to-sample learning task to study 'recognition memory'." Nature Protocols **1**(3): 1306-1311.

Blanchard, E. M., K. Iizuka, M. Christe, D. A. Conner, A. Geisterfer-Lowrance, F. J. Schoen, D. W. Maughan, C. E. Seidman and J. G. Seidman (1997).

"Targeted ablation of the murine α-Tropomyosin gene." Circulation Research **81**(6): 1005-1010.

Blasie, C. A. and J. M. Berg (1999). "Toward ligand identification within a CCHHC zinc-binding domain from the NZF/Myt1 family." Inorganic Chemistry **39**(2): 348-351.

Blomer, U., L. Naldini, T. Kafri, D. Trono, I. Verma and F. Gage (1997). "Highly efficient and sustained gene transfer in adult neurons with a lentivirus vector." Journal of Virology **71**(9): 6641-6649.

Bolivar, V., B. Caldarone, A. Reilly and L. Flaherty (2000). "Habituation of activity in an open field: a survey of inbred strains and F1 hybrids." Behavior Genetics **30**(4): 285-293.

Bonaglia, M. C., R. Giorda, A. Massagli, R. Galluzzi, R. Ciccone and O. Zuffardi (2008). "A familial inverted duplication/deletion of 2p25.1-25.3 provides new clues on the genesis of inverted duplications." European Journal of Human Genetics **17**(2): 179-186.

Bosker, F. J., C. A. Hartman, I. M. Nolte, B. P. Prins, P. Terpstra, D. Posthuma, T. van Veen, G. Willemsen, R. H. DeRijk, E. J. de Geus, W. J. Hoogendijk, P. F. Sullivan, B. W. Penninx, D. I. Boomsma, H. Snieder and W. A. Nolen (2011). "Poor replication of candidate genes for major depressive disorder using genome-wide association data." Molecular Psychiatry **16**(5): 516-532.

Boudreau, R. L., S. E. Garwick-Coppens, J. Liu, L. M. Wallace and S. Q. Harper (2011). Rapid cloning and validation of microRNA shuttle vectors: a practical guide. RNA Interference Techniques, Springer**:** 19-37.

Bourin, M. and M. Hascoët (2003). "The mouse light/dark box test." European Journal of Pharmacology **463**(1–3): 55-65.

Brennan, P. A. and E. B. Keverne (2004). "Something in the air? new insights into mammalian pheromones." Current Biology **14**(2): R81-R89.

Brivanlou, A. H. and J. E. Darnell (2002). "Signal transduction and the control of gene expression." Science **295**(5556): 813-818.

Brodal, P. (2010). Development, aging, and plasticity. The Central Nervous System. Oxford, Oxford University Press, USA**:** 115-156.

Brown, K. M., C.-y. Chu and T. M. Rana (2005). "Target accessibility dictates the potency of human RISC." Nature Structural & Molecular Biology **12**(5): 469-470.

Brown, T. A., M. F. Joanisse, J. S. Gati, S. M. Hughes, P. L. Nixon, R. S. Menon and S. G. Lomber (2013). "Characterization of the blood-oxygen level-dependent (BOLD) response in cat auditory cortex using high-field fMRI." NeuroImage **64**(0): 458-465.

Brummelkamp, T. R., R. Bernards and R. Agami (2002). "A system for stable expression of short interfering RNAs in mammalian cells." Science **296**(5567): 550-553.

Brunstein, J. (2010). Methods in molecular biology and genetic enfineering. Lewin's Genes X. J. E. G. E. S. K. Krebs, S. T., Jones and Bartlett**:** 42-78.

Bustin, S. A. and T. Nolan (2004). "Pitfalls of quantitative real-time reverse-transcription polymerase chain reaction." Journal of Biomolecular Techniques **15**(3): 155.

Calderón, F. H., A. Bonnefont, F. J. Muñoz, V. Fernández, L. A. Videla and N. C. Inestrosa (1999). "PC12 and Neuro 2a cells have different susceptibilities to acetylcholinesterase–amyloid complexes, amyloid25–35 fragment, glutamate, and hydrogen peroxide." Journal of Neuroscience Research **56**(6): 620-631.

Caplen, N. J. (2004). "Gene therapy progress and prospects. Downregulating gene expression: the impact of RNA interference." Gene Therapy **11**(16): 1241-1248.

Cartharius, K., K. Frech, K. Grote, B. Klocke, M. Haltmeier, A. Klingenhoff, M. Frisch, M. Bayerlein and T. Werner (2005). "MatInspector and beyond: promoter analysis based on transcription factor binding sites." Bioinformatics **21**(13): 2933-2942.

Carthew, R. W. and E. J. Sontheimer (2009). "Origins and mechanisms of miRNAs and siRNAs." Cell **136**(4): 642-655.

Carvalho, M. C., S. Masson, M. L. Brandão and M. A. de Souza Silva (2008). "Anxiolytic-like effects of substance P administration into the dorsal, but not ventral, hippocampus and its influence on serotonin." Peptides **29**(7): 1191-1200.

Cerbone, A. and A. G. Sadile (1994). "Behavioral habituation to spatial novelty: Interference and noninterference studies." Neuroscience & Biobehavioral Reviews **18**(4): 497-518.

Cetin, A., S. Komai, M. Eliava, P. H. Seeburg and P. Osten (2007). "Stereotaxic gene delivery in the rodent brain." Nature Protocols **1**(6): 3166-3173.

Chang, K., S. J. Elledge and G. J. Hannon (2006). "Lessons from Nature: microRNA-based shRNA libraries." Nature Methods **3**(9): 707-714.

Chédotal, A. and L. J. Richards (2010). "Wiring the brain: the biology of neuronal guidance." Cold Spring Harbor Perspectives in Biology **2**(6).

Chelly, J., M. Khelfaoui, F. Francis, B. Cherif and T. Bienvenu (2006). "Genetics and pathophysiology of mental retardation." European Journal of Human Genetics **14**(6): 701-713.

Chenn, A. and S. K. McConnell (1995). "Cleavage orientation and the asymmetric inheritance of notchl immunoreactivity in mammalian neurogenesis." Cell **82**(4): 631-641.

Cocks, G., N. Romanyuk, T. Amemori, P. Jendelova, O. Forostyak, A. Jeffries, L. Perfect, S. Thuret, G. Dayanithi, E. Sykova and J. Price (2013). "Conditionally immortalized stem cell lines from human spinal cord retain regional identity and generate functional V2a interneurons and motorneurons." Stem Cell Research & Therapy **4**(3): 69.

Coleman, J. E. (1992). "Zinc proteins: enzymes, storage proteins, transcription factors, and replication proteins." Annual Review of Biochemistry **61**(1): 897-946.

Colón-Ramos, D. A. and K. Shen (2008). "Cellular Conductors: Glial Cells as Guideposts during Neural Circuit Development." PLoS Biology **6**(4): e112.

Copp, A. J., N. D. E. Greene and J. N. Murdoch (2003). "The genetic basis of mammalian neurulation." Nature Reviews Genetics **4**(10): 784-793.

Courchesne, E., H. J. Chisum, J. Townsend, A. Cowles, J. Covington, B. Egaas, M. Harwood, S. Hinds and G. A. Press (2000). "Normal brain development and aging: quantitative analysis at in vivo MR Imaging in healthy Volunteers1." Radiology **216**(3): 672-682.

Crawley, J. and F. K. Goodwin (1980). "Preliminary report of a simple animal behavior model for the anxiolytic effects of benzodiazepines." Pharmacology Biochemistry and Behavior **13**(2): 167-170.

Crawley, J. N. (1999). "Behavioral phenotyping of transgenic and knockout mice: experimental design and evaluation of general health, sensory functions, motor abilities, and specific behavioral tests." Brain Research **835**(1): 18-26.

Crawley, J. N. (2007). Motor functions What's wrong with my mouse? behavioral phenotyping of transgenic and knockout mice. J. N. Crawley. United States of America, John Wiley & Sons, Inc.

Crews, F., J. He and C. Hodge (2007). "Adolescent cortical development: A critical period of vulnerability for addiction." Pharmacology Biochemistry and Behavior **86**(2): 189-199.

Crino, P., K. Khodakhah, K. Becker, S. Ginsberg, S. Hemby and J. Eberwine (1998). "Presence and phosphorylation of transcription factors in developing dendrites." Proceedings of the National Academy of Sciences of the United States of America **95**(5): 2313-2318.

Crusio, W. E. and H. Schwegler (1987). "Hippocampal mossy fiber distribution covaries with open-field habituation in the mouse." Behavioural Brain Research **26**(2–3): 153-158.

D'Amour, K. A. and F. H. Gage (2003). "Genetic and functional differences between multipotent neural and pluripotent embryonic stem cells." Proceedings of the National Academy of Sciences of the United States of America **100**(Suppl 1): 11866-11872.

D'Hooge, R. and P. P. De Deyn (2001). "Applications of the Morris water maze in the study of learning and memory." Brain Research Reviews **36**(1): 60-90.

Dahl, R. E. (2004). "Adolescent brain development: a period of vulnerabilities and opportunities." Annals of the New York Academy of Sciences **1021**(1): 1-22.

Davidson, B. L. and R. L. Boudreau (2007). "RNA interference: a tool for querying nervous system function and an emerging therapy." Neuron **53**(6): 781-788.

De Camilli, P., S. M. Harris, W. B. Huttner and P. Greengard (1983). "Synapsin I (Protein I), a nerve terminal-specific phosphoprotein. II. Its specific association with synaptic vesicles demonstrated by immunocytochemistry in agarose-embedded synaptosomes." The Journal of Cell Biology **96**(5): 1355-1373.

de Fougerolles, A., H.-P. Vornlocher, J. Maraganore and J. Lieberman (2007). "Interfering with disease: a progress report on siRNA-based therapeutics." Nature Reviews Drug Discovery **6**(6): 443-453.

de Lima, M. N., T. Luft, R. Roesler and N. Schröder (2006). "Temporary inactivation reveals an essential role of the dorsal hippocampus in consolidation of object recognition memory." Neuroscience Letters **405**(1–2): 142-146.

Deacon, R. M., D. M. Bannerman and J. N. P. Rawlins (2002). "Anxiolytic effects of cytotoxic hippocampal lesions in rats." Behavioral neuroscience **116**(3): 494.

Degroot, A. and D. Treit (2004). "Anxiety is functionally segregated within the septo-hippocampal system." Brain Research **1001**(1–2): 60-71.

Dekaban, A. S. and D. Sadowsky (1978). "Changes in brain weights during the span of human life: Relation of brain weights to body heights and body weights." Annals of Neurology **4**(4): 345-356.

Dere, E., J. P. Huston and M. A. De Souza Silva (2005). "Episodic-like memory in mice: simultaneous assessment of object, place and temporal order memory." Brain Research Protocols **16**(1–3): 10-19.

Dere, E., J. P. Huston and M. A. De Souza Silva (2007). "The pharmacology, neuroanatomy and neurogenetics of one-trial object recognition in rodents." Neuroscience & Biobehavioral Reviews **31**(5): 673-704.

Dermietzel, R. and D. C. Spray (1993). "Gap junctions in the brain: where, what type, how many and why?" Trends in Neurosciences **16**(5): 186-192.

Desai, A. R. and S. K. McConnell (2000). "Progressive restriction in fate potential by neural progenitors during cerebral cortical development." Development **127**(13): 2863-2872.

Dissen, G., J. McBride, A. Lomniczi, V. Matagne, M. Dorfman, T. Neff, F. Galimi and S. Ojeda (2012). Using lentiviral vectors as delivery vehicles for gene therapy. Controlled Genetic Manipulations. A. Morozov, Humana Press. **65:** 69-96.

Doherty, F. C., J. B. Schaack and C. D. Sladek (2011). "Comparison of the efficacy of four viral vectors for transducing hypothalamic magnocellular neurosecretory neurons in the rat supraoptic nucleus." Journal of Neuroscience Methods **197**(2): 238-248.

Draganski, B., C. Gaser, V. Busch, G. Schuierer, U. Bogdahn and A. May (2004). "Neuroplasticity: Changes in grey matter induced by training." Nature **427**(6972): 311-312.

Du, Q., H. Thonberg, J. Wang, C. Wahlestedt and Z. Liang (2005). "A systematic analysis of the silencing effects of an active siRNA at all single-nucleotide mismatched target sites." Nucleic Acids Research **33**(5): 1671-1677.

Dykxhoorn, D. M., C. D. Novina and P. A. Sharp (2003). "Killing the messenger: short RNAs that silence gene expression." Nature Reviews Molecular Cell Biology **4**(6): 457-467.

Elbashir, S. M., J. Harborth, W. Lendeckel, A. Yalcin, K. Weber and T. Tuschl (2001). "Duplexes of 21-nucleotide RNAs mediate RNA interference in cultured mammalian cells." Nature **411**(6836): 494-498.

Engin, E. and D. Treit (2007). "The role of hippocampus in anxiety: intracerebral infusion studies." Behavioural pharmacology **18**(5-6): 365-374.

Ennaceur, A. (2010). "One-trial object recognition in rats and mice: methodological and theoretical issues." Behavioural brain research **215**(2): 244.

Eren-Koçak, E., C. A. Turner, S. J. Watson and H. Akil (2011). "Short-hairpin RNA silencing of endogenous fibroblast growth factor 2 in rat hippocampus increases anxiety behavior." Biological psychiatry **69**(6): 534-540.

Erraji-Benchekroun, L., M. D. Underwood, V. Arango, H. Galfalvy, P. Pavlidis, P. Smyrniotopoulos, J. J. Mann and E. Sibille (2005). "Molecular aging in human prefrontal cortex is selective and continuous throughout adult life." Biological psychiatry **57**(5): 549-558.

Evans, M. J. and M. H. Kaufman (1981). "Establishment in culture of pluripotential cells from mouse embryos." Nature **292**(5819): 154-156.

Farkas, L. M. and W. B. Huttner (2008). "The cell biology of neural stem and progenitor cells and its significance for their proliferation versus differentiation during mammalian brain development." Current Opinion in Cell Biology **20**(6): 707-715.

Fellmann, C., T. Hoffmann, V. Sridhar, B. Hopfgartner, M. Muhar, M. Roth, Dan Y. Lai, Inês A. M. Barbosa, Jung S. Kwon, Y. Guan, N. Sinha and J. Zuber (2013). "An Optimized microRNA Backbone for Effective Single-Copy RNAi." Cell Reports **5**(6): 1704-1713.

Fernandes, C. and S. E. File (1996). "The influence of open arm ledges and maze experience in the elevated plus-maze." Pharmacology Biochemistry and Behavior **54**(1): 31-40.

Fernandes, C., L. Liu, J. Paya-Cano, S. Gregorová, J. Forejt and L. Schalkwyk (2004). "Behavioral characterization of wild derived male mice (Mus musculus musculus) of the PWD/Ph inbred strain: high exploration compared to C57BL/6J." Behavior Genetics **34**(6): 621-630.

Ferreira, A., L.-S. Chin, L. Li, L. M. Lanier, K. S. Kosik and P. Greengard (1998). "Distinct roles of synapsin I and synapsin II during neuronal development." Molecular Medicine **4**(1): 22.

Fewell, G. D. and K. Schmitt (2006). "Vector-based RNAi approaches for stable, inducible and genome-wide screens." Drug Discovery Today **11**(21–22): 975-982.

File, S. E., A. S. Lippa, B. Beer and M. T. Lippa (2001). Animal tests of anxiety. Current Protocols in Neuroscience, John Wiley & Sons, Inc.

Finlay, B. and R. Darlington (1995). "Linked regularities in the development and evolution of mammalian brains." Science **268**(5217): 1578-1584.

Fire, A., S. Xu, M. K. Montgomery, S. A. Kostas, S. E. Driver and C. C. Mello (1998). "Potent and specific genetic interference by double-stranded RNA in Caenorhabditis elegans." Nature **391**(6669): 806-811.

Francis, F., A. Koulakoff, D. Boucher, P. Chafey, B. Schaar, M.-C. Vinet, G. Friocourt, N. McDonnell, O. Reiner, A. Kahn, S. K. McConnell, Y. Berwald-Netter, P. Denoulet and J. Chelly (1999). "Doublecortin is a developmentally regulated, microtubule-associated protein expressed in migrating and differentiating neurons." Neuron **23**(2): 247-256.

Fukuchi-Shimogori, T. and E. A. Grove (2001). "Neocortex patterning by the secreted signaling molecule FGF8." Science **294**(5544): 1071-1074.

Gage, F. H. (2000). "Mammalian neural stem cells." Science **287**(5457): 1433-1438.

Gamsjaeger, R., M. K. Swanton, F. J. Kobus, E. Lehtomaki, J. A. Lowry, A. H. Kwan, J. M. Matthews and J. P. Mackay (2008). "Structural and biophysical analysis of the DNA binding properties of Myelin Transcription Factor 1." Journal of Biological Chemistry **283**(8): 5158-5167.

Gao, X. and P. Zhang (2007). "Transgenic RNA interference in mice." Physiology **22**(3): 161-166.

Garbett, K., P. J. Ebert, A. Mitchell, C. Lintas, B. Manzi, K. Mirnics and A. M. Persico (2008). "Immune transcriptome alterations in the temporal cortex of subjects with autism." Neurobiology of Disease **30**(3): 303-311.

Garbino, A., R. J. van Oort, S. S. Dixit, A. P. Landstrom, M. J. Ackerman and X. H. T. Wehrens (2009). "Molecular evolution of the junctophilin gene family." Physiological Genomics **37**(3): 175-186.

Genc, S., T. F. Koroglu and K. Genc (2004). "RNA interference in neuroscience." Molecular Brain Research **132**(2): 260-270.

Gharani, N., R. Benayed, V. Mancuso, L. M. Brzustowicz and J. H. Millonig (2004). "Association of the homeobox transcription factor, ENGRAILED 2, 3, with autism spectrum disorder." Molecular Psychiatry **9**(5): 474-484.

Ghashghaei, H. T., C. Lai and E. S. Anton (2007). "Neuronal migration in the adult brain: are we there yet?" Nature Reviews Neuroscience **8**(2): 141-151.

Giedd, J. N., J. Blumenthal, N. O. Jeffries, F. X. Castellanos, H. Liu, A. Zijdenbos, T. Paus, A. C. Evans and J. L. Rapoport (1999). "Brain development during childhood and adolescence: a longitudinal MRI study." Nature Neuroscience **2**(10): 861-863.

Gilbert, P. E. and R. P. Kesner (2003). Localization of function within the dorsal hippocampus: The role of the CA3 subregion in paired-associate learning. Washington, DC, ETATS-UNIS, American Psychological Association.

Gilbert, S. F. (2010). Developmental Biology. United States of America, Sinauer Associates.

Gingrich, J., T. Rubio and C. Karlak (2006). "Effect of RNA degradation on the data quality in quantitative PCR and microarray experiments." Bio-Rad Bulletin **5452**.

Glantz, L. A. and D. A. Lewis (2000). "Decreased dendritic spine density on prefrontal cortical pyramidal neurons in schizophrenia." Archives of general psychiatry **57**(1): 65-73.

Goridis, C. and J.-F. Brunet (1999). "Transcriptional control of neurotransmitter phenotype." Current Opinion in Neurobiology **9**(1): 47-53.

Gossen, M. and H. Bujard (2002). "Studying gene function in eukaryotes by conditional gene inactivation." Annual review of genetics **36**(1): 153-173.

Gössl, C., L. Fahrmeir, B. Pütz, L. M. Auer and D. P. Auer (2002). "Fiber Tracking from DTI Using Linear State Space Models: Detectability of the Pyramidal Tract." NeuroImage **16**(2): 378-388.

Gray, J. A. and N. McNaughton (2000). The neuropsychology of anxiety: an enquiry into the functions of the septo-hippocampal system. Great Britain, Oxford University Press.

Gray, P. A., H. Fu, P. Luo, Q. Zhao, J. Yu, A. Ferrari, T. Tenzen, D.-i. Yuk, E. F. Tsung, Z. Cai, J. A. Alberta, L.-p. Cheng, Y. Liu, J. M. Stenman, M. T. Valerius, N. Billings, H. A. Kim, M. E. Greenberg, A. P. McMahon, D. H. Rowitch, C. D.

Stiles and Q. Ma (2004). "Mouse brain organization revealed through direct genome-scale TF expression analysis." Science **306**(5705): 2255-2257.

Greene, L. A. and A. S. Tischler (1976). "Establishment of a noradrenergic clonal line of rat adrenal pheochromocytoma cells which respond to nerve growth factor." Proceedings of the National Academy of Sciences of the United States of America **73**(7): 2424-2428.

Greengard, P., F. Valtorta, A. Czernik and F. Benfenati (1993). "Synaptic vesicle phosphoproteins and regulation of synaptic function." Science **259**(5096): 780-785.

Gritsman, K., W. S. Talbot and A. F. Schier (2000). "Nodal signaling patterns the organizer." Development **127**(5): 921-932.

Gruchy, N., M.-L. Jacquemont, S. Lyonnet, P. Labrune, I. El Kamel, J.-P. Siffroi and M.-F. Portnoï (2007). "Recurrent inverted duplication of 2p with terminal deletion in a patient with the classical phenotype of trisomy 2p23-pter." American Journal of Medical Genetics Part A **143A**(20): 2417-2422.

Gu, S., L. Jin, Y. Zhang, Y. Huang, F. Zhang, Paul N. Valdmanis and Mark A. Kay (2012). "The Loop Position of shRNAs and Pre-miRNAs Is Critical for the Accuracy of Dicer Processing In Vivo." Cell **151**(4): 900-911.

Gurok, U., C. Steinhoff, B. Lipkowitz, H.-H. Ropers, C. Scharff and U. A. Nuber (2004). "Gene expression changes in the course of neural progenitor cell differentiation." The Journal of Neuroscience **24**(26): 5982-6002.

Haier, R. J., R. E. Jung, R. A. Yeo, K. Head and M. T. Alkire (2004). "Structural brain variation and general intelligence." NeuroImage **23**(1): 425-433.

Hammond, R. S., L. E. Tull and R. W. Stackman (2004). "On the delay-dependent involvement of the hippocampus in object recognition memory." Neurobiology of Learning and Memory **82**(1): 26-34.

Hammond, S. M. (2005). "Dicing and slicing: the core machinery of the RNA interference pathway." FEBS Letters **579**(26): 5822-5829.

Hannon, G. J. and J. J. Rossi (2004). "Unlocking the potential of the human genome with RNA interference." Nature **431**(7006): 371-378.

Heldt, S. A. and K. J. Ressler (2009). "The use of lentiviral vectors and Cre/loxP to investigate the function of genes in complex behaviors." Frontiers in molecular neuroscience **2**: 22.

Hof, P. R., B. D. Trapp, J. de Vellis, L. Claudio and D. R. Colman (2003). Cellular components of the nervous tissue. Fundamental Neuroscience. L. R. Squire, B. F. E., M. S. K. et al. United States of America, Academic Press**:** 49-78.

Hogg, S. (1996). "A review of the validity and variability of the Elevated Plus-Maze as an animal model of anxiety." Pharmacology Biochemistry and Behavior **54**(1): 21-30.

Hoheisel, J. D. (2006). "Microarray technology: beyond transcript profiling and genotype analysis." Nature Reviews Genetics **7**(3): 200-210.

Holmes, S. E., E. O'Hearn, A. Rosenblatt, C. Callahan, H. S. Hwang, R. G. Ingersoll-Ashworth, A. Fleisher, G. Stevanin, A. Brice, N. T. Potter, C. A. Ross and R. L. Margolis (2001). "A repeat expansion in the gene encoding junctophilin-3 is associated with Huntington disease-like 2." Nat Genet **29**(4): 377-378.

Hommel, J. D., R. M. Sears, D. Georgescu, D. L. Simmons and R. J. DiLeone (2003). "Local gene knockdown in the brain using viral-mediated RNA interference." Nature Medicine **9**(12): 1539-1544.

Howarth, J., Y. Lee and J. Uney (2010). "Using viral vectors as gene transfer tools (Cell Biology and Toxicology Special Issue: ETCS-UK 1 day meeting on genetic manipulation of cells)." Cell Biology and Toxicology **26**(1): 1-20.

Hüppi, P. S., S. Warfield, R. Kikinis, P. D. Barnes, G. P. Zientara, F. A. Jolesz, M. K. Tsuji and J. J. Volpe (1998). "Quantitative magnetic resonance imaging of brain development in premature and mature newborns." Annals of Neurology **43**(2): 224-235.

Hutsler, J. J. and H. Zhang (2010). "Increased dendritic spine densities on cortical projection neurons in autism spectrum disorders." Brain Research **1309**(0): 83-94.

Huttenlocher, P. R. (1990). "Morphometric study of human cerebral cortex development." Neuropsychologia **28**(6): 517-527.

Huttenlocher, P. R. (1991). "Dendritic and synaptic pathology in mental retardation." Pediatric Neurology **7**(2): 79-85.

Huttner, W., W. Schiebler, P. Greengard and P. De Camilli (1983). "Synapsin I (protein I), a nerve terminal-specific phosphoprotein. III. Its association with synaptic vesicles studied in a highly purified synaptic vesicle preparation." The Journal of Cell Biology **96**(5): 1374-1388.

Irizarry, R. A., D. Warren, F. Spencer, I. F. Kim, S. Biswal, B. C. Frank, E. Gabrielson, J. G. N. Garcia, J. Geoghegan, G. Germino, C. Griffin, S. C. Hilmer, E. Hoffman, A. E. Jedlicka, E. Kawasaki, F. Martinez-Murillo, L. Morsberger, H. Lee, D. Petersen, J. Quackenbush, A. Scott, M. Wilson, Y. Yang, S. Q. Ye and

W. Yu (2005). "Multiple-laboratory comparison of microarray platforms." Nature Methods **2**(5): 345-350.

Jaenisch, R. (1988). "Transgenic animals." Science **240**(4858): 1468-1474.

Jakobsson, J. and C. Lundberg (2006). "Lentiviral vectors for use in the central nervous system." Molecular Therapy **13**(3): 484-493.

Jeffries, A. R., L. W. Perfect, J. Ledderose, L. C. Schalkwyk, N. J. Bray, J. Mill and J. Price (2012). "Stochastic choice of allelic expression in human neural stem cells." Stem Cells **30**(9): 1938-1947.

Jernigan, T. L., W. F. C. Baaré, J. Stiles and K. S. Madsen (2011). Postnatal brain development: structural imaging of dynamic neurodevelopmental processess. Progress in Brain Research. O. Braddick, J. Atkinson and G. M. Innocenti. Great Britain, Elsevier. **189:** 77-92.

Jiang, Y., V. C. Yu, F. Buchholz, S. O'Connell, S. J. Rhodes, C. Candeloro, Y.-R. Xia, A. J. Lusis and M. G. Rosenfeld (1996). "A novel family of Cys-Cys, His-Cys zinc finger transcription factors expressed in developing nervous system and pituitary gland." Journal of Biological Chemistry **271**(18): 10723-10730.

Johnson, M. B., Y. I. Kawasawa, C. E. Mason, e. Krsnik, G. Coppola, D. Bogdanovi, D. H. Geschwind, S. M. Mane, M. W. State and N. estan (2009). "Functional and evolutionary insights into human brain development through global transcriptome analysis." Neuron **62**(4): 494-509.

Johnston, M. V. (2009). "Plasticity in the developing brain: implications for rehabilitation." Developmental Disabilities Research Reviews **15**(2): 94-101.

Kafri, T., U. Blomer, D. A. Peterson, F. H. Gage and I. M. Verma (1997). "Sustained expression of genes delivered directly into liver and muscle by lentiviral vectors." Nature Genetics **17**(3): 314-317.

Kakizawa, S., Y. Kishimoto, K. Hashimoto, T. Miyazaki, K. Furutani, H. Shimizu, M. Fukaya, M. Nishi, H. Sakagami, A. Ikeda, H. Kondo, M. Kano, M. Watanabe, M. Iino and H. Takeshima (2007). "Junctophilin-mediated channel crosstalk essential for cerebellar synaptic plasticity." The EMBO Journal **26**(7): 1924-1933.

Kandel, E. R. (2001). "The molecular biology of memory storage: a dialogue between genes and synapses." Science **294**(5544): 1030-1038.

Kandel, E. R. and C. Pittenger (1999). "The past, the future and the biology of memory storage." Philosophical Transactions of the Royal Society of London. Series B: Biological Sciences **354**(1392): 2027-2052.

Kang, H. J., B. Voleti, T. Hajszan, G. Rajkowska, C. A. Stockmeier, P. Licznerski, A. Lepack, M. S. Majik, L. S. Jeong, M. Banasr, H. Son and R. S. Duman (2012). "Decreased expression of synapse-related genes and loss of synapses in major depressive disorder." Nat Med **18**(9): 1413-1417.

Karsten, S. L., L. C. Kudo, R. Jackson, C. Sabatti, H. I. Kornblum and D. H. Geschwind (2003). "Global analysis of gene expression in neural progenitors reveals specific cell-cycle, signaling, and metabolic networks." Developmental Biology **261**(1): 165-182.

Kaufmann, W. E. and H. W. Moser (2000). "Dendritic anomalies in disorders associated with mental retardation." Cerebral cortex **10**(10): 981-991.

Keller, G. M. (1995). "In vitro differentiation of embryonic stem cells." Current Opinion in Cell Biology **7**(6): 862-869.

Keverne, E. B. and P. A. Brennan (1996). "Olfactory recognition memory." Journal of Physiology-Paris **90**(5–6): 399-401.

Keyvani, K. and T. Schallert (2002). "Plasticity-associated molecular and structural events in the injured brain." Journal of Neuropathology & Experimental Neurology **61**(10): 831-840.

Kim, J. G., R. C. Armstrong, D. v. Agoston, A. Robinsky, C. Wiese, J. Nagle and L. D. Hudson (1997). "Myelin transcription factor 1 (Myt1) of the oligodendrocyte lineage, along with a closely related CCHC zinc finger, is expressed in developing neurons in the mammalian central nervous system." Journal of Neuroscience Research **50**: 272-290.

Kim, K., S. O. Zakharkin and D. B. Allison (2010). "Expectations, validity, and reality in gene expression profiling." Journal of Clinical Epidemiology **63**(9): 950-959.

Kjelstrup, K. G., F. A. Tuvnes, H.-A. Steffenach, R. Murison, E. I. Moser and M.-B. Moser (2002). "Reduced fear expression after lesions of the ventral hippocampus." Proceedings of the National Academy of Sciences of the United States of America **99**(16): 10825-10830.

Klug, A. (2005). The discovery of zinc fingers and their practical applications in gene regulation: a personal account. Zinc Finger Proteins. S. Iuchi and N. Kuldell, Springer US**:** 1-6.

Klug, A. (2010). "The discovery of zinc fingers and their applications in gene regulation and genome manipulation." Annual Review of Biochemistry **79**(1): 213-231.

Knight, J. (2001). "When the chips are down." Nature **410**(6831): 860-861.

Kolb, B., R. Gibb and T. E. Robinson (2003). "Brain plasticity and behavior." Current Directions in Psychological Science **12**(1): 1-5.

Koudritsky, M. and E. Domany (2008). "Positional distribution of human transcription factor binding sites." Nucleic acids research **36**(21): 6795-6805.

Kubinová, Š., D. Horák, N. Kozubenko, V. Vaněček, V. Proks, J. Price, G. Cocks and E. Syková (2010). "The use of superporous Ac-CGGASIKVAVS-OH-modified PHEMA scaffolds to promote cell adhesion and the differentiation of human fetal neural precursors." Biomaterials **31**(23): 5966-5975.

Kuhlbrodt, K., B. Herbarth, E. Sock, I. Hermans-Borgmeyer and M. Wegner (1998). "Sox10, a novel transcriptional modulator in glial cells." The Journal of neuroscience **18**(1): 237-250.

Kuroda, H., R. H. Kutner, N. G. Bazan and J. Reiser (2008). "A comparative analysis of constitutive and cell-specific promoters in the adult mouse hippocampus using lentivirus vector-mediated gene transfer." The Journal of Gene Medicine **10**(11): 1163-1175.

Lapin, I. P. (1995). "Only controls: Effect of handling, sham injection, and intraperitoneal injection of saline on behavior of mice in an elevated plus-maze." Journal of Pharmacological and Toxicological Methods **34**(2): 73-77.

Larkin, J. E., B. C. Frank, H. Gavras, R. Sultana and J. Quackenbush (2005). "Independence and reproducibility across microarray platforms." Nature Methods **2**(5): 337-344.

Latchman, D. S. (1996). "Transcription-factor mutations and disease." New England Journal of Medicine **334**(1): 28-33.

Lattin, J., K. Schroder, A. Su, J. Walker, J. Zhang, T. Wiltshire, K. Saijo, C. Glass, D. Hume, S. Kellie and M. Sweet (2008). "Expression analysis of G Protein-Coupled Receptors in mouse macrophages." Immunome Research **4**(1): 5.

Lazarov, O., M. P. Mattson, D. A. Peterson, S. W. Pimplikar and H. van Praag (2010). "When neurogenesis encounters aging and disease." Trends in Neurosciences **33**(12): 569-579.

Lee, Y., A. Mattai, R. Long, J. L. Rapoport, N. Gogtay and A. M. Addington (2012). "Microduplications disrupting the MYT1L gene (2p25.3) are associated with schizophrenia." Psychiatric Genetics **22**(4): 206-209.

Leid, M., J. E. Ishmael, D. Avram, D. Shepherd, V. Fraulob and P. Dollé (2004). "CTIP1 and CTIP2 are differentially expressed during mouse embryogenesis." Gene Expression Patterns **4**(6): 733-739.

Lein, E. S., M. J. Hawrylycz, N. Ao, M. Ayres, A. Bensinger, A. Bernard, A. F. Boe, M. S. Boguski, K. S. Brockway, E. J. Byrnes, L. Chen, L. Chen, T.-M. Chen, M. Chi Chin, J. Chong, B. E. Crook, A. Czaplinska, C. N. Dang, S. Datta, N. R. Dee, A. L. Desaki, T. Desta, E. Diep, T. A. Dolbeare, M. J. Donelan, H.-W. Dong, J. G. Dougherty, B. J. Duncan, A. J. Ebbert, G. Eichele, L. K. Estin, C. Faber, B. A. Facer, R. Fields, S. R. Fischer, T. P. Fliss, C. Frensley, S. N. Gates, K. J. Glattfelder, K. R. Halverson, M. R. Hart, J. G. Hohmann, M. P. Howell, D. P. Jeung, R. A. Johnson, P. T. Karr, R. Kawal, J. M. Kidney, R. H. Knapik, C. L. Kuan, J. H. Lake, A. R. Laramee, K. D. Larsen, C. Lau, T. A. Lemon, A. J. Liang, Y. Liu, L. T. Luong, J. Michaels, J. J. Morgan, R. J. Morgan, M. T. Mortrud, N. F. Mosqueda, L. L. Ng, R. Ng, G. J. Orta, C. C. Overly, T. H. Pak, S. E. Parry, S. D. Pathak, O. C. Pearson, R. B. Puchalski, Z. L. Riley, H. R. Rockett, S. A. Rowland, J. J. Royall, M. J. Ruiz, N. R. Sarno, K. Schaffnit, N. V. Shapovalova, T. Sivisay, C. R. Slaughterbeck, S. C. Smith, K. A. Smith, B. I. Smith, A. J. Sodt, N. N. Stewart, K.-R. Stumpf, S. M. Sunkin, M. Sutram, A. Tam, C. D. Teemer, C. Thaller, C. L. Thompson, L. R. Varnam, A. Visel, R. M. Whitlock, P. E. Wohnoutka, C. K. Wolkey, V. Y. Wong, M. Wood, M. B. Yaylaoglu, R. C. Young, B. L. Youngstrom, X. Feng Yuan, B. Zhang, T. A. Zwingman and A. R. Jones (2007). "Genome-wide atlas of gene expression in the adult mouse brain." Nature **445**(7124): 168-176.

Lenroot, R. K. and J. N. Giedd (2006). "Brain development in children and adolescents: Insights from anatomical magnetic resonance imaging." Neuroscience & Biobehavioral Reviews **30**(6): 718-729.

Levine, M. and E. H. Davidson (2005). "Gene regulatory networks for development." Proceedings of the National Academy of Sciences of the United States of America **102**(14): 4936-4942.

Lewandoski, M. (2001). "Conditional control of gene expression in the mouse." Nature Reviews Genetics **2**(10): 743-755.

Li, W., X. Wang, J. Zhao, J. Lin, X. Q. Song, Y. Yang, C. Jiang, B. Xiao, G. Yang, H. X. Zhang and L. X. Lv (2012). "Association study of myelin transcription factor 1-like polymorphisms with schizophrenia in Han Chinese population." Genes, Brain and Behavior **11**(1): 87-93.

Li, W., Y. Xiong, C. Shang, K. Y. Twu, C. T. Hang, J. Yang, P. Han, C.-Y. Lin, C.-J. Lin, F.-C. Tsai, K. Stankunas, T. Meyer, D. Bernstein, M. Pan and C.-P. Chang (2013). "Brg1 governs distinct pathways to direct multiple aspects of mammalian neural crest cell development." Proceedings of the National Academy of Sciences of the United States of America **110**(5): 1738-1743.

Li, Z. and M. Sheng (2003). "Some assembly required: the development of neuronal synapses." Nature Reviews Molecular Cell Biology **4**(11): 833-841.

Lillien, L. (1998). "Neural progenitors and stem cells: mechanisms of progenitor heterogeneity." Current Opinion in Neurobiology **8**(1): 37-44.

Lin, Y., B. L. Bloodgood, J. L. Hauser, A. D. Lapan, A. C. Koon, T.-K. Kim, L. S. Hu, A. N. Malik and M. E. Greenberg (2008). "Activity-dependent regulation of inhibitory synapse development by Npas4." Nature **455**(7217): 1198-1204.

Lister, R. (1987). "The use of a plus-maze to measure anxiety in the mouse." Psychopharmacology **92**(2): 180-185.

Liu, F., W. Kuo, T.-K. Jenssen and E. Hovig (2012). Performance comparison of multiple microarray platforms for gene expression profiling. Next Generation Microarray Bioinformatics. J. Wang, A. C. Tan and T. Tian, Humana Press. **802:** 141-155.

Livak, K. J. and T. D. Schmittgen (2001). "Analysis of relative gene expression data using real-time quantitative PCR and the 2−ΔΔCT Method." Methods **25**(4): 402-408.

Lledo, P.-M., M. Alonso and M. S. Grubb (2006). "Adult neurogenesis and functional plasticity in neuronal circuits." Nature Reviews Neuroscience **7**(3): 179-193.

Lodge, D. J. and A. A. Grace (2007). "Aberrant hippocampal activity underlies the dopamine dysregulation in an animal model of schizophrenia." The Journal of Neuroscience **27**(42): 11424-11430.

Logue, S. F., R. Paylor and J. M. Wehner (1997). "Hippocampal lesions cause learning deficits in inbred mice in the Morris water maze and conditioned-fear task." Behavioral neuroscience **111**(1): 104.

Lumsden, A. and K. Chris (2003). Neural induction and pattern formation. Fundamental Neuroscience. L. R. Squire, B. F. E., M. S. K. et al. United States of America, Academic Press**:** 363-390.

Luscombe, N. M., S. E. Austin, H. M. Berman and J. M. Thornton (2000). "An overview of the structures of protein-DNA complexes." Genome Biology **1**(1): reviews001.001 - reviews001.037.

MacLean, P. D. (1949). "Psychosomatic disease and the" visceral brain" recent developments bearing on the papez theory of emotion." Psychosomatic medicine **11**(6): 338-353.

Maguire, E. A., D. G. Gadian, I. S. Johnsrude, C. D. Good, J. Ashburner, R. S. J. Frackowiak and C. D. Frith (2000). "Navigation-related structural change in the hippocampi of taxi drivers." Proceedings of the National Academy of Sciences of the United States of America **97**(8): 4398-4403.

Maniatis, T., S. Goodbourn and J. A. Fischer (1987). "Regulation of inducible and tissue-specific gene expression." Science **236**(4806): 1237-1245.

Manjunath, N., H. Wu, S. Subramanya and P. Shankar (2009). "Lentiviral delivery of short hairpin RNAs." Advanced Drug Delivery Reviews **61**(9): 732-745.

Mao, Y., X. Ge, C. L. Frank, J. M. Madison, A. N. Koehler, M. K. Doud, C. Tassa, E. M. Berry, T. Soda, K. K. Singh, T. Biechele, T. L. Petryshen, R. T. Moon, S. J. Haggarty and L.-H. Tsai (2009). "Disrupted in schizophrenia 1 regulates neuronal progenitor proliferation via modulation of GSK3β/β-Catenin signaling." Cell **136**(6): 1017-1031.

Mareschal, D., M. H. Johnson, S. Sirois, M. W. Spratling, M. S. C. Thomas and G. Westermann (2007). Neuroconstructivism: how the brain constructs cognition United States of America, Oxford University Press.

Martin, G. R. (1981). "Isolation of a pluripotent cell line from early mouse embryos cultured in medium conditioned by teratocarcinoma stem cells." Proceedings of the National Academy of Sciences of the United States of America **78**(12): 7634-7638.

Matsuzawa, J., M. Matsui, T. Konishi, K. Noguchi, R. C. Gur, W. Bilker and T. Miyawaki (2001). "Age-related volumetric changes of brain gray and white matter in healthy infants and children." Cerebral Cortex **11**(4): 335-342.

McBryant, S. J., B. Gedulin, K. R. Clemens, P. E. Wright and J. M. Gottesfeld (1996). "Assessment of major and minor groove DNA interactions by the zinc fingers of xenopus transcription factor IIIA." Nucleic Acids Research **24**(13): 2567-2574.

McHugh, S. B., M. Fillenz, J. P. Lowry, J. N. P. Rawlins and D. M. Bannerman (2011). "Brain tissue oxygen amperometry in behaving rats demonstrates functional dissociation of dorsal and ventral hippocampus during spatial processing and anxiety." European Journal of Neuroscience **33**(2): 322-337.

McIntyre, G. and G. Fanning (2006). "Design and cloning strategies for constructing shRNA expression vectors." BMC Biotechnology **6**(1): 1.

McKay, R. (1997). "Stem cells in the central nervous system." Science **276**(5309): 66-71.

McTigue, D. M. and R. B. Tripathi (2008). "The life, death, and replacement of oligodendrocytes in the adult CNS." Journal of Neurochemistry **107**(1): 1-19.

Meister, G. and T. Tuschl (2004). "Mechanisms of gene silencing by double-stranded RNA." Nature **431**(7006): 343-349.

Messier, C., S. Émond and K. Ethier (1999). "New techniques in stereotaxic surgery and anesthesia in the mouse." Pharmacology Biochemistry and Behavior **63**(2): 313-318.

Meyer, G., J. P. Schaaps, L. Moreau and A. M. Goffinet (2000). "Embryonic and early fetal development of the human neocortex." The Journal of Neuroscience **20**(5): 1858-1868.

Meyer, K. J., M. S. Axelsen, V. C. Sheffield, S. R. Patil and T. H. Wassink (2012). "Germline mosaic transmission of a novel duplication of PXDN and MYT1L to two male half-siblings with autism." Psychiatric Genetics **22**(3): 137-140.

Meyer, L. R., A. S. Zweig, A. S. Hinrichs, D. Karolchik, R. M. Kuhn, M. Wong, C. A. Sloan, K. R. Rosenbloom, G. Roe, B. Rhead, B. J. Raney, A. Pohl, V. S. Malladi, C. H. Li, B. T. Lee, K. Learned, V. Kirkup, F. Hsu, S. Heitner, R. A. Harte, M. Haeussler, L. Guruvadoo, M. Goldman, B. M. Giardine, P. A. Fujita, T. R. Dreszer, M. Diekhans, M. S. Cline, H. Clawson, G. P. Barber, D. Haussler and W. J. Kent (2013). "The UCSC Genome Browser database: extensions and updates 2013." Nucleic Acids Research **41**(D1): D64-D69.

Milner, B., L. R. Squire and E. R. Kandel (1998). "Cognitive neuroscience and the study of memory." Neuron **20**(3): 445-468.

Misquitta, L. and B. M. Paterson (1999). "Targeted disruption of gene function in Drosophila by RNA interference (RNA-i): a role for nautilus in embryonic somatic muscle formation." Proceedings of the National Academy of Sciences of the United States of America **96**(4): 1451-1456.

Moffat, J. and D. M. Sabatini (2006). "Building mammalian signalling pathways with RNAi screens." Nature Reviews Molecular Cell Biology **7**(3): 177-187.

Moretto, M., Â. de Mattos-Dutra, N. Arteni, R. Meirelles, M. de Freitas, C. Netto and R. Pessoa-Pureur (1999). "Effects of neonatal cerebral hypoxia-ischemia on the in vitro phosphorylation of synapsin 1 in rat synaptosomes." Neurochemical Research **24**(10): 1263-1269.

Morris, R. (1984). "Developments of a water-maze procedure for studying spatial learning in the rat." Journal of Neuroscience Methods **11**(1): 47-60.

Moser, E., M. Moser and P. Andersen (1993). "Spatial learning impairment parallels the magnitude of dorsal hippocampal lesions, but is hardly present following ventral lesions." The Journal of Neuroscience **13**(9): 3916-3925.

Mouse-Genome-Sequencing-Consortium (2002). "Initial sequencing and comparative analysis of the mouse genome." Nature **420**(6915): 520-562.

Muruganandan, S., H. J. Dranse, J. L. Rourke, N. M. McMullen and C. J. Sinal (2013). "Chemerin neutralization blocks hematopoietic stem cell osteoclastogenesis." Stem Cells: N/A-N/A.

Nadler, J. J., S. S. Moy, G. Dold, N. Simmons, A. Perez, N. B. Young, R. P. Barbaro, J. Piven, T. R. Magnuson and J. N. Crawley (2004). "Automated apparatus for quantitation of social approach behaviors in mice." Genes, Brain and Behavior **3**(5): 303-314.

Naldini, L., U. Blomer, F. Gage, D. Trono and I. Verma (1996). "Efficient transfer, integration, and sustained long-term expression of the transgene in adult rat brains injected with a lentiviral vector." Proceedings of the National Academy of Sciences of the United States of America **93**: 11382 - 11388.

Naldini, L., U. Blömer, P. Gallay, D. Ory, R. Mulligan, F. H. Gage, I. M. Verma and D. Trono (1996). "In vivo gene delivery and stable transduction of nondividing cells by a lentiviral vector." Science **272**(5259): 263-267.

Nelson, S. B., C. Hempel and K. Sugino (2006). "Probing the transcriptome of neuronal cell types." Current Opinion in Neurobiology **16**(5): 571-576.

Nielsen, J. A., J. A. Berndt, L. D. Hudson and R. C. Armstrong (2004). "Myelin transcription factor 1 (Myt1) modulates the proliferation and differentiation of oligodendrocyte lineage cells." Molecular and Cellular Neuroscience **25**(1): 111-123.

Nishi, M., A. Mizushima, K.-i. Nakagawara and H. Takeshima (2000). "Characterization of human junctophilin subtype genes." Biochemical and Biophysical Research Communications **273**(3): 920-927.

Nishi, M., H. Sakagami, S. Komazaki, H. Kondo and H. Takeshima (2003). "Coexpression of junctophilin type 3 and type 4 in brain." Molecular Brain Research **118**(1–2): 102-110.

Noldus, L. J. J., A. Spink and R. J. Tegelenbosch (2001). "EthoVision: a versatile video tracking system for automation of behavioral experiments." Behavior Research Methods, Instruments, & Computers **33**(3): 398-414.

O'Keefe, J. and L. Nadel (1978). Exploration. The Hippocampus as a Cognitive Map. Great Britain, Oxford University Press.

Ohuchi, H., S. Kimura, M. Watamoto and N. Itoh (2000). "Involvement of fibroblast growth factor (FGF)18-FGF8 signaling in specification of left-right asymmetry and brain and limb development of the chick embryo." Mechanisms of Development **95**(1–2): 55-66.

Olesen, P. J., Z. Nagy, H. Westerberg and T. Klingberg (2003). "Combined analysis of DTI and fMRI data reveals a joint maturation of white and grey matter in a fronto-parietal network." Cognitive Brain Research **18**(1): 48-57.

Oppenheim, R. W. (1991). "Cell death during development of the nervous system." Annual Review of Neuroscience **14**(1): 453-501.

Osen-Sand, A., J. K. Staple, E. Naldi, G. Schiavo, O. Rossetto, S. Petitpierre, A. Malgaroli, C. Montecucco and S. Catsicas (1996). "Common and distinct fusion proteins in axonal growth and transmitter release." The Journal of Comparative Neurology **367**(2): 222-234.

Overhoff, M., M. Alken, R. K.-K. Far, M. Lemaitre, B. Lebleu, G. Sczakiel and I. Robbins (2005). "Local RNA target structure influences siRNA efficacy: a systematic global analysis." Journal of Molecular Biology **348**(4): 871-881.

Pabo, C. O. and R. T. Sauer (1992). "Transcription factors: structural families and principles of DNA recognition." Annual Review of Biochemistry **61**(1): 1053-1095.

Paczkowski, C. M. and J. Chun (2009). Genomic disorder and gene expression in the developing CNS. Encyclopedia of Neuroscience. R. S. Editor-in-Chief: Larry. Oxford, Academic Press**:** 679-684.

Paddison, P. J., A. A. Caudy, E. Bernstein, G. J. Hannon and D. S. Conklin (2002). "Short hairpin RNAs (shRNAs) induce sequence-specific silencing in mammalian cells." Genes & Development **16**(8): 948-958.

Paddison, P. J., J. M. Silva, D. S. Conklin, M. Schlabach, M. Li, S. Aruleba, V. Balija, A. O'Shaughnessy, L. Gnoj, K. Scobie, K. Chang, T. Westbrook, M. Cleary, R. Sachidanandam, W. Richard McCombie, S. J. Elledge and G. J. Hannon (2004). "A resource for large-scale RNA-interference-based screens in mammals." Nature **428**(6981): 427-431.

Palka, J., K. E. Whitlock and M. A. Murray (1992). "Guidepost cells." Current Opinion in Neurobiology **2**(1): 48-54.

Pang, Z. P., N. Yang, T. Vierbuchen, A. Ostermeier, D. R. Fuentes, T. Q. Yang, A. Citri, V. Sebastiano, S. Marro, T. C. Sudhof and M. Wernig (2011). "Induction of human neuronal cells by defined transcription factors." Nature **476**(7359): 220-223.

Papez, J. W. (1937). "A proposed mechanism of emotion." Archives of neurology and psychiatry **38**(4): 725.

Paus, T. (2005). "Mapping brain maturation and cognitive development during adolescence." Trends in Cognitive Sciences **9**(2): 60-68.

Paus, T., A. Zijdenbos, K. Worsley, D. L. Collins, J. Blumenthal, J. N. Giedd, J. L. Rapoport and A. C. Evans (1999). "Structural maturation of neural pathways in children and adolescents: in vivo study." Science **283**(5409): 1908-1911.

Paxinos, G. and K. Franklin (2003). The Mouse Brain in Stereotaxic Coordinates. United States of America, Academic Press.

Pebernard, S. and R. D. Iggo (2004). "Determinants of interferon-stimulated gene induction by RNAi vectors." Differentiation **72**(2-3): 103-111.

Peeters, J. and P. Spek (2005). "Growing applications and advancements in microarray technology and analysis tools." Cell Biochemistry and Biophysics **43**(1): 149-166.

Pei, Y. and T. Tuschl (2006). "On the art of identifying effective and specific siRNAs." Nature methods **3**(9): 670-676.

Perez, J. A., S. M. Clinton, C. A. Turner, S. J. Watson and H. Akil (2009). "A new role for FGF2 as an endogenous inhibitor of anxiety." The Journal of Neuroscience **29**(19): 6379-6387.

Perycz, M., A. S. Urbanska, P. S. Krawczyk, K. Parobczak and J. Jaworski (2011). "Zipcode Binding Protein 1 regulates the development of dendritic arbors in hippocampal Neurons." The Journal of Neuroscience **31**(14): 5271-5285.

Pfefferbaum A, M. D. H. S. E. V. R. J. M. Z. R. B. L. K. O. (1994). "A quantitative magnetic resonance imaging study of changes in brain morphology from infancy to late adulthood." Archives of Neurology **51**(9): 874-887.

Pfeifer, A., M. Ikawa, Y. Dayn and I. M. Verma (2002). "Transgenesis by lentiviral vectors: Lack of gene silencing in mammalian embryonic stem cells and preimplantation embryos." Proceedings of the National Academy of Sciences of the United States of America **99**(4): 2140-2145.

Pfisterer, U., A. Kirkeby, O. Torper, J. Wood, J. Nelander, A. Dufour, A. Björklund, O. Lindvall, J. Jakobsson and M. Parmar (2011). "Direct conversion of human fibroblasts to dopaminergic neurons." Proceedings of the National Academy of Sciences of the United States of America.

Pfrieger, F. W. (2010). "Role of glial cells in the formation and maintenance of synapses." Brain Research Reviews **63**(1–2): 39-46.

Pham, P., A. Kamen and Y. Durocher (2006). "Large-scale transfection of mammalian cells for the fast production of recombinant protein." Molecular Biotechnology **34**(2): 225-237.

Poldrack, R. A. (2000). "Imaging Brain Plasticity: Conceptual and Methodological Issues— A Theoretical Review." NeuroImage **12**(1): 1-13.

Pollock, K., P. Stroemer, S. Patel, L. Stevanato, A. Hope, E. Miljan, Z. Dong, H. Hodges, J. Price and J. D. Sinden (2006). "A conditionally immortal clonal stem cell line from human cortical neuroepithelium for the treatment of ischemic stroke." Experimental Neurology **199**(1): 143-155.

Pongrac, J., F. Middleton, D. Lewis, P. Levitt and K. Mirnics (2002). "Gene expression profiling with DNA microarrays: advancing our understanding of psychiatric disorders." Neurochemical Research **27**(10): 1049-1063.

Posthuma, D., E. J. C. De Geus, W. F. C. Baare, H. E. H. Pol, R. S. Kahn and D. I. Boomsma (2002). "The association between brain volume and intelligence is of genetic origin." Nature Neuroscience **5**(2): 83-84.

Prut, L. and C. Belzung (2003). "The open field as a paradigm to measure the effects of drugs on anxiety-like behaviors: a review." European Journal of Pharmacology **463**(1-3): 3-33.

Ramalho-Santos, M., S. Yoon, Y. Matsuzaki, R. C. Mulligan and D. A. Melton (2002). ""Stemness": transcriptional profiling of embryonic and adult stem cells." Science **298**(5593): 597-600.

Rao, D. D., J. S. Vorhies, N. Senzer and J. Nemunaitis (2009). "siRNA vs. shRNA: similarities and differences." Advanced Drug Delivery Reviews **61**(9): 746-759.

Raymond, G. V., M. L. Bauman and T. L. Kemper (1995). "Hippocampus in autism: a Golgi analysis." Acta Neuropathologica **91**(1): 117-119.

Reiss, A. L., M. T. Abrams, H. S. Singer, J. L. Ross and M. B. Denckla (1996). "Brain development, gender and IQ in children: a volumetric imaging study." Brain **119**(5): 1763-1774.

Restrepo, D., J. Arellano, A. M. Oliva, M. L. Schaefer and W. Lin (2004). "Emerging views on the distinct but related roles of the main and accessory olfactory systems in responsiveness to chemosensory signals in mice." Hormones and Behavior **46**(3): 247-256.

Reynolds, A., D. Leake, Q. Boese, S. Scaringe, W. S. Marshall and A. Khvorova (2004). "Rational siRNA design for RNA interference." Nature Biotechnology **22**(3): 326-330.

Reynolds, B. A. and S. Weiss (1992). "Generation of neurons and astrocytes from isolated cells of the adult mammalian central nervous system." Science **255**(5052): 1707-1710.

Rezayat, M., A. Roohbakhsh, M.-R. Zarrindast, R. Massoudi and B. Djahanguiri (2005). "Cholecystokinin and GABA interaction in the dorsal hippocampus of rats in the elevated plus-maze test of anxiety." Physiology & Behavior **84**(5): 775-782.

Rietze, R. L. and B. A. Reynolds (2006). Neural stem cell isolation and characterization. Methods in Enzymology. K. Irina and L. Robert, Academic Press. **419:** 3-23.

Rio, M., G. Royer, S. Gobin, M. C. de Blois, C. Ozilou, A. Bernheim, M. Nizon, A. Munnich, J. P. Bonnefont, S. Romana, M. Vekemans, C. Turleau and V. Malan (2012). "Monozygotic twins discordant for submicroscopic chromosomal anomalies in 2p25.3 region detected by array CGH." Clinical Genetics: n/a-n/a.

Rodgers, R. J. and N. J. T. Johnson (1995). "Factor analysis of spatiotemporal and ethological measures in the murine elevated plus-maze test of anxiety." Pharmacology Biochemistry and Behavior **52**(2): 297-303.

Rodriguez-Lebron, E., E. M. Denovan-Wright, K. Nash, A. S. Lewin and R. J. Mandel (2005). "Intrastriatal rAAV-mediated delivery of anti-huntingtin shRNAs induces partial reversal of disease progression in R6/1 Huntington's disease transgenic mice." Molecular Therapy **12**(4): 618-633.

Rose, C. R. and A. Konnerth (2001). "Stores Not Just for Storage: Intracellular Calcium Release and Synaptic Plasticity." Neuron **31**(4): 519-522.

Rosenthal, N. and S. Brown (2007). "The mouse ascending: perspectives for human-disease models." Nature Cell Biology **9**(9): 993-999.

Rozema, D. B. and D. L. Lewis (2003). "siRNA delivery technologies for mammalian systems." TARGETS **2**(6): 253-260.

Rubinson, D. A., C. P. Dillon, A. V. Kwiatkowski, C. Sievers, L. Yang, J. Kopinja, D. L. Rooney, M. Zhang, M. M. Ihrig, M. T. McManus, F. B. Gertler, M. L. Scott and L. Van Parijs (2003). "A lentivirus-based system to functionally silence genes in primary mammalian cells, stem cells and transgenic mice by RNA interference." Nature Genetics **33**(3): 401-406.

Růžička, J., A. Nataliya Romanyuk, M. Vetrík, M. Hrubý, G. Cocks, J. Cihlář, M. Přádný, J. Price, E. Syková and P. Jendelová (2013). "Treating spinal cord injury in rats with a combination of human fetal neural stem cells and hydrogels modified with serotonin." Acta Neurobiol Experimentalis **73**: 102-115.

Sanes, J. R. and M. Yamagata (1999). "Formation of lamina-specific synaptic connections." Current Opinion in Neurobiology **9**(1): 79-87.

Sanford, L. P., I. Ormsby, A. C. Gittenberger-de Groot, H. Sariola, R. Friedman, G. P. Boivin, E. L. Cardell and T. Doetschman (1997). "TGFbeta2 knockout mice have multiple developmental defects that are non-overlapping with other TGFbeta knockout phenotypes." Development **124**(13): 2659-2670.

Schena, M., D. Shalon, R. W. Davis and P. O. Brown (1995). "Quantitative monitoring of gene expression patterns with a complementary DNA microarray." Science **270**(5235): 467-470.

Schmitt, U. and C. Hiemke (1998). "Strain differences in open-field and elevated plus-maze behavior of rats without and with pretest handling." Pharmacology Biochemistry and Behavior **59**(4): 807-811.

Semenza, G. L. (1998). Transcription Factors and Human Diseases. United States of America, Oxford University Press, Inc.

Seong, E., A. F. Seasholtz and M. Burmeister (2002). "Mouse models for psychiatric disorders." Trends in Genetics **18**(12): 643-650.

Shen, C., A. K. Buck, X. Liu, M. Winkler and S. N. Reske (2003). "Gene silencing by adenovirus-delivered siRNA." FEBS letters **539**(1): 111-114.

Shi, L., X. Chang, P. Zhang, M. P. Coba, W. Lu and K. Wang (2013). "The functional genetic link of NLGN4X knockdown and neurodevelopment in neural stem cells." Human Molecular Genetics.

Shi, Y. (2003). "Mammalian RNAi for the masses." Trends in Genetics **19**(1): 9-12.

Shoichet, S. A., K. Hoffmann, C. Menzel, U. Trautmann, B. Moser, M. Hoeltzenbein, B. Echenne, M. Partington, H. van Bokhoven, C. Moraine, J.-P. Fryns, J. Chelly, H.-D. Rott, H.-H. Ropers and V. M. Kalscheuer (2003). "Mutations in the ZNF41 gene are associated with cognitive deficits: identification of a new candidate for X-Linked mental retardation." The American Journal of Human Genetics **73**(6): 1341-1354.

Silva, J. M., M. Z. Li, K. Chang, W. Ge, M. C. Golding, R. J. Rickles, D. Siolas, G. Hu, P. J. Paddison, M. R. Schlabach, N. Sheth, J. Bradshaw, J. Burchard, A. Kulkarni, G. Cavet, R. Sachidanandam, W. R. McCombie, M. A. Cleary, S. J. Elledge and G. J. Hannon (2005). "Second-generation shRNA libraries covering the mouse and human genomes." Nature Genetics **37**(11): 1281-1288.

Silva, R. C. B. and M. L. Brandão (2000). "Acute and chronic effects of gepirone and fFluoxetine in rats tested in the elevated plus-maze: an ethological analysis." Pharmacology Biochemistry and Behavior **65**(2): 209-216.

Singh, M., N. S. Spoelstra, A. Jean, E. Howe, K. C. Torkko, H. R. Clark, D. S. Darling, K. R. Shroyer, K. B. Horwitz, R. R. Broaddus and J. K. Richer (2008). "ZEB1 expression in type I vs type II endometrial cancers: a marker of aggressive disease." Modern Pathology **21**(7): 912-923.

Sinicropi, D., M. Cronin and M.-L. Liu (2007). Gene expression profiling utilizing microarray technology and RT-PCR. BioMEMS and biomedical nanotechnology, Springer**:** 23-46.

Skarnes, W. C., B. Rosen, A. P. West, M. Koutsourakis, W. Bushell, V. Iyer, A. O. Mujica, M. Thomas, J. Harrow, T. Cox, D. Jackson, J. Severin, P. Biggs, J. Fu, M. Nefedov, P. J. de Jong, A. F. Stewart and A. Bradley (2011). "A conditional knockout resource for the genome-wide study of mouse gene function." Nature **474**(7351): 337-342.

Son, E. Y., J. K. Ichida, B. J. Wainger, J. S. Toma, V. F. Rafuse, C. J. Woolf and K. Eggan (2011). "Conversion of mouse and human fibroblasts into functional spinal motor neurons." Cell stem cell **9**(3): 205-218.

Southall, T. D. and A. H. Brand (2009). "Neural stem cell transcriptional networks highlight genes essential for nervous system development." EMBO J **28**(24): 3799-3807.

Spear, L. P. (2000). "The adolescent brain and age-related behavioral manifestations." Neuroscience & Biobehavioral Reviews **24**(4): 417-463.

Specht, K., T. Richter, U. Müller, A. Walch, M. Werner and H. Höfler (2001). "Quantitative gene expression analysis in microdissected archival formalin-fixed and paraffin-embedded tumor tissue." The American Journal of Pathology **158**(2): 419-429.

Spedding, M., T. Jay, J. C. e Silva and L. Perret (2005). "A pathophysiological paradigm for the therapy of psychiatric disease." Nature Reviews Drug Discovery **4**(6): 467-476.

Spink, A. J., R. A. J. Tegelenbosch, M. O. S. Buma and L. P. J. J. Noldus (2001). "The EthoVision video tracking system—A tool for behavioral phenotyping of transgenic mice." Physiology & Behavior **73**(5): 731-744.

Srivastava, D. P., K. M. Woolfrey and P. Penzes (2011). "Analysis of dendritic spine morphology in cultured CNS neurons." Journal of Visualized Experiments(53).

Stankiewicz, P. and J. R. Lupski (2010). "Structural variation in the human genome and its role in disease." Annual review of medicine **61**: 437-455.

Stefanko, D. P., R. M. Barrett, A. R. Ly, G. K. Reolon and M. A. Wood (2009). "Modulation of long-term memory for object recognition via HDAC inhibition." Proceedings of the National Academy of Sciences of the United States of America **106**(23): 9447-9452.

Stevens, S. J. C., C. M. A. van Ravenswaaij-Arts, J. W. H. Janssen, J. S. Klein Wassink-Ruiter, A. J. van Essen, T. Dijkhuizen, J. van Rheenen, R. Heuts-Vijgen, A. P. A. Stegmann, E. E. J. G. L. Smeets and J. J. M. Engelen (2011). "MYT1L is a candidate gene for intellectual disability in patients with 2p25.3 (2pter) deletions." American Journal of Medical Genetics Part A **155**(11): 2739-2745.

Stiles, J. (2008). The fundamentals of brain development. United States of America, Harvard University Press.

Stiles, J. (2011). Brain development and the nature versus nurture debate. Progress in Brain Research. O. Braddick, J. Atkinson and G. M. Innocenti. Great Britain, Elsevier. **189:** 3-22.

Stiles, J. and T. Jernigan (2010). "The basics of brain development." Neuropsychology Review **20**(4): 327-348.

Stiles, J., J. S. Reilly, S. C. Levine, D. A. Trauner and R. Nass (2012). The basics of brain development. Neural Plasticity and Cognitive Development: Insights from Children with Perinatal Brain Injury. United States of America, Oxford University Press, Inc.**:** 31-81.

Stormo, G. D. (2000). "DNA binding sites: representation and discovery." Bioinformatics **16**(1): 16-23.

Stott, S. R. W., E. Metzakopian, W. Lin, K. H. Kaestner, R. Hen and S.-L. Ang (2013). "Foxa1 and Foxa2 are required for the maintenance of dopaminergic properties in ventral midbrain neurons at late embryonic stages." The Journal of Neuroscience **33**(18): 8022-8034.

Strand, A. D., A. K. Aragaki, Z. C. Baquet, A. Hodges, P. Cunningham, P. Holmans, K. R. Jones, L. Jones, C. Kooperberg and J. M. Olson (2007). "Conservation of regional gene expression in mouse and human brain." PLoS Genetics **3**(4): e59.

Studer, M. (2011). "The use and re-use of transcription factors during brain development." Developmental Neurobiology **71**(8): 663-664.

Su, A. I., T. Wiltshire, S. Batalov, H. Lapp, K. A. Ching, D. Block, J. Zhang, R. Soden, M. Hayakawa, G. Kreiman, M. P. Cooke, J. R. Walker and J. B. Hogenesch (2004). "A gene atlas of the mouse and human protein-encoding transcriptomes." Proceedings of the National Academy of Sciences of the United States of America **101**(16): 6062-6067.

Tabara, H., M. Sarkissian, W. G. Kelly, J. Fleenor, A. Grishok, L. Timmons, A. Fire and C. C. Mello (1999). "The rde-1 Gene, RNA Interference, and transposon silencing in C. elegans." Cell **99**(2): 123-132.

Takeshima, H., S. Komazaki, M. Nishi, M. Iino and K. Kangawa (2000). "Junctophilins: a novel family of junctional membrane complex proteins." Molecular Cell **6**(1): 11-22.

Tam, P. P. and R. S. Beddington (1987). "The formation of mesodermal tissues in the mouse embryo during gastrulation and early organogenesis." Development **99**(1): 109-126.

Tanaka, T. S., T. Kunath, W. L. Kimber, S. A. Jaradat, C. A. Stagg, M. Usuda, T. Yokota, H. Niwa, J. Rossant and M. S. H. Ko (2002). "Gene expression profiling of embryo-derived stem cells reveals candidate genes associated with pluripotency and lineage specificity." Genome Research **12**(12): 1921-1928.

Tang, B., P. Di Lena, L. Schaffer, S. R. Head, P. Baldi and E. A. Thomas (2011). "Genome-wide identification of Bcl11b gene targets reveals role in brain-derived neurotrophic factor signaling." PLoS ONE **6**(9): e23691.

Tau, G. Z. and B. S. Peterson (2009). "Normal development of brain circuits." Neuropsychopharmacology **35**(1): 147-168.

Taylor, S., M. Wakem, G. Dijkman, M. Alsarraj and M. Nguyen (2010). "A practical approach to RT-qPCR—Publishing data that conform to the MIQE guidelines." Methods **50**(4): S1-S5.

Thakker, D. R., F. Natt, D. Hüsken, R. Maier, M. Müller, H. van der Putten, D. Hoyer and J. F. Cryan (2004). "Neurochemical and behavioral consequences of widespread gene knockdown in the adult mouse brain by using nonviral RNA interference." Proceedings of the National Academy of Sciences of the United States of America **101**(49): 17270-17275.

The-International-Mouse-Knockout-Consortium (2007). "A Mouse for All Reasons." Cell **128**(1): 9-13.

Thibault, K., B. Calvino, S. Dubacq, M. Roualle-de-Rouville, V. Sordoillet, I. Rivals and S. Pezet (2012). "Cortical effect of oxaliplatin associated with sustained neuropathic pain: Exacerbation of cortical activity and down-regulation of potassium channel expression in somatosensory cortex." Pain **153**(8): 1636-1647.

Thiel, C. M., C. P. Müller, J. P. Huston and R. K. W. Schwarting (1999). "High versus low reactivity to a novel environment: behavioural, pharmacological and neurochemical assessments." Neuroscience **93**(1): 243-251.

Thompson, P. M., T. D. Cannon, K. L. Narr, T. van Erp, V.-P. Poutanen, M. Huttunen, J. Lonnqvist, C.-G. Standertskjold-Nordenstam, J. Kaprio, M. Khaledy, R. Dail, C. I. Zoumalan and A. W. Toga (2001). "Genetic influences on brain structure." Nature Neuroscience **4**(12): 1253-1258.

Tiscornia, G., O. Singer, M. Ikawa and I. M. Verma (2003). "A general method for gene knockdown in mice by using lentiviral vectors expressing small interfering RNA." Proceedings of the National Academy of Sciences of the United States of America **100**(4): 1844-1848.

Tiscornia, G., O. Singer and I. M. Verma (2006). "Design and cloning of lentiviral vectors expressing small interfering RNAs." Nature Protocols **1**(1): 234-240.

Tkachev, D., M. L. Mimmack, M. M. Ryan, M. Wayland, T. Freeman, P. B. Jones, M. Starkey, M. J. Webster, R. H. Yolken and S. Bahn (2003). "Oligodendrocyte dysfunction in schizophrenia and bipolar disorder." The Lancet **362**(9386): 798-805.

Toga, A. W. and P. M. Thompson (2005). "Genetics of brain structure and intelligence " Annual Review of Neuroscience **28**(1): 1-23.

Tomar, R. S., H. Matta and P. M. Chaudhary (2003). "Use of adeno-associated viral vector for delivery of small interfering RNA." Oncogene **22**(36): 5712-5715.

Tong, C., G. Huang, C. Ashton, P. Li and Q.-L. Ying (2011). "Generating gene knockout rats by homologous recombination in embryonic stem cells." Nature Protocols **6**(6): 827-844.

Toro, C. T. and J. F. W. Deakin (2007). "Adult neurogenesis and schizophrenia: A window on abnormal early brain development?" Schizophrenia Research **90**(1-3): 1-14.

Torres, R., A. García, M. Payá and J. C. Ramirez (2011). "Non-integrative lentivirus drives high-frequency cre-mediated cassette exchange in human cells." PLoS ONE **6**(5): e19794.

Treit, D., J. Menard and C. Royan (1993). "Anxiogenic stimuli in the elevated plus-maze." Pharmacology Biochemistry and Behavior **44**(2): 463-469.

Tremblay, R. G., M. Sikorska, J. K. Sandhu, P. Lanthier, M. Ribecco-Lutkiewicz and M. Bani-Yaghoub (2010). "Differentiation of mouse Neuro 2A cells into dopamine neurons." Journal of Neuroscience Methods **186**(1): 60-67.

Tuschl, T., P. D. Zamore, R. Lehmann, D. P. Bartel and P. A. Sharp (1999). "Targeted mRNA degradation by double-stranded RNA in vitro." Genes & Development **13**(24): 3191-3197.

Vallier, L., P. J. Rugg-Gunn, I. A. Bouhon, F. K. Andersson, A. J. Sadler and R. A. Pedersen (2004). "Enhancing and diminishing gene function in human embryonic stem cells." Stem Cells **22**(1): 2-11.

Valouev, A., D. S. Johnson, A. Sundquist, C. Medina, E. Anton, S. Batzoglou, R. M. Myers and A. Sidow (2008). "Genome-wide analysis of transcription factor binding sites based on ChIP-Seq data." Nature Methods **5**(9): 829-834.

van den Haute, C., K. Eggermont, B. Nuttin, Z. Debyser and V. Baekelandt (2003). "Lentiviral vector-mediated delivery of short hairpin RNA results in persistent knockdown of gene expression in mouse brain." Human gene therapy **14**(18): 1799-1807.

van der Staay, F. J. (2000). "Effects of the size of the Morris water tank on spatial discrimination learning in the CFW1 mouse." Physiology & Behavior **68**(4): 599-602.

van Hooijdonk, L., M. Ichwan, T. Dijkmans, T. Schouten, M. de Backer, R. Adan, F. Verbeek, E. Vreugdenhil and C. Fitzsimons (2009). "Lentivirus-mediated transgene delivery to the hippocampus reveals sub-field specific differences in expression." BMC Neuroscience **10**(1): 2.

Van Loo, K. and G. Martens (2007). "Genetic and environmental factors in complex neurodevelopmental disorders." Current genomics **8**(7): 429.

van Os, J., B. P. Rutten and R. Poulton (2008). "Gene-environment interactions in schizophrenia: review of epidemiological findings and future directions." Schizophrenia Bulletin **34**(6): 1066-1082.

Vaquerizas, J. M., S. K. Kummerfeld, S. A. Teichmann and N. M. Luscombe (2009). "A census of human transcription factors: function, expression and evolution." Nature Reviews Genetics **10**(4): 252-263.

Venter, J. C., M. D. Adams, E. W. Myers, P. W. Li, R. J. Mural, G. G. Sutton, H. O. Smith, M. Yandell, C. A. Evans, R. A. Holt, J. D. Gocayne, P. Amanatides, R. M. Ballew, D. H. Huson, J. R. Wortman, Q. Zhang, C. D. Kodira, X. H. Zheng, L. Chen, M. Skupski, G. Subramanian, P. D. Thomas, J. Zhang, G. L. Gabor Miklos, C. Nelson, S. Broder, A. G. Clark, J. Nadeau, V. A. McKusick, N. Zinder, A. J. Levine, R. J. Roberts, M. Simon, C. Slayman, M. Hunkapiller, R. Bolanos, A. Delcher, I. Dew, D. Fasulo, M. Flanigan, L. Florea, A. Halpern, S. Hannenhalli, S. Kravitz, S. Levy, C. Mobarry, K. Reinert, K. Remington, J. Abu-Threideh, E. Beasley, K. Biddick, V. Bonazzi, R. Brandon, M. Cargill, I. Chandramouliswaran, R. Charlab, K. Chaturvedi, Z. Deng, V. D. Francesco, P. Dunn, K. Eilbeck, C. Evangelista, A. E. Gabrielian, W. Gan, W. Ge, F. Gong, Z. Gu, P. Guan, T. J. Heiman, M. E. Higgins, R.-R. Ji, Z. Ke, K. A. Ketchum, Z. Lai, Y. Lei, Z. Li, J. Li, Y. Liang, X. Lin, F. Lu, G. V. Merkulov, N. Milshina, H. M. Moore, A. K. Naik, V. A. Narayan, B. Neelam, D. Nusskern, D. B. Rusch, S.

Salzberg, W. Shao, B. Shue, J. Sun, Z. Y. Wang, A. Wang, X. Wang, J. Wang, M.-H. Wei, R. Wides, C. Xiao, C. Yan, A. Yao, J. Ye, M. Zhan, W. Zhang, H. Zhang, Q. Zhao, L. Zheng, F. Zhong, W. Zhong, S. C. Zhu, S. Zhao, D. Gilbert, S. Baumhueter, G. Spier, C. Carter, A. Cravchik, T. Woodage, F. Ali, H. An, A. Awe, D. Baldwin, H. Baden, M. Barnstead, I. Barrow, K. Beeson, D. Busam, A. Carver, A. Center, M. L. Cheng, L. Curry, S. Danaher, L. Davenport, R. Desilets, S. Dietz, K. Dodson, L. Doup, S. Ferriera, N. Garg, A. Gluecksmann, B. Hart, J. Haynes, C. Haynes, C. Heiner, S. Hladun, D. Hostin, J. Houck, T. Howland, C. Ibegwam, J. Johnson, F. Kalush, L. Kline, S. Koduru, A. Love, F. Mann, D. May, S. McCawley, T. McIntosh, I. McMullen, M. Moy, L. Moy, B. Murphy, K. Nelson, C. Pfannkoch, E. Pratts, V. Puri, H. Qureshi, M. Reardon, R. Rodriguez, Y.-H. Rogers, D. Romblad, B. Ruhfel, R. Scott, C. Sitter, M. Smallwood, E. Stewart, R. Strong, E. Suh, R. Thomas, N. N. Tint, S. Tse, C. Vech, G. Wang, J. Wetter, S. Williams, M. Williams, S. Windsor, E. Winn-Deen, K. Wolfe, J. Zaveri, K. Zaveri, J. F. Abril, R. Guigó, M. J. Campbell, K. V. Sjolander, B. Karlak, A. Kejariwal, H. Mi, B. Lazareva, T. Hatton, A. Narechania, K. Diemer, A. Muruganujan, N. Guo, S. Sato, V. Bafna, S. Istrail, R. Lippert, R. Schwartz, B. Walenz, S. Yooseph, D. Allen, A. Basu, J. Baxendale, L. Blick, M. Caminha, J. Carnes-Stine, P. Caulk, Y.-H. Chiang, M. Coyne, C. Dahlke, A. D. Mays, M. Dombroski, M. Donnelly, D. Ely, S. Esparham, C. Fosler, H. Gire, S. Glanowski, K. Glasser, A. Glodek, M. Gorokhov, K. Graham, B. Gropman, M. Harris, J. Heil, S. Henderson, J. Hoover, D. Jennings, C. Jordan, J. Jordan, J. Kasha, L. Kagan, C. Kraft, A. Levitsky, M. Lewis, X. Liu, J. Lopez, D. Ma, W. Majoros, J. McDaniel, S. Murphy, M. Newman, T. Nguyen, N. Nguyen, M. Nodell, S. Pan, J. Peck, M. Peterson, W. Rowe, R. Sanders, J. Scott, M. Simpson, T. Smith, A. Sprague, T. Stockwell, R. Turner, E. Venter, M. Wang, M. Wen, D. Wu, M. Wu, A. Xia, A. Zandieh and X. Zhu (2001). "The sequence of the human genome." Science **291**(5507): 1304-1351.

Vierbuchen, T., A. Ostermeier, Z. P. Pang, Y. Kokubu, T. C. Südhof and M. Wernig (2010). "Direct conversion of fibroblasts to functional neurons by defined factors." Nature **463**(7284): 1035-1041.

Vorhees, C. V. and M. T. Williams (2006). "Morris water maze: procedures for assessing spatial and related forms of learning and memory." Nature Protocols **1**(2): 848-858.

Vrijenhoek, T., J. E. Buizer-Voskamp, I. van der Stelt, E. Strengman, C. Sabatti, A. Geurts van Kessel, H. G. Brunner, R. A. Ophoff and J. A. Veltman (2008). "Recurrent CNVs disrupt three candidate genes in schizophrenia patients." The American Journal of Human Genetics **83**(4): 504-510.

Wall, D. P., F. J. Esteban, T. F. DeLuca, M. Huyck, T. Monaghan, N. Velez de Mendizabal, J. Goñí and I. S. Kohane (2009). "Comparative analysis of neurological disorders focuses genome-wide search for autism genes." Genomics **93**(2): 120-129.

Wang, T., Z. Zeng, T. Li, J. Liu, J. Li, Y. Li, Q. Zhao, Z. Wei, Y. Wang, B. Li, G. Feng, L. He and Y. Shi (2010). "Common SNPs in Myelin Transcription Factor 1-Like MYT1L: association with major depressive disorder in the chinese Han population." PLoS ONE **5**(10): e13662.

Wang, Z., E. Oron, B. Nelson, S. Razis and N. Ivanova (2012). "Distinct lineage specification roles for NANOG, OCT4, and SOX2 in human embryonic stem cells." Cell Stem Cell **10**(4): 440-454.

Washbourne, P., P. M. Thompson, M. Carta, E. T. Costa, J. R. Mathews, G. Lopez-Bendito, Z. Molnar, M. W. Becher, C. F. Valenzuela, L. D. Partridge and M. C. Wilson (2002). "Genetic ablation of the t-SNARE SNAP-25 distinguishes mechanisms of neuroexocytosis." Nature Neuroscience **5**(1): 19-26.

Weber, K., U. Bartsch, C. Stocking and B. Fehse (2008). "A multicolor panel of novel lentiviral "Gene Ontology" (LeGO) vectors for functional gene analysis." Molecular Therapy **16**(4): 698-706.

Wen, T., P. Gu, T. Minning, Q. Wu, M. Liu, F. Chen, H. Liu and H. Huang (2002). "Microarray analysis of neural stem cell differentiation in the striatum of the fetal rat." Cellular and Molecular Neurobiology **22**(4): 407-416.

Werring, D. J., C. A. Clark, G. J. M. Parker, D. H. Miller, A. J. Thompson and G. J. Barker (1999). "A direct demonstration of both structure and function in the visual system: combining diffusion tensor imaging with functional magnetic resonance imaging." NeuroImage **9**(3): 352-361.

Wilson, P. A., G. Lagna, A. Suzuki and A. Hemmati-Brivanlou (1997). "Concentration-dependent patterning of the Xenopus ectoderm by BMP4 and its signal transducer Smad1." Development **124**(16): 3177-3184.

Winslow, J. T. (2001). Mouse social recognition and preference. Current Protocols in Neuroscience, John Wiley & Sons, Inc.

Woolfrey, K. M., D. P. Srivastava, H. Photowala, M. Yamashita, M. V. Barbolina, M. E. Cahill, Z. Xie, K. A. Jones, L. A. Quilliam, M. Prakriya and P. Penzes (2009). "Epac2 induces synapse remodeling and depression and its disease-associated forms alter spines." Nature Neuroscience **12**(10): 1275-1284.

Workman, A. D., C. J. Charvet, B. Clancy, R. B. Darlington and B. L. Finlay (2013). "Modeling transformations of neurodevelopmental sequences across mammalian species." The Journal of Neuroscience **33**(17): 7368-7383.

Wu, C., C. Orozco, J. Boyer, M. Leglise, J. Goodale, S. Batalov, C. Hodge, J. Haase, J. Janes, J. Huss and A. Su (2009). "BioGPS: an extensible and customizable portal for querying and organizing gene annotation resources." Genome Biology **10**(11): R130.

Wu, M.-T., R.-H. Wu, C.-F. Hung, T.-L. Cheng, W.-H. Tsai and W.-T. Chang (2005). "Simple and efficient DNA vector-based RNAi systems in mammalian cells." Biochemical and Biophysical Research Communications **330**(1): 53-59.

Wurm, F. and A. Bernard (1999). "Large-scale transient expression in mammalian cells for recombinant protein production." Current Opinion in Biotechnology **10**(2): 156-159.

Yamaguchi, T. P. (2001). "Heads or tails: Wnts and anterior posterior patterning." Current biology : CB **11**(17): R713-R724.

Yang, M. and J. N. Crawley (2001). Simple behavioral assessment of mouse olfaction. Current Protocols in Neuroscience, John Wiley & Sons, Inc.

Yang, M., J. L. Silverman and J. N. Crawley (2001). Automated three-chambered social approach task for mice. Current Protocols in Neuroscience, John Wiley & Sons, Inc.

Yip, K. Y., C. Cheng, N. Bhardwaj, J. B. Brown, J. Leng, A. Kundaje, J. Rozowsky, E. Birney, P. Bickel and M. Snyder (2012). "Classification of human genomic regions based on experimentally determined binding sites of more than 100 transcription-related factors." Genome Biol **13**(9): R48.

Yoo, A. S., A. X. Sun, L. Li, A. Shcheglovitov, T. Portmann, Y. Li, C. Lee-Messer, R. E. Dolmetsch, R. W. Tsien and G. R. Crabtree (2011). "MicroRNA-mediated conversion of human fibroblasts to neurons." Nature **476**(7359): 228-231.

Zaehres, H., M. W. Lensch, L. Daheron, S. A. Stewart, J. Itskovitz-Eldor and G. Q. Daley (2005). "High-efficiency RNA interference in human embryonic stem cells." Stem Cells **23**(3): 299-305.

Zamore, P. D. and B. Haley (2005). "Ribo-gnome: The Big World of Small RNAs." Science **309**(5740): 1519-1524.

Zeng, L., P. Zhang, L. Shi, V. Yamamoto, W. Lu and K. Wang (2013). "Functional impacts of NRXN1 knockdown on neurodevelopment in stem cell models." PLoS ONE **8**(3): e59685.

Zhou, T., B. Xu, H. Que, Q. Lin, S. Lv and S. Liu (2006). "Neurons derived from PC12 cells have the potential to develop synapses with primary neurons from rat cortex." Acta neurobiologiae experimentalis **66**(2): 105.

Zou, Y. S., D. L. Van Dyke and J. W. Ellison (2007). "Microarray comparative genomic hybridization and FISH studies of an unbalanced cryptic telomeric 2p deletion/16q duplication in a patient with mental retardation and behavioral problems." American Journal of Medical Genetics Part A **143A**(7): 746-751.